PB82-249897

Sampling and Data Handling Methods for Inhalable Particulate Sampling

Southern Research Inst.
Birmingham, AL

Prepared for

Industrial Environmental Research Lab.
Research Triangle Park, NC

May 82

U.S. Department of Commerce
National Technical Information Service
NTIS

PB82-249897

EPA-600/7-82-036
MAY 1982

SAMPLING AND DATA HANDLING METHODS FOR INHALABLE PARTICULATE SAMPLING

by

Wallace B. Smith, Kenneth M. Cushing, Jean W. Johnson,
Christine T. Parsons, Ashley D. Williamson, and Rufus R. Wilson,Jr.

Southern Research Institute
2000 Ninth Avenue, South
Birmingham, Alabama 35255

Contract 68-02-3118

Project 4181-37

Report SoRI-EAS-81-245R

EPA Project Officer: D. Bruce Harris

Industrial Environmental Research Laboratory
Office of Environmental Engineering and Technology
Research Triangle Park, NC 27711

U.S. ENVIRONMENTAL PROTECTION AGENCY
OFFICE OF RESEARCH AND DEVELOPMENT
WASHINGTON, D.C. 20460

REPRODUCED BY
NATIONAL TECHNICAL
INFORMATION SERVICE
U.S. DEPARTMENT OF COMMERCE
SPRINGFIELD, VA. 22161

IERL-RTP-1283

TECHNICAL REPORT DATA
(Please read Instructions on the reverse before completing)

1. REPORT NO.
EPA-600/7-82-036

2.

3. RECIPIENT'S ACCESSION NO.
PB82 249897

4. TITLE AND SUBTITLE
Sampling and Data Handling Methods for Inhalable Particulate Sampling

5. REPORT DATE
May 1982

6. PERFORMING ORGANIZATION CODE

7. AUTHOR(S)
W. B. Smith, K. M. Cushing, J. W. Johnson, C. T. Parsons, A. D. Williamson, and R. R. Wilson, Jr.

8. PERFORMING ORGANIZATION REPORT NO.
SoRI-EAS-81-245R

9. PERFORMING ORGANIZATION NAME AND ADDRESS
Southern Research Institute
2000 Ninth Avenue, South
Birmingham, Alabama 35225

10. PROGRAM ELEMENT NO.

11. CONTRACT/GRANT NO.
68-02-3118

12. SPONSORING AGENCY NAME AND ADDRESS
EPA, Office of Research and Development
Industrial Environmental Research Laboratory
Research Triangle Park, NC 27711

13. TYPE OF REPORT AND PERIOD COVERED
Final; 11/78-12/80

14. SPONSORING AGENCY CODE
EPA/600/13

15. SUPPLEMENTARY NOTES IERL-RTP project officer is D. Bruce Harris, Mail Drop 62, 919/541-7807.

16. ABSTRACT The report reviews the objectives of a research program on sampling and measuring particles in the inhalable particulate (IP) size range in emissions from stationary sources, and describes methods and equipment required. A computer technique was developed to analyze data on particle-size distributions of samples taken with cascade impactors from industrial process streams. Research in sampling systems for IP matter included concepts for maintaining isokinetic sampling conditions, necessary for representative sampling of the larger particles, while flowrates in the particle-sizing device were constant. Laboratory studies were conducted to develop suitable IP sampling systems with overall cut diameters of 15 micrometers and conforming to a specified collection efficiency curve. Collection efficiencies were similarly measured for a horizontal elutriator. Design parameters were calculated for horizontal elutriators to be used with impactors, the EPA SASS train, and the EPA FAS train. Two cyclone systems were designed and evaluated. Tests on an Andersen Size Selective Inlet, a 15-micrometer precollector for high-volume samplers, showed its performance to be with the proposed limits for IP samplers. A stack sampling system was designed in which the aerosol is diluted in flow patterns and with mixing times simulating those in stack plumes.

17. KEY WORDS AND DOCUMENT ANALYSIS

a. DESCRIPTORS		b. IDENTIFIERS/OPEN ENDED TERMS	c. COSATI Field/Group	
Pollution	Measurement	Pollution Control	13B	
Flue Gases	Cyclone Separators	Stationary Sources	21B	07A, 13I
Sampling		Particulate	14B	
Dust		Inhalable Particulate	11G	
Aerosols			07D	
Data Processing			09B	

18. DISTRIBUTION STATEMENT
Release to Public

19. SECURITY CLASS *(This Report)*
Unclassified

20. SECURITY CLASS *(This page)*
Unclassified

21. NO. OF PAGES
297

22. PRICE

EPA Form 2220-1 (9-73)

NOTICE

THIS DOCUMENT HAS BEEN REPRODUCED FROM THE BEST COPY FURNISHED US BY THE SPONSORING AGENCY. ALTHOUGH IT IS RECOGNIZED THAT CERTAIN PORTIONS ARE ILLEGIBLE, IT IS BEING RELEASED IN THE INTEREST OF MAKING AVAILABLE AS MUCH INFORMATION AS POSSIBLE.

NOTICE

Mention of trade names or commercial products does not consititute endorsement or recommendation for use.

ABSTRACT

The objectives of a research program on the sampling and measurement of particles in the inhalable particulate (IP) size range in emissions from stationary sources were reviewed and methods and equipment required are described. A summary is given of research programs conducted in support of the development of new and improved techniques for sampling IP emissions, instruments that are especially suited for IP measurements, and data-handling methods.

A computer technique was developed for analysis of data on particle-size distributions of samples taken with cascade impactors from industrial process gas streams. The plot of cumulative mass concentration vs particle size could be extrapolated from the limit of the impactor (the first stage cut diameter of 10 μm) to 15 μm by using a third degree polynomial of first order osculation. To estimate the accuracy of the method, simulated unimodal and bimodal log-normal particle-size distributions were sampled according to the impactor stage collection efficiency curves. Errors inherent to the method were found to be negligible. Concentrations of particles < 15 μm in diameter could be calculated from existing data to within a factor of 3 and probably within the sampling error if the impactor data were corrected for nozzle and precollector effects. Impactor data were also subjected to a modal analysis in which the data were fitted with multi-component log-normal distributions by a simplex minimization method. The results were comparable to those obtained with the polynomial: IP concentrations could be estimated within a factor of two or better.

Research on sampling systems for IP matter included the consideration of concepts for maintaining isokinetic sampling conditions, necessary for representative sampling of the larger particles, while flowrates in the particle-sizing device were constant. Techniques and devices that were considered were nozzles with cross-sectional areas that could be varied mechanically, split-stream probes and shrouded probes, and gas recycle systems. All the techniques involve the difficulty of manipulation of equipment from outside the stack.

Laboratory studies were conducted to develop suitable IP sampling systems with overall cut diameters of 15 μm and conforming to a specified collection efficiency curve. Cascade impactors, cyclones, and horizontal elutriators were used as collectors. Laboratory experiments were conducted with monodisperse aerosols on commercially available impactors and buttonhook nozzles to characterize them for measurements in the IP range of particle sizes.

Collection efficiencies were similarly measured for a horizontal elutriator. The measured values agreed well with values calculated from theory, allowing the preparation of design nomographs for inlet precollectors in sampling systems.

Design parameters were calculated for horizontal elutriators to be used with impactors, operated at 14.2 ℓ/min at 149°C; the EPA Source Assessment Sampling System, operated at 185 ℓ/min at 204°C; and the EPA Fugitive Ambient Sampling Train, operated at 5,282 ℓ/min and 23°C.

Two cyclone systems were designed and evaluated: a cyclone to be used as a precollector for impactors, and a system of two cyclones and a filter in series, to be used as the primary system for measuring IP and fine particulate matter concentrations. Both systems were designed for high-temperature service in process gas streams.

Tests on the Andersen Size Selective Inlet, a 15-μm precollector for hi-vol samplers, showed its performance to be within the proposed limits for IP samplers.

A stack sampling system was designed in which the aerosol is diluted in flow patterns and with mixing times simulating those in stack plumes. The system was thus designed to characterize aerosols formed from condensable vapors in stack gas as the plume is diluted and cooled by the atmosphere. Tests with the system on emissions from a domestic oil-fired furnace indicated that condensation of organic chemical vapors took place in the system as expected.

Procedures for the use of impactors for measuring particle-size distributions in industrial process gas streams were modified in order to measure IP concentrations. The modifications included refinements in preparation, calibration, and operation of the impactors and in processing the data.

This report was submitted in fulfillment of Contracts No. 68-02-2131 and 68-02-3118 by Southern Research Institute under the sponsorship of the U.S. Environmental Protection Agency. This report covers the period November 1, 1978 to December 31, 1980.

CONTENTS

Page

Abstract. iii
Figures viii
Tables xiv

1. Introduction and Background. 1
  - Consultant Workshop. 3
    - General Comments on the EPA Program. 3
    - Development of an IP Sampler Performance Curve 4
    - State of the Art in Sampling 7
      - Ambient Samplers 7
      - Fugitive Emission Samplers 7
      - In-Stack Sampling. 8
    - Design and Sampling Considerations for IP Measurement 8
      - Precollector Efficiency Curves 8
      - Isokinetic Sampling. 9
      - Large Particles. 10
      - Condensable Material 10
      - Fugitive Emissions 11
      - Calibration. 11
    - Recommended Research Program 12
      - For Immediate Action 12
      - Six Months Program 12
      - Long Term Research and Development 16
    - Summary of Studies Completed 18
2. Development of Methods for Sampling and Data Analysis 20
  - Data Analysis for Cascade Impactors. 20
    - Summary. 20
    - Previous CIDRS 20
    - Proposed CIDRS 22
    - Extending Accuracy in the Mass Size Distribution Calculated Beyond the First Stage D_{50}. 27
    - The Osculating Polynomial. 28
    - Accuracy of the Extrapolation Technique. . . 31
    - Testing with Unimodal Particle-size Distributions. 33
      - Variation of the Particulate Mass Median Diameter. 33

Variation of the Geometric Standard Deviation of the Particulate Size Distribution 33
Variation of the Geometric Standard Deviation (Slope) of the Collection Efficiency Curve 34
Variation of the Assumed Largest Particle Diameter in the Distribution 34
Testing with Bimodal Particle-size Distributions 37
Variation of Geometric Standard Deviation of the Particle-size Distribution 37
Variation of the Mass Median Diameter of the Second Mode 37
Variation in Fraction of the Total Mass Contained in Each of the Modes. 40
Effect of Operating Problems 40
Isokinetic Sampling by Constant Flowrate Particle-sizing Devices. 51
Sampling Concepts 52
Variable Area Nozzles. 53
In-stack Split Stream Probe. 61
Gas Recycle Concept. 67
In-stack Probe Shroud. 71
3. Design, Fabrication, and Testing of Prototype Sampling Systems for Inhalable Particulate Matter. 73
Summary. 73
Evaluation of Commercial Cascade Impactors and Buttonhook Nozzles--Effect on Measurement of Inhalable Particulate Matter 74
Experimental Procedures 74
Results and Evaluation. 79
Buttonhook Nozzles 79
Impactors. 79
The Horizontal Elutriator as an IP Precollector. 85
Background. 85
Experimental Procedures 91
Results 93
Collector Design. 98
The FAST Elutriator Inlet. 98
Horizontal Elutriator Inlet for Fugitive Emissions Sampler 98
Cyclones as IP Collectors. 104
Background. 104
Calibration of the Brink Cyclone. 105
Calibration of the Sierra Cyclone 105
Calibration of the Southern Research Institute Five-Stage Cyclone. 105
An Inhalable Particulate Precollector and Sampling Train 109
Development and Fabrication 109

Calibration 111
Results 115
Size-selective Inlet for the Andersen Hi-Vol Sampler. 122
A Stack Dilution Sampling System 122
Design and Testing of Laboratory Prototype Sampler 125
Prototype Design 125
Performance Characterization of Laboratory Prototype Sampler 127
Domestic Furnace Test. 132
Results of Dilution Sampling Measurements . 133
Gravimetric Measurements 133
Temporal Behavior. 134
Effect of Dilution Ratio on Particle Size Distribution. 137
Conclusions. 138
4. Operation and Sampling Parameters for the Inhalable Particulate Sampling System 140
Cascade Impactor Calibration and Operation . . . 140
The Inhalable Particulate Sampling System. . . . 140
The Dual-Cyclone Train. 141
Cleaning, Inspection, and Assembly . . 146
Sampling Parameters. 147
Sampling 152
Sample Retrieval and Weighing. 155
Data Analysis and Reports. 157
The Stack Dilution Sampling System. 159
Design and Operating Procedures. . . . 159
System Description 159
Assembly 166
Sampling Parameters. 167
Sampling 169
Sample Retrieval and Weighing. 171
Data Analysis and Reports. 171

References 171

Appendices

A. Modifications to CIDRS Cumulative Mass Curve Fitting Programs for Inhalable Particulate Determination. . . 175
B. Modeling of SRI Impactor Data and Calculation of IP Concentration 191
C. Design Drawings of the Inhalable Particulate Sampling Train 267
D. Design Drawings of the Inhalable Particulate Precutter Cyclone 276
E. Metric System Conversion Factors. 281

FIGURES

Number Page

1 Calibration of the hi-vol and dichotomous sampler inlets. 5

2 Recommended IP sampler collection specifications. . . 6

3 Cumulative size distribution from raw impactor data . 23

4 Start of development of interpolated points between first and last D_{50}. 23

5 Continued generation of interpolated points 24

6 Continued generation of interpolated points 24

7 Generation of interpolated points on parabola which includes DMAX 25

8 Generation of interpolated points on hyperbola through $D_{50}(1)$ and DMAX 25

9 Generation of interpolated points on osculating polynomial and zero slope line at total mass concentration 26

10 Fitting the cumulative mass distribution for $D(1)<D<DMAX$ using a first-order osculating polynomial P (D). 32

11 Ratio of recovered to true IP concentration versus mass median diameter of a unimodal log-normal particle-size distribution. 34

12 Ratio of recovered to true IP concentration versus aerosol geometric standard deviation of a unimodal log-normal particle-size distribution 35

13 Ratio of recovered to true IP concentration versus stage efficiency standard deviation using a unimodal log-normal particle-size distribution 35

Figures (Continued)

Number Page

14 Ratio of recovered to true IP concentration versus assumed largest particle diameter using a unimodal log-normal particle-size distribution 36

15 Ratio of recovered to true IP concentration versus aerosol geometric standard deviation of a bimodal log-normal mass distribution. 38

16 Ratio of recovered to true inhalable particle concentration versus second mode mass median diameter of a bimodal log-normal particle-size distribution . . 39

17 Ratio of recovered to true IP concentration versus fractional contribution of mass from each mode of a bimodal log-normal mass distribution. 41

18 Cumulative particle-size distribution at inlet to electrostatic precipitator. 43

19 Differential particle-size distribution at inlet to electrostatic precipitator. 44

20 Cumulative particle-size distribution at outlet of electrostatic precipitator. 45

21 Differential particle-size distribution at outlet of electrostatic precipitator. 46

22 Calculated IP concentration vs. assumed D_{MAX} at electrostatic precipitator inlet. Coal-fired power plant 47

23 Calculated IP concentration vs. assumed D_{MAX} at electrostatic precipitator outlet. Coal-fired power plant 48

24 Calculated IP concentration vs. assumed D_{MAX} at electrostatic precipitator inlet. Cement kiln. . . 49

25 Calculated IP concentration vs. assumed D_{MAX} at electrostatic precipitator outlet. Cement kiln . . 50

26 Conceptual design of variable area nozzle attached to an impactor. 54

Figures (Continued)

Number Page

27 A variable area nozzle attached to a cyclone 55

28 A diamond-shaped nozzle 56

29 Conceptual drawing of an elliptical nozzle 58

30 A multiple nozzle revolver configuration 59

31 An iris nozzle 62

32 In-stack split-stream probe 63

33 Split-stream probe: sliding-cone probe 65

34 Split-stream probe: adjustable flap probe 65

35 A split-stream nozzle 66

36 A hot gas recycle concept 67

37 Cool gas recycle concept 69

38 In-stack probe shroud 72

39 Configuration of apparatus used in evaluation of cascade impactor and nozzle 75

40 Andersen Mark III cascade impactor situated in isokinetic sampling apparatus 76

41 Isokinetic sampling apparatus adjacent to vibrating orifice aerosol generator 77

42 Isokinetic sampling apparatus adjacent to vibrating orifice aerosol generator 78

43 Calibration data for the first three stages of the University of Washington Mark V cascade impactor 84

44 Particle collection efficiency for the impactor 85

45 Settling velocity in air for unit density spheres 88

46 Velocity profile and particle trajectory between parallel plates 89

Figures (Continued)

Number Page

47 Zone of 100% particle collection. 90

48 Theoretical collection efficiency by particle settling in rectangular and circular tubes 91

49 Apparatus used to measure the collection efficiency of the settling chamber 92

50 Profile of the air velocity immediately upstream from the blower of the settling chamber before the plates were positioned 94

51 Profile of the air velocity upstream from the plates of the settling chamber 95

52 Theoretical and experimental collection efficiencies for a horizontal elutriator with rectangular cross-section, plate length 38.1 cm, average gas velocity 70 cm/sec 96

53 Theoretical and experimental collection efficiencies for a horizontal elutriator with rectangular cross-section, plate length 20 cm, average gas velocity 40 cm/sec 97

54 Relationship of design parameters for horizontal elutriators with D_{50} cutpoints of 15 μm aerodynamic diameter used as precollectors for in-stack cascade impactors 99

55 Relationship of design parameters for horizontal elutriators with D_{50} cutpoints of 15 μm aerodynamic diameter to be used with SASS trains. 100

56 Relationship of design parameters for horizontal elutriators with D_{50} cutpoints of 15 μm aerodynamic diameter to be used with FAST trains. 101

57 Laboratory set-up for testing FAST horizontal elutriator inlet. 103

58 Collection efficiency versus flowrate for a Brink precollector cyclone sampling 15 μm aerodynamic diameter ammonium fluorescein particles at 22, 100, and 150°C 106

Figures (Continued)

Number Page

59 Flowrate versus viscosity to maintain a D_{50}=15 μm aerodynamic for Brink precollector cyclone. 107

60 Calibration curves for the five-stage cyclone system. Flowrate 1.0 ft^3/min, temperature 22°C. 109

61 Schematic of a cascade impactor-precollector cyclone system. 112

62 Schematic of two-cyclone system 112

63 Summary of cyclone dimensions 113

64 Calibration system for heated aerosols. 114

65 Collection efficiency of Cyclone IX versus flowrate for particles of 15±0.6 μm aerodynamic diameter . . 116

66 Collection efficiency of Cyclone X versus flowrate for particles of 15±0.6 μm aerodynamic diameter . . 117

67 Collection efficiency versus aerodynamic particle diameter for Cyclone III at 22°C and 11.3 ℓ/min (□), 93°C and 19.8 ℓ/min (○), and 150°C and 22.7 ℓ/min (Δ) 118

68 Calibration data for Cyclone IX at 14 ℓ/min and 150°C 119

69 Schematic of size-selective inlet 123

70 Block diagram of dilution sampling system 126

71 Concentration profile of salt aerosol across diluter. 128

72 Temperature dependence of cross-section of diluted aerosol plume 129

73 Particle-size distribution of glycerol smoke aerosol. 131

74 Time variation of particle number concentration per unit flue gas as measured after dilution. Dilution ratio=19.6 (standard) 135

75 Time variation of particle mass concentration per unit flue gas as measured after dilution. Dilution ratio=19.6 (standard) 136

Figures (Continued)

Number Page

76 Particle mass concentration per unit flue gas as measured at different dilution ratios. All concentrations measured eight minutes after beginning of combustion cycle 139

77 Schematic drawing of inhalable particulate sampler. . 142

78 The critical internal dimensions of a cyclone 145

79 Nomograph for selecting proper sampling duration. . . 148

80 Recommended sampling points for circular and square or rectangular ducts. 151

81 Gas flowrate versus viscosity at D_{50}=15 μm aerodynamic diameter for IP Cyclone SRI-X 153

82 Nomograph for selecting nozzles for isokinetic sampling, using cyclone samplers. 154

83 Diagram of Stack Dilution Sampling System 160

84 Sample probe and heated hose for the Stack Dilution Sampling System 162

85 The dilution air line of the Stack Dilution Sampling System. 162

86 Inlet assembly for the dilution chamber 163

87 Hi-vol filter and impactor assembly of the Stack Dilution Sampling System. 164

88 Pressure and flow measurement module. 165

89 Heater and flow control module. 166

TABLES

Number Page

1 EPA Needs and Priorities for Data on Emissions of Inhalable Particulate Matter from Stationary Sources 2

2 Recommended Program to Develop Methods for Measurement of Inhalable Particulate Matter 13

3 Techniques Recommended for Use in Obtaining Data to Set IP Emission Factors for Industrial Sources. . . 14

4 Systems Available for Measuring Particle Size and Mass 17

5 Summary of Studies that have been Performed at Southern Research Institute Towards Completion of the IP Program. 19

6 CIDRS Programs and Output 22

7 Sampling Parameters from a Hypothetical Sampling Test Using the Multiple Nozzle Revolver Configuration. . 60

8 Change in Stage D_{50}'s for an Andersen Impactor as a Function of Moisture Content of Sampled Gas 70

9 Evaluation of Buttonhook Nozzles. 79

10 Evaluation of Commercial Cascade Impactors Using Fifteen-Micron Aerodynamic Diameter Particles . . . 80

11 FAST Horizontal Elutriator Inlet Test Data. 102

12 Calibration Results for the Brink Cyclone 108

13 Sierra Cyclone Calibration Data 108

14 Laboratory Calibration of the Five-Stage Cyclones D_{50} Cut Points. 110

15 Operating Parameters of SRI Cyclones. 121

16 Size-selective Inlet Calibration Data 124

SECTION 1

INTRODUCTION AND BACKGROUND

The U.S. Environmental Protection Agency expects to set air pollution standards for emission of inhalable particulate (IP) matter from stationary sources. Inhalable particulate matter is defined in terms of particle size, since the extent of penetration of inhaled particles into the lungs depends on their size.

Adequate characterization of a source of IP matter requires measurement of stack or fugitive emissions from the source and also background levels of ambient atmospheric particles in the relevant size ranges. The concentration and particle-size distribution of the suspended particulate matter and, in some instances, its chemical composition and biological properties must be determined. The first step in obtaining information of this kind is usually sampling of the gas stream or atmosphere for particles of the appropriate sizes.

To assist the EPA in planning research on the IP sampling and analysis problem, a workshop was held at Research Triangle Park, NC, in December 1978. The workshop was attended by consultants and other investigators experienced in aerosol sampling and characterization.

At that time, it was generally recognized that there were no methods in use that were suitable for measuring inhalable particulate matter per se. Thus a need was recognized for information on methods that could yield or could be adapted to yield IP data, and also on the research that would be necessary for the development of instruments and procedures for that purpose.

Table 1 lists the needs of the Environmental Protection Agency for data on IP emissions from stationary sources, as seen by the EPA at the time, and priorities assigned by the agency for filling them.

TABLE 1. EPA NEEDS AND PRIORITIES FOR DATA ON EMISSIONS OF INHALABLE PARTICULATE MATTER FROM STATIONARY SOURCES

Priority	Program Element	Description
1	1a	Total mass $\leq$ 15 μm aerodynamic diameter Mass- cut to match ambient monitor Mass- D_{50} = 15 μm $\pm$ 2 μm Mass- slope to match ambient monitor
2	1b or 2c	Condensable fraction of total mass Discrete size fractions $\leq$ 15 μm
3	2a	Size distribution - continuum $\leq$ 80 μm
4	2b	Size distribution - continuum $\leq$ 15 μm
5	3	Chemical composition of material in program elements 1 and 2
6	4	Bioassay of material in program elements 1 and 2

The present report contains (1) recommendations on EPA research prepared in the workshop and (2) a detailed summary of research done at Southern Research Institute on the IP sampling problem under contract with the EPA. Except as noted in the text and in the references at the end of the text, the information in the report has not been published.

CONSULTANT WORKSHOP*

The purposes of the workshop were:

(1) to discuss the EPA objectives,
(2) to discuss any restrictions or ground rules in developing or applying measurement techniques,
(3) to define the current state of the art,
(4) to identify ongoing programs and establish lines of communication, and
(5) to lay the ground work for a position paper recommending methods and research programs on the development of methods.

At the workshop, elements 1 and 2 of the EPA program (Table 1) were addressed in order of priority. The following is a summary of the comments and recommendations of the workshop participants, as recorded by Southern Research Institute staff members attending.

General Comments on the EPA Program

The workshop participants agreed that the objectives of the EPA program appeared to be logical and reasonable. It was understood that the definition of inhalable particulate matter and the "standard" particle-size curve had resulted from prior decisions by the EPA and were not subject to review or revision. All particles smaller than 80 µm, including condensable materials, were to be considered of interest. Condensables were included because they were recognized as constituting most of the mass of emissions from many sources. On the other hand, any emphasis on particles larger than 20-30 μm was not considered to be justified for most sources. It was argued that very large particles are typically not emitted in large quantities and that they do not travel far from the source. Frequently, samples of large particles in ambient aerosols have been found to consist primarily of dust generated by the wind, automobiles, or farming, rather than being emitted from stationary sources. Another practical problem associated with large particles was seen in the difficulty involved in sampling them. It was recognized that great care would be required in developing sampling systems and protocols to ensure that representative samples would be obtained.

---

*EPA personnel who participated or attended were: John Backman, Fred Miller, Dennis Drehmel, John Nader, Bruce Harris, Jim Abbott, Ken Knapp, Jack Wagman, Charles Rhodes, and Frank Noonan.

Consultants and other investigators who attended were: Wallace Smith (Southern Research Institute), Kenneth Whitby (University of Minnesota), Richard Parker (Air Pollution Technology), Virgil Marple (University of Minnesota), Dale Lundgren (University of Florida), Thomas Mercer (University of Rochester), Carl Peterson (Environmental Research Corporation), Michael Pilat (University of Washington), Walter John (California Dept. of Health Services), Morton Lippmann (New York University Medical Center), Robert Heinsohn (Pennsylvania State University), Richard Flagan (California Institute of Technology), Joe McCain (Southern Research Institute), Ray Wilson (Southern Research Institute), and Henry Kolnsberg (The Research Corporation of New England).

The workshop participants agreed that the greatest problem associated with the EPA's proposed program would be the lack of time available for the development of adequate measurement methods. Although it appeared to be reasonable to design and evaluate survey systems for in-stack, ambient, and fugitive emissions in 6 months to a year, a number of the systems would have to be fabricated and procedures written before they could be put to widespread use. It was expected that 3 to 5 years would be required before reliable methods would be available that could be used to obtain all of the detailed data needed. The only practical course appeared to be the use of survey techniques to obtain less comprehensive data as soon as possible while research programs were initiated to develop more advanced and accurate methods for future use.

Development of an IP Sampler Performance Curve

Figure 1 shows some calibration data for inlets for the hi-vol sampler and dichotomous sampler. The data approximate the "standard" curve for IP samplers. It was strongly recommended that these data be confirmed and extended by independent research. It was recommended that the EPA adopt a standard mathematical performance curve for samplers used in measuring IP matter, with specified tolerances. Any newly developed devices would have to be calibrated and shown to fit the curve within the tolerances specified. Suggested performance criteria for IP samplers are shown in Figure 2. The performance curves of all samplers would be required to fall within the shaded area. The shaded area is bounded by log-normal curves drawn through the (13 μm, 50%) and (17 μm, 50%) points with geometric standard deviations (σ_g) of 1.0 and 1.7. After allowing 10% for wall losses of small particles and 10% penetration of large particles, the area is completely defined as shown. After more thorough characterization of existing and newly developed sampling systems, it might be possible to place more stringent tolerances on the standard curve.*

---

*Subsequent to the workshop, the curve in Figure 2 was indeed adopted as the standard IP curve by the EPA.

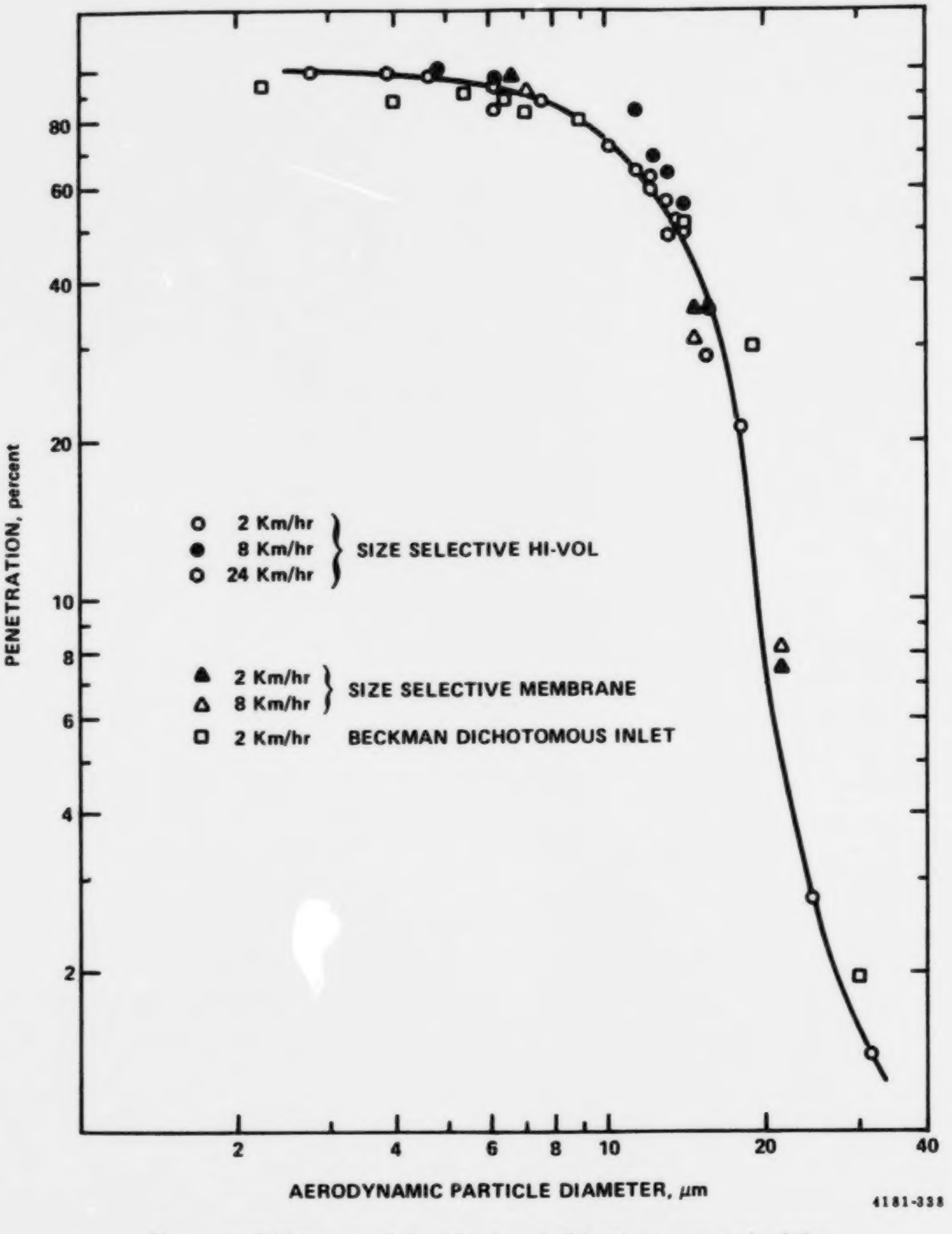

Figure 1. Calibration of the hi-vol and dichotomous sampler inlets.

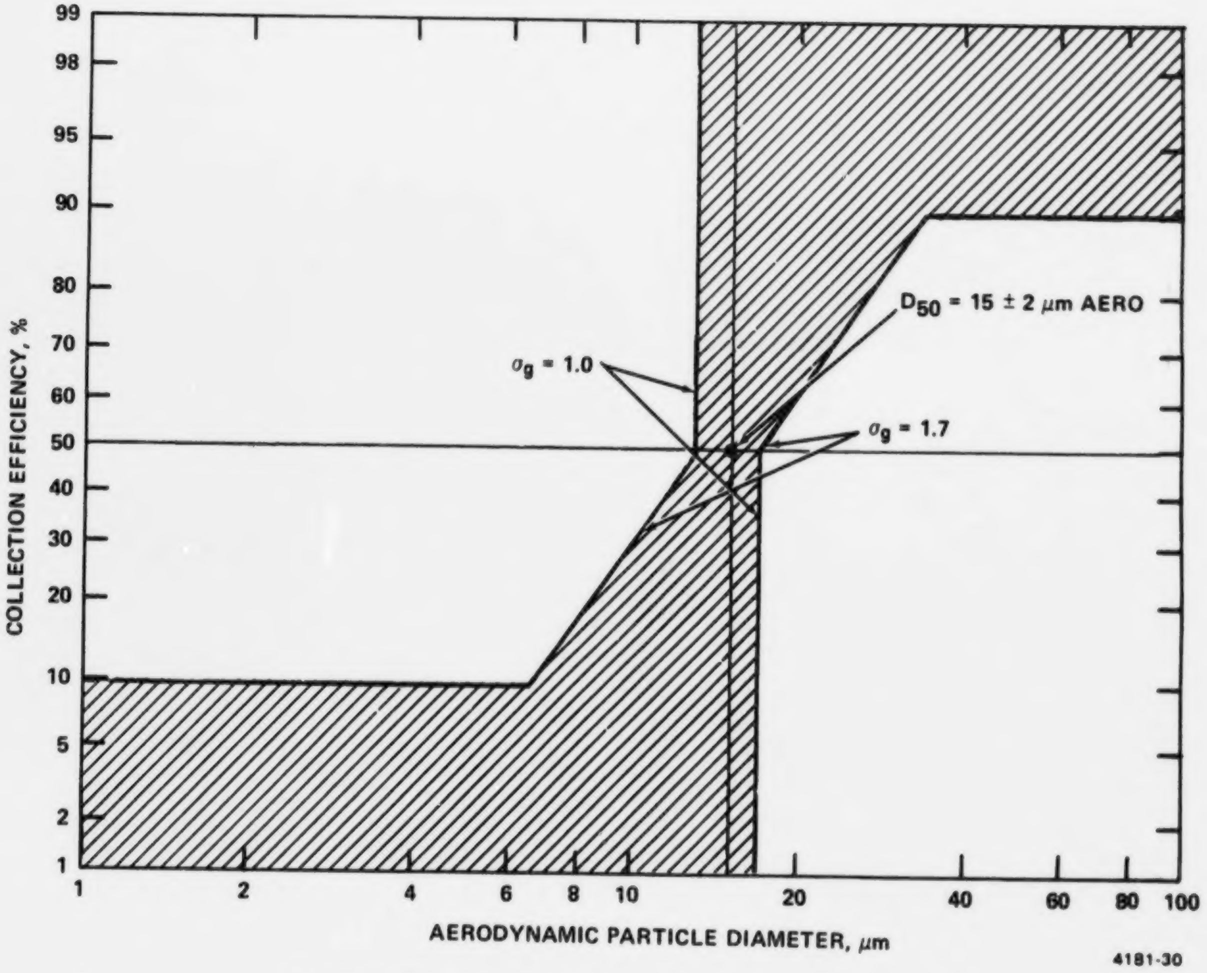

Figure 2. Recommended IP sampler collection specifications.

State of the Art in Sampling

The following techniques were those available at the beginning of the research program.

Ambient Samplers--

Suitable inlets were currently under development for the dichotomous sampler and the hi-vol sampler. The performance characteristics of the devices other than the inlets were presumed to be well-characterized and satisfactory. It was expected that after thorough characterization of the new inlets they would be available for acquiring IP mass data.

Standardized instruments for acquiring detailed information on particle size were not available. It was expected that diffusion batteries and electrical aerosol analyzers could be made available within 6 months to a year for measuring very fine particles, but that measuring particle sizes up to 80 µm would require extensive research.

No real-time monitors were currently available for measuring mass or particle size on a routine basis.

Condensable materials were not expected to be present in ambient and fugitive aerosols as vapors, and hence were not considered to have a high research priority.

Fugitive Emission Samplers--

The hi-vol and dichotomous samplers were presumed to be suitable for sampling fugitive emissions. The FAST system, a 200 ft^3/min sampler, would require the development of a new IP inlet before it could be used. Prototype FAST units were projected as being available in about 6 months. The FAST instrument yields limited information on particle size (as does the dichotomous sampler) as well as on the concentration of organic chemical vapors.

The comments made above with reference to particle size and real-time analysis were considered to apply to fugitive emissions as well as to ambient sampling.

The greatest problem in sampling fugitive emissions was considered to be the development of suitable sampling strategies. There was no protocol available for selecting sampling methods or locations to characterize fugitive emissions.

In-Stack Sampling--

It was expected that both cyclones and impactors could be used as in-stack devices to approximate the IP performance curve. Nevertheless, it was recognized that additional calibration and perhaps modification would be required before practical systems could be assembled.

In measuring the condensable fraction, it is important to simulate the dilution and cooling process that occurs at the stack-ambient interface. It was noted that a system under development would allow the operator to mix the sample with filtered ambient air before it reached the filter. This method appeared to be suitable for measuring mass, but it was recognized that it would require refinement before the dilution sufficiently represented the stack-ambient interaction to allow accurate measurement of particle size. In addition, the collectors that would be used would have to satisfy the requirements of the IP performance curve.

It was noted that some advanced types of data analysis had not been exploited efficiently to obtain in-stack information on particle-size distribution. Specifically, it was noted that methods had been developed in treating ambient sampling data to extrapolate particle-size distribution curves to larger particle sizes, thus yielding data on IP concentrations. This was thought to be a technique that was immediately available for making progress in the search for IP data on stationary sources. The technique would not provide direct information on the condensable fraction, but if the gas composition were known, it might be possible to make some general inferences.

It was pointed out that any method that involves extrapolation must be carefully examined and verified before extensive application to stack gas, especially at the outlet of a control device, where the original particle-size distribution would have been distorted by the removal of particles in a non-linear fashion.

Design and Sampling Considerations for IP Measurement

Precollector Efficiency Curves--

The mass of inhalable particulate matter that is measured is relatively insensitive to the standard deviation, σ_g, of the inlet collection efficiency curve for most samplers, but the particle-size distribution may be greatly affected. However, if the complete particle-size distribution smaller than 80 μm (or even 20-30 μm) was to be measured, there appeared to be little value in having any stage in the sampler match a standard IP performance curve. It was thought that all the information could be retrieved from the measured particle-size distribution. If the material was to be used for bioassay, however, a stage that matched the standard IP curve would be desirable.

Another point that was considered concerning the interpretation of data obtained from ambient samplers was the problem of recovering the portion of the sample containing particles larger than 15 µm, so that the ratio of the inhalable fraction to the total could be obtained. It was recognized that theoretically the information could be obtained by operating a standard hi-vol sampler at the same location as the IP sampler and attributing the difference in the amounts collected to particles larger than 15 µm. However, this would be a secondary measurement and might lead to undesirably large errors; therefore, it was recommended that some thought be given to recovering the larger particles.

It was noted that IP precollectors for in-stack samplers might be larger than desirable and that size constraints might force the operation of sampling trains at lower flowrates than desired. For example, with a cyclone precollector, the Method 5 trains might be restricted to a maximum sampling rate of 0.5 ft^3/min.

A problem that had recently been observed and accepted as a fundamental limitation of impactor performance was particle bounce at large particle sizes or high impaction velocities. Although it is not evident in Figure 1, a typical collection efficiency curve for an impactor exhibits very low values for particles much larger than the D_{50} value. Thus, it was recognized as imperative that all proposed inlets be calibrated with dry particles much larger than the D_{50} value.

Isokinetic Sampling--

It was recognized that in stack sampling when precollectors such as cyclones or impactors are used with a mass train, it is necessary to maintain a fixed constant flowrate, in order to avoid changes in the sampling characteristics of the precollector. Any alternative to using a fixed flowrate would involve the development of new, complicated sampling systems. It would not be expected that errors introduced by limited traverses and non-isokinetic sampling would significantly affect the quality or reliability of the IP data obtained.

In ambient and fugitive sampling systems, the inlet would have to be designed to minimize the effects of varying wind speed and direction. The magnitude of errors due to non-isokinetic sampling would have to be determined by careful calibration.

Large Particles--

Because of their high inertia, large particles are extremely difficult to sample in a representative fashion. Also their concentration is usually low, and so counting statistics might be poor. Large particles have to be sampled isokinetically and cannot be transported around bends or through long sampling lines. It was judged that special systems involving manual operation and perhaps microscopic analysis would be required to measure size distributions of large particles. It appeared doubtful that real-time analysis could be achieved in the near future.*

Condensable Material--

It was recognized that accurate measurement of the amount of condensable material existing in a process stream and determination of its physical and chemical properties in the atmosphere presented perhaps the most important and challenging task of the IP research program.

Many process streams contain materials in the vapor state which condense to form homogeneous or heterogeneous aerosol particles. Some "condensable" vapors do not actually appear as particles in the air downwind of the source since their equilibrium vapor pressure is high enough that they will not condense, or condensed vapors may re-evaporate as dilution is increased. In order to measure the properties of the aerosol emitted to the atmosphere, the condensation in the sampling system would have to simulate plume behavior. Dilution ratios on the order of 1000:1 might be required. Lower dilution rates might maximize the super saturation and overestimate the contribution of condensed vapors to the IP matter.

It was noted that the rate of dilution might be important. Studies of the aerosols produced by diesel engines (Kittelson, University of Minnesota) have shown that rapid dilution of 1000:1 can prevent condensation of organic vapors.

It was also pointed out that condensed vapors can contribute significantly to mass emissions under some circumstances. The example of a coal-fired boiler burning coal with 10% ash was given. If all the ash appeared in the flue gas and if 99% of this fly ash was collected, 1% of the fly ash would be omitted from the stack. The fly ash emissions would amount to 0.1% of the mass of the original coal. If the coal contained 1% sulfur, and if 5% of the sulfur was emitted from the stack, it would amount to 0.05% of the mass of the coal. Furthermore, since the sulfur is emitted as sulfur oxides or sulfuric acid, the mass contributed to the emissions would be multiplied 2-or 3-fold. Thus it could equal or exceed fly ash emissions.

---

*Subsequent to the workshop, the measurement of very large particles was relegated to a lower priority by the EPA.

In other processes, notably smelting, the fraction of the emissions emitted as vapors and condensing at the stack-ambient interface could far exceed the amount existing as solid particles within the stack.

It was noted that it would be preferable in the sampling to dilute and cool the entire aerosol as it exists in the stack. However, because of the unacceptably high losses in transporting large particles through sampling lines and dilution systems, the workshop participants recognized that it would almost certainly be necessary to collect and size particles larger than 2-3 μm in the stack. The smaller particles would then pass to the dilution system outside the stack for further characterization. Removing particles from the sample aerosol would remove surfaces on which condensation would likely occur upon cooling and dilution. Thus, to some extent, the result would be biased and the mass concentration of the aerosol and its particle-size distribution in the diluter would be distorted.

In view of these complications, it was recognized that experimental and theoretical studies had to be performed to determine the magnitude and nature of the errors associated with this compromise procedure.

Fugitive Emissions--

The development of realistic sampling protocols was seen as perhaps the most difficult problem in measuring fugitive emissions. It was noted that a great deal of research would be required for the development of suitable sampling strategies. In addition to deploying networks of fixed sensors, mobile laboratories and the use of chemical tracers were considered to be methods that could be applied to isolating and measuring fugitive emissions.

Calibration--

It was recognized that instruments and systems must be calibrated with standards and that the development of calibration procedures would require considerable time and effort. As a minimum, the following calibration parameters would have to be considered:

- particle type - wet, dry, monodisperse, polydisperse
- velocity of gas
- particle diameter - aerodynamic, standard set for verifying size
- sampling efficiency vs. particle size
- wall loss vs. particle size

- aerosol concentration - it could affect the operation of some devices
- temperature - it would have to simulate sampling conditions
- wind direction
- gas loading and reentrainment
- frequency of calibration
- number of devices calibrated - initial prototypes, or all

The workshop participants noted that in the early stages of a research and development program, it would be important to have the opportunity of calibrating devices at more than one facility, so that results could be compared and verified.

Recommended Research Program

The research plan outlined in this section was developed within the context of the three-phase program illustrated in Table 2. The participants pointed out other work being done at several laboratories that would ultimately benefit the IP program. Table 3 summarizes the research program recommended by the workshop participants.

For Immediate Action--

The only activities (other than initiating a comprehensive research and development program) that appeared profitable for immediate action were:

(1) Additional analysis of existing data. Two techniques were to be evaluated: the University of Minnesota modal analysis and the Southern Research Institute curve-fitting procedure.

(2) Calibration of sampler inlets. It was recognized that the new inlets for the hi-vol and dichotomous samplers needed to be calibrated and their performance verified, and that a total mass sampler (lo-vol) with the same flowrate and inlet as the dichotomous sampler was needed for field comparisons between total mass samplers and the dichotomous sampler.

Six Months Program--

The picture projected at six months appeared somewhat brighter. It was envisioned that systems could be made available to acquire much of the survey data required for the IP program. Nevertheless, the participants noted that the sampling program could not be fully implemented, adequate data obtained, data reviewed, and the method accepted by the scientific community before several (3-5) years would have elapsed.

TABLE 2. RECOMMENDED PROGRAM TO DEVELOP METHODS FOR MEASUREMENT OF INHALABLE PARTICULATE MATTER

Phase I -	Develop Program Outline Set Specifications Assess Methods Available Identify R&D Areas Set Milestones Contact Consultants and Subcontractors for Phases II and III	← Start 2 months
Phase II -	Short Term Tasks Identify Methods Where Specifications May Be Met By Changing Only Sampling Protocol Identify Methods Where Specifications May Be Met By Minor Hardware and Procedure Modifications Bread Board Hardware and Test Demonstrate/Test as Time Allows Draft New Protocols	6 months
Phase III -	Research and Development Identify Systems That Can Meet All Program Ojectives Develop Prototype Systems Develop Calibration and Test Protocols and Systems Calibrate and Demonstrate Systems Write Technical Reports, Operator's Manuals, and Procedures Manuals	Initial Milestones → to be Set in Phase I

TABLE 3. TECHNIQUES RECOMMENDED FOR USE IN OBTAINING DATA TO SET IP EMISSION FACTORS FOR INDUSTRIAL SOURCES

TIME SCALE	PROGRAM ELEMENT	STACK	AMBIENT	FUGITIVE
Immediate	1a. Total Mass ≤15 μm 1b. Condensable Mass 2c. Size Distribution ≤15 μm,,Discrete 2a. Size Distribution ≤80 μm 2b. Size Distribution ≤15 μm, Continuous	Re-Analyze Data		
Six Months	1a. 1b. 2c.	Cyclones + Impingers, for 1a, 1b, 2c Also SASS Train	Lo-Vol, Hi-Vol, Dichotomous (Similar inlets requiring more calibration and performance verification) 1b, N/A	FAST Train, New Inlet
	2a.		Deposition on Suitable Substrate, with Automatic or Manual Image Analysis.	
	2b.	Cyclones, Impactors		
Longer Term:	1a. 1b. 2c.	15 μm, 2.5 μm Cyclones Followed by Dilution Run in Parallel with Method 17		
Nine Months Two Years	2a.	15 μm, 2.5 μm Cyclones Dilution, Out of Stack Sizing. (Impactor, Optical, Diffusional, Electrical) Body Impactor for 2-80 μm	Rotating, Body Impactor, Optical, Diffusional, Electrical, Centrifugal Mobile Labs	

For in-stack use, a train was suggested that would include in-stack cyclones with D_{50} values of 15 μm and 2.5 μm. This would be a modified EPA Method 5 train with a conventional filter box and a modified impinger train. A study of impinger solutions would be required to reduce artifact formation. Dilution would be preferred over impingers as a means of promoting condensation in collecting volatile components of the aerosol.

It was appreciated that isokinetic sampling of stack gas would not be possible with fixed flowrate sampling systems unless a very large number of nozzle sizes were available and the nozzles were changed at each sampling point of a stack traverse. Therefore a simplified (compared to EPA Method 5) sampling procedure was suggested. In the light of the accuracy of stack sampling procedures, no significant loss of accuracy is expected to result from the simplification.

It was recommended that two simultaneous samples should be obtained using four sampling sites positioned at 90-degree intervals along the centroid of the gas flow in a circular duct (or the equivalent in a rectangular duct) consisting of:

(1) a total particulate mass sample obtained using a standard EPA Method 5 or Method 17 sampling train at the isokinetic flowrate,

(2) IP samples obtained with the cyclone-impinger or cyclone-diluter train described above.

With respect to the sampling velocity, a reasonable compromise was judged to be operation at ± 20% of isokinetic using a fixed sampling rate and a set of 14 nozzles ranging from 2 to 20 mm in diameter in steps of 1.2 (20% diameter increase). This arrangement would allow ± 20% isokinetic rate sampling at 0.3 ℓ/sec and a gas velocity range of 1-100 m/sec, which would be expected to cover almost all stack-sampling situations.

Cascade impactors, cascade cyclones, diffusion-condensation nuclei counters, and electrical mobility analyzers would be used for detailed investigations of the in-stack aerosol (≤ 15 μm, without condensables).

For ambient work, it was suggested that more calibration of the new inlets to the hi-vol and dichotomous samplers was needed, in addition to the development of the lo-vol instrument mentioned above. In order to size particles up to 80 μm, particle collection by settling (dust fall) or a rotating impactor was considered practical, with microscopic analysis for sizing.

The ambient systems would also be used for sampling fugitive emissions, but in addition sampling strategy was noted to be a very important problem requiring strong emphasis. Also, the FAST equipment would require a new inlet. A horizontal elutriator was envisioned for this use.

Continued development and adaptation of the more complex data analysis techniques was seen as needed to ensure that the maximum amount of information would be obtained from the data.

Long-Term Research and Development--

It was recommended that long-term research activities should consist of refining and documenting the procedures that were developed in haste to make surveys of IP sources, developing standdardized methods for obtaining more detailed information, and performing specialized experiments to obtain data on unusual sources.

The techniques that were suggested for widespread application based on current technology are indicated in Table 3. Additional methods that might be used are given in Table 4.

In-stack sampling--It was recommended that a stack sampling system with dilution that simulates the cooling-dilution process in a plume be developed for measuring the particle-size distribution of the diluted aerosol after condensation occurs. This should be coupled to the development or refinement of a dynamic, theoretical model of aerosol behavior during cooling and dilution.

Standard hardware systems and procedures would need to be developed for measuring the particle-size distribution of the diluted aerosol.

For collecting samples for chemical analysis, cascade impactors were favored, although diffusion batteries and cyclones could also be used. In many instances, real-time data acquisition would be desired, and optical, diffusional, or electrical methods would have to be used. Optical counters would have to be calibrated for aerodynamic sizing, using cyclones or impactors on the inlet.

For measuring very large particles, up to 80 μm, a body impactor, consisting of a number of cylinders or rectangular areas of diminishing width, was considered most practical. The performance of the device would have to be determined, and sampling and analyzing procedures developed.

It was recognized that chemical analysis must be coupled with particle sizing in all sampling programs, and that these techniques required additional research.

It was also recognized that it would be possible to eliminate conflicting requirements for fixed flowrates and isokinetic

TABLE 4. SYSTEMS AVAILABLE FOR MEASURING PARTICLE SIZE AND MASS

Mass	Particle Size
Ambient Sampling	
Filter	Impactor
Hi-Vol	Hi-Vol
Other	Mega Vol
Piezoelectric	Other
Nephelometer	Dichotomous Sampler
Beta Gauge	Diffusion Battery
	Electrical Mobility Analyzer
	Optical Counter
	Piezoelectric
	Impactor
	Centrifuge
	Cyclone
	Centrifuge
Fugitive Sampling	
Filter	Filter
Hi-Vol	Hi-Vol
Other	Mega-Vol
Piezoelectric	Other
Nephelometer	Dichotomous Sampler
Beta Gauge	Diffusion Battery
Lidar	Electrical Mobility Analyzer
	Optical Counter
	Piezoelectric
	Impactor
	Centrifuge
	Cyclone
	Fugitive Assessment Sampling Train (FAST)
	Centrifuge
Stack Sampling	
Filter	Impactor
Charge Transfer	Cyclone
Beta Gauge	Optical Counter
Piezoelectric	Electrical Mobility Analyzer
Optical	
Transmissometer	
Lidar	
Other	

sampling if recirculation loops or variable inlets were used. Research on the practicality of both approaches was recommended.

Also recommended was the study of the errors associated with sampling IP matter in turbulent streams with nozzles of different sizes and at non-isokinetic flowables.

An adequate theory of cyclone performance under stack conditions was considered to be needed more than ever. Further application of advanced data analysis techniques, if not completed under the short-term study, were recommended for further investigation.

Ambient sampling--Continued refinement of the rotating impactor method for sampling large particles and advanced methods of data analysis were recommended for further study.

Real-time systems in mobile laboratories were recommended as an important means of characterizing emission sources. Mobile vans were viewed as more versatile than fixed sampling networks, and less expensive for a large survey program. It was noted that chemical analysis of particulate matter would be of great value in relating ambient aerosol compositions to stack emissions or non-stationary sources (especially for large particles) and suitable procedures would have to be established for incorporating the analyses into the survey program.

It was noted that research would be required to develop methods of sampling large particles accurately and for transposing real-time particle size and concentration data to an aerodynamic basis.

Fugitive emissions--It was suggested that in addition to the methods used in ambient sampling, techniques that employed remote sensing or balloon-lofted instruments might be especially applicable to sampling fugitive emissions. Here also, mobile laboratories would be valuable in characterizing fugitive emissions rapidly and efficiently.

An extensive research program was seen as needed to develop sampling strategies. Decisions would have to be made on how to sample in space and time, and on what meteorological data would be required. Statistical techniques and modelling would be used to optimize the procedures, and chemical analysis would help in discriminating between source and non-source aerosols.

Summary of Studies Completed

The remainder of this report summarizes the work that has been done at Southern Research Institute under contract with the EPA on the IP program. A list of the studies included in this report that originated from the recommendations described in the previous section is shown in Table 5. This table also lists the page number corresponding to the section of the report in which each topic is discussed. References to published information resulting from these studies are listed following the text.

TABLE 5. SUMMARY OF STUDIES THAT HAVE BEEN PERFORMED AT SOUTHERN RESEARCH INSTITUTE TOWARDS COMPLETION OF THE IP PROGRAM

	Page
Data handling methods for determination of inhalable particulate matter in previously obtained data	20
Isokinetic sampling by constant flowrate sizing devices	51
Evaluation of commercial cascade impactors and buttonhook nozzles - effects on measurement of inhalable particulate matter	74
The horizontal elutriator as an IP precollector	85
The FAST elutriator inlet	98
Calibration of available cyclones at stack conditions	105
An IP precollector cyclone	109
An IP cyclone train (D_{50} values 15 μm and 2.5 μm)	109
Calibration of a hi-vol sampler size-selective inlet	122
A stack dilution sampling system for measurement of condensation aerosols	122
Procedures for cascade impactor operation in process streams	140
Operation of the IP sampling system	140
Operation of the stack dilution sampling system	159

SECTION 2

DEVELOPMENT OF METHODS FOR SAMPLING AND DATA ANALYSIS

This section contains information on (1) a computer technique that allows the extrapolation of particle-size data from cascade impactors, and (2) techniques and devices for maintaining isokinetic sampling with particle-sizing equipment that is operated at constant flowrates.

DATA ANALYSIS FOR CASCADE IMPACTORS

Summary

Because of the increased interest in the health effects of particles up to 15 μm diameter, it has become desirable to accurately extrapolate particle-size data above the effective limit of the first stage D_{50} (approximately 10 μm) of a cascade impactor. To do this, a first-order osculating polynomial is used in conjunction with the Computer Impactor Data Reduction System[1] for fitting the cumulative mass curve between the first stage D_{50} and the maximum particle size. The function is a third degree polynomial which uses the known characteristics of the cumulative mass curve for its solution over the range of particle sizes. Tests of this technique on a number of theoretical unimodal and bimodal size distributions demonstrate a high degree of accuracy in recovering the true cumulative particle concentration up to 15 μm. This technique, as described below, can be used for recovering inhalable particulate concentrations from existing impactor data within a factor of about 3 if no information is available on the type of nozzle or precollector that was used. If the effects of these devices are known, the errors in the IP data are probably within the experimental error of sampling.

Further testing of the data reduction technique is recommended to evaluate the effect on its accuracy of random errors in the measured size distribution.

Previous CIDRS

EPA Report 600/7-78-042, "A Computer-Based Impactor Data Reduction System"[1] described a series of five computer programs, known by the acronym CIDRS, which are designed to reduce the field data taken by commercially available round jet cascade impactors. An outline of the CIDRS programs is illustrated in Table 6 with a listing of the program names and their functions.

In brief, the sampling hardware information, sampling conditions, and particulate catch information are used as input to CIDRS to determine effective cut sizes of the various impactor stages and the particle concentration at each of these stages. This cumulative mass concentration $<D_{50}$ vs. D_{50} is fitted by a set of continuous, modified spline curves. The mass and number size distributions may also be found from the derivative of this cumulative mass concentration curve. Since both the cumulative mass concentration curve and its first derivative are continuous, averaging of cumulative mass concentrations and mass size distributions over many runs is possible. This is done independently of stage D_{50} and stage geometric mean diameters. The averaged mass size distribution values, respective particle sizes, and upper and lower 50% confidence limits are stored in files. A separate file for inlet and outlet data is kept in this manner so that, on the final program execution, penetration-efficiency fractions and confidence limits are calculated at the various particle sizes. Both tabular and graphical outputs are produced at each of the data reduction levels described.

The curve fit to the cumulative mass distribution is a critical point in this data reduction system. After the fit is made in program SPLIN1, the stage by stage values of cumulative mass, the D_{50}'s, the stage values of $\Delta M/\Delta \log D$, and the geometric mean diameters are ignored. Averaging and penetration-efficiency calculations are based strictly on the fitting coefficients as stored by SPLIN1 execution.

The method of fitting used in SPLIN1 is a graphical technique, or a "programmed French curve". The $\log_{10}$ (cumulative mass concentration) vs. $\log_{10}$ (D_{50}) points are input to SPLIN1 as illustrated in Figure 3. Then a parabola is fitted to each set of three consecutive cumulative mass points. As shown in Figures 4 through 6, interpolated points are defined at equal log diameter intervals between the first two of each set of three D_{50}'s. (A parabola having a negative first derivative in this interpolation area is overridden by a straight line between the two D_{50}'s to ensure a continuously increasing cumulative mass curve.) The final interpolation parabola (Figure 7) is fitted through the second D_{50}, first D_{50}, and maximum particle size DMAX.

In the original version of SPLIN1, a hyperbolic function of the form

$$M = a_1 + \frac{a_2}{\log D} \qquad (1)$$

TABLE 6. CIDRS PROGRAMS AND OUTPUT

MPROG

Cumulative Mass Concentration $<D_{50}$
Cumulative % Mass Concentration $<D_{50}$
$\Delta M/\Delta \text{Log } D$ vs. GMD
$\Delta N/\Delta \text{Log}$ vs. GMD

SPLIN1

Fitting Coefficients to Generated Set of Cumulative Mass Concentration Points.

GRAPH

Cumulative Mass Concentration
Cumulative % Mass Concentration
Mass vs. Particle-size Distribution
Number vs. Particle-size Distribution

STATIS

Averages With Confidence Bars	Cumulative Mass Concentration Cumulative % Mass Concentration Mass vs. Particle-size Distribution Number vs. Particle-size Distribution

PENTRA OR PENLOG

Percent Penetration-efficiency vs. Particle Size with Confidence Bars

is used to define the interpolation points between the first D_{50} and DMAX where M is the mass concentration (mg/am^3) less than particle diameter D(μm) and a_1 and a_2 are constants. Seven equally log-spaced interpolated points are defined over this broad particle range. The hyperbolic function as used for point interpolation is illustrated in Figure 8.

Proposed CIDRS

The function which is proposed to replace the hyperbola, a third-degree polynomial of first-order osculation, is the subject of the remainder of this section. Such a function, used to interpolate points between the first stage D_{50} and the maximum particle diameter, is illustrated in Figure 9. Note that as

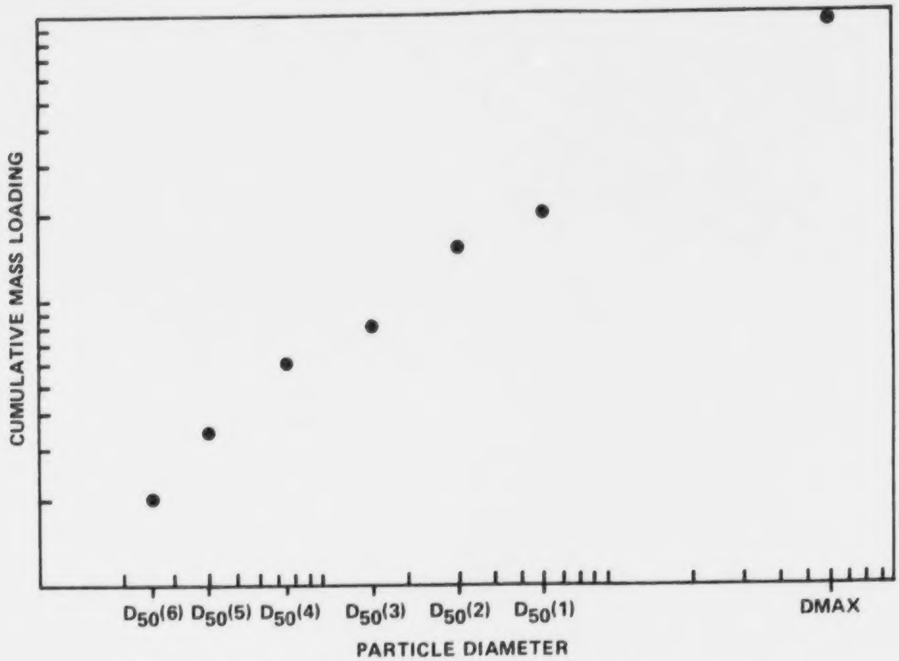

Figure 3. Cumulative size distribution from raw impactor data.

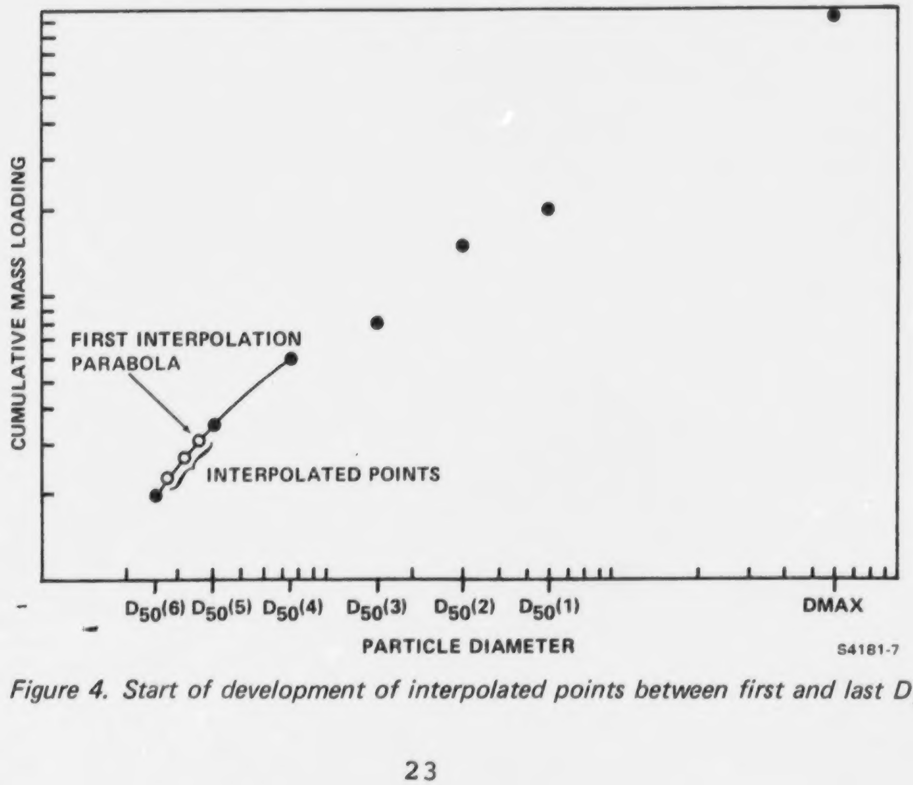

Figure 4. Start of development of interpolated points between first and last D_{50}.

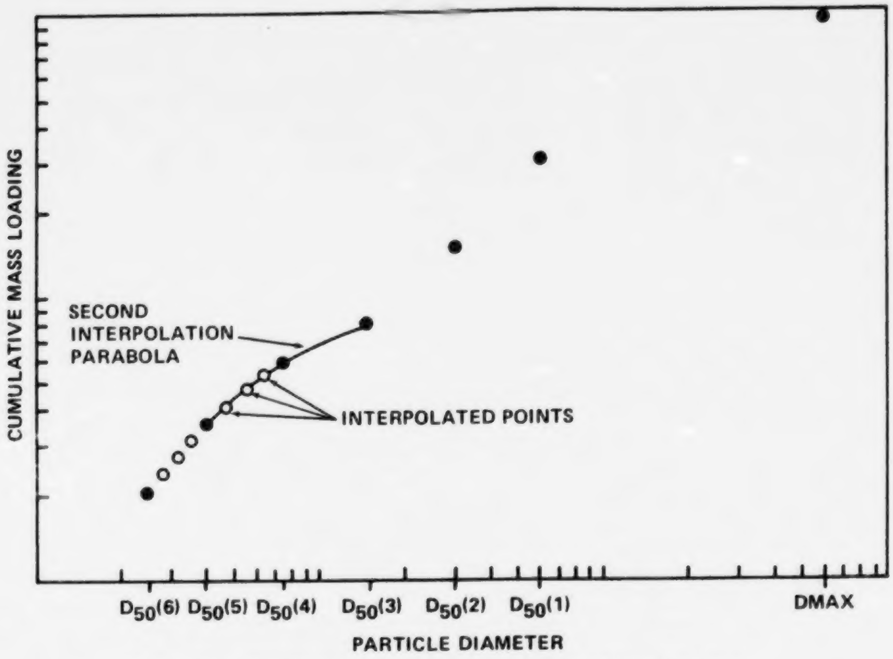

Figure 5. Continued generation of interpolated points

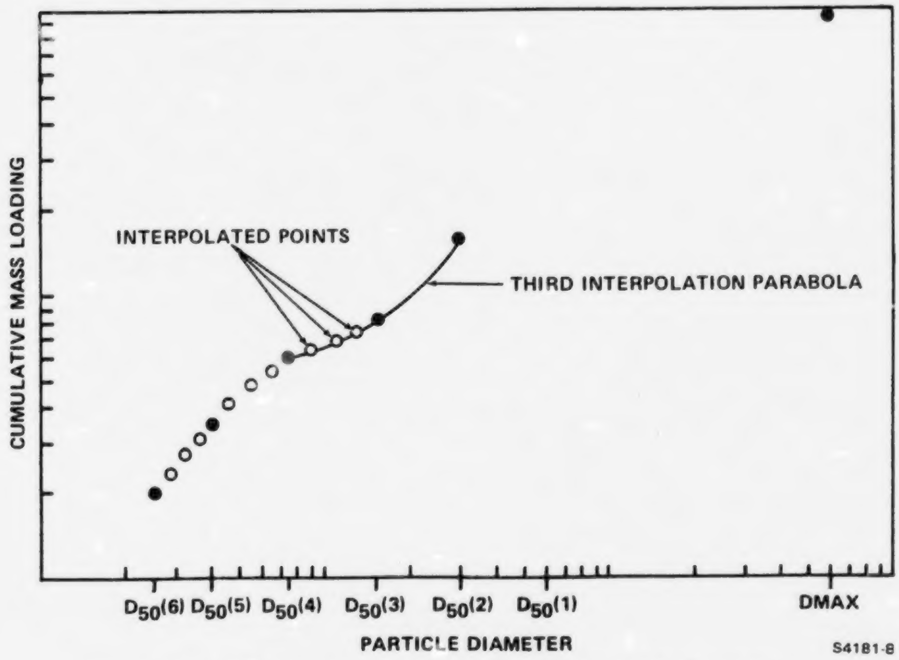

Figure 6. Continued generation of interpolated points

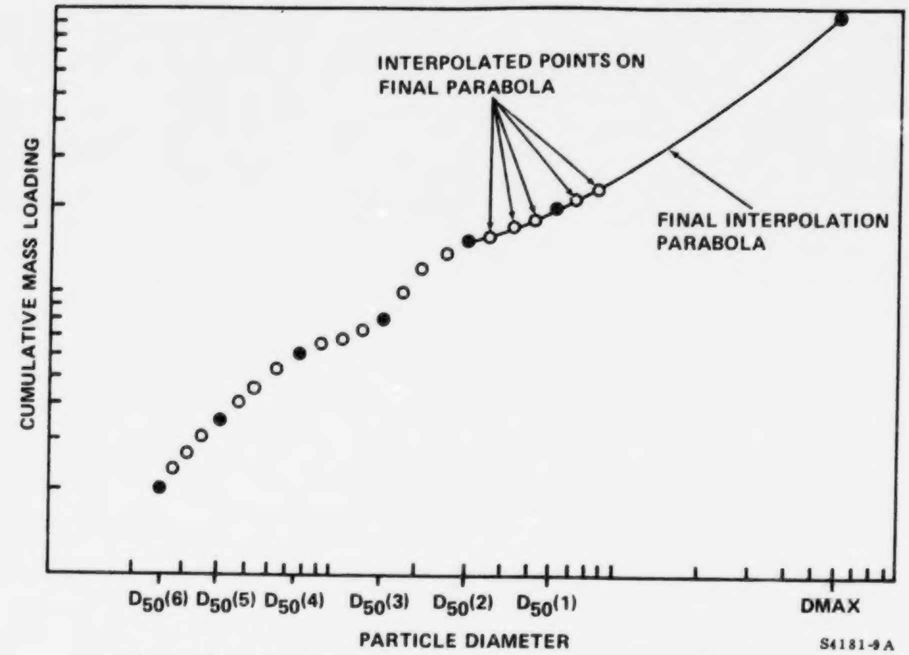

Figure 7. Generation of interpolated points on parabola which includes DMAX.

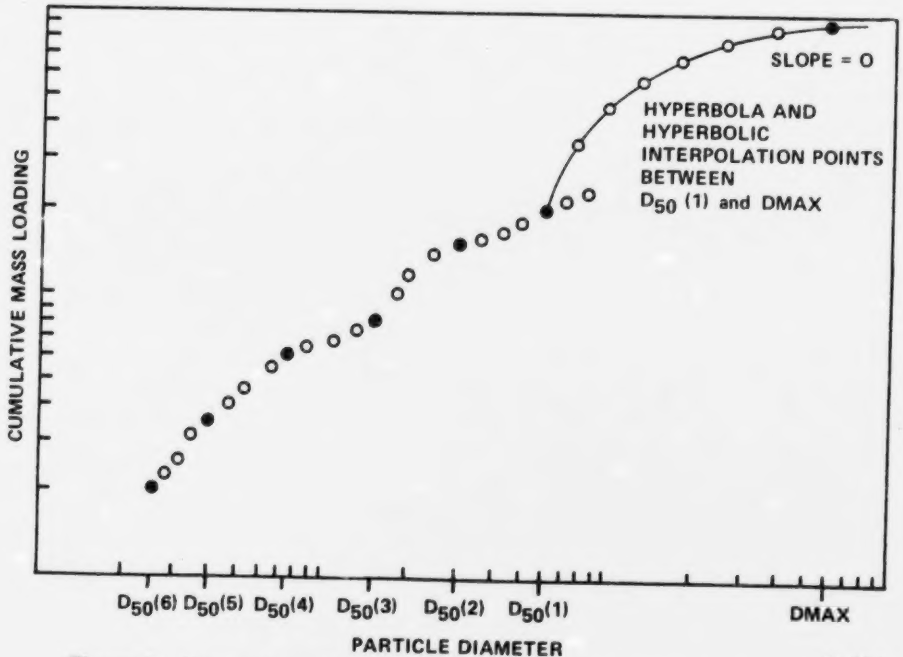

Figure 8. Generation of interpolated points on hyperbola through $D_{50}(1)$ and DMAX.

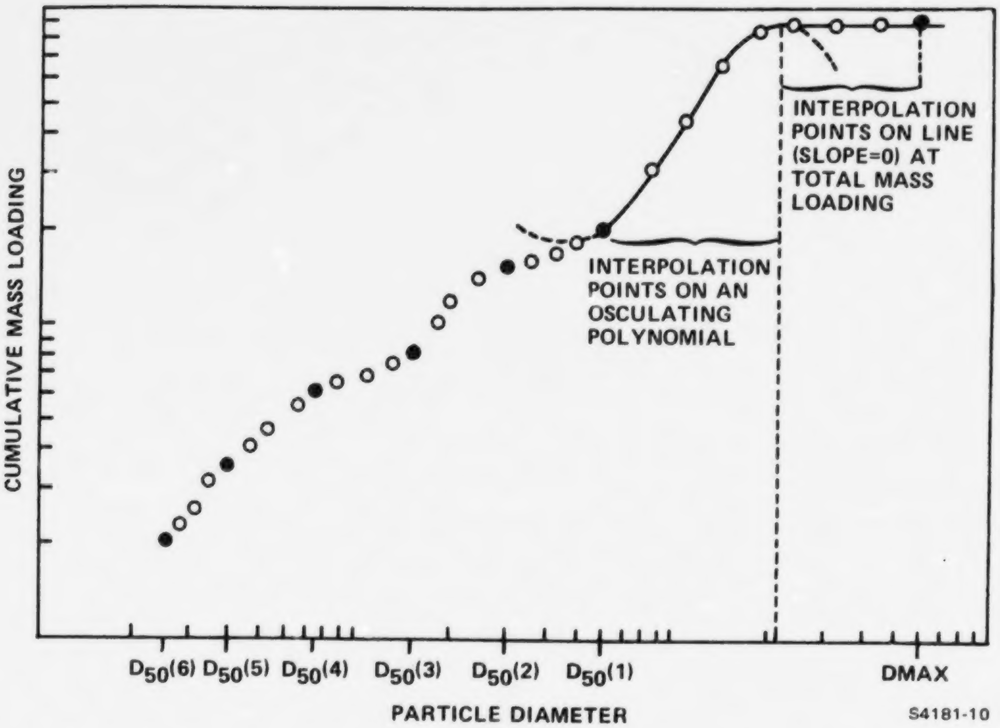

Figure 9. Generation of interpolated points on osculating polynomial and zero slope line at total mass concentration.

the osculating polynomial approaches the total mass loading, its first derivative goes to zero. For log diameters greater than this zero slope point (ZSPT) the cumulative mass loading is at its total value. The functional form of the osculating polynominal is discussed below. Its importance lies in the fact that it is a better suited function than the hyperbola for recovering the inhalable particulate matter, i.e., cumulative mass concentration <15.0 µm which lies in this fitting region beyond the first stage D_{50} (~10.0 µm).

The set of interpolated points and original D_{50} points is used in fitting a series of continuous, second-degree polynomials. The fitting coefficients along with their boundary points (the set of cumulative mass concentration vs. particle size used in making the fit) are stored in files. Using these coefficients, the cumulative mass curve and the mass and number size distribution curves may be recovered for use in any subsequent program.

Extending Accuracy in the Mass Size Distribution Calculated Beyond the First Stage D_{50}

CIDRS has proven to be an accurate and time saving tool for impactor data reduction over the size region of approximately 0.25 μm up to 10 μm or the first stage D_{50}.[2] Because of the present construction of cascade impactors, there is a large span of particle size in the distribution. Since an extrapolation to 15.0 μm extends the data only slightly beyond the first stage D_{50}, calculating IP mass concentration appears feasible if proper extrapolation techniques are used.

The known or obtainable properties of the distribution are:

(1) The first (largest) D_{50} is known.
(2) The cumulative mass at the first D_{50} is known.
(3) The slope of the cumulative mass curve at this D_{50} can be calculated.
(4) The largest particle diameter is known or can be estimated.
(5) The total cumulative mass at the largest particle diameter is known.
(6) The first derivative of the cumulative mass curve at the largest particle diameter = 0.0.
(7) The first derivative of the cumulative mass distribution is non-negative.

As mentioned previously, the function that has been used in CIDRS for fitting data beyond the first stage D_{50} has been a hyperbola of the form given in Equation 1.

Properties 1, 2, 4, and 5 are automatically satisfied by this two point fit (Equation 1). In addition, the form of the hyperbolic function generates a close approximation to properties 6 and 7 in that the slope of this function for real data is never negative and approaches zero at large D.

However, the hyperbolic function has drawbacks which limit its usefulness for extrapolation to inhalable particle sizes above the first stage D_{50}. First, property 6 is never rigorously satisfied. While the slope of the hyperbolic function approaches zero for large values of the maximum particle size, it will not be zero for a finite maximum particle size as is required. More seriously, there is no correlation between the slope of the hyperbola at the first stage D_{50} and the slope determined by the spline fitting routine. This discontinuity in slope violates property 3 of the true cumulative mass distribution and thus the hyperbolic function will not define proper mass concentrations for diameters slightly above the first stage D_{50}.

The Osculating Polynomial

The new technique employs a polynomial of first-order osculation to fit cumulative mass concentration from the first stage D_{50} to the maximum particle size.[3] It not only passes through the two end points, but also may be constructed to have zero slope at the maximum particle size and have a slope at the first stage D_{50} equal to that of the spline fit through the first stage D_{50}. The osculating polynomial may also be constrained to have a non-negative slope over the specified range of particle sizes. In other words, all seven of the known or obtainable properties of the mass distribution in this particle range can be satisfied by the proposed technique.

A polynomial of first-order osculation is used as an approximation to a given function. By definition it matches both the function and its first derivatives at a finite number of points. In general, there exists a unique (2n-1) degree polynomial fit to a set of n points. For the case of impactor data, let particle diameter be represented by the variable D, the cumulative mass loading by M(D), and the osculating polynomial approximation of this function by P(D); then properties 1-6 require

$$P(D_i) = M(D_i), \text{ and } P'(D_i) = M'(D_i) \tag{2}$$

for i = 0, 1 where the first point corresponds to the first stage D_{50} and the second to the maximum particle diameter. For the approximating equation to be physically realistic it is also necessary that property 7 be satisfied, therefore

$$P'(D) \geq 0 \text{ for } D_0 \leq D \leq D_1. \tag{3}$$

To first order osculation, the polynomial P(D) can be described by Hermite's formula,[3]

$$P(D) = \sum_{i=0}^{n} U_i(D)M(D_i) + \sum_{i=0}^{n} V_i(D)M'(D_i) \tag{4}$$

where $M(D_i)$ and $M'(D_i)$ are the known values of mass concentration and its derivatives at D_0 and D_1; thus n has values of 0 and 1 only. The functions $U_i(D)$ and $V_i(D)$ can be expressed in terms of the Lagrange multipliers $L_i(D)$ and their derivatives $L_i'(D)$ such that

$$U_i(D) = \left[1-2L_i'(D_i)\ (D-D_i)\right] \left[L_i(D)\right]^2 \tag{5}$$

$$V_i(D) = (D-D_i)\left[L_i(D)\right]^2 \tag{6}$$

where

$$L_i(D) = \prod_{\substack{j=0\\ j\neq i}}^{n} \frac{(D-D_j)}{(D_i-D_j)} \qquad i = 0,1,2,----,n. \tag{7}$$

For the two points i = 0, i = 1 we have from Equation 7

$$L_0(D) = \frac{D - D_1}{D_0 - D_1} \tag{8}$$

$$L_1(D) = \frac{D - D_0}{D_1 - D_0} \tag{9}$$

and their derivatives are

$$L_0'(D) = \frac{1}{D_0 - D_1} \tag{10}$$

$$L_1'(D) = \frac{1}{D_1 - D_0}\;. \tag{11}$$

For the points i = 0, i = 1 Equation 4 becomes

$$P(D) = U_0(D)M(D_0) + U_1(D)M(D_1) + V_0(D)M'(D_0) + V_1(D)M'(D_1). \tag{12}$$

Combining Equations 5 and 6 with 8, 9, 10, and 11, the osculating polynomial then becomes

$$P(D) = \left[1 - \frac{2(D - D_0)}{(D_0 - D_1)}\right]\left[\frac{D - D}{D_0 - D_1}\right]^2 M(D_0)$$

$$+\left[1 - \frac{2(D - D_1)}{(D_1 - D_0)}\right]\left[\frac{D - D_0}{D_1 - D_0}\right]^2 M(D_1)$$

$$+ \left[\frac{(D - D_0)\ (D - D_1)^2\ M'(D_0)}{(D_0 - D_1)^2}\right]$$

$$+ \left[\frac{(D - D_1)\ (D - D_0)^2\ M'(D_1)}{(D_1 - D_0)^2}\right] . \tag{13}$$

Equation 13 can be put into a simpler form by defining the following constants:

$$k_1 = \frac{M(D_0)}{(D_0 - D_1)^2}\ ,\ k_2 = -\frac{2M(D_0)}{(D_0 - D_1)^3}\ ,\ k_3 = \frac{M(D_1)}{(D_1 - D_0)^2}$$

$$k_4 = -\frac{2M(D_1)}{(D_1 - D_0)^3}\ ,\ k_5 = \frac{M'(D_0)}{(D_0 - D_1)^2}\ ,\ k_6 = \frac{M'(D_1)}{(D_1 - D_0)^2} . \tag{14}$$

$$a_1 = k_2 + k_4 + k_5 + k_6$$

$$a_2 = [k_1 + k_3 - (2D_1 + D_0)(k_2 + k_5) - (2D_0 + D_1)(k_4 + k_6)]$$

$$a_3 = [(k_2 + k_5)(D_1^2 + 2D_0D_1) + (k_4 + k_6)(D_0^2 + 2D_0D_1) - 2k_1D_1 - 2k_3D_0]$$

$$a_4 = [k_1D_1^2 + k_3D_0^2 - D_0D_1^2(k_2 + k_5) - D_0^2D_1(k_4 + k_6)] .$$

In terms of these constants, the first order osculating polynomial can be written as a cubic equation in particle diameter D such that

$$P(D) = a_1D^3 + a_2D^2 + a_3D + a_4 \tag{15}$$

and its first derivative is

$$P'(D) = 3a_1D^2 + 2a_2D + a_3. \tag{16}$$

Property 7 above for impactor data limits the acceptable solutions to 15 and 16 to those for which

$$P'(D) \geq 0, \; D_0 \leq D \leq D_1. \tag{17}$$

For some combinations of impactor data, particularly those for which the slope $M'(D_0)$ of the cumulative mass distribution at the first D_{50} is large, property 7 places an upper limit on the range (D_0 to D_1) of permissible particle diameters. For those cases, physically acceptable solutions can be found for a reduced range of particle diameters wherein the maximum size is somewhat smaller than the original D_1 or assumed maximum particle size. Figure 10 illustrates this. The first fitting osculating polynomial has the proper cumulative mass loading value at the first D_{50} and at the maximum particle diameter. The first derivative of the function at these two particle sizes is also correct, i.e., the first derivative of the osculating polynomial with respect to log diameter is the same as that for the spline fit at the first D_{50} and is zero at the maximum particle size. However, since the osculating polynomial does have negative first derivative values for $D_0 \leq D \leq D_1$ (where D_1 here equals DMAX), the D_1 is "stepped" to a smaller value, and a second osculating polynomial is fitted. This second osculating polynomial is then tested for negative first derivative values for $D_0 \leq D \leq D_1$. The particle size D_1 continues to be redefined at smaller values, and the osculating polynomial is fitted between D_0 and D_1 until D_1 is defined at a critical value such that there are no negative derivatives over the tested particle size range for the osculating polynomial. D_1, renamed "zero slope point", ZSPT, marks the maximum of the osculating polynomial at the total cumulative mass loading. As illustrated in Figure 9, interpolation points for the cumulative mass distribution are then defined along the osculating polynomial for $D_{50}(1) \leq D \leq \text{ZSPT}$ and are defined as the total cumulative mass loading for $\text{ZSPT} \leq D \leq \text{DMAX}$.

Accuracy of the Extrapolation Technique

In order to have confidence in the value of the particulate concentration consisting of particles smaller than 15.0 μm as derived from a set of impactor data, one must be assured that the curve fitted to impactor data is a correct fit and that any extrapolation is reasonable. In order to test the "applicability" of the osculating polynomial for generating a cumulative mass distribution beyond approximately 10.0 μm, a theoretical mass distribution was assumed. The distribution was fitted with the proposed technique, and the recovered distribution was examined. For this purpose, both unimodal and bimodal distributions were theoretically sampled and the resulting data reduced using the CIDRS programs. The recovered distributions were then compared to the original, theoretical distribution. The characteristics

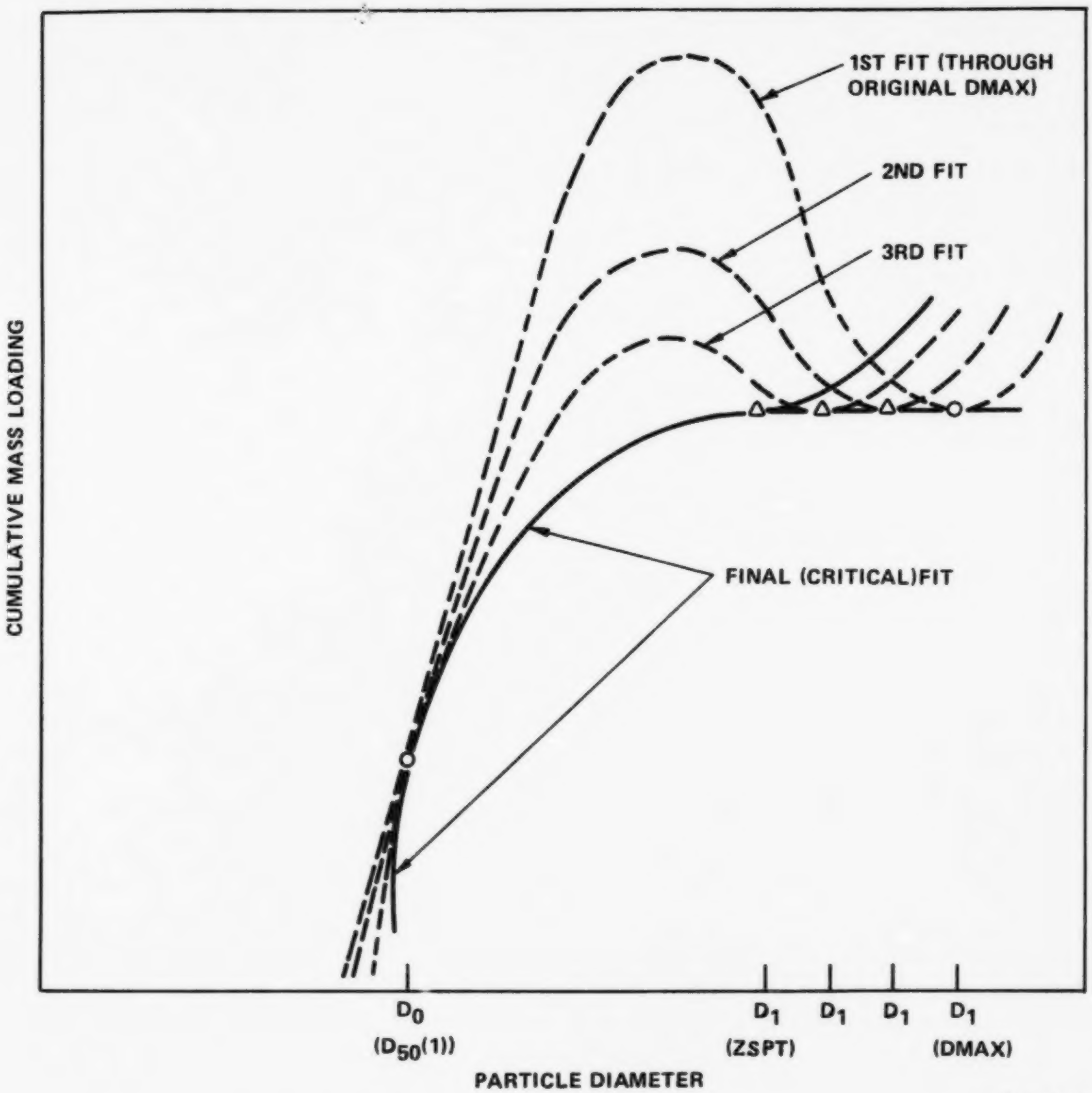

S4181-11 A

Figure 10. Fitting the cumulative mass distribution for $D(1) < D < DMAX$ using a first-order osculating polynomial $P(D)$. The maximum diameter of the fitting function, D_1, is decreased until a critical fit is obtained with $P'D \geq 0$ for $D_0 < D < D_1$.

of the particulate distribution which were individually varied were the mass median diameter MMD, the geometric standard deviation σ_g, and for bimodal size distributions, the fractional distribution of mass in each mode. Also varied were the assumed largest particle diameter DMAX and the geometric standard deviation of the stage efficiency curves σ_{gs}. Since there were no experimental errors or uncertainties, the size distributions calculated from the modified CIDRS program are a true test of the extrapolation technique.

Testing with Unimodal Particle-size Distributions

For unimodal testing a log-normal size distribution was used with MMD = 5.0 μm and σ_g = 2.5 unless otherwise specified in the text. Also, unless otherwise specified in the text, DMAX was input as 100.0 μm, and the masses were collected using log-normal stage efficiency curves with σ_{gs} value of 1.06 to simulate impactor behavior using greased substrates, and with a σ_{gs} of 1.3 to simulate impactor behavior using glass fiber substrates.

Variation of the Particulate Mass Median Diameter--

The polynomial used in conjunction with the modified spline technique in CIDRS shows a high degree of accuracy in recovering the cumulative inhalable particulate concentration (<15.0 μm) for a wide range of MMD values. Figure 11 illustrates this with a plot of the ratio of the recovered inhalable particulate to the true inhalable particulate, IP_R/IP_T, vs. MMD for stage efficiency curves with σ_{gs} values of 1.3 and 1.06. For MMD's of 1.0, 2.0, 5.0, 10.0, and 20.0 μm, the recovery is near a perfect 1.00 except at one point. For σ_{gs} of 1.3 the IP_R/IP_T ratio is at its highest value of 1.06 at an MMD of 20.0 μm. This greater error in IP recovery may be caused by assuming a largest particle diameter (100.0 μm here) which is too small with respect to the 20.0 μm MMD.

Variation of the Geometric Standard Deviation of the Particulate Size Distribution--

To test the sensitivity of this fitting technique to different values of the aerosol geometric standard deviation, σ_g, unimodal particle-size distributions having σ_g values of 1.5 to 3.5 were tested. Figure 12 shows the ratio of recovered over true inhalable particulate IP_R/IP_T vs. these values of σ_g for stages having collection curves with geometric standard deviations of 1.3 and 1.06. The technique shows good accuracy in recovering the true IP concentration. The highest ratio value here is 1.04 and a relatively sharp mass distribution with standard deviation of 1.5. The accuracy increases as the particle-size distribution broadens.

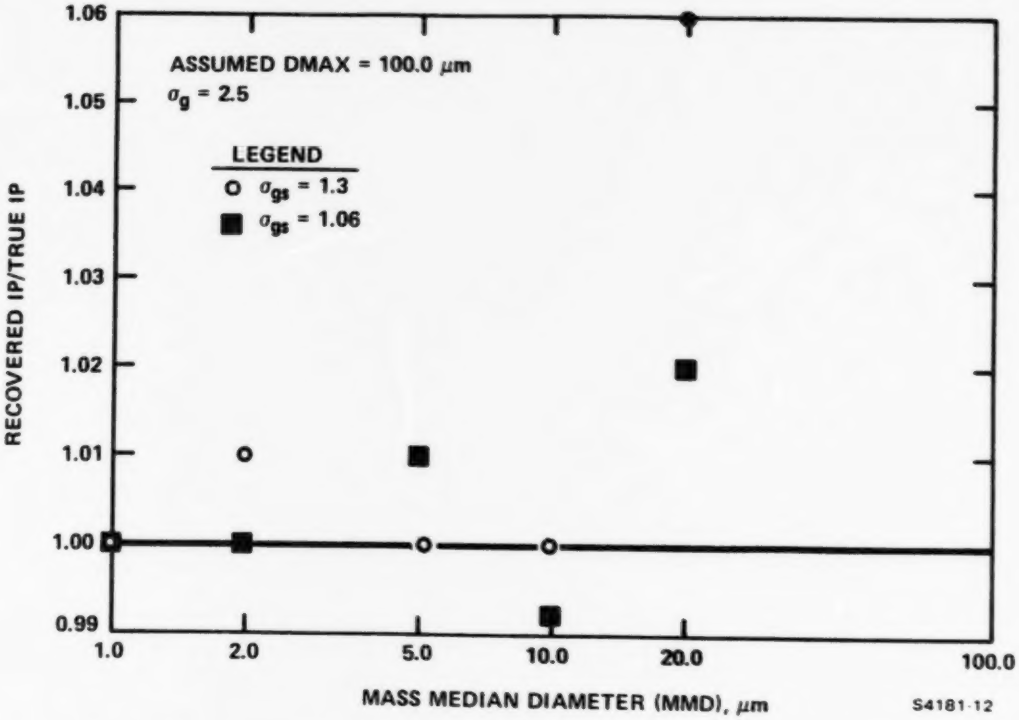

Figure 11. Ratio of recovered to true IP concentration versus mass median diameter of a unimodal log-normal particle-size distribution.

Variation of the Geometric Standard Deviation (Slope) of the Collection Efficiency Curve--

The geometric standard deviation of the collection efficiency curve of the sampler, σ_{gs}, ranges from a near perfect cut value of 1.01 to 1.7 in this test. As shown in Figure 13 the variation of σ_g has little effect on an accurate recovery of the inhalable particle concentration. The maximum error for IP recovery occurs for a sampler efficiency σ_{gs} of 1.01. Here the recovered over true inhalable particulate ratio, IP_R/IP_T, is only 1.02.

Variation of the Assumed Largest Particle Diameter in the Distribution--

In this test the assumed largest particle diameter, DMAX, is varied from 20.0 μm up to 999.0 μm for the same unimodal log-normal size distribution. The results, as seen in Figure 14, show

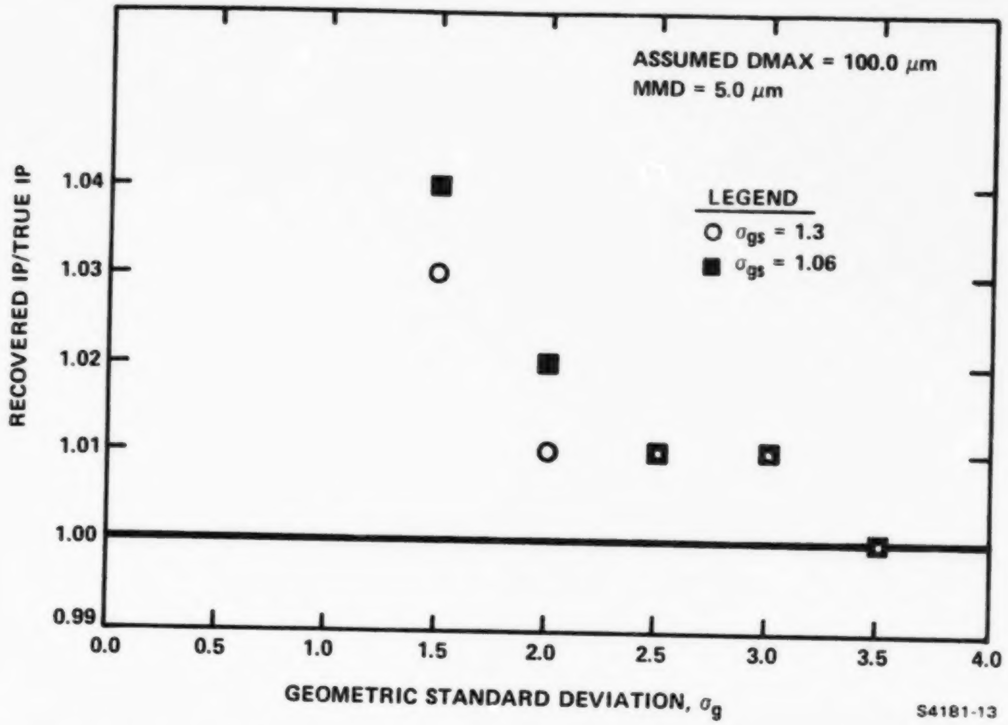

Figure 12. *Ratio of recovered to true IP concentration versus aerosol geometric standard deviation of a unimodal log-normal particle-size distribution.*

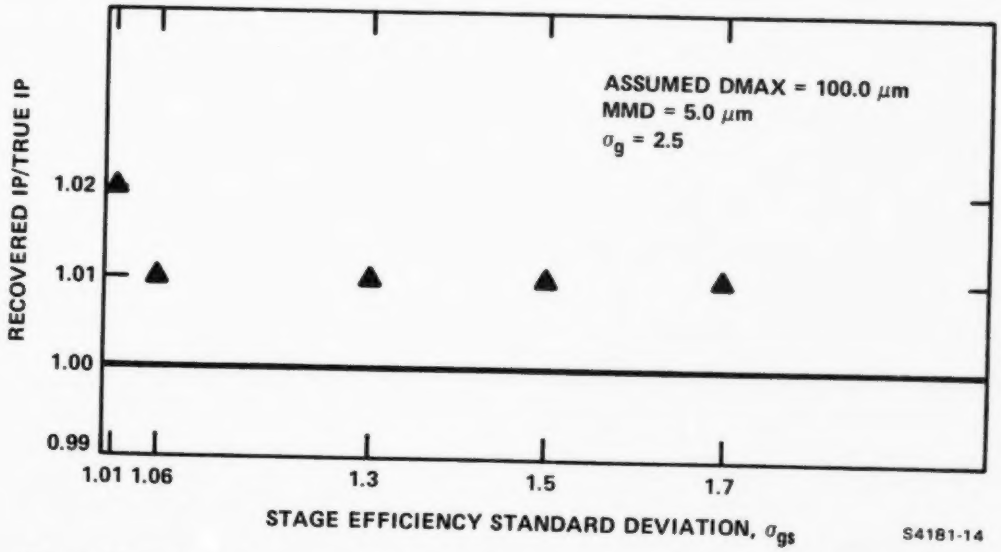

Figure 13. *Ratio of recovered to true IP concentration versus stage efficiency standard deviation using a unimodal log-normal particle-size distribution.*

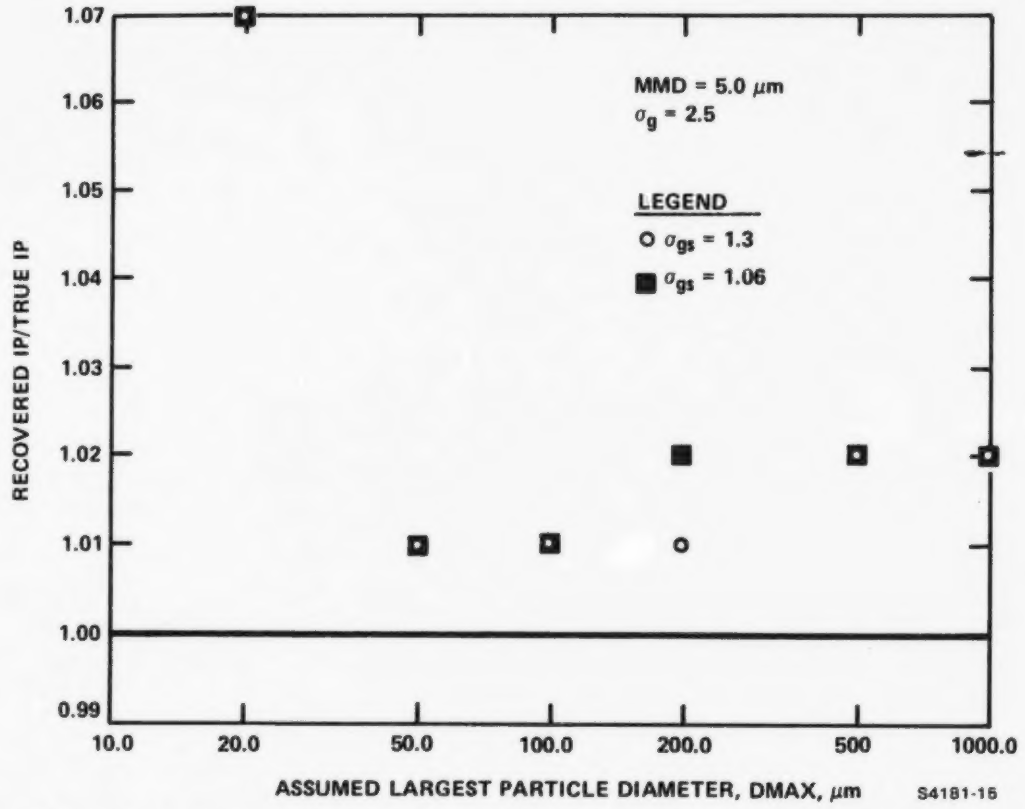

Figure 14. *Ratio of recovered to true IP concentration versus assumed largest particle diameter using a unimodal log-normal particle-size distribution.*

that accurate IP recovery is relatively insensitive to assumed DMAX unless it is extremely under-valued. In this distribution the ratio of recovered to true inhalable particulate IP_R/IP_T has its highest values of 1.07 (for σ_{gs} = 1.06) and 1.06 (for σ_{gs} = 1.3) for an assumed DMAX of 20.0 μm. However, for this size distribution having a mass median diameter of 5.0 μm, an assumed DMAX of 20.0 μm is unreasonably low. The other IP_R/IP_T values are on the order of 1.01 to 1.02. It is concluded then that only an extremely low guess of DMAX might cause large errors in IP recovery. This data reduction method still produces good IP recovery if the assumed DMAX is over approximated.

Testing with Bimodal Particle-size Distributions

For bimodal testing a log-normal size distribution is used having mass median diameters of 2.0 μm (MMD_1) and 15.0 μm (MMD_2) and geometric standard deviations, σ_{g_1} and σ_{g_2}, of 2.0 for each mode unless otherwise specified in the text. As in unimodal testing the masses are collected using stage efficiency standard deviations, σ_{gs}, of both 1.06 and 1.3 to simulate greased substrates and glass fiber substrates, respectively. Also, unless otherwise specified, the assumed largest particle diameter, DMAX, is input as 100.0 μm, and there is an equal contribution of mass from each of the two modes.

Variation of Geometric Standard Deviation of the Particle-size Distribution--

In this test, the geometric standard deviations of each mode of the particle-size distribution, σ_{g_1} and σ_{g_2}, were varied from 1.5 to 3.0. As seen in Figure 15, the recovery of inhalable particulate appears more sensitive to this change of parameter than any other test. For a stage efficiency σ_{gs} of 1.06, the recovered IP is as much as 14% low for a distinctly bimodal distribution where geometric standard deviations $\sigma_{g_1} = \sigma_{g_2} = 1.5$. As the modes broaden, the recovered to true inhalable particulate ratio IP_R/IP_T approaches 1.0. This should be expected since the degree of curvature decreases in the cumulative mass distribution as these modes broaden; i.e., the distribution becomes more unimodal and the spline fitting technique must make less drastic attempts to adjust to curvature.

Variation of the Mass Median Diameter of the Second Mode--

As seen in Figure 16, variation of the mass median diameter of the second mode, MMD_2, has little effect on the accuracy of IP recovery. The recovered to true inhalable particulate ratio, IP_R/IP_T, remains at or less than 1.05 as the MMD_2 ranges from

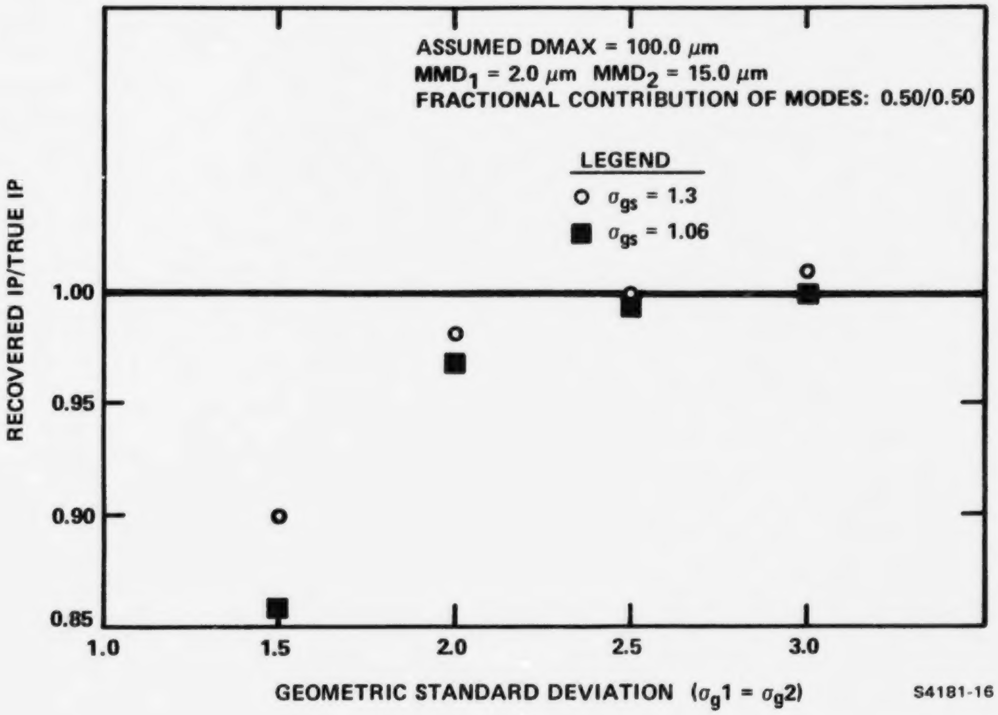

Figure 15. Ratio of recovered to true IP concentration versus aerosol geometric standard deviation of a bimodal log-normal mass distribution.

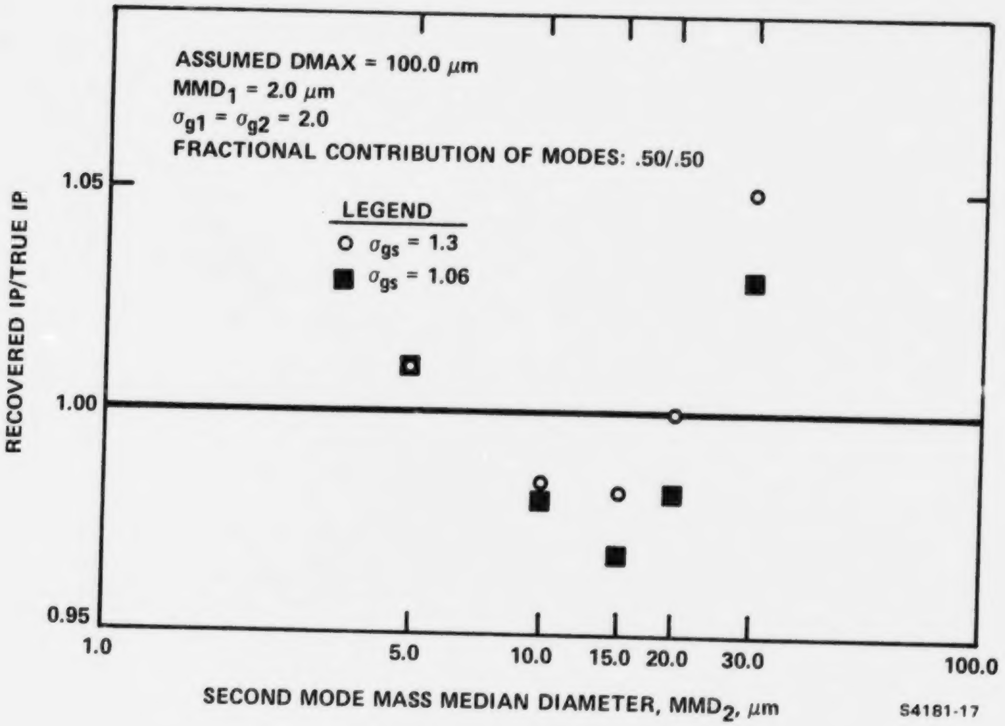

Figure 16. Ratio of recovered to true inhalable particle concentration versus second mode mass median diameter of a bimodal log-normal particle-size distribution.

5.0 to 30.0 μm. The highest value of IP_R/IP_T of 1.05 occurs for an MMD of 30.0 μm. This may be attributed to the large amount of mass in the second mode which falls beyond the first D_{50}.

Variation in Fraction of the Total Mass Contained in Each of the Modes--

In this test the ratio of mass contributed by each of the two modes in the bimodal distribution was varied. Beginning with a 25% contribution of mass in the first mode and a 75% contribution of mass in the second mode, the ratio was changed on each trial with a greater fraction of mass being contributed by the first mode in each successive trial. Figure 17 shows that the recovery of inhalable particulate less than 15.0 μm of this bimodal distribution is acceptable regardless of the ratio of modes. The ratio of recovered to true inhalable particulate IP_R/IP_T is at its lowest value of 0.931 for glass fiber substrates where the ratio of first mode mass to second mode mass is 0.25/0.75. As mass becomes less concentrated at sizes greater than the first stage D_{50}, i.e., as the mass mode ratio approaches 0.75/0.25, IP_R/IP_T approaches a perfect 1.00.

Effect of Operating Problems--

Further tests were conducted in an attempt to estimate the effect of operating problems. Some questions that might arise are: (1) were the impactors properly calibrated and operated? (2) was the largest particle diameter known? and (3) was a buttonhook nozzle or improperly calibrated cyclone precollector used?

Although it is not possible to determine exactly how large the errors are that might be introduced by the three parameters mentioned above, it is possible to determine the sensitivity of the calculated IP concentration to them, and thus establish probable bounds for the errors.

For the sensitivity tests, data from two sources were chosen. One was a coal-fired power plant and the other a cement kiln. Both sources employed electrostatic precipitators as pollution control devices.

Size distributions were calculated for the aerosols at the control device inlet and outlet at each source using theoretical stage constants and constants determined at Southern Research Institute by calibration. A range of values for DMAX was used. It was further assumed that the first, and possibly the second, stages of the impactors were interfered with by collection in a buttonhook nozzle or improperly calibrated cyclone. To eliminate the latter as an interference, the extrapolation was started from the second and third stages, ignoring the first or second as appropriate. This of course, results in a loss of resolution as a compromise to eliminate possible errors.

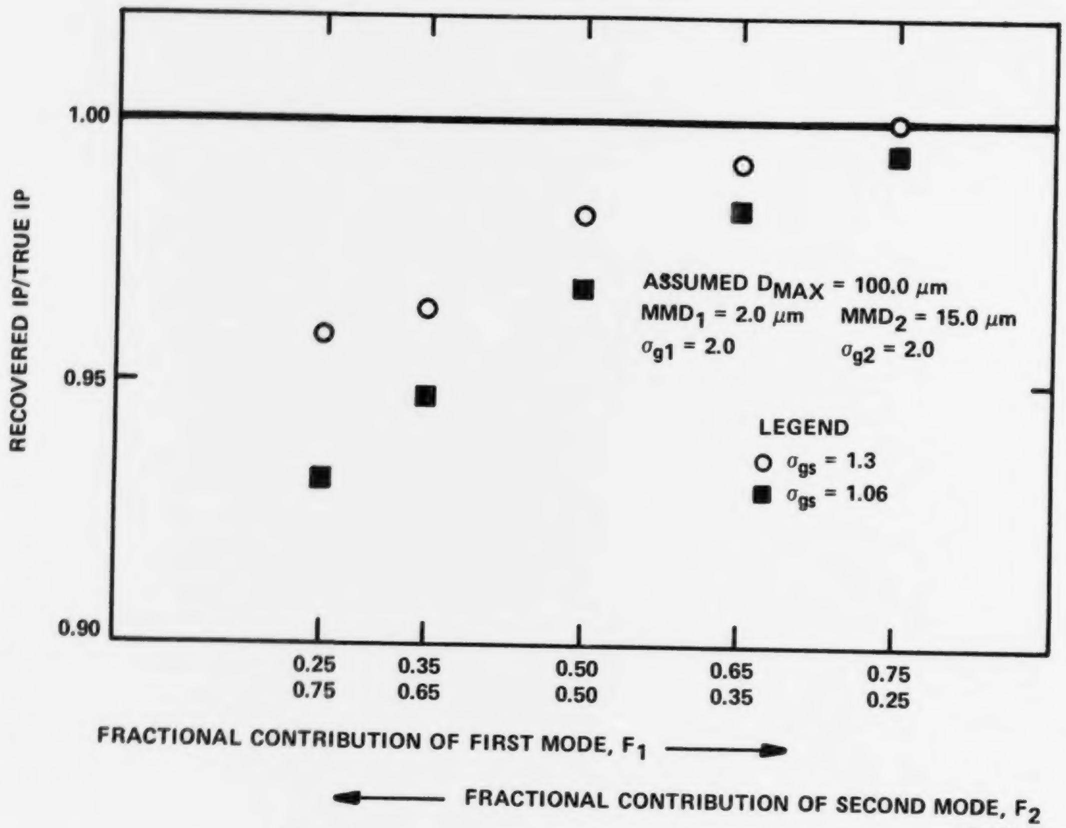

Figure 17. *Ratio of recovered to true IP concentration versus fractional contribution of mass from each mode of a bimodal log-normal mass distribution.*

Figures 18-21 are typical results from the study. In this series of graphs, impactor stage constants determined by calibration at Southern Research Institute were used for the impactors and the DMAX was chosen to be 100 μm at the inlet and 20 μm for the aerosols at the outlet of the precipitator. As shown, extrapolations were made from the 1st, 2nd, and 3rd D_{50}'s of the impactors.

Similar tests were made with theoretical impactor stage constants, and a range of DMAX. In all tests, the variations in calculated IP are less at the control device outlet than the inlet as the parameters are changed, as expected.

Figures 22-25 summarize the results from the sensitivity/accuracy analysis. In these figures the calculated IP concentration is plotted versus the assumed largest particle diameter. Data are shown for uncalibrated impactors, calibrated impactors, and with the first and second D_{50}'s omitted from the curve fit. Although these results are also source specific to some extent, the emissions from coal-fired boilers and cement kilns are quite different and allow some estimate of the variation from source to source.

Referring to Figure 22, note that the difference between the IP concentrations calculated assuming calibrated and uncalibrated impactors is small. However, omitting the first stage, or first two stages, from the fit makes a large difference. It can be seen here, as in the theoretical challenge, that the choice of DMAX does not introduce large errors.

In Figure 23, outlet data of the same size are treated. Since there is little mass above the largest D_{50}, the calculated IP concentration is rather insensitive to all of the test parameters.

Data taken at a cement kiln are shown in Figures 24 and 25. Since this source has a much larger size distribution it is not surprising to see a stronger variation in the calculated IP concentration at the inlet to the precipitator, as the parameters are changed. At the outlet, there is little variation in the calculated IP concentration because the control device removes most of the larger particles.

The results of this study indicate that, although it is desirable to make an accurate estimate of DMAX, it is not vital and should not greatly affect the accuracy of IP concentrations calculated from data stored in the EPA's Fine Particle Emissions Information System (FPEIS). Also, it is indicated that valid data can be recovered, even in tests where the impactors were uncalibrated. By far the largest uncertainty, other than improper operation and unidentified experimental errors, is introduced by the lack of knowledge with respect to the types of nozzles

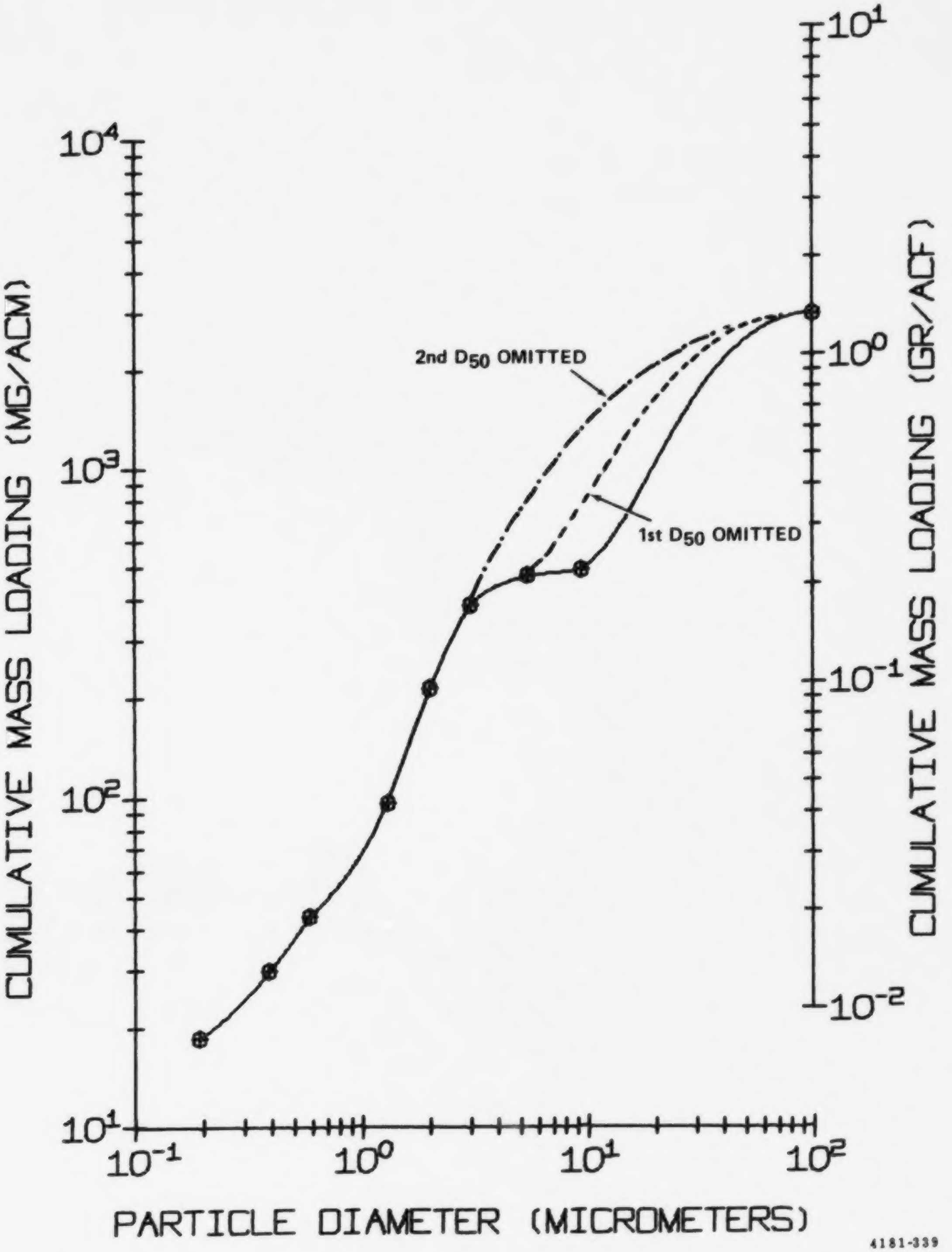

Figure 18. Cumulative particle-size distribution at inlet to electrostatic precipitator.

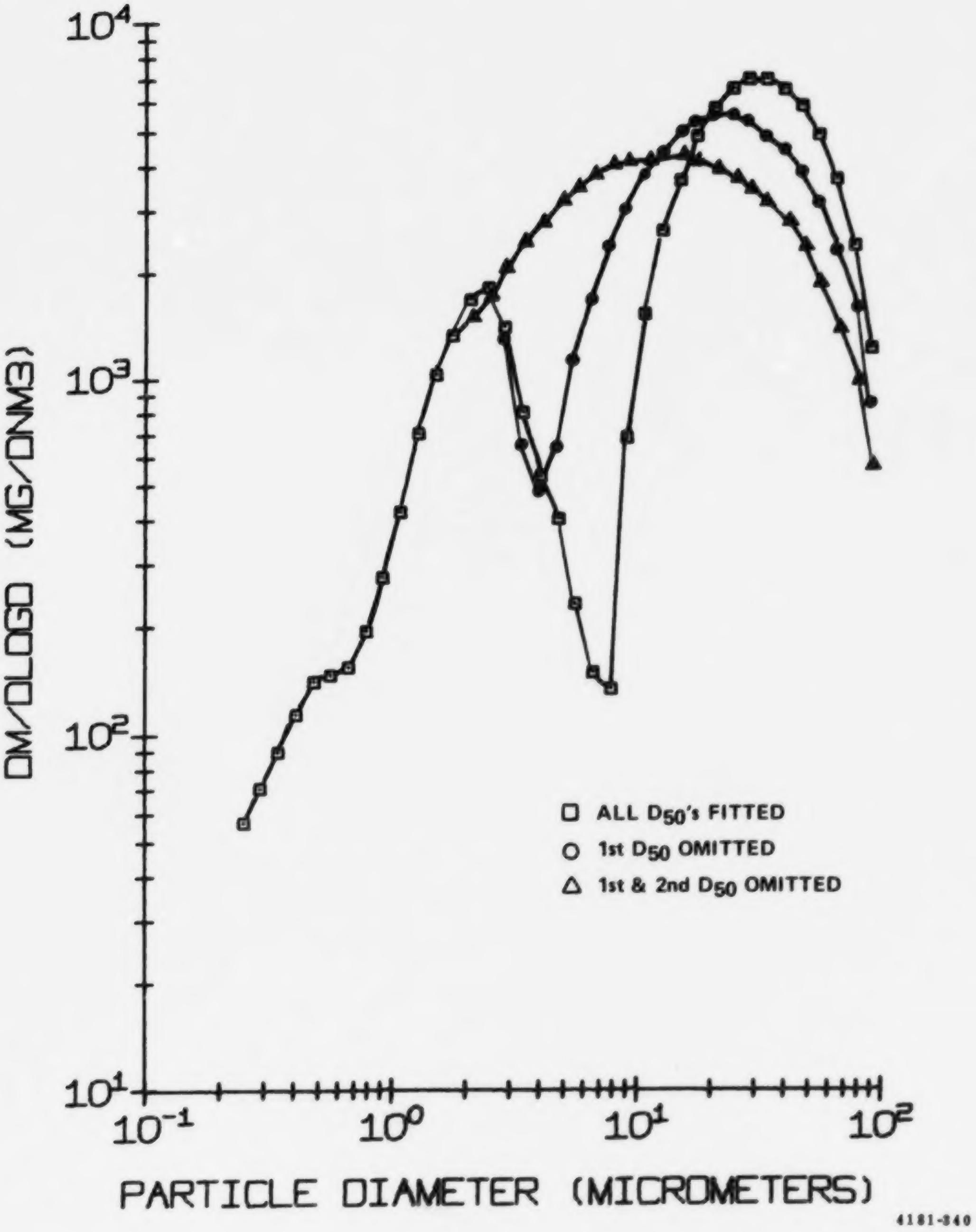

Figure 19. Differential particle-size distribution at inlet to electrostatic precipitator.

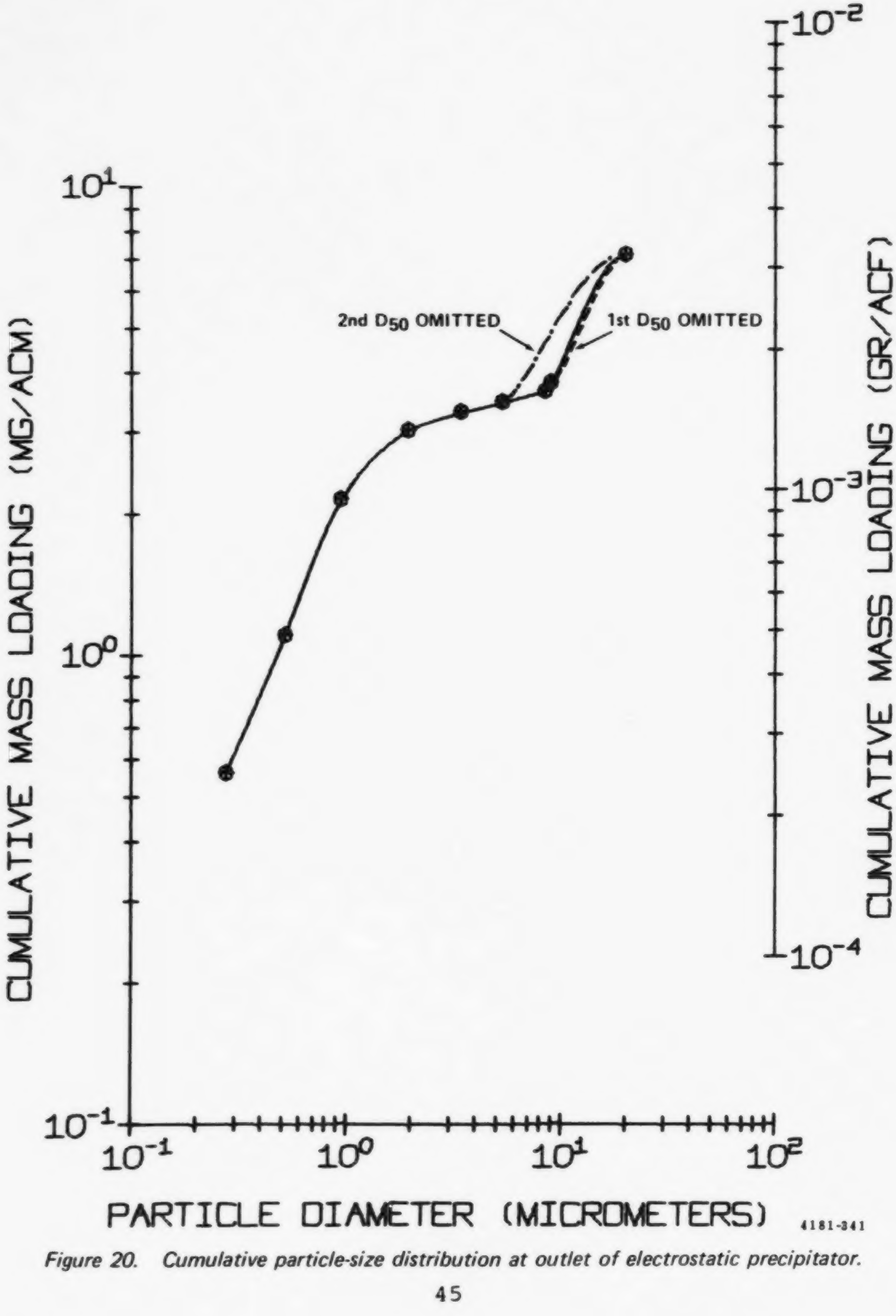

Figure 20. Cumulative particle-size distribution at outlet of electrostatic precipitator.

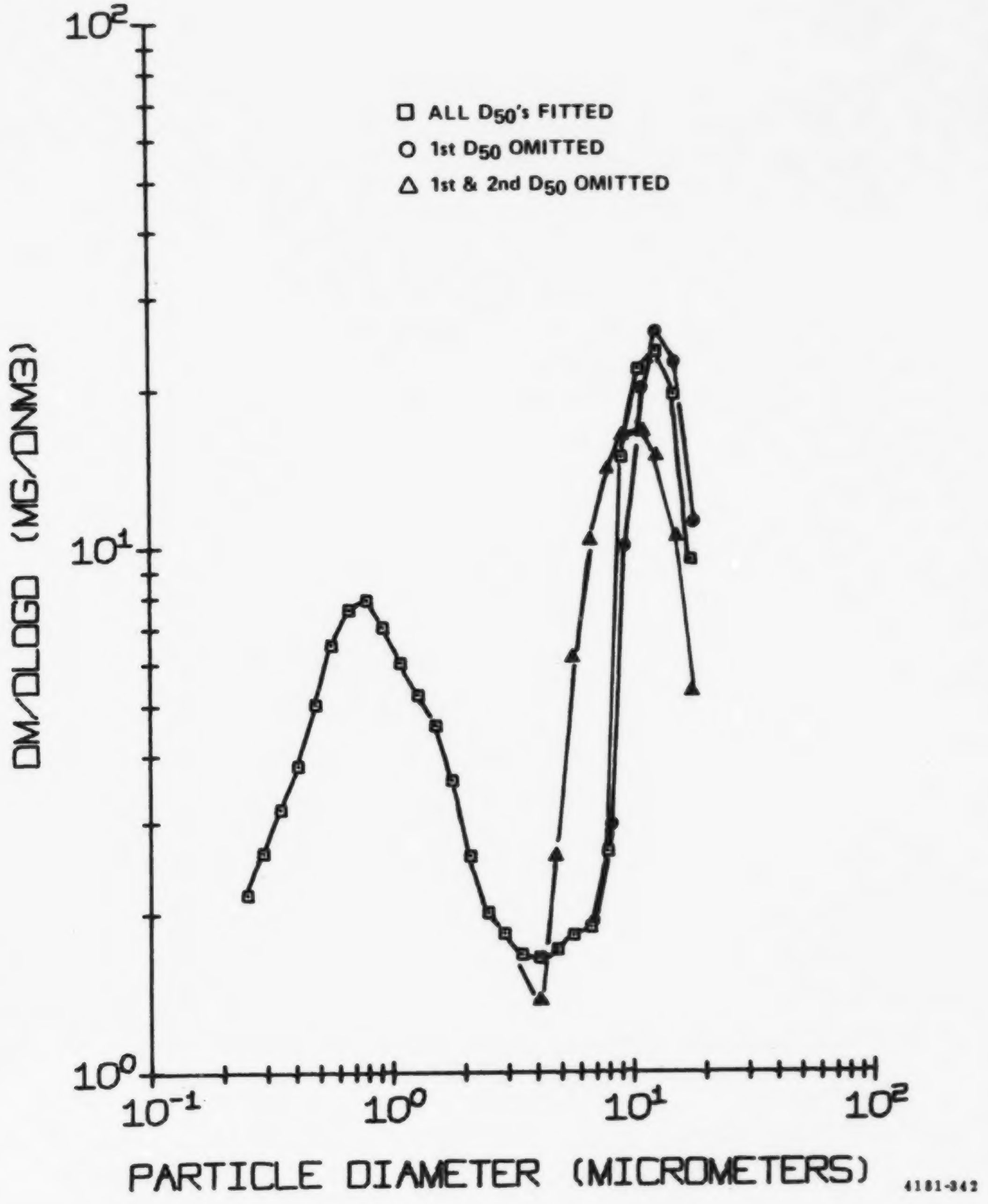

Figure 21. Differential particle-size distribution at outlet of electrostatic precipitator.

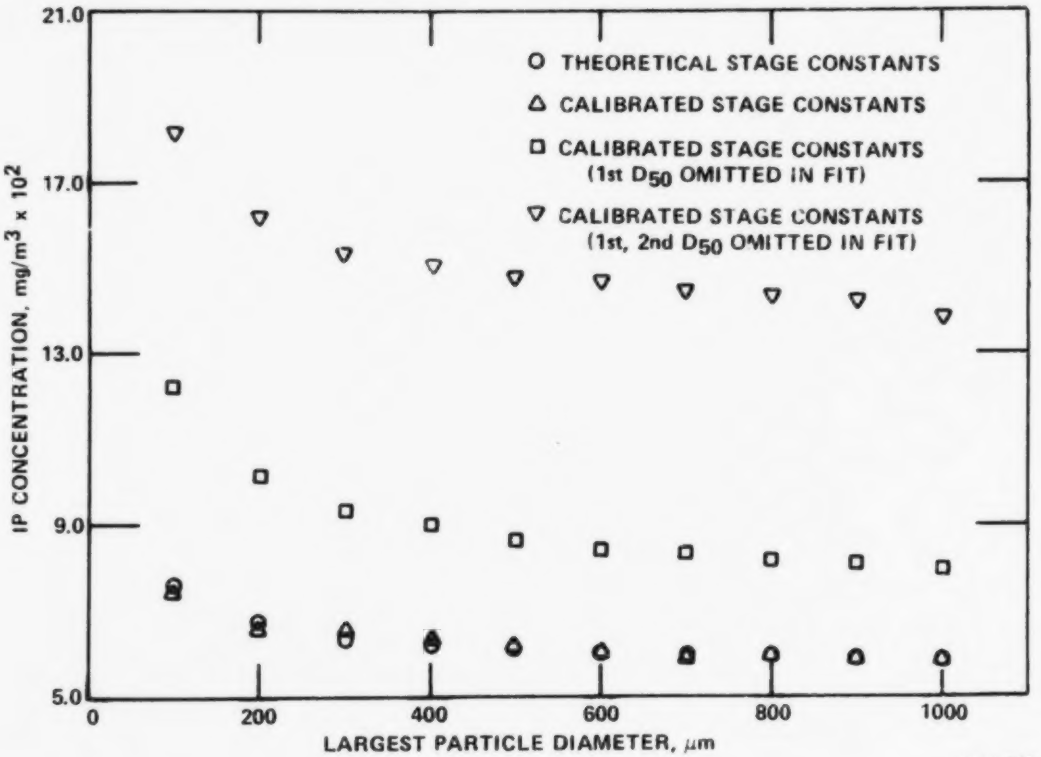

Figure 22. Calculated IP concentration vs. assumed D_{MAX} at electrostatic precipitator inlet. Coal-fired power plant.

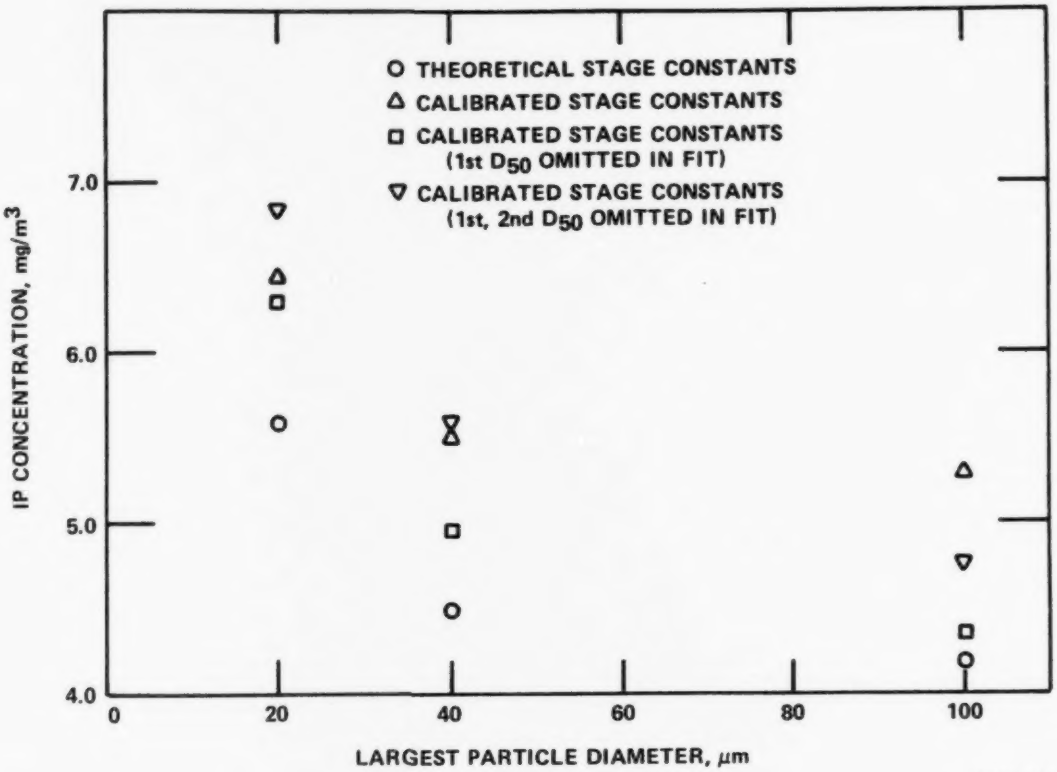

4181-344

Figure 23. Calculated IP concentration vs. assumed D_{MAX} at electrostatic precipitator outlet. Coal-fired power plant.

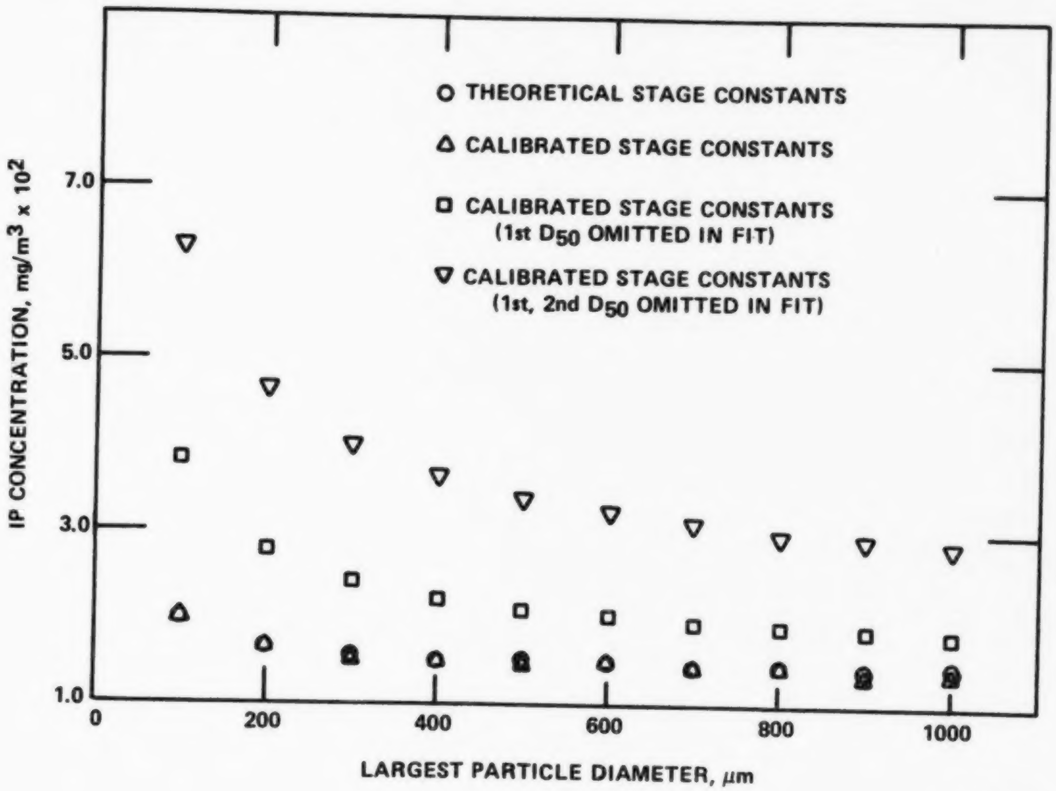

4181-346

Figure 24. Calculated IP concentration vs. assumed D_{MAX} at electrostatic precipitator inlet. Cement kiln.

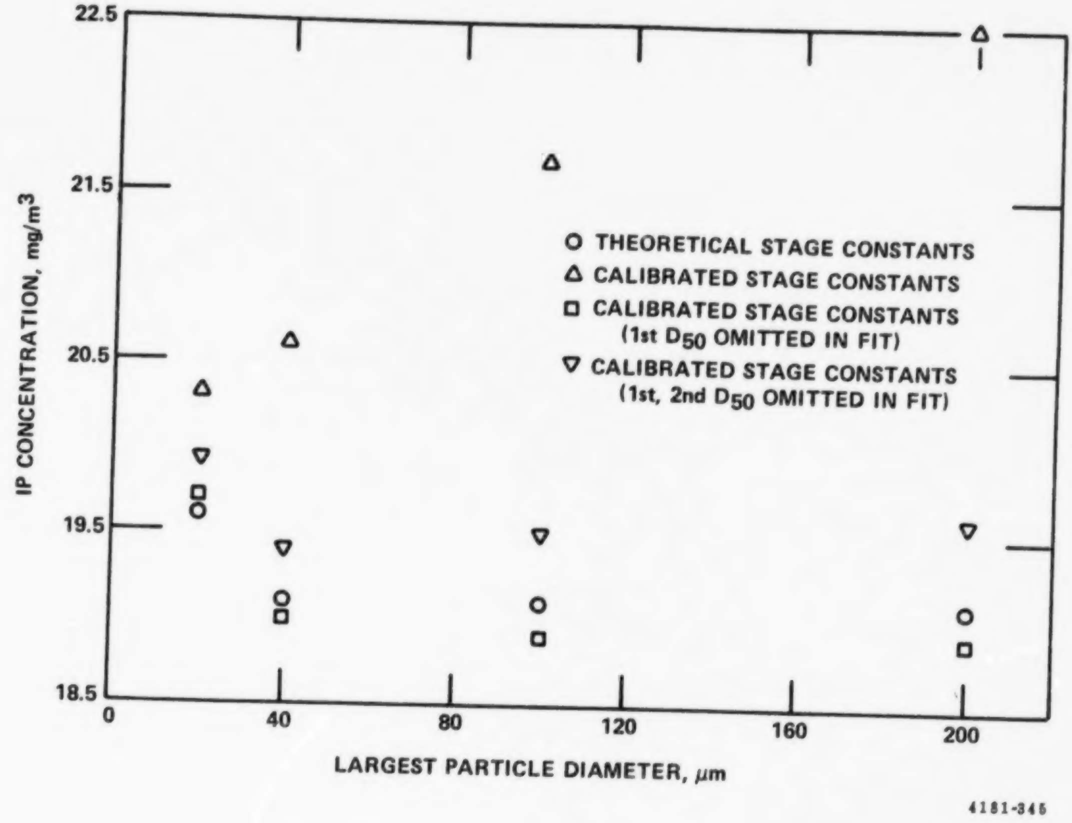

Figure 25. Calculated IP concentration vs. assumed D_{MAX} at electrostatic precipitator outlet. Cement kiln.

and precollectors that were used. The difference in calculated IP when the first D_{50} point was included and omitted in these studies was about a factor of two. It is therefore highly desirable that the effect of using buttonhook nozzles and cyclone precollectors is determined quantitatively before retrieving IP data from FPEIS in order to minimize the probable error.

New data--It has been demonstrated in the previous section that the modified CIDRS program can be used to accurately calculate the IP concentration from raw impactor data if no experimental errors exist; that is, the program itself does not appear to introduce large errors. If the sampling protocols outlined in the following sections are used, CIDRS can be used routinely to yield the IP concentration. Again, as new sampling systems become available, no extrapolations will be required.

Impactor data were also subjected to a modal analysis at the University of Minnesota, in which the data were fitted with multicomponent log-normal distributions by a simplex minimization method. Data were extrapolated to 100 μm particle diameter by fitting the portion of the size distribution for which data were available. Results were similar to those obtained with the curve-fitting polynomial procedure. IP concentrations could be estimated within a factor of two or better. The results of this analysis are given in Appendix B.

ISOKINETIC SAMPLING BY CONSTANT FLOWRATE PARTICLE-SIZING DEVICES

The research at Southern Research Institute on a sampling system for inhalable particulate matter includes the consideration of concepts for maintaining isokinetic sampling at constant flowrates in the sizing device. Isokinetic sampling is necessary to obtain a representative sample of suspended particles, notably those larger than 2 μm in diameter.[4]

Various techniques for achieving this goal have been proposed or used in previous work. Isokinetic sampling is maintained in EPA Method 5 by varying the flowrate through the filter in the sample train.[5] A single fixed-diameter nozzle is generally used throughout the sampling to avoid interrupting the tests to change nozzles.

For a sizing device such as a cyclone or an impactor, the particle sizing characteristics are a function of flowrate. Consequently, these devices are generally operated at constant flowrates.[6] The velocity in the nozzle is set equal to the average velocity in the duct at the point where the sample is taken, or to the average velocity at points on a sampling traverse. However, sampling at the average velocity of the gas stream is not accurate enough to yield a good measure of the concentration of inhalable particulate matter.

Several techniques and devices that were considered for sampling isokinetically at a constant flowrate in the sizing and measuring device are described in this section of the report, and their advantages and disadvantages are discussed. These items are: (1) variable area nozzles, (2) split-stream probes, (3) combinations of (1) and (2), (4) gas recycle systems, and (5) probe shrouds.

All these techniques involve measurement of the gas velocity in the flue, and they all require methods for producing, controlling, and measuring mechanical motion of parts of the apparatus from outside the stack. This is probably the most difficult problem to be solved in the design of such a device. The sampling device must be able to withstand the harsh environment in the flue or stack, which may contain corrosive gases, abrasive dusts, and moisture, often mixed with condensed acids, all at high temperatures and velocities.

The sampler must also be able to withstand the thermal shock of being placed in and removed from this environment into an ambient environment, which may consist of rain, snow, or ice at freezing temperatures. Some mechanical designs may require that all parts be made of materials that have the same thermal coefficient of expansion. The mobility of the parts and the integrity of seals are limited or destroyed by accumulated dust, especially in industrial process streams containing sticky or abrasive particles.

The isokinetic sampling device must be constructed so that small adjustments are predictable and accurate. In the case of a variable area nozzle, for example, it is essential that the sampling area is known exactly. As the nozzle is closed, a small change in radius of a round nozzle or width of a rectangular nozzle produces a large change in total area.

Three possible methods of producing mechanical motion inside a flue at the end of a probe are a sliding rod or cable, a rotating rod or cable, and a fluid-pressure to mechanical-motion transducer. A rod or cable attached to the device at the end of the probe and extending outside the stack could operate the device through a push or pull by the operator. Alternatively, the rod could be twisted if a rotary motion were needed or perhaps to give a finer adjustment. The use of a fluid under pressure to move a small piston on the device would eliminate the need for moving parts extending outside the probe. Such a fluid would have to perform adequately at stack gas temperatures. In this case, a separate measurement of the piston position would be necessary. All of these concepts have obvious and subtle problems and would require further investigation to determine which is best.

Sampling Concepts

Sampling concepts which allow isokinetic sampling with constant flowrate devices have been examined previously by Blake[7] and Elder, Littlefield, Tillery and Ettinger.[8] In this report, the concepts are classified as those which require mechanical motion at the probe such as the variable area nozzle and the split stream probe, and those which do not, such as the probe shroud and the gas recycle concepts.

Variable Area Nozzles--

The sampling velocity at the nozzle is the sampling flowrate divided by the area of the open face of the nozzle. Since the flowrate must be kept constant for inertial sizing devices such as impactors or cyclones, the sampling velocity may be changed by varying the area of the nozzle. The five techniques discussed below all include the problem of mechanical motion as a prime concern and the method will be a desirable technique only to the extent to which this problem can be solved. The five nozzles are the rectangular, the diamond or lozenge, the round or iris, the ellipse, and the multiple nozzle revolver configuration.

Rectangular nozzle--A variable area nozzle with rectangular geometry is shown in Figure 26. The cross-sectional area of the nozzle is varied by moving one side of the nozzle, thus varying the height of the rectangle formed by the edges of the nozzle. A screw provides the fine adjustment and is connected to a cable which leads to a control knob outside the stack. A hose clamp on the nozzle holds the cable and keeps it from twisting when the screw turns. The screw threads are fine enough that a small change in the nozzle area is made with each revolution of the screw.

For some sampling situations, a cyclone is used to remove the large fraction of dust and thus decrease the loading on the upper stages of the main sizing device. A variable area nozzle attached to a cyclone is shown in Figure 27 with the cyclone connected to a probe. The nozzle is attached to the inlet of the cyclone and a push-pull motion is used to vary the nozzle area.

There is a possibility that in some sampling situations dust may cause the movable nozzle wall to jam by wedging between it and the two nozzle walls flanking it. If that should prove to be a problem, a small clamping device could be used to press those walls together against the movable wall, releasing them only momentarily when the nozzle needed adjustment. A small "lip" directly upstream of the movable wall or flap would help keep dust out.

The nozzle would have a largest and smallest "realistic" area. The largest area would be defined by the size of the nozzle when it was fully opened. The smallest area would be defined by the sharpness of the nozzle edges, their tapers, and the ability of the mechanical mechanism to make small adjustments in the area of the nozzle. For blunter nozzle edges larger nozzle areas are required to reduce errors associated with impaction around the nozzle edge and deviations of the flow streamlines.

Diamond nozzle--Figure 28 illustrates a diamond or lozenge-shaped nozzle. The area is changed by moving one corner away from or closer to its opposite corner. The area then changes

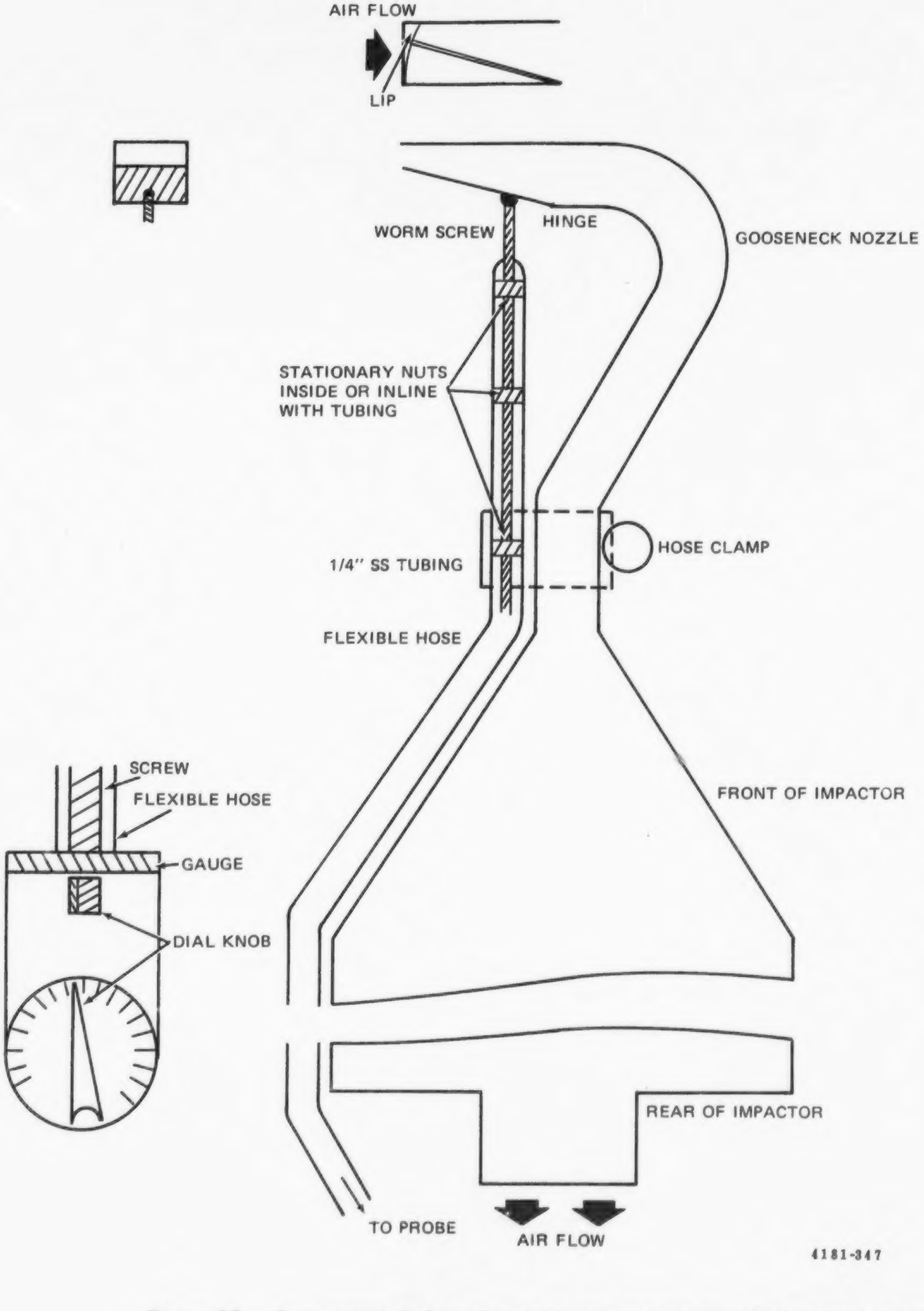
AIR FLOW
LIP
WORM SCREW
HINGE
GOOSENECK NOZZLE
STATIONARY NUTS
INSIDE OR INLINE
WITH TUBING
1/4" SS TUBING
HOSE CLAMP
FLEXIBLE HOSE
SCREW
FLEXIBLE HOSE
FRONT OF IMPACTOR
GAUGE
DIAL KNOB
REAR OF IMPACTOR
TO PROBE
AIR FLOW
4181-347

Figure 26. Conceptual design of variable area nozzle attached to an impactor.

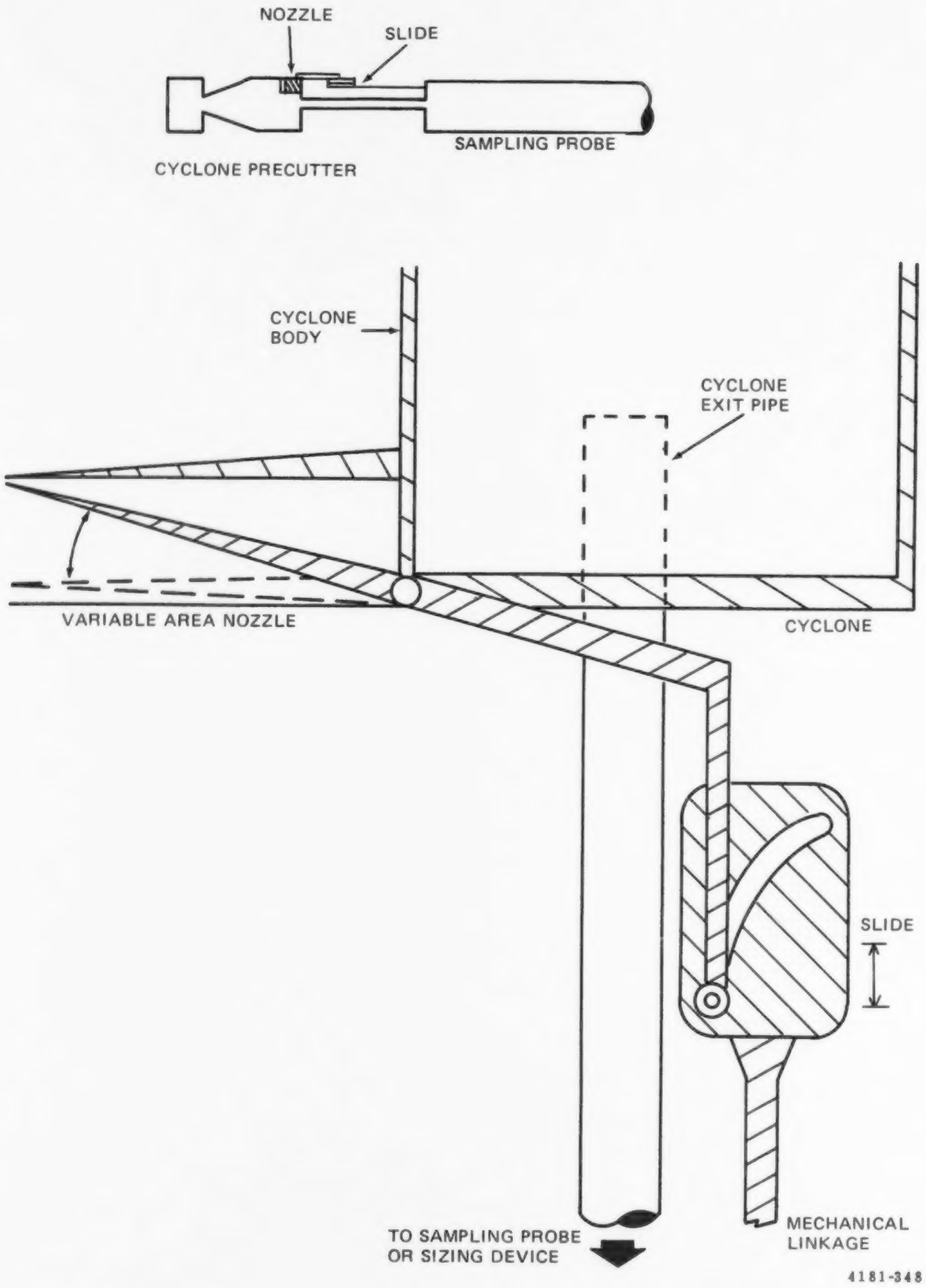
NOZZLE
SLIDE
SAMPLING PROBE
CYCLONE PRECUTTER
CYCLONE BODY
CYCLONE EXIT PIPE
VARIABLE AREA NOZZLE
CYCLONE
SLIDE
TO SAMPLING PROBE OR SIZING DEVICE
MECHANICAL LINKAGE
4181-348

Figure 27. A variable area nozzle attached to a cyclone.

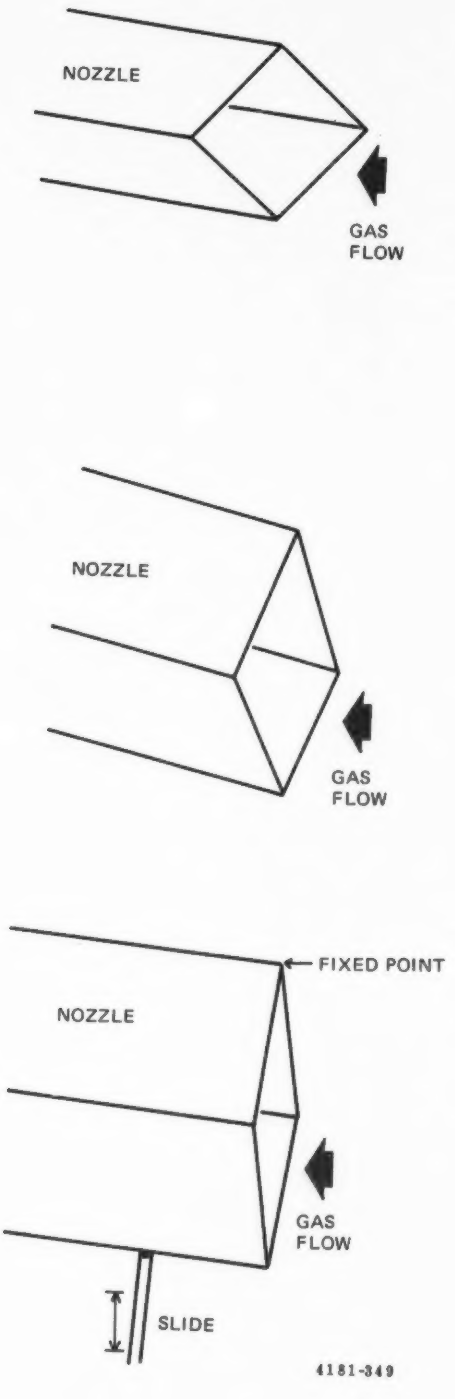
NOZZLE
GAS FLOW
NOZZLE
GAS FLOW
FIXED POINT
NOZZLE
GAS FLOW
SLIDE
4181-349

Figure 28. A diamond-shaped nozzle.

according to the area of the parallelogram the nozzle describes (area = base x height). A push-pull mechanical motion is used with this concept. Since every corner moves, they must be connected with hinges or similar connectors that allow motion. The size of the connectors will determine whether they will interrupt the flow streamlines appreciably. Perhaps the major problem with this concept is designing a transform connection from the movable to the fixed part of the nozzle.

Ellipse nozzle--The ellipse nozzle shown in Figure 29 is made of thin spring metal. Two arms squeeze the metal on opposite sides and deform the original circle into an elliptical or oval shape. It is doubtful that the various cross-sectional faces are actually ellipses but their areas may be approximated as such for design purposes. Calibration of the nozzle would determine the true area. A nozzle might be made of shim stock of alloys such as Inconel.

Multiple nozzle revolver configuration--The multiple nozzle revolver configuration is not a continuously variable nozzle but a set of variously sized nozzles which can be interchanged while sampling. Figure 30 illustrates an example. Before sampling, nozzles are selected which will allow isokinetic sampling at a range of velocities around the average velocity in the flue, and they are connected to a spoked wheel attached to the probe. The operator then selects the correct sampling nozzle to match the measured gas velocity by adjusting a mechanical linkage extending outside the stack wall. Nozzle selections are made to maintain isokinetic sampling within a certain percentage error. For flues which do not have great changes in velocity, the nozzles are selected so that anisokinetic errors are very low. For example, for a sizing device sampling at a constant flowrate of 28.3 ℓ/min (1.0 ft^3/min) in a flue with a gas velocity ranging from 6.2 to 12.3 m/sec (20 to 40 ft/sec) the nozzles selected would be 7.0, 7.5, 8.0, 8.5, 9.0, and 9.5 mm in diameter. The gas velocity is given for each sampling point in Table 7. The operator adjusts the nozzle set so that the 8.0 mm nozzle is the initial sampling nozzle. After sampling the necessary time at point one, the probe is moved to point two and the operator uses the mechanical linkage to adjust the nozzle set so that the 7.0 mm nozzle is the sampling nozzle. Remaining sampling points are sampled with the appropriate nozzle indicated in Table 7. The adjustment occurs essentially instantaneously and the seal between the sampling head and the sampling nozzle is obtained by close tolerance machining. Since the nozzles are hollow, flow disturbance around the sampling nozzle is minimized. As calculated by Reference Method 5 Subsection 6.11, the isokinetic variation is given in Table 7 and is well within the limits required of Method 5 tests ($90\% \leq I \leq 110\%$).[2] Using this particular set of nozzles, the maximum isokinetic variation in sampling at any velocity from 6.1 to 13.0 m/sec (20 to 43 ft/sec) is 107.5%. The use of more nozzles per

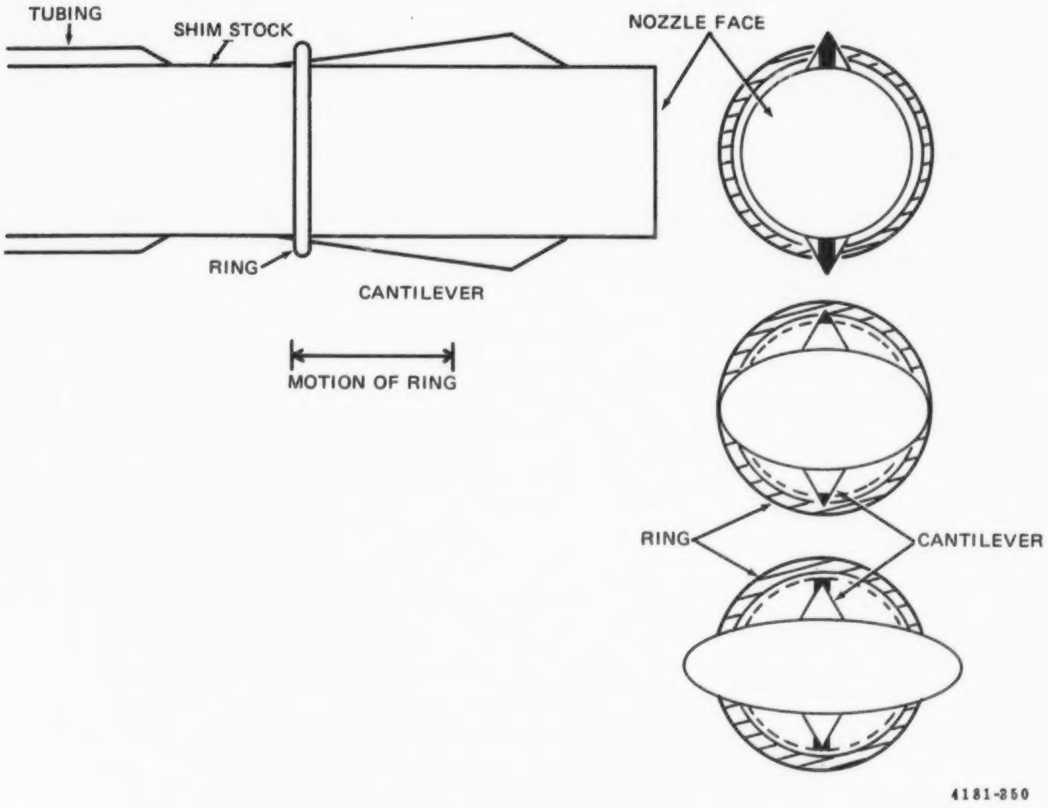
TUBING
SHIM STOCK
NOZZLE FACE
RING
CANTILEVER
MOTION OF RING
RING
CANTILEVER
4181-350

Figure 29. Conceptual drawing of an elliptical nozzle.

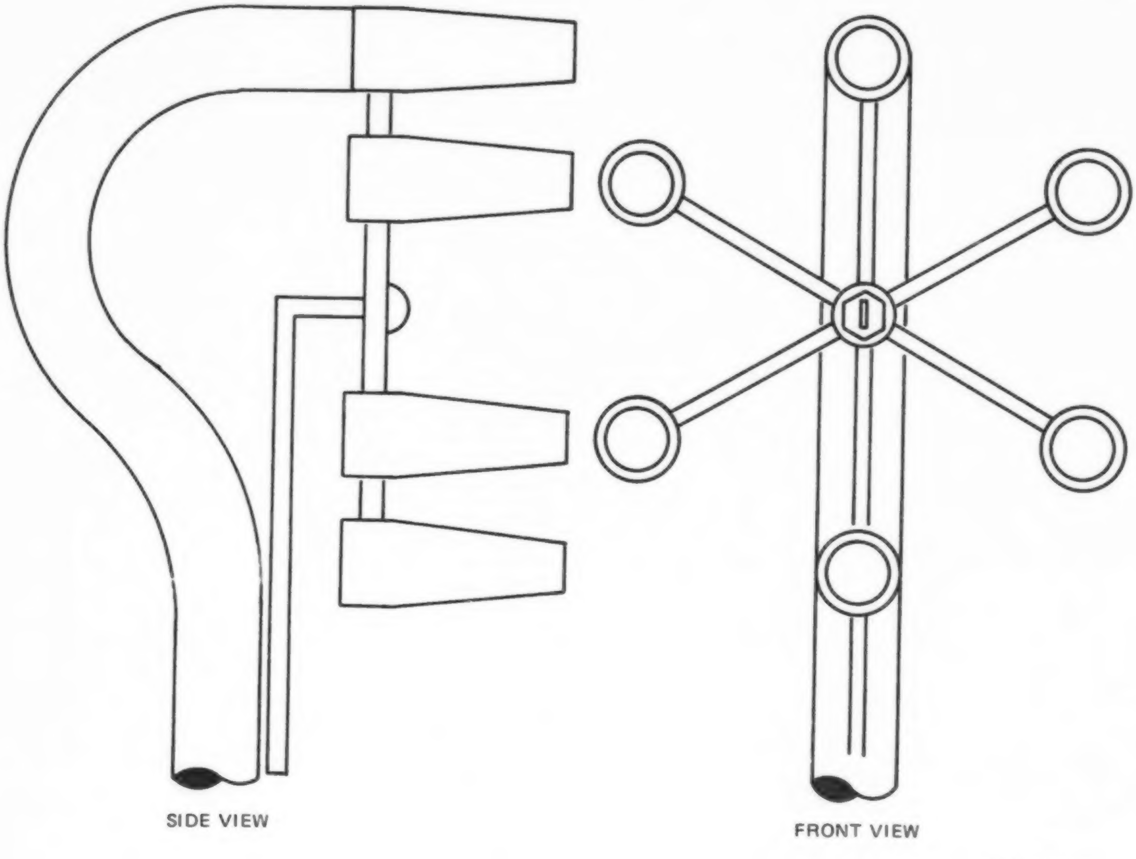
SIDE VIEW
FRONT VIEW
4181-351

Figure 30. A multiple nozzle revolver configuration.

TABLE 7. SAMPLING PARAMETERS FROM A HYPOTHETICAL SAMPLING TEST USING THE MULTIPLE NOZZLE REVOLVER CONFIGURATION

Sampling Point	1	2	3	4	5	6	7	8	9	10	11	12
Nozzle Used (diameter, in mm)	8.0	7.0	7.0	7.0	7.5	7.5	8.0	8.5	8.5	9.0	9.5	9.5
Sampling Velocity (m/sec)	9.28	12.13	12.13	12.13	10.56	10.56	9.28	8.22	8.22	7.34	6.58	6.58
Gas Velocity (m/sec)	9.9	11.7	12.3	11.9	11.1	10.5	9.7	8.6	7.9	7.2	6.7	6.2
Error in Sampling Velocity (%)	-6.3	+3.7	-1.4	+1.9	-4.9	+0.6	-4.3	-4.4	+4.1	+1.9	-1.8	+6.1
Per Cent Isokineticity	93.7	103.7	98.6	101.9	95.1	100.6	95.7	95.6	104.1	101.9	98.2	106.1

set (7, 8, or 9 instead of 6) would allow reduction of the isokinetic variation or extension of the velocity range.

Iris nozzle--The round or iris nozzle is only mentioned briefly here as a design concept. The nozzle consists of two or more very thin strips of a suitable metal alloy held together in an overlapping conical shape (see Figure 31). The nozzle face would be opened or closed by adjusting the position of the collar. As the collar is moved toward the face of the nozzle, the metal leaves would spring outward and increase the face area. The face area would decrease as the collar is moved in the opposite direction.

The major difficulties with this concept are the design and engineering problems. The overlapping leaves may experience metal fatigue due to thermal and mechanical stress and cease operating properly. It is necessary that the leaves retain their tendency to be flat so that they will spring out as the collar is moved toward the face of the nozzle. The collar must be designed so that it slides smoothly along the nozzle and does not interfere appreciably with the gas flow at the nozzle face.

In-Stack Split Stream Probe--

An in-stack, split-stream probe would allow true isokinetic sampling at the nozzle and yet maintain a constant flowrate through the sizing device. It does not require the use of a separate pump and cooling and condensing components. Instead, a valving arrangement adds cleaned stack gas to the sample gas stream at the rate needed to maintain a constant flowrate. Only the nozzle would need to be modified, and it could be used with any sizing device. The nozzle probably would not need to be larger than the sizing device in cross-section and thus not require a larger port than normally needed.

A schematic showing the general operation and necessary components of the split-stream probe is shown in Figure 32. The flowrate into the sizing device is set at a constant value. The nozzle is chosen to be a size such that isokinetic sampling can be maintained throughout the test. The minimum velocity that can be sampled isokinetically is equal to the sizing device flowrate divided by the cross-sectional area of the nozzle. The practical maximum velocity is that which does not cause unacceptable particle deposition in the nozzle and on the control valve and which does not lengthen sampling time unreasonably. As stack gas velocity, pressure, and temperature change and as the dilution air flowrate changes (due to stack gas changes or dilution filter load-up), an automatic monitor/controller adjusts the control valve to maintain isokinetic conditions.[7,9,10] At the minimum stack gas velocity, the control valve closes and no dilution air flows. At the maximum stack gas velocity, the control valve opens so that the dilution air is a substantial percentage of the total flow into the sizing device.

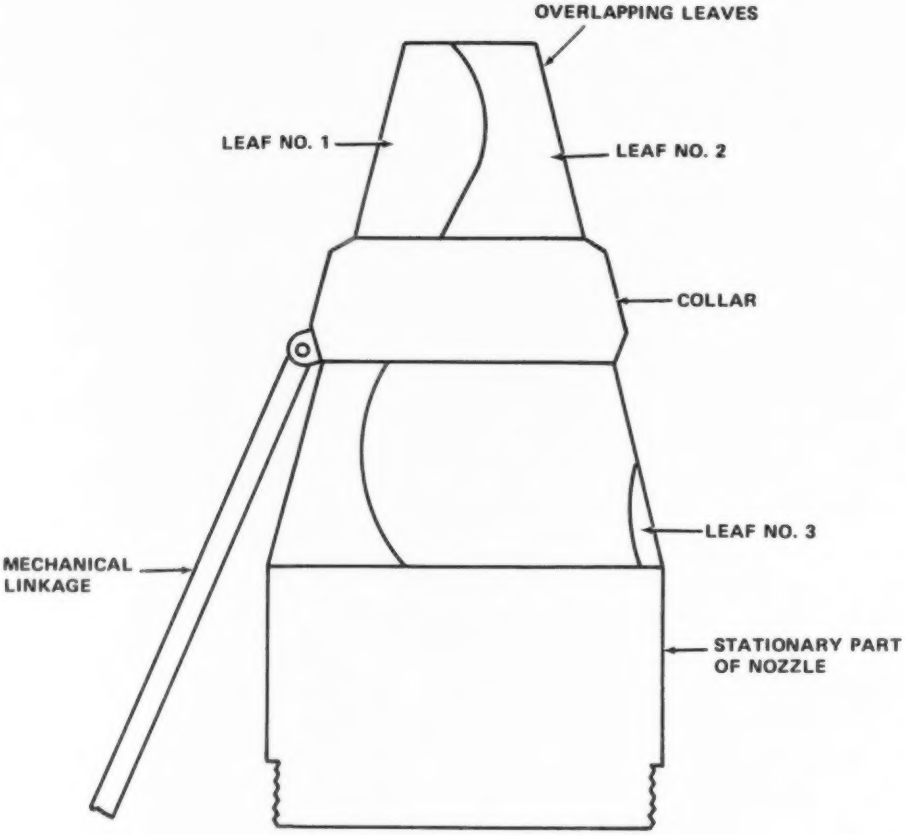
OVERLAPPING LEAVES
LEAF NO. 1
LEAF NO. 2
COLLAR
LEAF NO. 3
MECHANICAL LINKAGE
STATIONARY PART OF NOZZLE

4181-352

Figure 31. An iris nozzle.

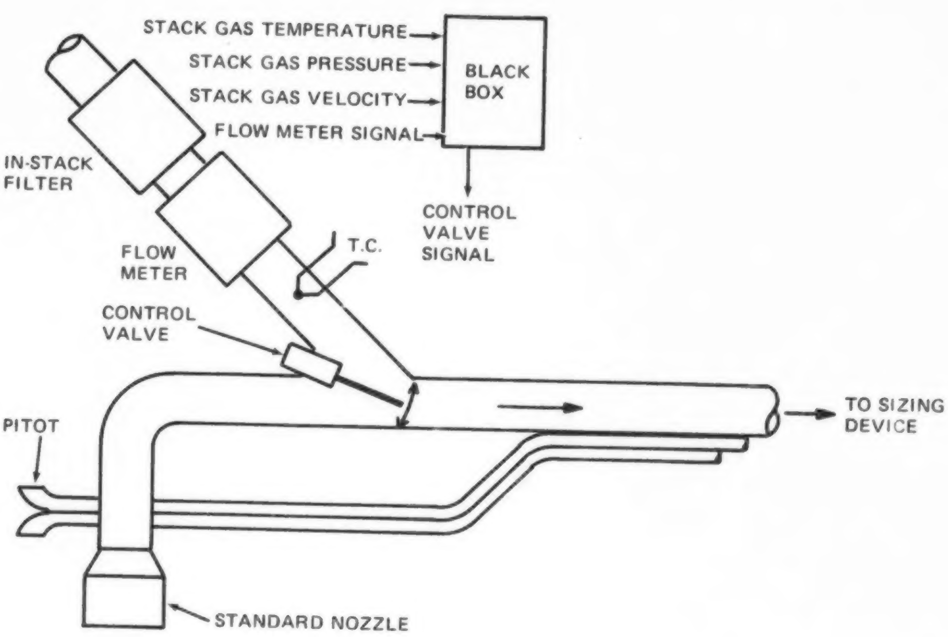
STACK GAS TEMPERATURE
STACK GAS PRESSURE
STACK GAS VELOCITY
FLOW METER SIGNAL
BLACK BOX
CONTROL VALVE SIGNAL
IN-STACK FILTER
FLOW METER
T.C.
CONTROL VALVE
PITOT
TO SIZING DEVICE
STANDARD NOZZLE

4181-353

Figure 32. In-stack split-stream probe, from Blake.[7]

Several observations can be made about this concept. As pointed out by Blake[7], the design and development of the monitor/controller would be expensive and the volume of gas sampled is not directly measured. Sampling in dusty streams could cause the pressure drop across the dilution filter to increase and thus necessitate constant adjustment of the control valve, even when the stack gas velocity is constant. For extremely dirty streams and a large variation of stack gas velocity from the constant gas velocity entering the sizing device, the dilution air filter could become plugged and interrupt the test. Since the control valve must restrict the sample flow in order to increase the dilution air flow, there will be wall losses on the control valve and other nearby parts. High temperature- and corrosion-resistant components for the filter housing, the flowmeter, and the control valve will be necessary. No separate cooling system or pump is required, and except for a slightly longer and larger nozzle, the sizing device and probe would not be modified.

Sliding-cone probe--One type of split-stream probe, shown in Figure 33, uses a sliding cone to vary the amount of sample gas pulled into the nozzle. As the cone slides in and reduces the amount of sample gas, small holes are spaced around the wall of the probe (or a small screen is used) to allow dilution air to enter. One advantage is that the dilution air can form an envelope around the sample air, thus minimizing wall losses beyond that point. Of course, the wall losses at the cone where the sample air enters an annular ring may be unacceptable at certain sampling velocities. Considerable thought would have to be given to the mechanical linkage that would adjust the position of the slide.

Adjustable-flap probe--Another type of split- stream probe is shown in Figure 34. It consists of a rectangular probe with two "flaps" which adjust the ratio of dilution air to sample air by opening and closing. A small bar which slides along the length of the probe can be used to adjust the setting. The dilution air would form layers on two sides of the stack gas stream instead of completely surrounding it. Otherwise, this design is much like the sliding cone probe.

Split-stream nozzle--A concept incorporating both the variable nozzle and the split-stream probe concepts is illustrated in Figure 35. The gas is sampled isokinetically by a fixed area nozzle and then split into two gas streams. One stream is pulled at a constant flowrate through a sizing device. The other stream flowrate is adjusted so that the nozzle face velocity equals the stack gas velocity. The excess gas is drawn out of the main flow "isokinetically". Two sampling trains are used: one for the sizing device and the other for the excess gas. The excess gas is filtered and provides a bulk sample for chemical analysis. The main advantages of this concept over the split-stream probe

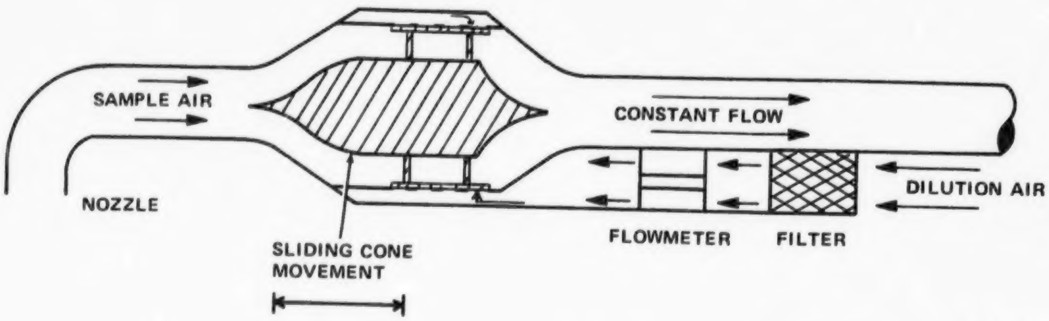
SAMPLE AIR
CONSTANT FLOW
DILUTION AIR
NOZZLE
SLIDING CONE MOVEMENT
FLOWMETER
FILTER
4181-354

Figure 33. Split-stream probe: sliding-cone probe.

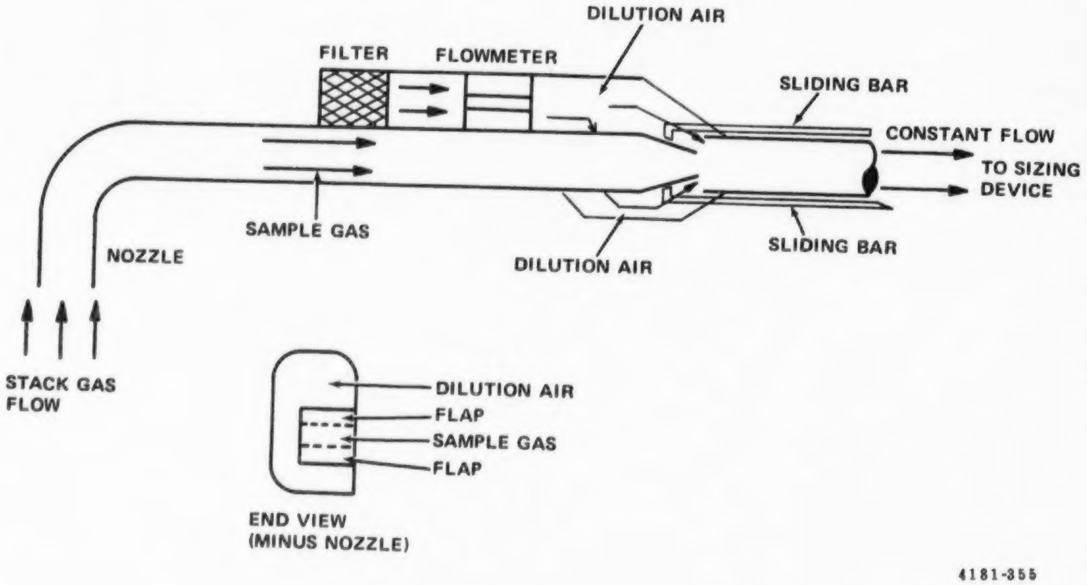
DILUTION AIR
FILTER
FLOWMETER
SLIDING BAR
CONSTANT FLOW
TO SIZING DEVICE
SAMPLE GAS
NOZZLE
DILUTION AIR
SLIDING BAR
STACK GAS FLOW
DILUTION AIR
FLAP
SAMPLE GAS
FLAP
END VIEW (MINUS NOZZLE)
4181-355

Figure 34. Split-stream probe: adjustable flap probe.

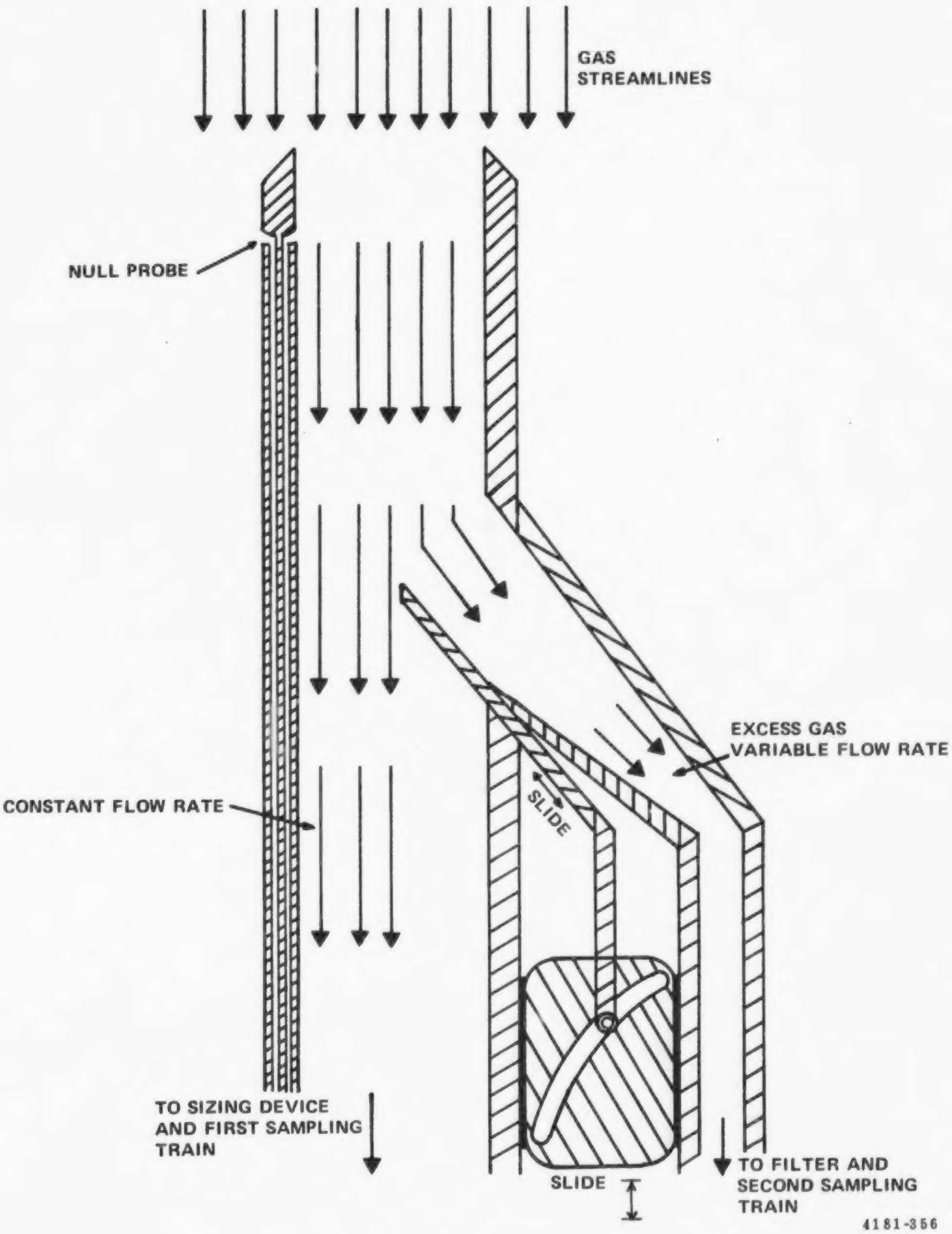
GAS STREAMLINES
NULL PROBE
CONSTANT FLOW RATE
SLIDE
EXCESS GAS VARIABLE FLOW RATE
TO SIZING DEVICE AND FIRST SAMPLING TRAIN
SLIDE
TO FILTER AND SECOND SAMPLING TRAIN
4181-356

Figure 35. A split-stream nozzle.

are: there is no need for in-stack filters and flowmeters; there is no particle loss due to the introduction of dilution air; and the sampling time is reduced since the stack particle concentration is maintained. The advantage this concept has over the variable area nozzle is the location of flow disturbances caused by mechanical linkages and sampling tubes away from the face of the nozzle. Disadvantages include the need for a second sampling train and the fact that the sample gas has been sampled "twice" essentially, once from the stack gas stream and once from the split. Also, it might be difficult to operate the movable flap so that isokinetic sampling takes place in the probe.

Gas Recycle Concept--

Similar to the split-stream probe is the gas recycle concept. Instead of separately filtering dirty stack gas to use as dilution air, the gas exiting the sizing device is used as the dilution air. Thus there is no separate filter to clog, because the sizing device final filter is cleaning the gas of particles. The gas can be introduced as an annular envelope around the stack gas and since there are no restrictions in the line, wall losses can be decreased. Since part of the gas entering the sizing device is clean, the sampling time to collect a given amount of mass would be lengthened.

Hot gas recycle--Figure 36 illustrates the method of recycling the stack gas while it is still at stack conditions (temperature and moisture). Stack gas entering the nozzle would be surrounded by clean dilution air immediately prior to its entrance into

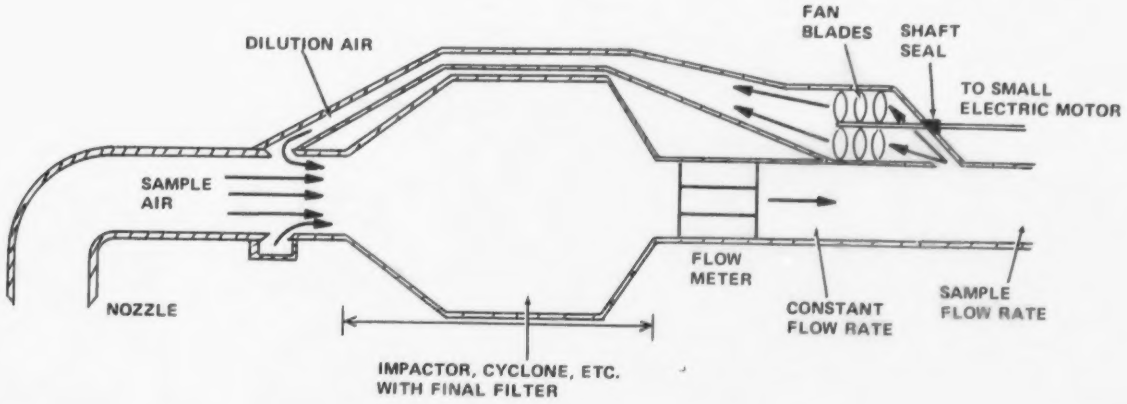

Figure 36. A hot gas recycle concept.

the sizing device. Upon exiting the final filter, a portion of the flow would be pumped back to the entrance of the sizing device through a bypass line. This would necessitate that the port be large enough for both the sizing device and the bypass line to pass through. The pumping device would have to be capable of high temperature operations and able to overcome the pressure drop of the sizing device. The sizing device flowrate and the sample flowrate are both monitored. Adjustments of the recycle gas flowrate and the sample flowrate maintain a constant sizing device flowrate and isokinetic sampling conditions.

Cool gas recycle--A cool gas recycle system is shown schematically in Figure 37. This system incorporates components that are more readily available than for any system discussed so far. Similar to the hot gas recycle concept, the cool gas recycle concept has less stringent requirements on the recycle pump. The stack gas is sampled isokinetically at the nozzle. Between the nozzle and the sizing device enough heated, dry air is added to the sample air to maintain a constant flowrate through the sizing device. After exiting the sizing device, the clean gas flows through a regular sampling train where it is cooled, dried, and measured. Part of the gas is then pumped through a gas heater which raises it to stack temperature. The gas is then used to provide the constant flowrate required by the sizing device by combining with the sample gas flow immediately downstream of the nozzle.

The cool gas recycle concept involves one consideration not present in the other systems. Since the dilution air is dry, the sizing device flow will consist of a gas with varying amounts of moisture, all of them less than the moisture in the stack gas. How this will affect the operation of the sizing device, and whether it will be a significant effect, is dependent on what the sizing device is and how it works. An investigation of the change in stage D_{50} for an Andersen impactor as a function of gas moisture content for three different temperatures is summarized in Table 8. The largest change in stage D_{50} for a run in which the moisture content varies from 5 to 20 percent is 3.4 percent for a gas temperature of 38°C (100°F), 2.7 percent for 149°C (300°F) and 2.3 percent for 316°C (600°F). The variation in stage D_{50} will be smaller for smaller variations in moisture content.

The major advantage this concept has over the other concepts is its lack of moving components in the stack environment. The flow adjustment and pumping of the gas stream can be performed on the cool gas thus allowing the use of conventional equipment. All the other items used such as the gas heater, temperature controller, and piping are stock items except for the flowrate monitor/controller. Unless the sizing device has an easily accessible, constant pressure drop component (such as a cyclone) which can be monitored by a differential pressure controller,

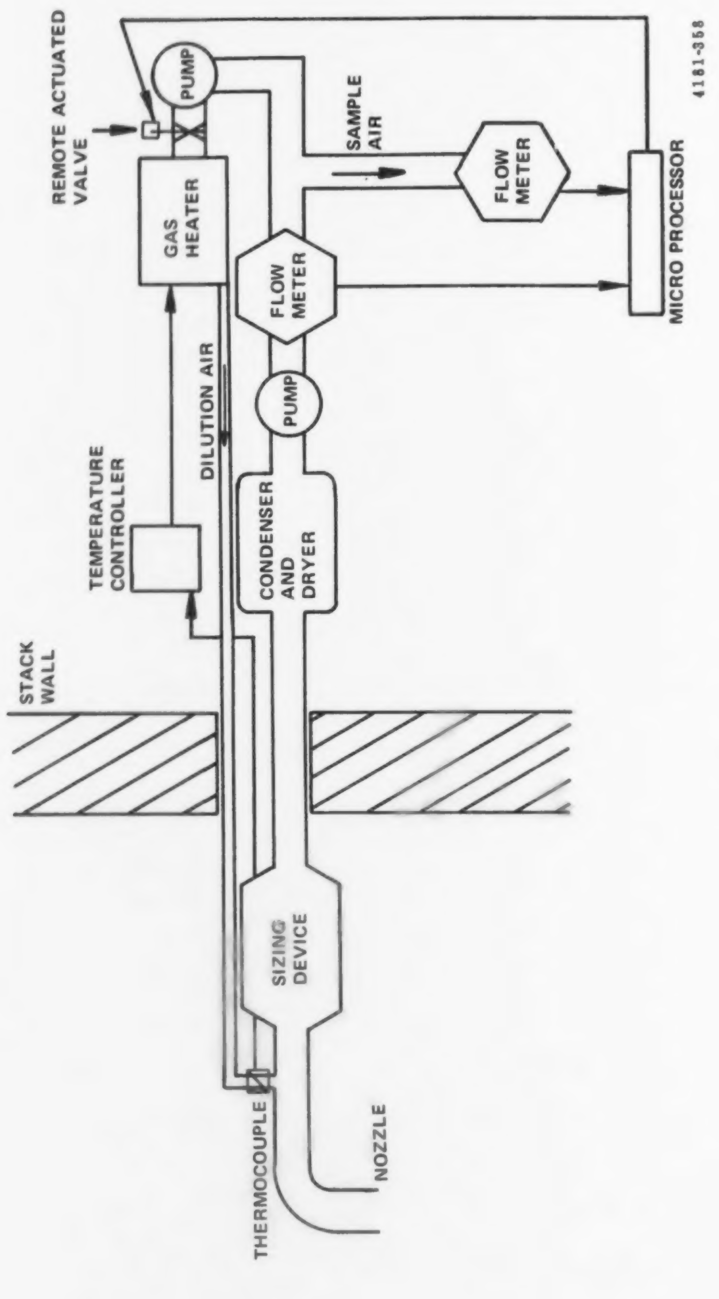
REMOTE ACTUATED VALVE
PUMP
GAS HEATER
SAMPLE AIR
FLOW METER
FLOW METER
MICRO PROCESSOR
4181-358
TEMPERATURE CONTROLLER
DILUTION AIR
PUMP
CONDENSER AND DRYER
STACK WALL
SIZING DEVICE
THERMOCOUPLE
NOZZLE

Figure 37. Cool gas recycle concept.

TABLE 8. CHANGE IN STAGE D_{50}'S FOR AN ANDERSEN IMPACTOR AS A FUNCTION OF MOISTURE CONTENT OF SAMPLED GAS

Temperature, °C (°F)		38 (100)					149 (300)					316 (600)				
Viscosity, micropoise		177	173	169	165		223	219	215	213		284	281	278	274	
Moisture, percent		5	10	15	20	Largest Difference (Percent)	5	10	15	20	Largest Difference (Percent)	5	10	15	20	Largest Difference (Percent)
D_{50}, µm	Stage															
	S1	10.59	10.47	10.35	10.23	3.44	11.86	11.75	11.65	11.54	2.66	13.35	13.27	13.19	13.10	1.85
	S2	10.10	9.98	9.87	9.75	3.44	11.30	11.20	11.10	11.00	2.66	12.72	12.64	12.57	12.49	1.85
	S3	6.20	6.14	6.07	5.99	3.44	6.93	6.87	6.81	6.75	2.67	7.79	7.74	7.69	7.65	1.86
	S4	4.17	4.12	4.08	4.03	3.44	4.65	4.61	4.57	4.53	2.67	5.21	5.18	5.15	5.11	1.87
	S5	2.34	2.31	2.28	2.26	3.44	2.59	2.57	2.55	2.53	2.68	2.89	2.87	2.85	2.83	1.91
	S6	1.13	1.12	1.10	1.09	3.42	1.24	1.23	1.22	1.21	2.69	1.36	1.35	1.34	1.34	1.99
	S7	0.727	0.719	0.711	0.703	3.40	0.791	0.784	0.777	.770	2.70	0.854	0.849	0.843	0.837	2.07
	S8	0.372	0.368	0.364	0.360	3.30	0.394	0.391	0.387	.384	2.73	0.408	0.405	0.402	0.398	2.28

a microprocessor will have to be used to calculate the flowrates at stack conditions from the measured cool, dry gas flowrates. For example, a commercial cascade impactor does not have any accessible points at which the pressure drop across a stage could be measured. However, a small series cyclone system would allow the pressure drop across any of its components to be read with a minimum of modification.

In-Stack Probe Shroud--

As shown in Figure 38, this design consists of a standard sampling nozzle centered in a large shroud.[7] Both the nozzle and the shroud have the same velocity at the inlets. The concept is based on the fact that the nozzle samples isokinetically from the shroud gas stream and on the assumption that the part of the shroud gas stream that enters the nozzle is representative of the stack gas at that point. It is argued that this system would work for stack gas velocities both higher and lower than the shroud velocity due to the fact that the flow streamlines of the gas entering the nozzle are not disturbed greatly. In actuality, the flow streamlines entering the nozzle must be bent but not, perhaps, at the immediate entrance to the nozzle. In the case of the stack gas velocity being less than the sampling velocity a larger gas volume is flowing through the nozzle area than is flowing through an equal, coaxial area located a distance upstream from the nozzle. This extra volume must come from the gas immediately outside that area. Thus the flow streamlines outside that area must bend and flow into that area to give the higher velocity. In this case the bending may not be as abrupt or sharp as when a nozzle is used without a shroud, so that the effect of sampling anisokinetically is reduced. Blake reports ". . . a preliminary evaluation indicates that the concept is valid over relatively wide stack/shroud velocity mismatches (3:1 and more) for particles of 30 μm diameter or less."[7] The extent to which anisokinetic effects are reduced would have to be determined by calculation and each user would have to decide whether the limits of error of the device would be compatible with the goals of the sampling program.

Other considerations of this method are the relatively large size of the probe, the need for a large, interchangeable cartridge filter, a large pump or exhaust blower, a large capacity flowmeter for the shroud flow, the need to place the in-situ sizing device inside the shroud, and the need to remove the shroud "nozzle" in order to remove the sizing device. Unless the shroud gas is cooled by a cooling component and the moisture is removed by a condenser, the blower would have to be capable of operation at stack temperatures. A valving arrangement would be used in conjunction with a large capacity flowmeter to set the shroud velocity equal to the nozzle velocity and to correct for increasing pressure drop across the shroud filter as it loads up.

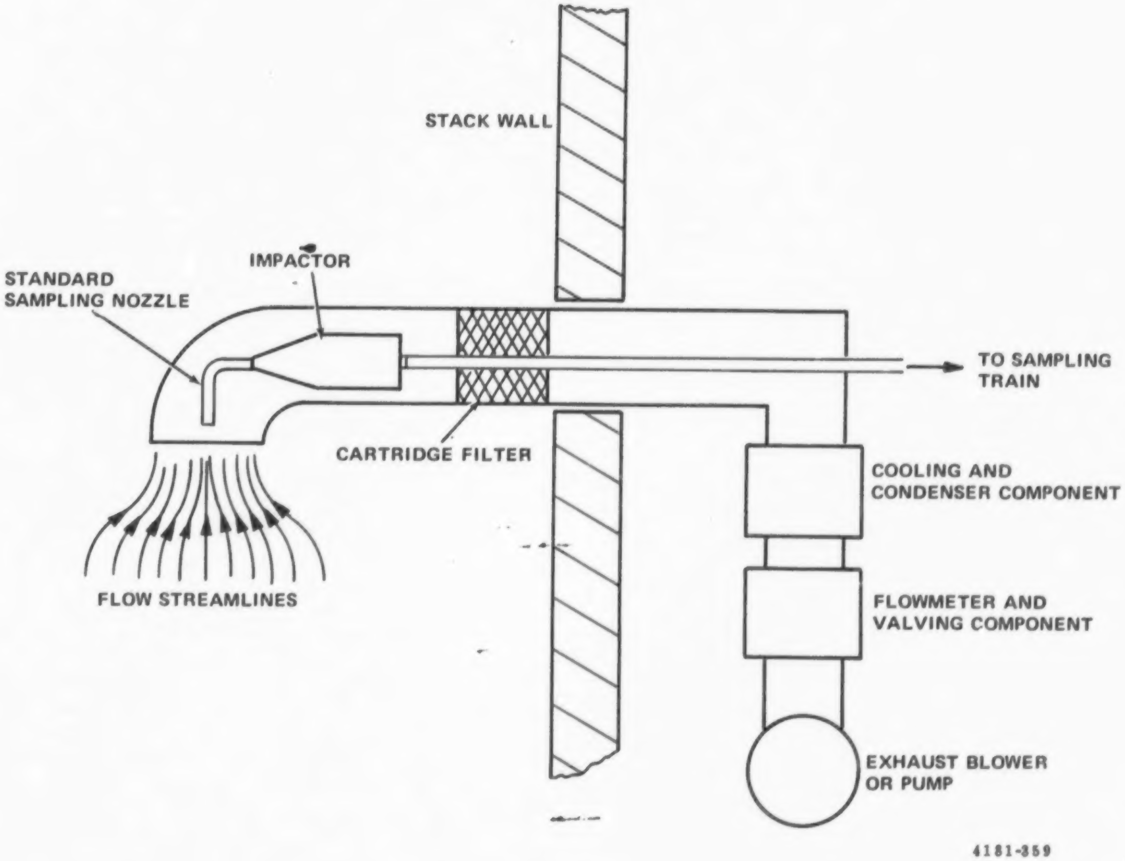
STACK WALL
IMPACTOR
STANDARD SAMPLING NOZZLE
TO SAMPLING TRAIN
CARTRIDGE FILTER
COOLING AND CONDENSER COMPONENT
FLOWMETER AND VALVING COMPONENT
FLOW STREAMLINES
EXHAUST BLOWER OR PUMP
4181-359

Figure 38. In-stack probe shroud, after Blake.[7]

SECTION 3

DESIGN, FABRICATION, AND TESTING OF PROTOTYPE SAMPLING SYSTEMS FOR INHALABLE PARTICULATE MATTER

A variety of aerosol sampling systems have been studied for use in measuring the concentration of inhalable particulate (IP) matter.[11] The system must be designed to separate particles larger and smaller than 15 μm in aerodynamic diameter (i.e., have a D_{50} value of 15 μm) according to a specified efficiency curve.

This section describes laboratory studies made at Southern Research Institute to develop suitable IP sampling systems that will fit EPA specifications. These systems are based on impactors, cyclones, and elutriators as collectors. All of these devices have features that limit their applicability. Impactors do not always retain particles efficiently that are much larger than the stage cut point (D_{50}). The particles bounce and are re-entrained into the gas stream, resulting in contamination of the smaller particle fraction.[12,13,14] Cyclones are not subject to that problem, but they are larger and their performance is difficult to predict.[15] Virtual impactors can have significant losses of small particles.[16] Horizontal elutriators are bulky and their performance is sensitive to orientation. However, re-entrainment is not a problem in elutriators for reasonable velocities, and the theory describing their performance is straightforward and accurate.

SUMMARY

The significant results that were attained may be summarized as follows:

Tests were conducted with monodisperse aerosols on several commercially available cascade impactors and buttonhook nozzles to characterize them for measurements in the IP range of particle sizes.

Collection efficiencies were measured for a horizontal elutriator. The measured values agreed well with values calculated from theory, allowing the preparation of design nomographs for inlet precollectors in sampling systems. Design parameters were calculated for horizontal elutriators to be used with cascade impactors, operated at 14.2 ℓ/min and 149°C, the EPA Source Assessment Sampling System, operated at 185 ℓ/min and 204°C, and the EPA Fugitive Ambient Sampling Train, operated at 5,282 ℓ/min and 23°C.

Two cyclone systems were designed and evaluated: a cyclone to be used as a precollector for cascade impactors, and a system of two cyclones and a filter in series, to be used as the primary system for measuring IP and fine particle concentrations. Both systems were designed for high-temperature operation in process streams.

Tests on the Andersen Size Selective Inlet, a 15-μm precollector for hi-vol samplers, showed its performance to be within the proposed limits for IP samplers.

A sampling system was designed in which the aerosol is diluted in flow patterns and with mixing times simulating those in stack plumes. The system is thus designed to characterize aerosols formed from condensable vapors in stack gas as the plume is diluted and cooled by the atmosphere. Tests with the system on a domestic oil-fired furnace indicated that condensation of organic chemical vapors took place in the system as expected.

EVALUATION OF COMMERCIAL CASCADE IMPACTORS AND BUTTONHOOK NOZZLES--EFFECT ON MEASUREMENT OF INHALABLE PARTICULATE MATTER

This part of Section 3 describes various tests that were made on commercial cascade impactors and buttonhook nozzles to determine their applicability to inhalable particulate measurement.[4]

Experimental Procedures

Using the apparatus shown in Figures 39 through 42, various buttonhook nozzles and commercial impactors were allowed to sample large monodisperse aerosols to determine their collection efficiency. The buttonhook nozzles tested were 0.32, 0.64, and 0.95 cm (1/8, 1/4, and 3/8 in.) in diameter. The cascade impactors tested were the Modified Brink, the Andersen Mark III, the Sierra Model 226, the MRI Model 1502, and the University of Washington Model V.

The particles used in this calibration were generated with a vibrating orifice aerosol generator (VOAG) using a solution of methylene blue dye in 1:1 distilled water and ethyl alcohol. The particles were dried and lofted up through a 30-in. Plexiglas column and were drawn by a high volume blower into a small Plexiglas wind tunnel via another smaller Plexiglas tube. The flow rates of the blower and pump were set so that sampling could be accomplished isokinetically.

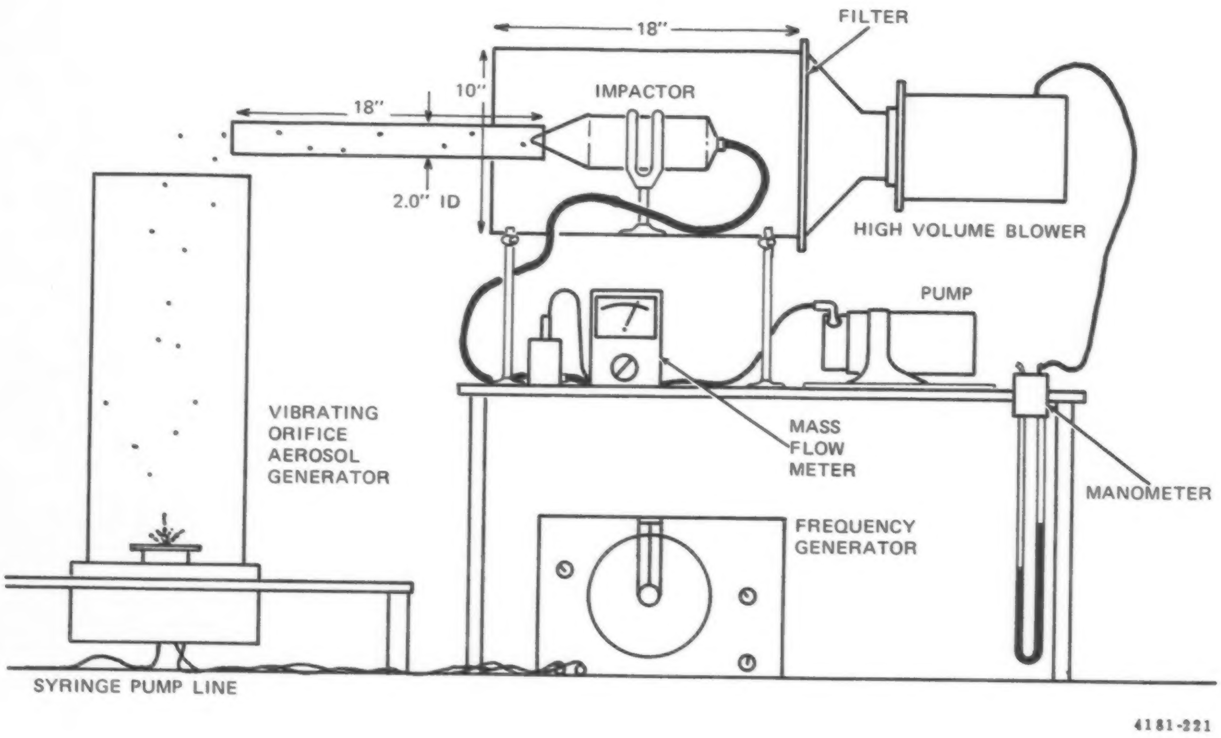
18"
FILTER
10"
IMPACTOR
18"
2.0" ID
HIGH VOLUME BLOWER
PUMP
VIBRATING
ORIFICE
AEROSOL
GENERATOR
MASS
FLOW
METER
MANOMETER
FREQUENCY
GENERATOR
SYRINGE PUMP LINE
4181-221

Figure 39. Configuration of apparatus used in evaluation of cascade impactor and nozzle.

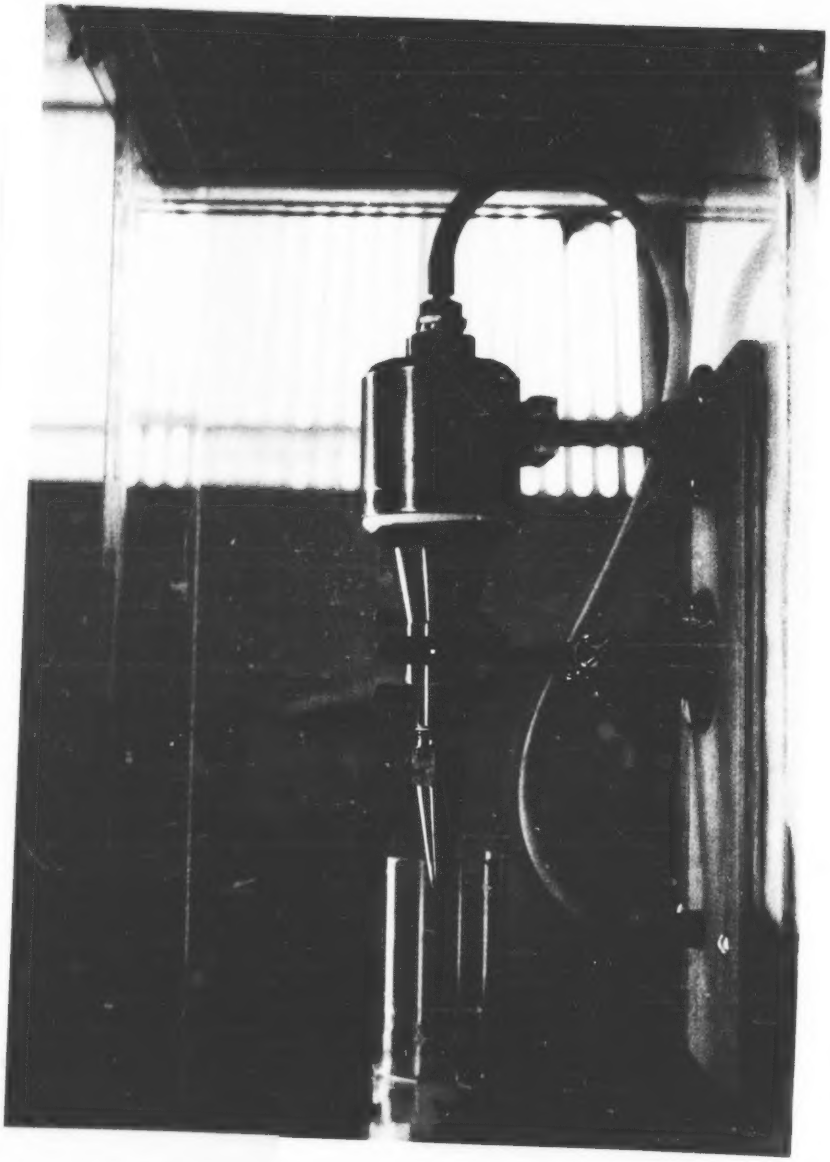

4181-363

Figure 40. Andersen Mark III cascade impactor situated in isokinetic sampling apparatus.

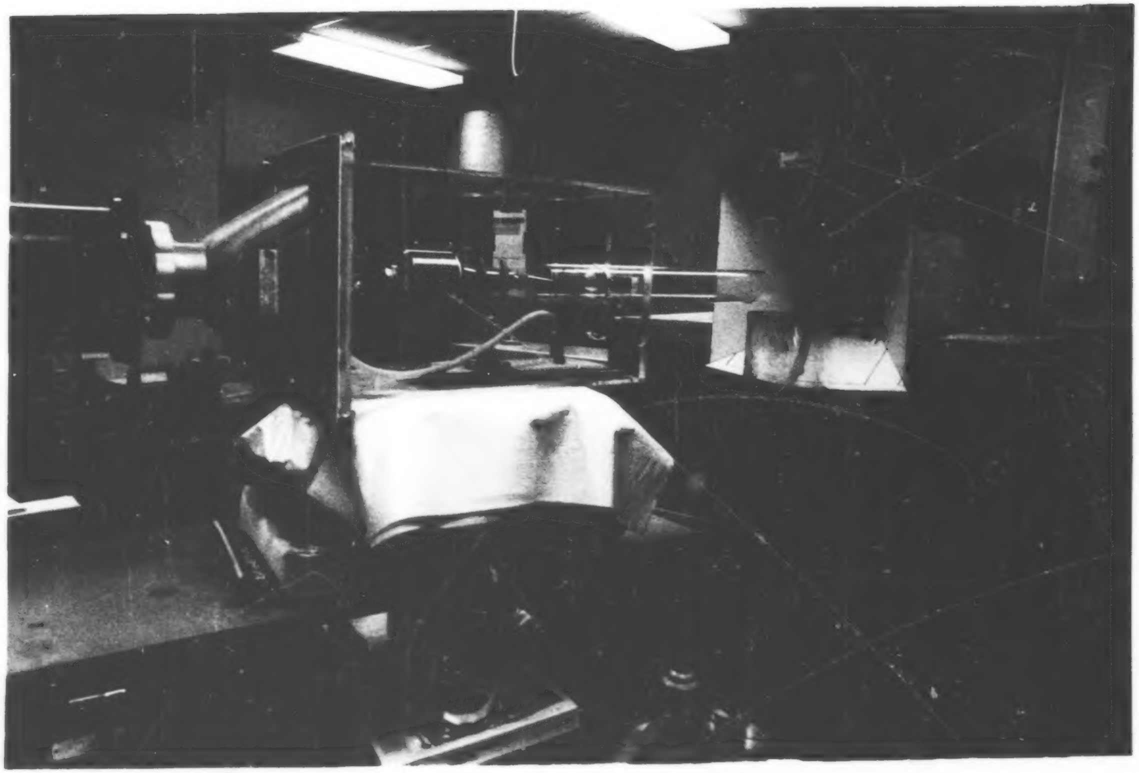

4181-362

Figure 41. Isokinetic sampling apparatus adjacent to vibrating orifice aerosol generator.

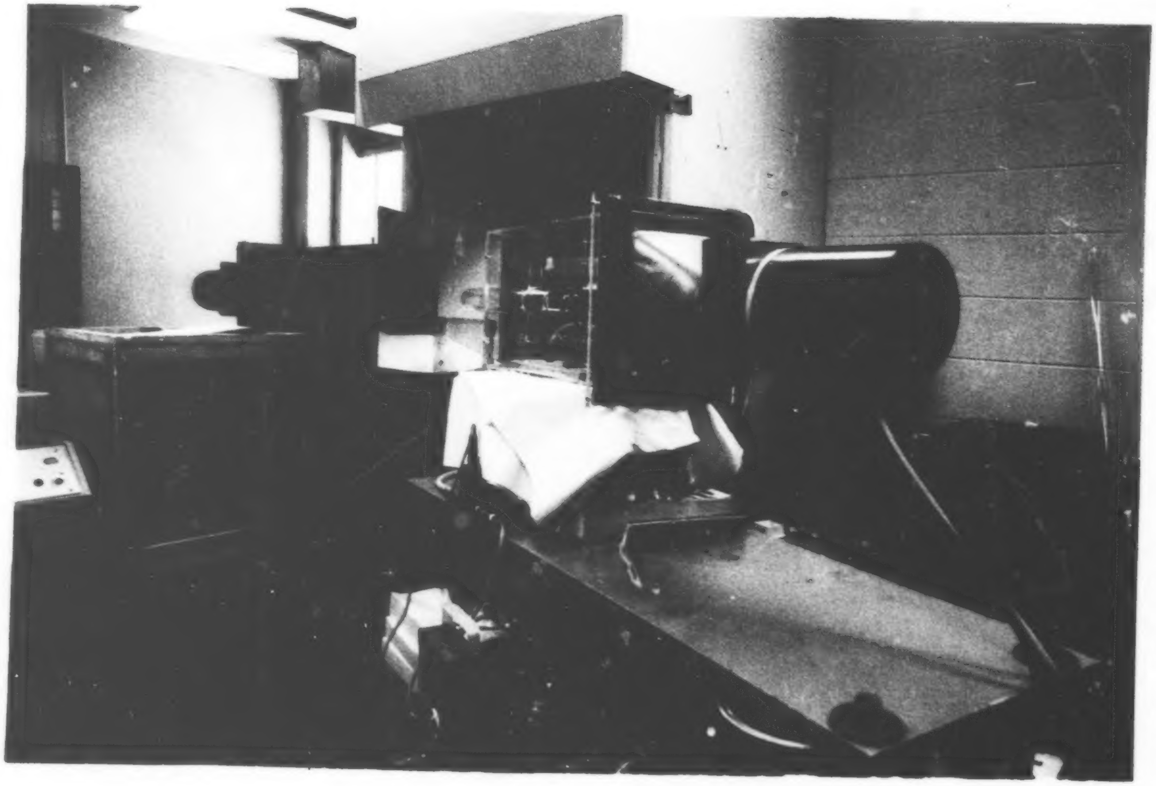

4181-361

Figure 42. Isokinetic sampling apparatus adjacent to vibrating orifice aerosol generator.

The buttonhook nozzles were allowed to sample for about 1.5 hours in each run, corresponding to one 500-ml syringe of solution being put through the VOAG. It was necessary to double the sampling time for the impactors in order to collect a measurable amount of material on each of the components and stages. In the tests on the buttonhook nozzles, filters were installed after the nozzles to collect all penetrating particles. After sampling, each impactor or nozzle was disassembled and each component was washed with a known amount of water, thus providing solutions with concentrations, and hence amounts of dissolved material that could be determined by absorption spectroscopy. When the component was, or contained, a glass fiber filter, it was washed by placing the filter in water in a container and leaving it in an ultrasonic cleaner for several minutes. Any glass fibers suspended in the resulting solution were removed by centrifugation.

Results and Evaluation

Buttonhook Nozzles--

The data from the nozzle evaluations are shown in Table 9. Nozzles larger than 0.95 cm (3/8 in.) in diameter could not be tested because higher air flow systems were not available. Generally it can be said that for the same flowrate, larger particles penetrated the buttonhook nozzles better, probably a result of higher inertia and subsequent bounce and re-entrainment.

TABLE 9. EVALUATION OF BUTTONHOOK NOZZLES

Nozzle Diameter, in.	Particle Size, μm	Flowrate, ℓ/min	Inlet Velocity, m/sec	Collection, %
1/8	15.2	7.22	15.2	27.6[a]
1/8	10.7	7.22	15.2	33.6
1/8	14.4	7.22	15.2	31.9
1/8	14.1	10.8	22.6	23.9
1/4	15.6	23.2	12.2	17.4
1/4	16.4	23.2	12.2	15.6
1/4	21.7	23.2	12.2	2.9[b]
1/4	14.1	28.3	15.2	30.7
1/4	14.2	23.2	12.2	42.0
3/8	10.6	56.5	13.1	52.7
3/8	15.2	65.1	15.2	27.3

a) Difficulty with particle generator
b) Low collection efficiency probably due to large particle bounce

Impactors--

Test data for the cascade impactors are shown in Table 10. Because of the design of the University of Washington Mark V, it was considered to have the best chance of having upper stages

TABLE 10. EVALUATION OF COMMERCIAL CASCADE IMPACTORS USING FIFTEEN-MICRON AERODYNAMIC DIAMETER PARTICLES

Impactor	Sierra Model 226		Sierra Model 226		Sierra Model 226		Sierra Model 226	
Orientation	Horizontal		Horizontal		Vertical		Vertical	
Substrate	Sierra glass fiber		Sierra glass fiber		Glass fiber		Glass fiber	
Nozzle	Straight		Straight		Straight		Straight	
Nozzle Diameter (inches)	5/32		5/32		5/32		7/32	
Inlet Velocity (m/sec)	8.53		8.53		8.63		9.72	
Aerodynamic Particle Size (microns)	14.5		15.2		18.3 µm		14.5 µm	
Flow rate (lpm)	6.40		6.40		6.40		14.2	
	% of Total Mass	% Eff.	% of Total Mass	% Eff.	% of Total Mass	% Effic.	% of Total Mass	% Effic.
Nozzle	27.8	27.8	28.9	28.9	24.4	24.4%	35.1	35.1%
Nozzle Holder	9.8	13.6	16.9	23.7	10.8	14.3	8.0	12.3
Total Wall Loss	37.6	37.6	45.8	45.8	35.2	35.2	43.1	43.1
Stage 0	6.8	10.9	4.7	8.7	NA	NA	NA	NA
Stage 1	7.6	13.7	7.4	14.9	3.8	5.9	4.6	8.1
Stage 2	17.0	35.5	26.5	62.8	13.2	21.7	19.6	37.6
Stage 3	16.7	53.9	8.5	54.0	40.0	83.7	18.2	55.8
Stage 4	7.1	50*	3.6	50.6	5.5	70.1	9.1	62.9
Stage 5	3.6*	50*	3.6	100*	1.9	79.7	3.0	56.5
Stage 6	1.8*	50*	-	-	0.5	100	2.3	100
Stage 7	NA	NA	NA	NA	-	-	-	-
Stage 8	NA	NA	NA	NA				
Back-up	1.8*	100*	-	-				
Comments	*Assumed Particles observed microscopically on all stages		*Assumed Particles observed microscopically on each stage				Water spilled on Stage 3 during washdown	

- Collected mass too little to measure
NA-stage does not exist in this model

TABLE 10. (Continued)

Impactor:	MRI Model 1506		MRI Model 1506		Andersen Mark III		Andersen Mark III	
Orientation:	Horizontal		Horizontal		Horizontal		Horizontal	
Substrate:	Glass fiber		Grease		Andersen glass fiber		Andersen glass fiber	
Nozzle:	Straight		Straight		Straight		Straight	
Noz. Diam.: (inches)	1/4		.25		0.24		0.24	
Inlet Vel.: m/sec	8.23		8.20		8.84		8.84	
Part. Diam.: μm	14.6		14.8		14.2		14.7	
Flowrate: lpm	15.6		15.6		15.6		15.6	
	% of Total Mass	% Eff.	% of Total Mass	% Effic.	% of Total Mass	% Eff.	% of Total Mass	% Eff.
Nozzle	7.8	7.8	6.9	6.9%	26.3	26.3	23.6	23.6
Holder	62.6	67.8	42.3	45.4	16.3	22.1	18.9	24.7
Wall Loss:	70.3	70.3	49.2	49.2	42.5	42.5	42.5	42.5
Stage 0	NA	NA	7.1	13.9	11.9	20.8	5.4	9.5
Stage 1	4.7	15.8	26.5	60.5	13.9	30.6	19.5	37.5
Stage 2	18.1	72.3	14.8	85.8	9.6	30.6	25.4	78.1
Stage 3	6.9	100*	2.5	100	13.3	60.7	7.1	100*
Stage 4	-	-	-	-	8.6	100*	-	-
Stage 5	-	-	-	-	-	-	-	-
Stage 6	-	-	-	-	-	-	-	-
Stage 7	-	-	-	-	-	-	-	-
	NA	NA			-	-	-	-
	-	-			-	-	-	-
Comments	*Assumed				Inter-Stage o-rings leaked during run. *Assumed		*Assumed	

TABLE 10. (Continued)

Impactor:	Brink		Brink		Brink	
Orientation:	Vertical		Vertical		Vertical	
Substrate:	Grease		Grease		Grease	
Nozzle:	Straight		Straight		Straight	
Nozzle Diameter:(mm)	1.5		1.7		1.7	
Inlet Velocity: m/sec	8.02		12.5		12.5	
Particle Diameter: μm	15.2		15.0		12.8	
Flowrate: lpm	0.85		1.70		1.70	
	% of Total Mass	% Efficiency	% of Total Mass	% Efficiency	% of Total Mass	% Efficiency
Nozzle	28.4%	28.4%	57.1%	57.1%	25.5%	25.5%
Cyclone	71.6	100	42.9	100	37.2	49.9
Stage 0	-	-	-	-	34.5	92.2
Stage 1	-	-	-	-	2.9	100
Stage 2	-	-	-	-	-	-
Filter	-	-	-	-	-	-

Impactor:	Brink		Brink		Brink	
Orientation:	Vertical		Vertical		Vertical	
Substrate:	Grease		Grease		Grease	
Nozzle:	Straight		Straight		Straight	
Nozzle Diameter:(mm)	1.5		1.5		1.7	
Inlet Velocity:m/sec	8.02		8.02		12.5	
Particle Diameter:μm	12.6		9.5		9.3	
Flowrate: lpm	0.85		1.13		1.70	
	% of Total Mass	% Efficiency	% of Total Mass	% Efficiency	% of Total Mass	% Efficiency
Nozzle	13.3%	13.3%	18.6%	18.6%	29.9%	29.9%
Cyclone	57.3	66.1	36.7	45.1	22.4	32.0
Stage 0	23.0	78.2	9.2	20.6	43.5	91.1
Stage 1	6.4	100	31.8	89.7	4.2	100
Stage 2	-	-	3.7	100	-	-
Filter	-	-	-	-	-	-

TABLE 10. (Continued)

Impactor:	Univ. of Wash.	Univ. of Wash.	Univ. of Wash.
Orientation:	Vertical	Vertical	Vertical
Substrate:	Grease	Grease	Grease
Nozzle:	Straight	Straight	Straight
Nozzle Diam. (inches)	3/16	3/16	¼
Inlet Velocity: m/sec	7.96	7.96	11.9
Particle Size: μm	15.2	16.4	15.2
Flowrate: lpm	8.49	8.49	22.7

	% of Total Mass	Collection Efficiency	% of Total Mass	Collection Efficiency	% of Total Mass	Collection Efficiency
Nozzle	37.9	37.9	43.6	43.6	27.9	27.9
Nozzle Holder	6.3	10.1	10.7	18.9	9.8	13.5
Stage 0	18.8	33.7	15.6	34.1	41.3	66.3
Stage 1	16.3	44.0	19.9	66.1	20.3	96.3
Stage 2	18.0	86.6	10.2	100.0	0.8	100.0
Stage 3	2.1	74.3	-	-	-	-
Stage 4	0.2	33.5	-	-	-	-
Spacers	0.5	100	-	-	-	-
Filter	-	-	-	-	-	-
Wall Loss	44.2	44.2	54.2	54.2	37.6	37.6

Comments: Stage Zero inverted in assembly.

Impactor:	Univ. of Wash.	Univ. of Wash.	Univ. of Wash.
Orientation:	Horizontal	Horizontal	Horizontal
Substrate:	Grease	Grease	Grease
Nozzle.	Straight	Straight	Straight
Nozzle Diam. (inches)	¼	3/26	3/16
Inlet Velocity: m/sec	11.9	7.96	13.3
Particle Size: μm	14.5	14.9	14.5
Flowrate: lpm	22.7	8.49	14.2

	% of Total Mass	Collection Efficiency	% of Total Mass	Collection Efficiency	% of Total Mass	Collection Efficiency
Nozzle	24.8	24.8	41.6	41.6	34.3	34.3
Nozzle Holder	8.2	10.9	3.7	6.4	7.4	11.3
Stage 0	40.7	60.8	9.8	17.9	27.8	47.6
Stage 1	25.0	95.3	16.9	37.6	26.1	85.3
Stage 2	1.2	100.0	25.2	90.3	4.5	100.0
Stage 3	-	-	2.7	100.0	-	-
Stage 4	-	-	-	-	-	-
Spacers	-	-	-	-	-	-
Filter	-	-	-	-	-	-
Wall Loss	33.0	33.0	45.4	45.4	41.7	41.7

which might have 15 µm aerodynamic diameter D_{50}'s at particular flowrates, 22.7, 14.2, and 8.49 ℓ/min (0.8, 0.5, and 0.3 acfm). These results are shown graphically in Figure 43, where the stage collection efficiency is shown as a function of the value of the dimensionless impaction parameter $\sqrt{\psi}$. For both the zero stage (nozzle) and the first stage, a $\sqrt{\psi_{50}}$ value could be clearly defined. For stage zero this value is 0.19, and for stage one $\sqrt{\psi_{50}} = 0.34$. The behavior of the zero stage is similar to results from previous calibration studies. Using these values of $\sqrt{\psi_{50}}$ it can be calculated that stage zero will have a D_{50} of 15 µm aerodynamic diameter at a flowrate of 15 ℓ/min (0.53 acfm) and that stage one will have the same D_{50} value at 9.35 ℓ/min (0.33 acfm). At 9.35 ℓ/min, stage zero would have a D_{50} of 19 µm aerodynamic diameter.

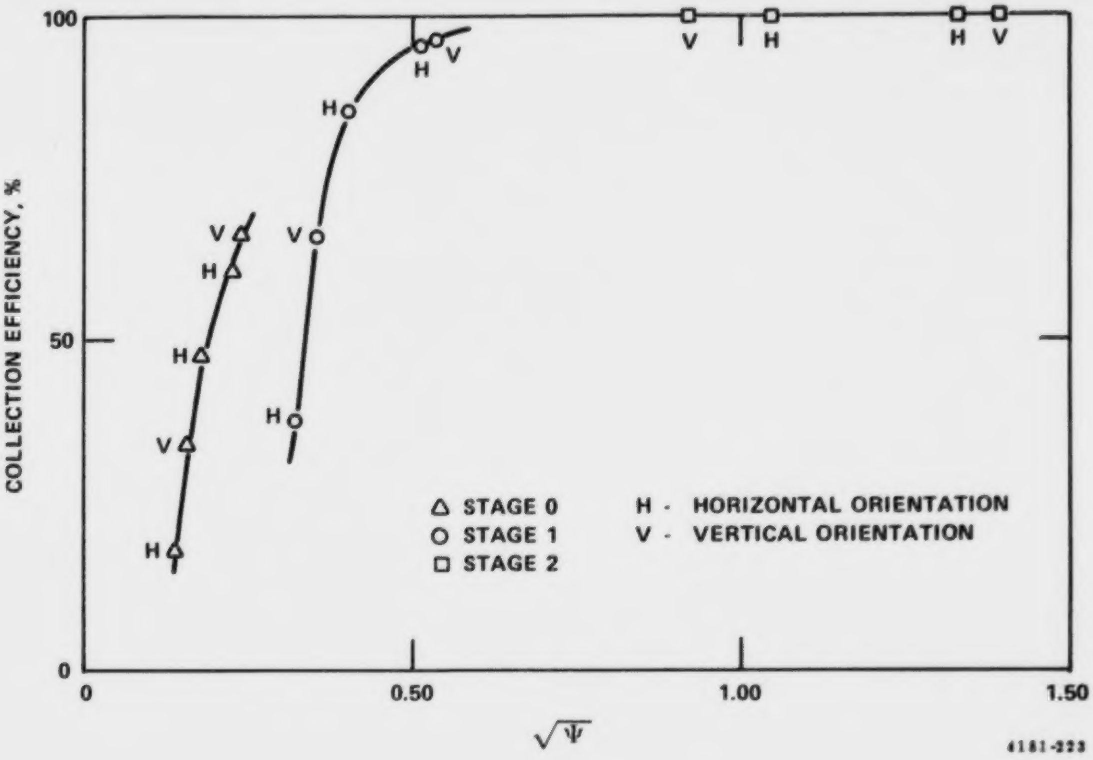

Figure 43. Calibration data for the first three stages of the University of Washington Mark V cascade impactor.

Even though a 15 µm D_{50} stage does exist for this impactor, overloading of large particles on either stage zero or stage one could result in serious re-entrainment problems.

In addition to the studies done to evaluate in-stack cascade impactors as IP collectors, tests were made of the Sierra Model

236 high-volume cascade impactor. This impactor was evaluated with glass fiber collection substrates and greased substrates with the intent of using it as a precollector for the Fugitive Ambient Sampling Train (FAST). The results of this evaluation are shown in Figure 44. Because of severe particle bounce, the Sierra impactor was rejected as an IP collector in favor of the horizontal elutriator described below.

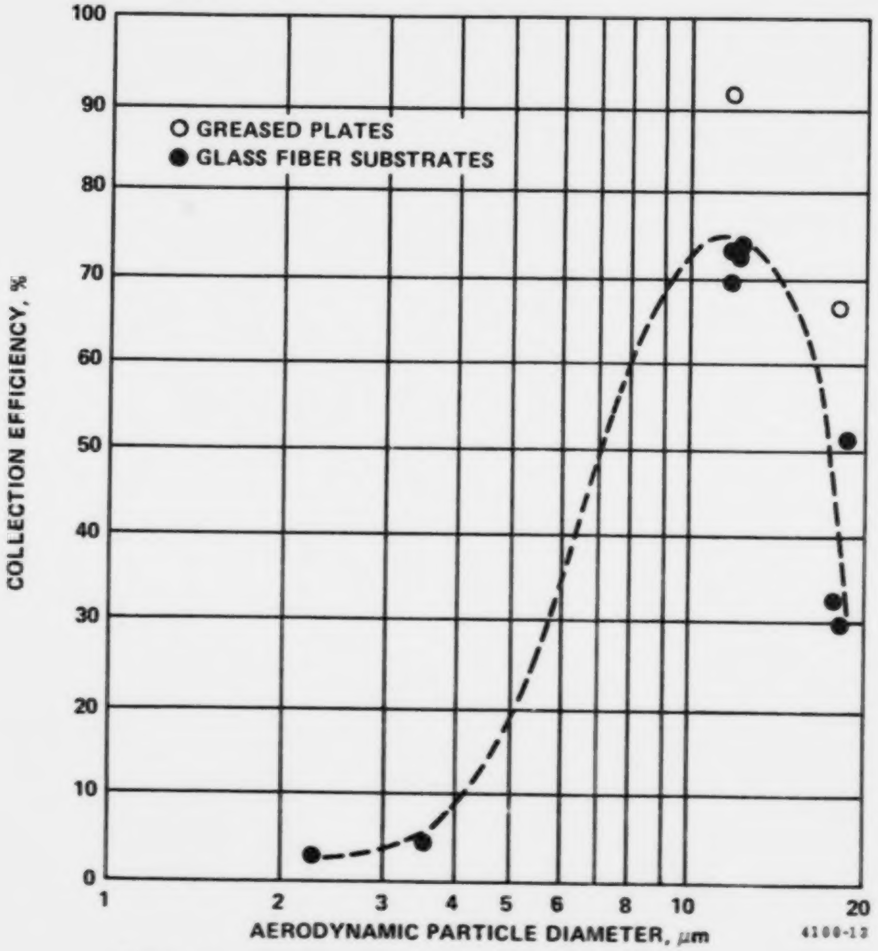

Figure 44. Particle collection efficiency for the impactor.

THE HORIZONTAL ELUTRIATOR AS AN IP PRECOLLECTOR

Background

Horizontal elutriators have been used extensively as devices for measuring and collecting particles and as apparatus for a variety of aerosol experiments.[17-20] The British Medical Research Council adopted the penetration curve of a particular horizontal elutriator as the definition of respirable particles.[21] Mercer has reviewed many of the practical applications of elutriators for sampling respirable particles.[22] Hamilton and Walton[21] have established the criterion that re-entrainment of deposited particles may occur if the ratio of mean air velocity to duct height (rectangular geometry) reaches a critical value which lies between 240 and 650 sec.$^{-1}$.

The experiments at Southern Research Institute on horizontal elutriators were performed to verify the theory of particle collection by settling and to develop design criteria for inlet collectors to be used in conjunction with two sampling systems developed for the Environmental Protection Agency: the Fugitive Ambient Sampling Train (FAST) and the Source Assessment Sampling System (SASS). Designs were also developed for the use of elutriators with in-stack cascade impactors.

The initial concept of the horizontal elutriator was the result of studies to measure quantitatively the deposition of aerosol particles on surfaces adjacent to, or suspended in, moving gas streams flowing through laboratory apparatus. Natanson[23] and Thomas[19] independently solved this problem theoretically for a circular horizontal tube of radius a. Although the derivations are somewhat complex, the results can be summarized and simplified in terms of the collection efficiency (Eff) by the following equation:

$$\text{Eff} = \frac{2}{\pi}\left[2\varepsilon\sqrt{1-\varepsilon^{2/3}} - \varepsilon^{1/3}\sqrt{1-\varepsilon^{2/3}} + \arcsin\varepsilon^{1/3}\right] \quad (18)$$

where

$$\varepsilon = \frac{3V_sL}{8a\bar{V}}$$

V_s is the settling velocity,

L is the length of tube,

a is the radius of tube, and

$\bar{V}$ is the average velocity of the gas.

The theory describing the performance of a rectangular flat plate elutriator is considerably less complex and is re-derived here to give the reader a better understanding of the particle motion in the elutriator. The settling velocity of spheres in a gas stream in laminar flow is given by the equation

$$V_s = \frac{C\rho g d^2}{18\ \mu} \tag{19}$$

where

V_s is the settling velocity,

g is the acceleration due to gravity,

C is the slip correction factor,

ρ is the particle density,

d is the particle diameter, and

μ is the viscosity of the gas.

In health-related studies, the aerodynamic behavior of the particles is of interest. It is therefore convenient to relate the settling velocity of all particles, whatever their shape or density, to that of spheres having unit density. The aerodynamic diameter is defined as the diameter of a unit density sphere having the same settling velocity as the particle of interest. The aerodynamic diameter is given from Equation 19 by setting $\rho = 1\ g/cm^3$ (the units must be retained). Also, for particles larger than about 2 μm, the slip correction factor is approximately equal to unity. A graph of settling velocity vs. diameter is shown in Figure 45.

For laminar flow between parallel plates, the velocity profile of a gas is parabolic with the maximum velocity equal to 1.5 times the average and with zero velocity at the plates:

$$V_x = \left(\frac{6y}{h} - \frac{6y^2}{h^2}\right)\bar{V} \tag{20}$$

where V_x is the velocity parallel to the plates, at a point y,

y is the displacement above the bottom plate,

h is the spacing between plates, and

$\bar{V}$ is the average velocity of the gas

The velocity profile and a typical particle trajectory are illustrated in Figure 46.

The efficiency with which particles are collected is determined by the dimensions of the channel, the velocity of the gas,

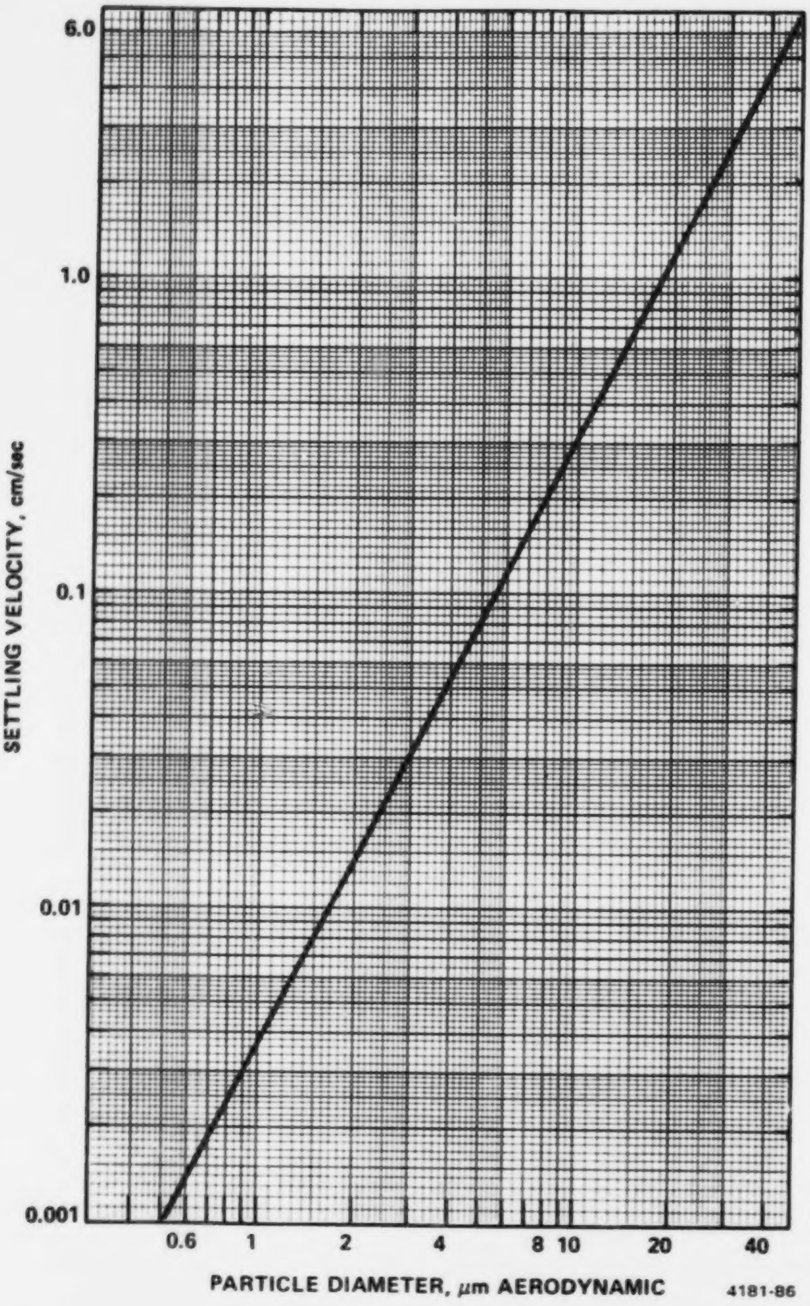

Figure 45. Settling velocity in air for unit density spheres.

the settling velocity of the particles, and the height at which the particles enter the channel.

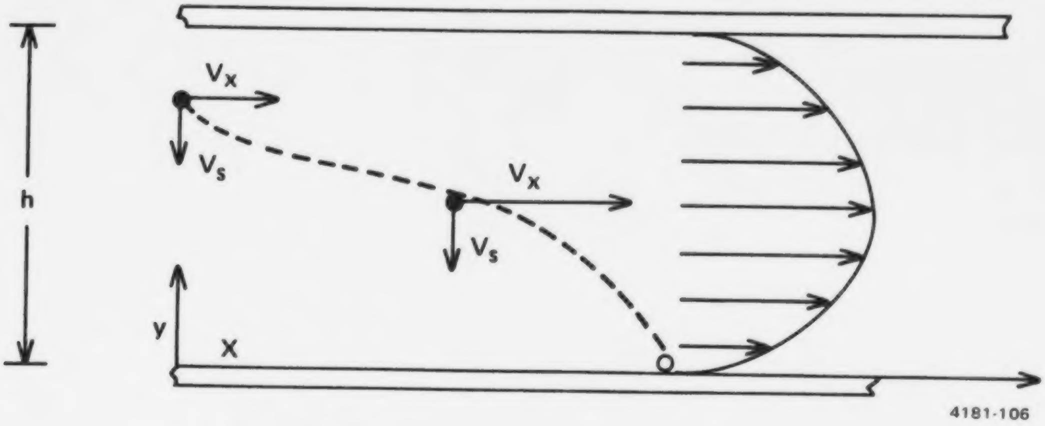

Figure 46. Velocity profile and particle trajectory between parallel plates.

Consider a particle which enters the channel at position y_o as shown in Figure 47 and which has a trajectory of length L (the length of the channel). All particles of this diameter or larger entering at or below position y_o will be captured. All particles of this diameter entering the channel at positions higher than y_o will penetrate the channel.

Now, from Equation 20:

$$\frac{dx}{dt} = \left(\frac{6y}{h} - \frac{6y^2}{h^2}\right) \bar{V}$$

but dy is given by dy = $-V_s dt$; therefore

$$\int_0^L dx = \frac{\bar{V}}{V_s} \int_{y_o}^{0} \left(\frac{6y}{h} - \frac{6y^2}{h^2}\right) dy; \text{ and } V_s L = \left(\frac{3y_o}{h} - \frac{2y_o^3}{h^2}\right) \bar{V} \qquad (21)$$

from which the settling velocity of the particle may be determined.

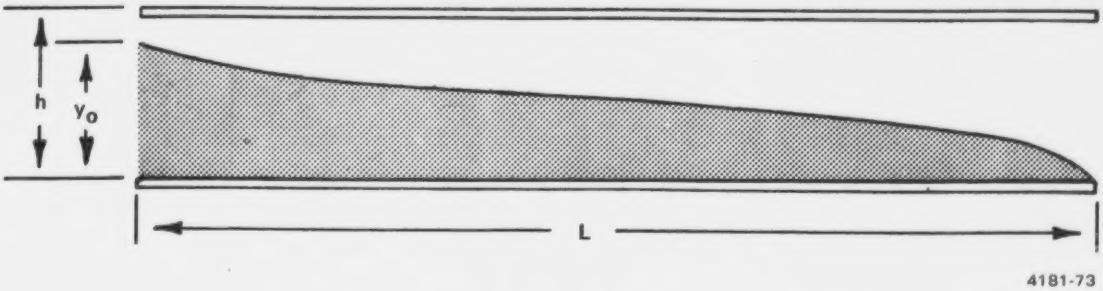

Figure 47. Zone of 100% particle collection.

If the particles are uniformly distributed within the gas, the fractional collection efficiency of the particle illustrated in Figure 46 is equal to the ratio of the volume of gas passing below position y_o to the total volume; thus:

$$\text{Eff} = \frac{W \int_{o}^{y_o} V_x \, dy}{W \int_{o}^{h} V_x \, dy}$$

where W is the width of the channel.

Now, from Equation 21,

$$\text{Eff} = \frac{V_s L}{h \, \overline{V}} = \frac{C \rho g d^2 L}{18 \, \mu h \, \overline{V}} \qquad (22)$$

The theoretical efficiency curves for a horizontal elutriator with a circular cross-section (from Equation 18) and for a horizontal elutriator with a rectangular cross-section (from Equation 22), both designed to have a cut point of 15 µm aerodynamic diameter, are shown for comparison in Figure 48.

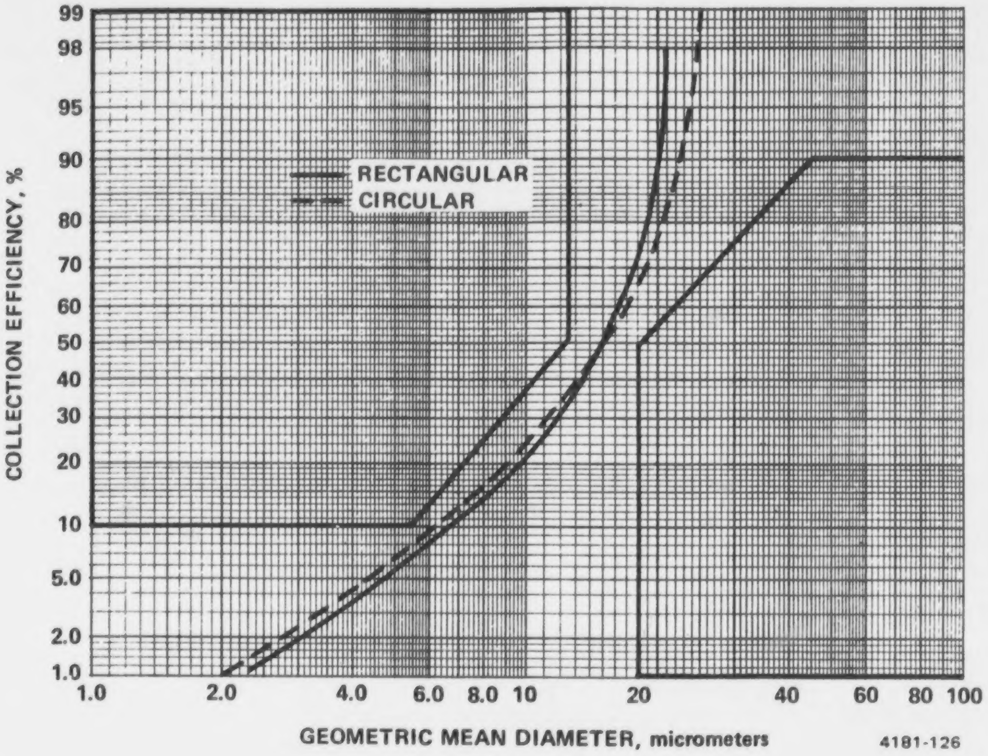

Figure 48. Theoretical collection efficiency by particle settling in rectangular and circular tubes.

The efficiency is found to be independent of the vertical velocity profile and, as Fuchs[17] observed, Equation 22 can be derived more easily assuming plug flow.

Experimental Procedures

Experiments were conducted to verify Equation 22 and to set design parameters for the FAST and SASS inlets. It should be noted that the systems tested here are designed so that the length and width are large relative to the height of the channels. This was done so that end and edge effects could be ignored.

Figure 49 is a schematic diagram of the experimental apparatus used to investigate the performance of a horizontal elutriator designed to have a cut point (D_{50}) of 15 μm aerodynamic diameter. The settling chamber consists of 28 channels, each 7 mm high, 17.8 cm wide, and 38.1 or 20 cm long. A high volume blower (Model 305, Sierra Instruments) connected in series with a variable voltage transformer was used to supply the desired air flow rate through the chamber. Monodisperse particles of

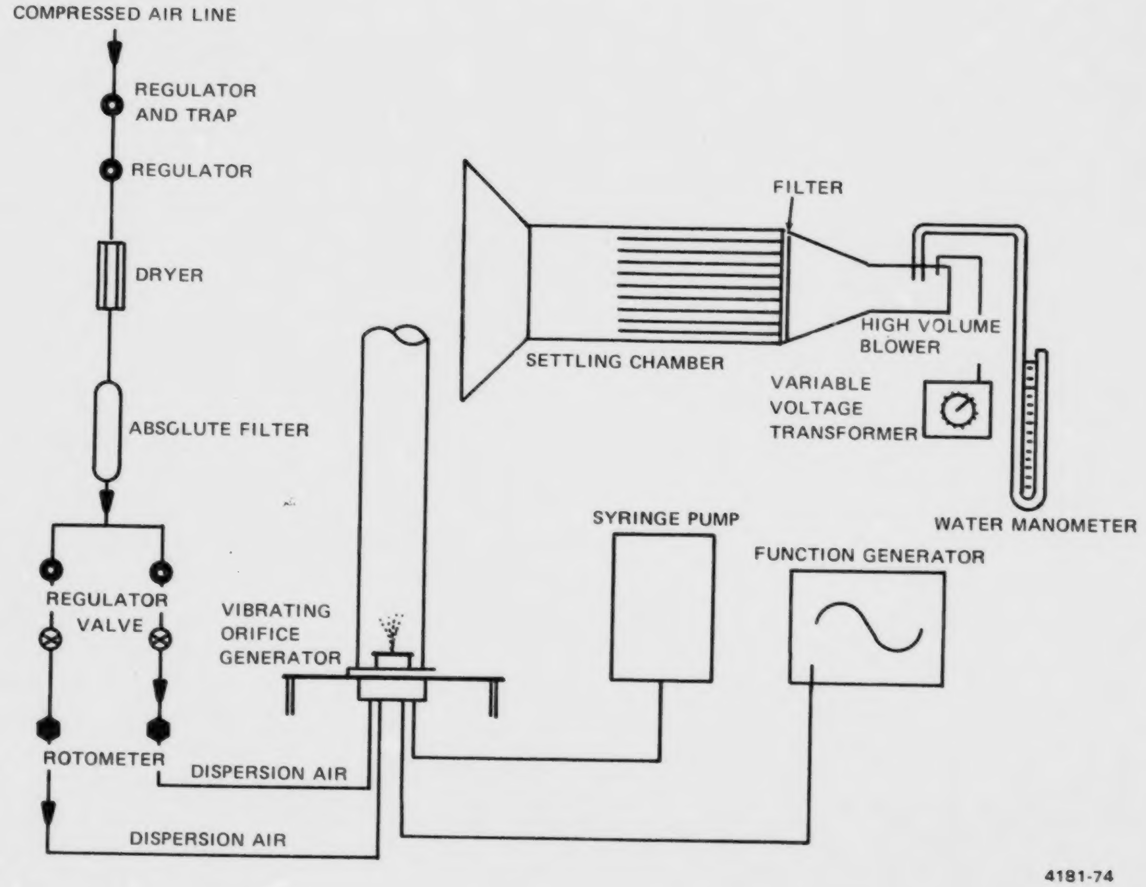
COMPRESSED AIR LINE
REGULATOR AND TRAP
REGULATOR
DRYER
ABSOLUTE FILTER
REGULATOR
VALVE
ROTOMETER
DISPERSION AIR
DISPERSION AIR
VIBRATING ORIFICE GENERATOR
SETTLING CHAMBER
FILTER
HIGH VOLUME BLOWER
VARIABLE VOLTAGE TRANSFORMER
WATER MANOMETER
SYRINGE PUMP
FUNCTION GENERATOR
4181-74

Figure 49. Apparatus used to measure the collection efficiency of the settling chamber.

methylene blue were generated using a vibrating orifice aerosol generator (VOAG) for particles larger than 4 μm aerodynamic diameter. During each test, the particles were sampled and checked frequently by optical microscopy to ensure constant monodispersity. All particles entering the horizontal elutriator were collected either by settling on the plates or on the 8 in. x 10 in. (20.3 cm x 25.4 cm) filter downstream from the plates.

Upon completion of each test, the plates and filter were washed separately with water. Samples from each wash were centrifuged to remove debris, and the amounts of methylene blue collected on the plates and on the filter were determined by absorption spectroscopy.

The velocity distribution through the settling chamber was studied to determine the configuration necessary to obtain uniform flow. The use of two filters and an extended flared inlet was necessary to provide the desired velocity distribution. Figure 50 is a velocity profile measured using a thermal anemometer immediately upstream from the blower before the plates were in position. From these data, it was evident that the blower was pulling uniformly across the rectangular opening where the 20.3 cm x 25.4 cm filter was positioned. Figure 51 shows the velocity profile measured upstream of the collector plates.

The velocity profiles shown in Figures 50 and 51 were considered satisfactory, and the overall average velocity was used to calculate the theoretical performance curves for the system. The average velocity through the chamber, measured using the thermal anemometer, was in agreement with previous calibration of the blower.

Results

Two sets of experimental data were obtained from the testing of the horizontal elutriator. The first set was acquired while operating the settling chamber at an average gas velocity of 70 cm/sec and a plate length of 38.1 cm. The second data set was obtained by operating the system at 40 cm/sec after shortening the plate length to 20 cm. The theoretical curves of the collection efficiency versus aerodynamic particle diameter shown in Figures 52 and 53 were developed from Equation 22 using the following parameter values:

Figure 52

ρ = 1.35 g/cm^3
g = 9.8 m/sec^2
L = 38.1 cm
μ = 181 micropoise
$\underline{h}$ = 0.701 cm
$\overline{V}$ = 70 cm/sec
Reynolds No. = 315

Figure 53

ρ = 1.35 g/cm^3
g = 9.8 m/sec^2
L = 20 cm
μ = 181 micropoise
$\underline{h}$ = 0.701 cm
$\overline{V}$ = 40 cm/sec
Reynolds No. = 180

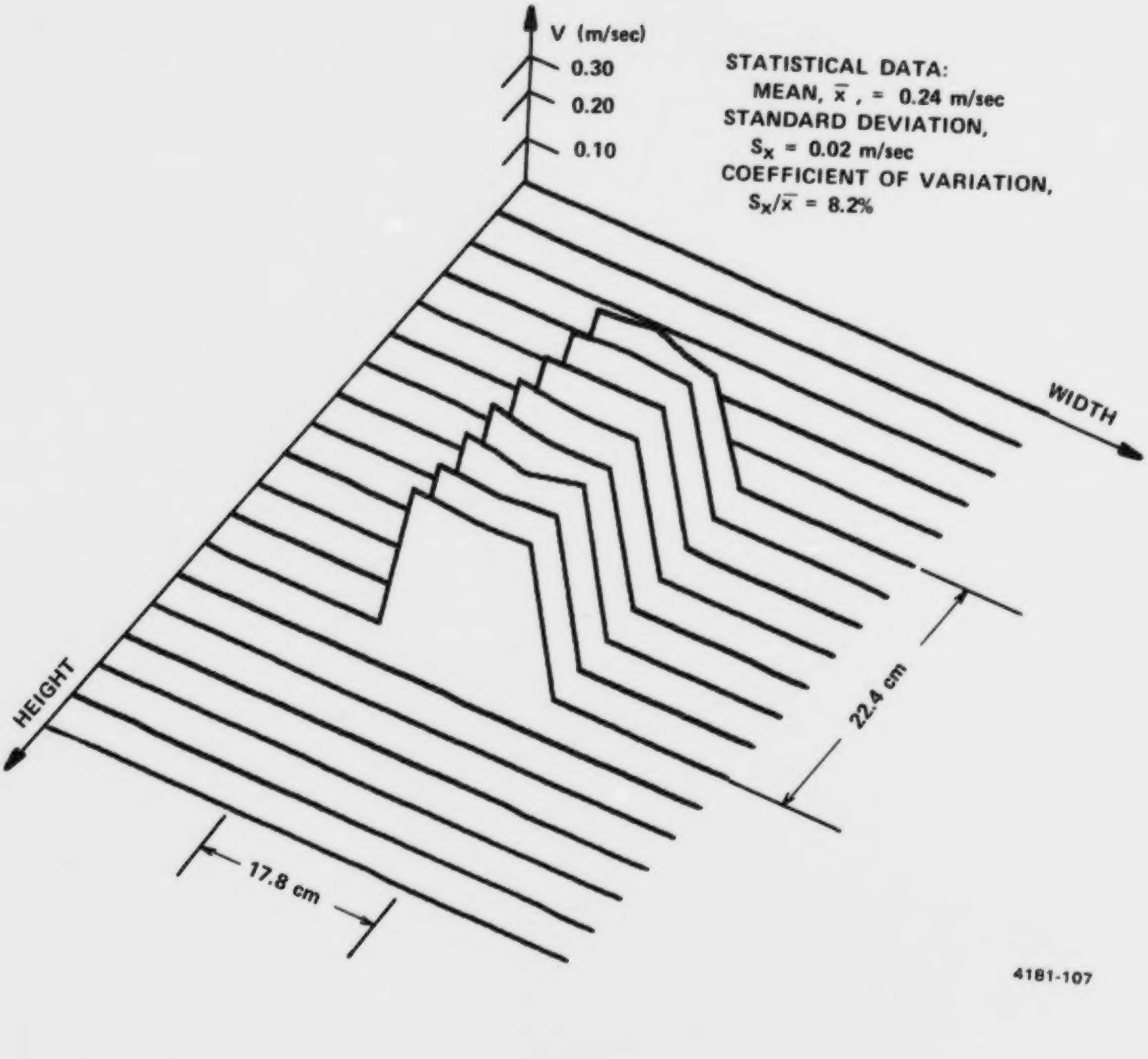

4181-107

Figure 50. Profile of the air velocity immediately upstream from the blower of the settling chamber before the plates were positioned.

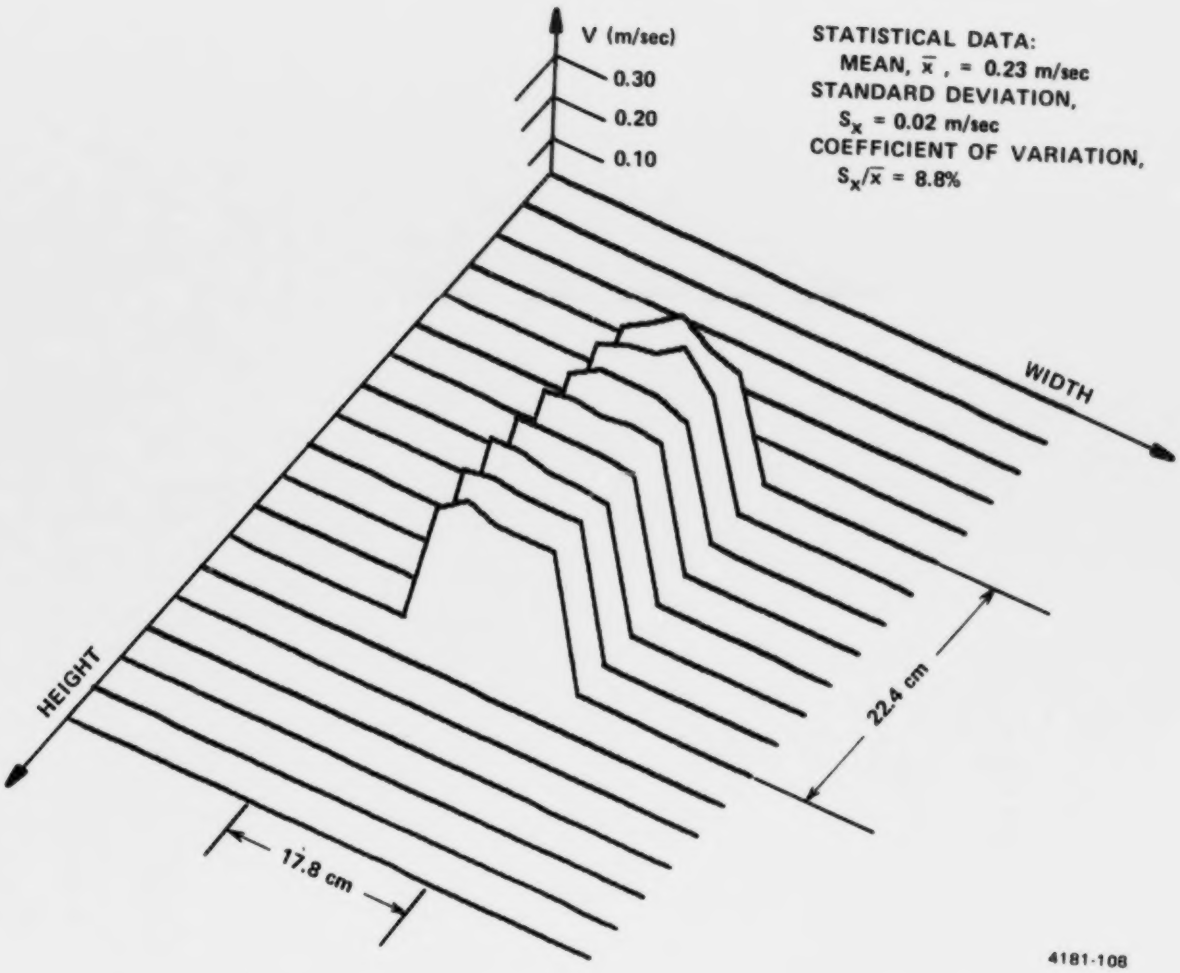

Figure 51. Profile of the air velocity upstream from the plates of the settling chamber.

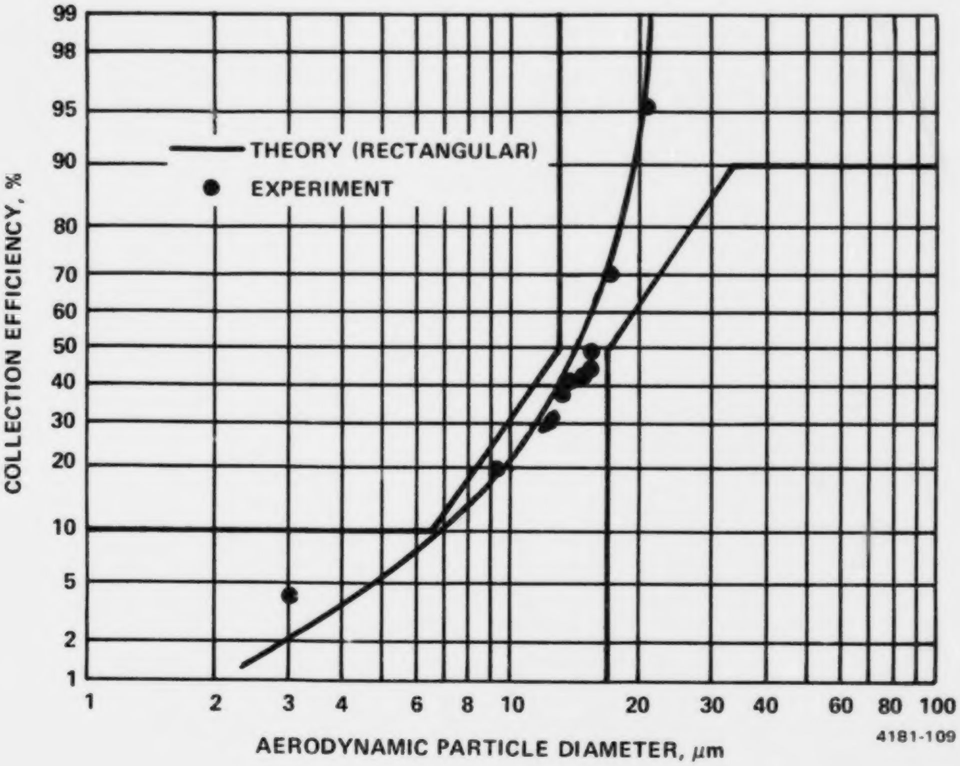

Figure 52. Theoretical and experimental collection efficiencies for a horizontal elutriator with rectangular cross-section, plate length 38.1 cm, average gas velocity 70 cm/sec.

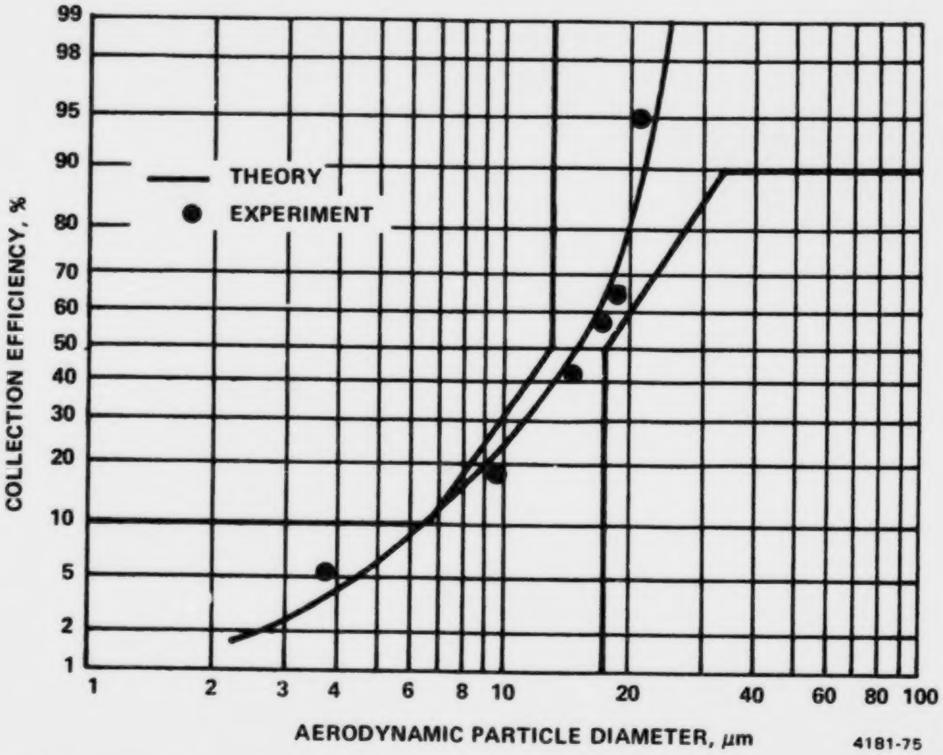

Figure 53. Theoretical and experimental collection efficiencies for a horizontal elutriator with rectangular cross-section, plate length 20 cm, average gas velocity 40 cm/sec.

The calculated values from theory for the collection efficiency were found to be in excellent agreement with the measured values. No corrections were made for end effects.

Collector Design

The experiments described above indicated that the theoretical equations can be used to predict particle collection by horizontal elutriators to a high degree of accuracy. Consequently, the equations were used to create design nomographs for inhalable particulate precollectors to be used in conjunction with the three systems of interest. Design parameters were calculated for horizontal elutriators to be used with: (1) cascade impactors operated at 14.2 ℓ/min and 149°C, (2) SASS trains operated at 185 ℓ/min and 204°C, and (3) FAST trains operated at 5,282 ℓ/min and 23°C.

Figures 54, 55, and 56 are the design nomographs for the three trains. On the vertical axis is the open area required, neglecting the thickness of the tube walls. The horizontal axis is the length of the elutriator required to yield the inhalable particulate performance at the specified flowrate and temperature. In constructing the graphs, it is assumed that the rectangular channels have widths much greater than their heights, so that the vertical walls will not have a significant effect on the gas flow.

THE FAST ELUTRIATOR INLET

Upon completion of the theoretical and prototype study of horizontal elutriators, an elutriator inlet was designed and fabricated for the Fugitive Assessment Sampling Train. It was designed to have a 15 μm aerodynamic diameter cut point at the normal operating flowrate. This inlet section was calibrated using ammonium fluorescein particles of 15 and 16 μm aerodynamic diameter generated with the VOAG. The collection efficiencies of the elutriator were 48% and 59%, respectively, for the two particle sizes. This is well within the designed collection efficiency for these particle sizes. The data obtained during this testing procedure are summarized in Table 11. Figure 57 depicts the experimental arrangement in the laboratory.

Horizontal Elutriator Inlet for Fugitive Emissions Sampler

The final application of this study of horizontal elutriators was the design of an inlet to be used with high volume impactors to measure the size and concentration of inhalable particulate matter in fugitive emission plumes.

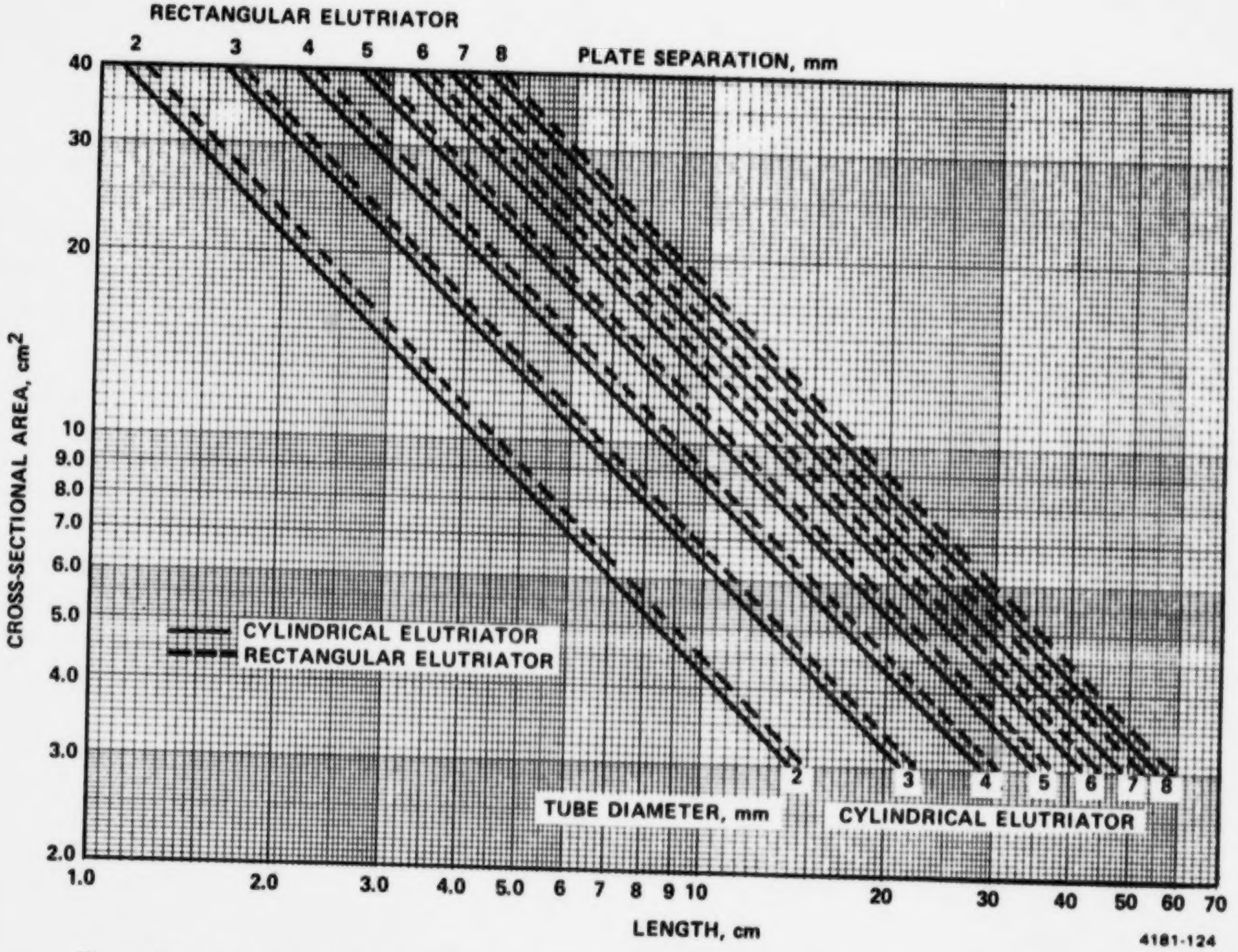

Figure 54. Relationship of design parameters for horizontal elutriators with D_{50} cutpoints of 15 µm aerodynamic diameter used as precollectors for in-stack cascade impactors.

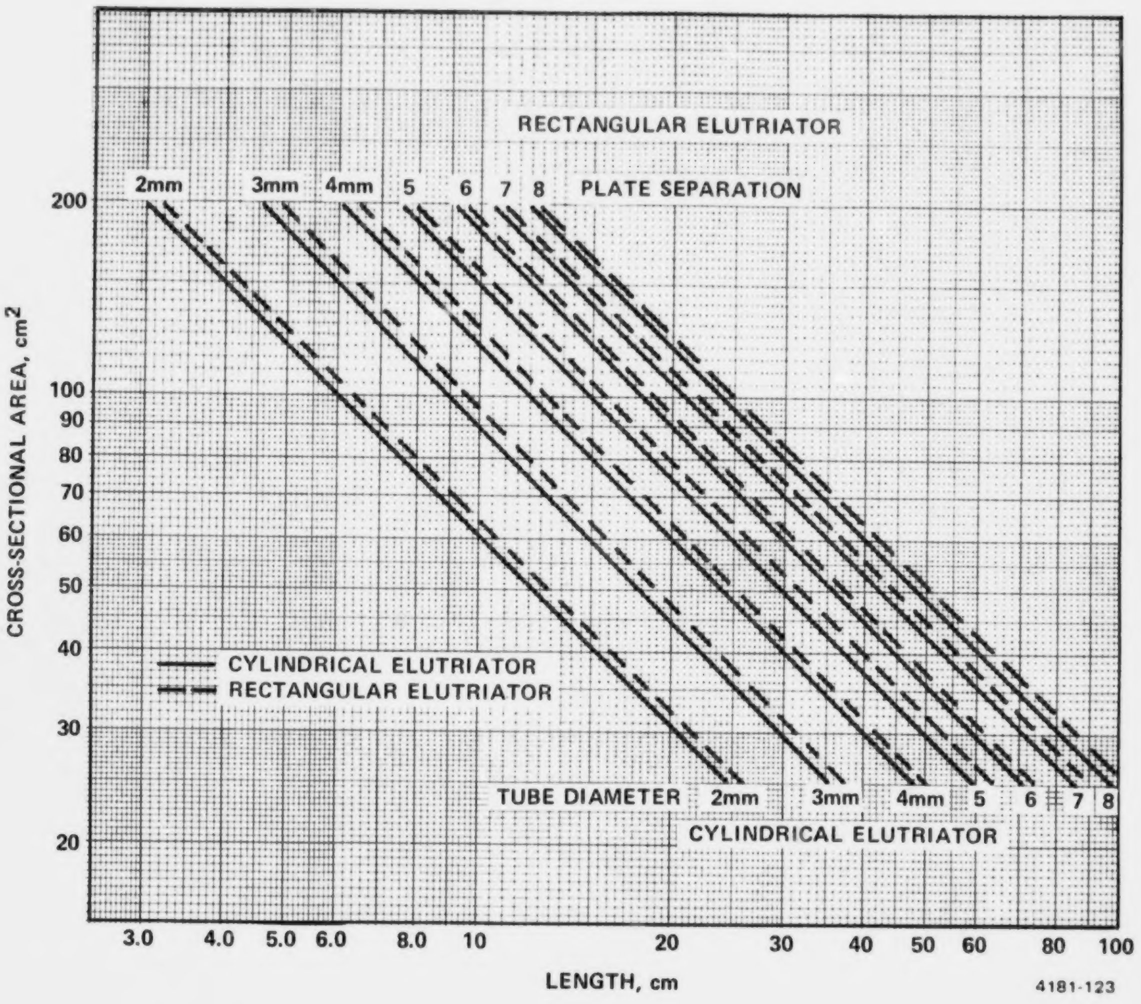

Figure 55. Relationship of design parameters for horizontal elutriators with D_{50} cutpoints of 15 μm aerodynamic diameter to be used with SASS trains.

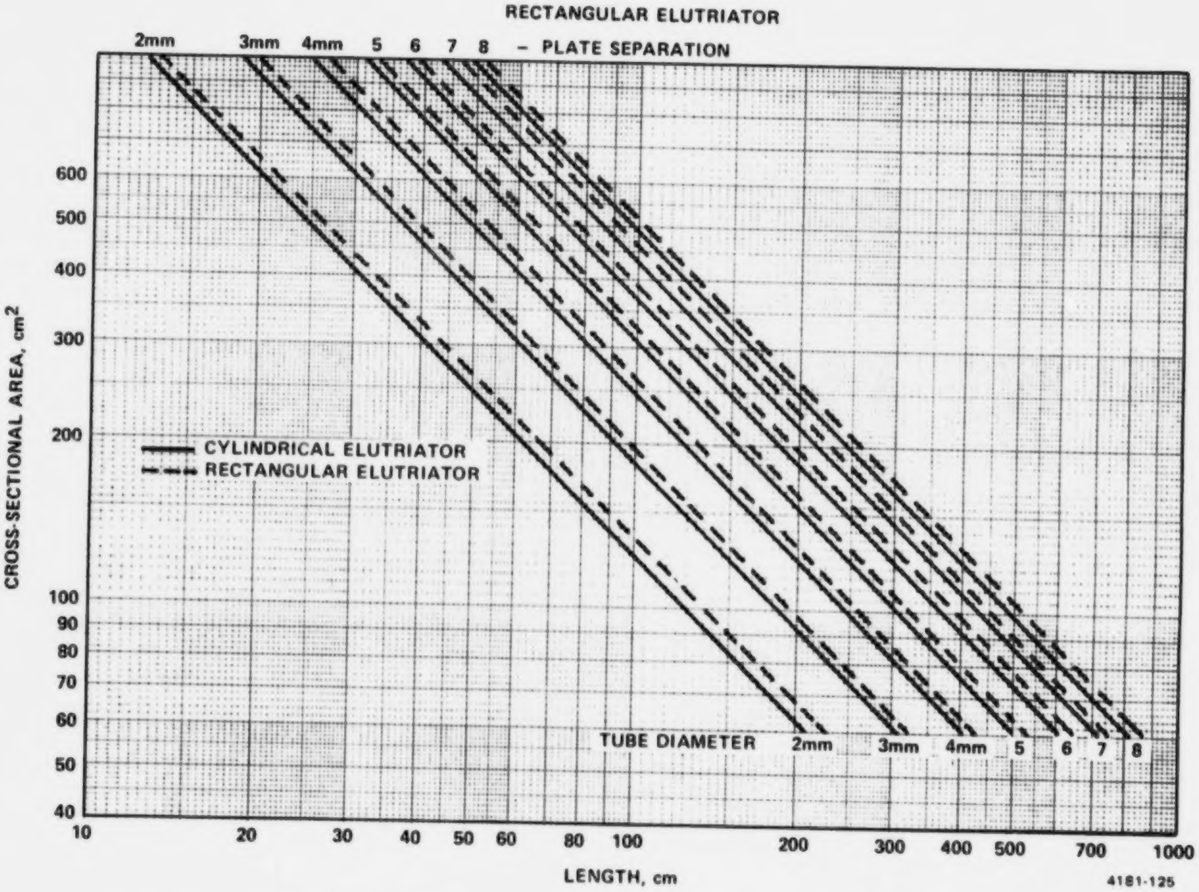

Figure 56. Relationship of design parameters for horizontal elutriators with D_{50} cutpoints of 15 µm aerodynamic diameter to be used with FAST trains.

TABLE 11. FAST HORIZONTAL ELUTRIATOR INLET TEST DATA

Test No.	1		2	
Aerodynamic Particle Diameter (μm)	16.0		15.0	
Filter Pressure Drop (in mercury)	2.0		2.2	
Sampling Duration (hr)	4		2.5	
	% of Total Mass	% Collection Efficiency	% of Total Mass	% Collection Efficiency
Inlet Louvre Section	0.75*	0.75	28.2	28.1
Screen	0.0009*	0.0009	5.34	7.4
Screen to Elutriator Transform	3.63	3.65	1.56	2.4
Elutriator Plates	56.2	58.8	31.2	47.8
Plate Holder Section	0.5	1.27	0.14	0.4
Filter Transform and Filter	38.9	100.0	33.7	100.0

*Questionable results due to inaccurate washing technique.

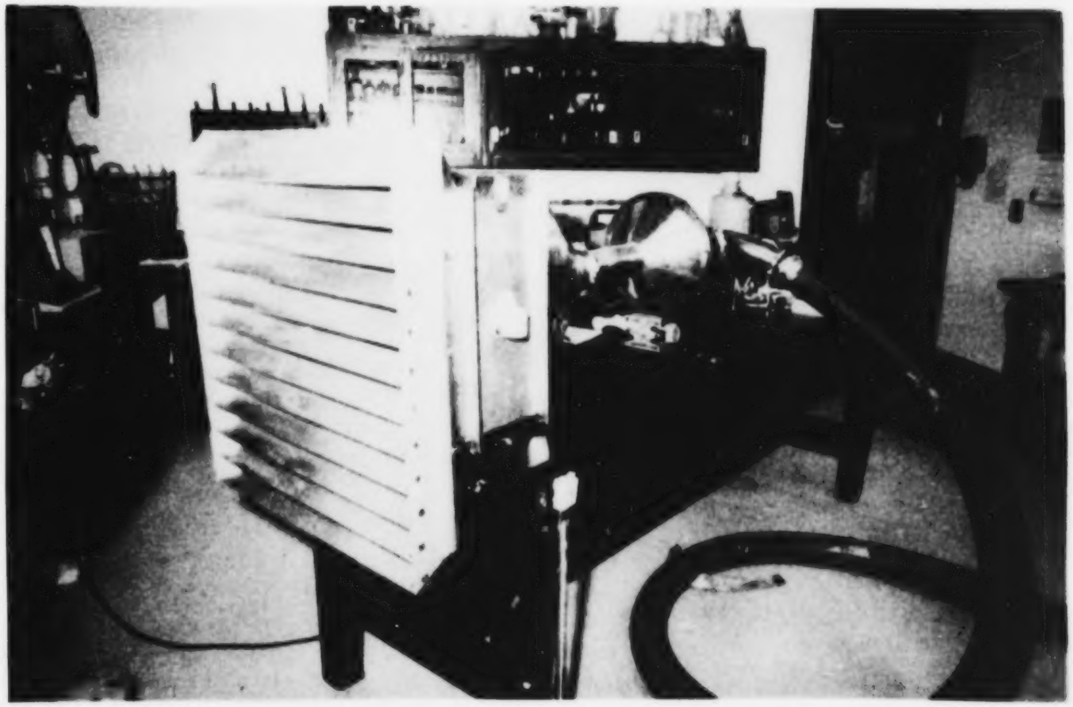

Figure 57. Laboratory set-up for testing FAST horizontal elutriator inlet.

The laboratory sampling device illustrated in Figure 49 was modified slightly by the addition of a cascade impactor between the horizontal elutriator section and the filter. The resulting system will be mounted on masts and arranged in a vertical, planar grid for measuring the plume "profile".

CYCLONES AS IP COLLECTORS

Background

Although no theory exists to adequately predict cyclone behavior, several experimental investigations have been performed demonstrating their utility for separating and sizing small particles.[24-26] Smith et al.[15] and John et al.[27] have demonstrated that the curves of particle collection efficiency for small cyclones can be as steep as those of impactors, and significant re-entrainment does not occur. Chan and Lippmann[28] have shown that experimental efficiency data for small cyclones can be fitted well using the empirical relationship:

$$\mathrm{Eff} = 0.5 + 0.5 \tanh \left[\left(\frac{D_p}{KQ^n} \right)^2 + \left(A - 2B \right) \frac{D_{pn}}{KQ^n} + B - A \right] \qquad (23)$$

where

Q is the sample flow rate, cm^3/sec,

D_p is the diameter of the sampled particle, cm, and

A,B,K,n are empirical constants.

Also it was shown that the D_{50} vs. flowrate relationship is given over a limited range of sampling conditions by:

$$D_{50} = KQ^n. \qquad (24)$$

From their own research and data reported by others, Chan and Lippmann reported values of K ranging from 6.17 to 4591, and values of n from -0.636 to -2.13. Smith et al. reported values of K from 14.0 to 44.6, and n from -0.63 to -1.11. Although the trend in the data is for n to have larger values for small cyclones (D_{50}'s) and K to be larger, the correlation is not consistent enough to be predicted from the cyclone geometry, and no data are reported for temperatures other than ambient. Furthermore, there are definite discontinuities and hysteresis effects in the relationship given in Equation 24, even for individual cyclones, as the flow is increased and decreased. The discontinuous and hysteresis effects are generally attributed to transitions from turbulent to laminar flow, or the reverse, in the outlet tube of the cyclone as the flow is changed.[25-28]

Smith et al.[15] found the D_{50} of cyclones to increase linearly as the gas temperature and viscosity were increased; but again the rate of increase was not predictable from the cyclone geometry. Certainly a modification to Equation 24 would be required to predict any temperature dependence. Lacking an adequate theory for predicting the performance of cyclones before they are designed and calibrated, it was found necessary in this study, as in previous work, to extrapolate the dimensions for a new cyclone to give the desired performance from those of similar cyclones of known performance. Several cyclones were calibrated to determine a basis for extrapolation for the new IP Sampler cyclone dimensions.

However, because of these difficulties, and the requirement that the inhalable particulate cyclones always be operated to yield D_{50}'s at 15 ± 2 µm, it was still considered necessary to calibrate them over a range of temperatures and flowrates similar to those expected in field operation.

Calibration of the Brink Cyclone

The Brink precollector cyclone (Southern Research Institute design) was calibrated at ambient temperature and at 100 and 150°C. Ammonium fluorescein particles of 15 µm aerodynamic diameter were generated by a vibrating orifice aerosol generator, heated, and then sampled by the cyclone. The flowrate was varied to determine the flowrate at which the cyclone collected 15 µm particles with 50% efficiency. The results of these tests are shown in Figures 58 and 59 and in Table 12. The Brink cyclone has a D_{50} of 15 µm at 0.51 ℓ/min at ambient temperatures, 0.79 ℓ/min at 100°C and 1.1 ℓ/min at 150°C.

Calibration of the Sierra Cyclone

The first cyclone in the Sierra Instruments, Inc. Model 283 Cyclade (TM) four-stage instack cascade cyclone sampler was calibrated at ambient temperature with 15 µm aerodynamic diameter ammonium fluorescein particles. The cyclone was found to have a D_{50} of 15 µm at 5 ℓ/min. The calibration data are presented in Table 13.

Calibration of the Southern Research Institute Five-Stage Cyclone

The individual cyclones of the Southern Research Institute Five-Stage Cyclone System were calibrated in the laboratory under conditions similar to those frequently encountered in the field.

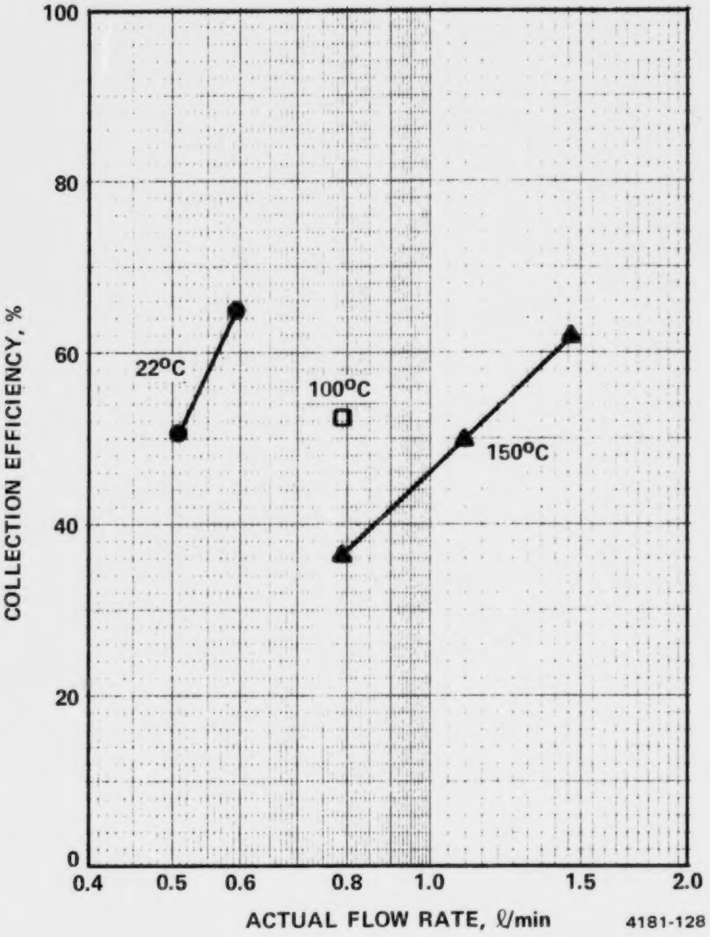

Figure 58. Collection efficiency versus flowrate for a Brink precollector cyclone sampling 15 μm aerodynamic diameter ammonium fluorescein particles at 22, 100, and 150°C.

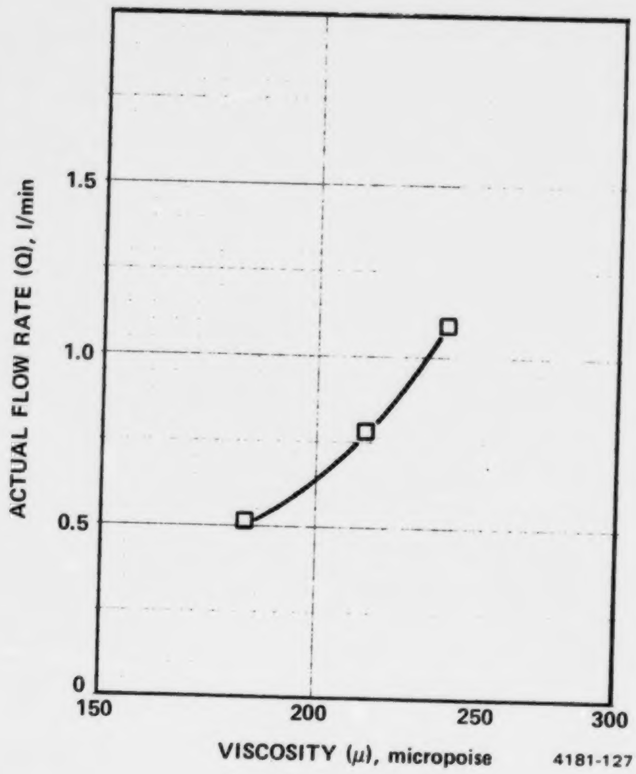

Figure 59. Flowrate versus viscosity to maintain a D_{50} = 15 μm aerodynamic for Brink precollector cyclone.

TABLE 12. CALIBRATION RESULTS FOR THE BRINK CYCLONE

D_p = 15 μm Aerodynamic

Temperature, °C	Flowrate, ℓ/min	Collection Efficiency, %
150	0.79	37
150	1.5	62
150	1.1	50
100	0.79	53
23	0.60	65
21	0.51	51

TABLE 13. SIERRA CYCLONE CALIBRATION DATA

Flowrate, ℓ/min	Temperature, °C	Aerodynamic Particle Diameter, μm	Collection Efficiency, %
7	23	15.1	96.1
7	23	15.0	95.6
14	23	14.5	64.6
14	23	14.3	58.0
14	23	9.9	27.4
14	23	7.1	14.1
21	23	7.1	10.1
21	23	10.3	40.1
21	23	15.4	71.9

The D_{50} cut points of these cyclones at various operating conditions are given in Table 14. For laboratory conditions (temperature 22°C, flowrate 28.3 ℓ/min, and particle density 1.0 g/cm^3) the cut points are 5.6, 2.1, 1.4, 0.63, and 0.33 μm, as shown by the calibration curve of efficiency vs. aerodynamic particle diameter in Figure 60.

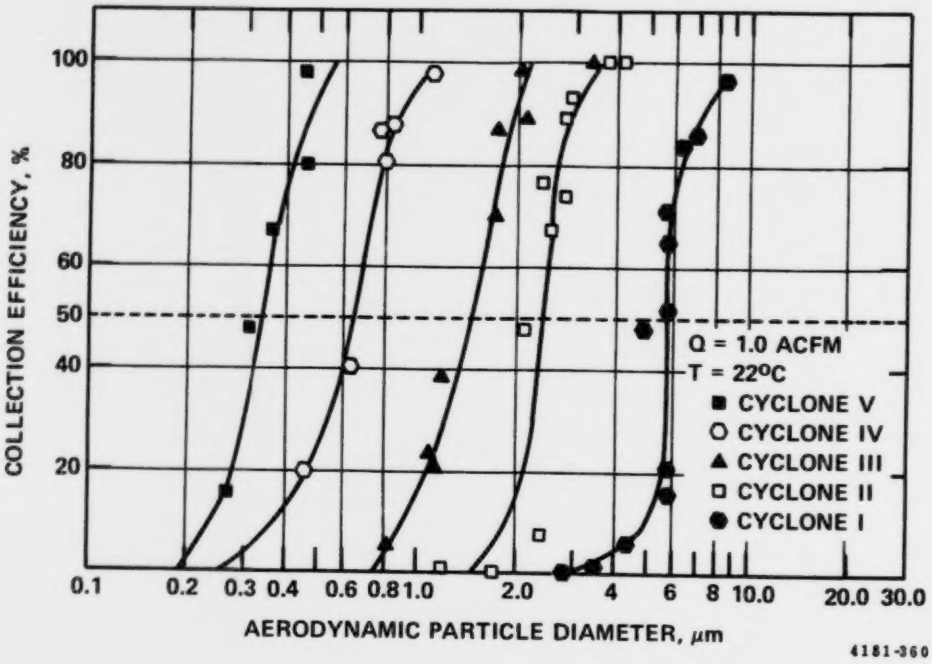

Figure 60. Calibration curves for the five-stage cyclone system. Flow rate 1.0 ft^3/min, temperature 22°C.

AN INHALABLE PARTICULATE PRECOLLECTOR AND SAMPLING TRAIN

Development and Fabrication

The objective of this phase of the program on the development of samplers for inhalable particles was the design and evaluation of two systems: (1) a cyclone to be used as a precollector for cascade impactors, and (2) a system, consisting of two cyclones and a filter in series, to be used as the primary system for measuring the total particulate concentration, the inhalable particulate concentration, and the fine particle concentration (<2.5 μm). Both systems are to be used in process streams where the particle concentration and temperature are generally much higher than in the atmosphere. The precollector for impactors and the first cyclone in the series train must have

TABLE 14. LABORATORY CALIBRATION OF THE FIVE-STAGE CYCLONES D_{50} CUT POINTS

Flowrate, ℓ /min	Temperature, °C	D_{50} Cut Points, μm (ρ = 1.0 gm/cm^3) Cyclone I	Cyclone II	Cyclone III	Cyclone IV	Cyclone V
7	22	-	-	-	2.6	1.6
9.7	22	-	-	3.1	-	-
14	22	8.2	3.6	2.3	1.4	0.84
20	22	-	3.1	-	-	-
21	22	-	2.8	-	-	-
21	22	-	2.3	-	-	0.65
28	22	5.6	2.1	1.4	0.63	0.33
19.8	93	-	-	2.5	-	-
28	93	6.4	3.1	1.8	-	-
14	151	-	-	5.0	-	-
19.4	151	-	-	2.5	-	-
28	151	-	3.4	2.9	-	-
28	204	8.6	4.1	3.1	-	-

efficiency curves satisfying the specifications for inhalable particulate samplers shown in Figure 2. The second cyclone in the series train must be designed to have a D_{50} of 2.5 ± 0.5 μm aerodynamic.

The nominal operating conditions used in designing the systems were flowrates of 14 ℓ/min and 21 ℓ/min at 150°C, respectively, for the precollector and cyclone systems. With these operating conditions as a goal, the dimensions of the cyclones were extrapolated from those previously evaluated.[15]

Figures 61 and 62 are schematic illustrations of the two new systems. The precollector cyclone is designated SRI-IX and the large cyclone in the series train, SRI-X. Cyclone SRI-III, which had been previously evaluated as part of the SRI/EPA 5-stage cyclone train, was found to be adequate for the smaller cyclone in the new system.

The critical dimensions of all three cyclones are given in Figure 63.

Calibration

In order to calibrate the cyclones at elevated temperatures, the heating arrangement shown in Figure 64 was used in conjunction with the vibrating orifice aerosol generator described above. Tests were made at temperatures of 23°C, 93°C, and 150°C. Ammonium fluorescein particles were used for calibrating the cyclones. Samples were taken frequently of the heated aerosol to ensure that the calibration system was stable and that the particles were spherical and of the proper size.

In this study, the primary objective was to determine the operating conditions under which the cyclones satisfied the design criteria. For this purpose, it was sufficient to use an abbreviated calibration procedure and thus to reduce the extensive amount of testing that would be needed for complete calibration. At a specific temperature, monodisperse particles having nominal aerodynamic diameters of 15 μm were generated and sampled. Tests were made at a variety of flowrates to determine the sampling rate required to yield a D_{50} of 15 μm at the given temperature. Only limited data were taken to determine collection efficiency vs. particle diameter.

When preparing to generate monodisperse particles using the vibrating orifice method, it is necessary to know the solution flowrate and frequency of vibration in order to calculate the concentration of solute required to yield the desired particle diameter after drying. In practice, the flowrate can be selected and the solution prepared precisely, but the frequency at which the generator is finally found to yield maximum stability is

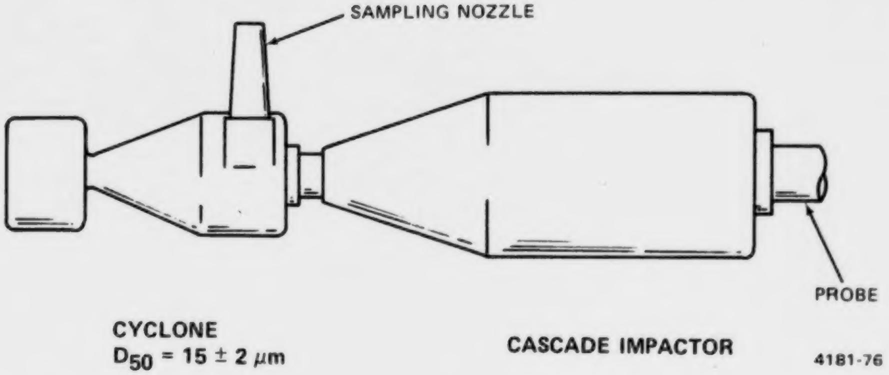

SAMPLING NOZZLE
PROBE
CYCLONE
D_{50} = 15 ± 2 μm
CASCADE IMPACTOR
4181-76

Figure 61. Schematic of a cascade impactor-precollector cyclone system.

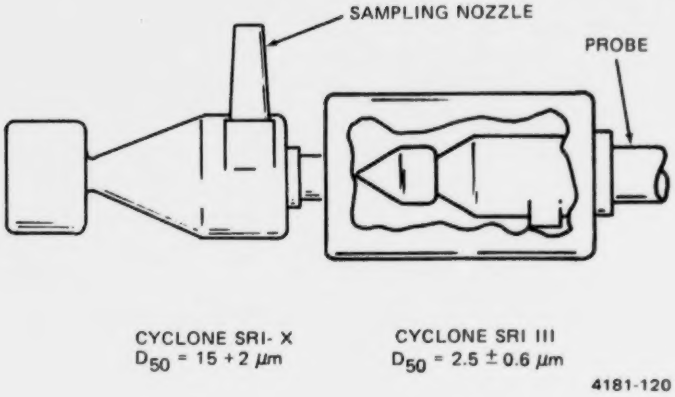

SAMPLING NOZZLE
PROBE
CYCLONE SRI- X
D_{50} = 15 + 2 μm
CYCLONE SRI III
D_{50} = 2.5 ± 0.6 μm
4181-120

Figure 62. Schematic of two-cyclone system.

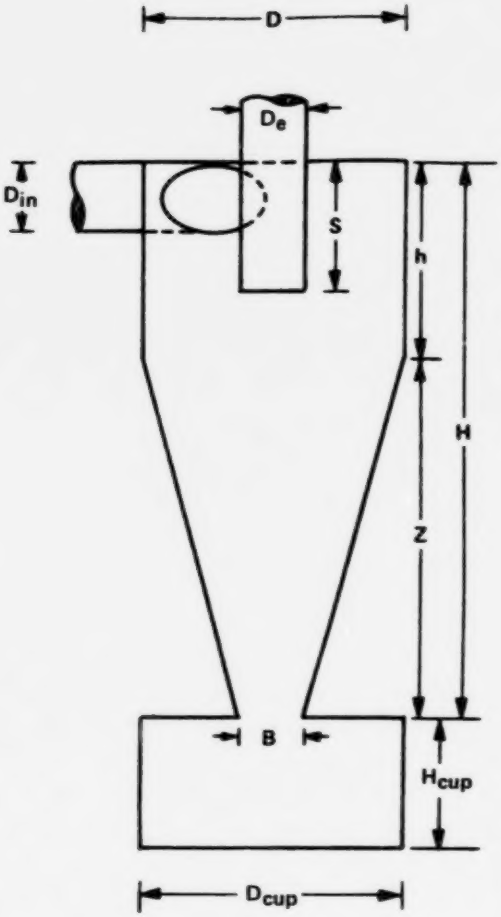

DIMENSIONS (CENTIMETERS)

CYCLONE	D	D_{in}	D_e	B	H	h	Z	S	H_{cup}	D_{cup}
SRI-X	6.14	1.83	2.17	2.92	8.47	2.82	5.65	2.40	2.635	6.14
SRI-III	3.11	0.75	0.83	0.76	4.91	1.40	3.51	1.08	2.22	3.10
SRI-IX	5.12	1.53	1.81	2.43	7.06	2.35	4.71	2.00	2.26	5.12

4181-22

Figure 63. Summary of cyclone dimensions.

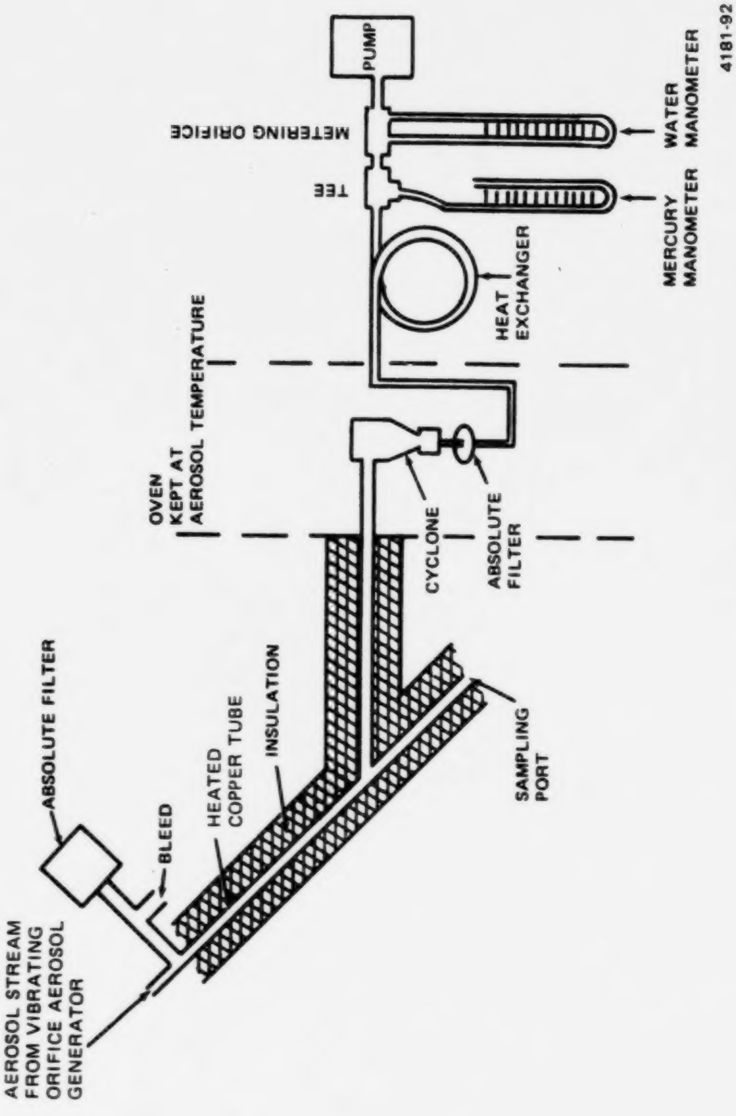
AEROSOL STREAM FROM VIBRATING ORIFICE AEROSOL GENERATOR
ABSOLUTE FILTER
BLEED
HEATED COPPER TUBE
INSULATION
SAMPLING PORT
OVEN KEPT AT AEROSOL TEMPERATURE
CYCLONE
ABSOLUTE FILTER
HEAT EXCHANGER
TEE
METERING ORIFICE
PUMP
MERCURY MANOMETER
WATER MANOMETER
4181-92

Figure 64. Calibration system for heated aerosols.

unpredictable to some extent. Therefore, as indicated in the figure captions, the actual particle diameters differed slightly from 15 μm. In these tests the particles had aerodynamic diameters of 15.0 ± 0.6 μm.

Results

Figures 65-68 show the calibration data for the three cyclones. In Figure 65, the particle collection efficiency is plotted vs. flowrate for cyclone SRI-IX.

As indicated in the figure, data were taken at 23°C, 93°C, and 150°C. Similar data are shown in Figure 66 for cyclone SRI-X.

The settling velocity in air of 15 μm particles is 0.7 cm/sec and there was some concern that settling might influence the collection efficiency of the larger cyclones by making them sensitive to orientation. In Figure 66, which contains calibration data for cyclone SRI-X, data are shown taken with the cyclone in both vertical and horizontal orientations. It can be seen that there is little, if any, effect due to particle settling.

The data reported in Figures 65 and 66 will be used to select the flowrates of the new sampling trains. Since there is no adequate theory for calculating cyclone efficiency, cyclone SRI-III was calibrated at the same flowrates required for proper operation of cyclone SRI-X. These calibration data are shown in Figure 67. D_{50}'s and flow conditions for the three cyclones, as derived from the graphs, are:

Cyclone SRI-III

3.1 μm (aerodynamic) D_{50} at 23°C, 11 ℓ/min
2.6 μm (aerodynamic) D_{50} at 93°C, 20 ℓ/min
2.3 μm (aerodynamic) D_{50} at 150°C, 23 ℓ/min

Cyclone SRI-IX

15 μm (aerodynamic) D_{50} at 23°C, 6.8 ℓ/min
15 μm (aerodynamic) D_{50} at 93°C, 12 ℓ/min
15 μm (aerodynamic) D_{50} at 150°C, 14 ℓ/min

Cyclone SRI-X

15 μm (aerodynamic) D_{50} at 23°C, 11 ℓ/min
15 μm (aerodynamic) D_{50} at 93°C, 20 ℓ/min
15 μm (aerodynamic) D_{50} at 150°C, 23 ℓ/min

Also, limited data were taken with particles with diameters other than 15 μm using cyclone IX. These are shown plotted with the inhalable particulate performance specifications in Figure 68.

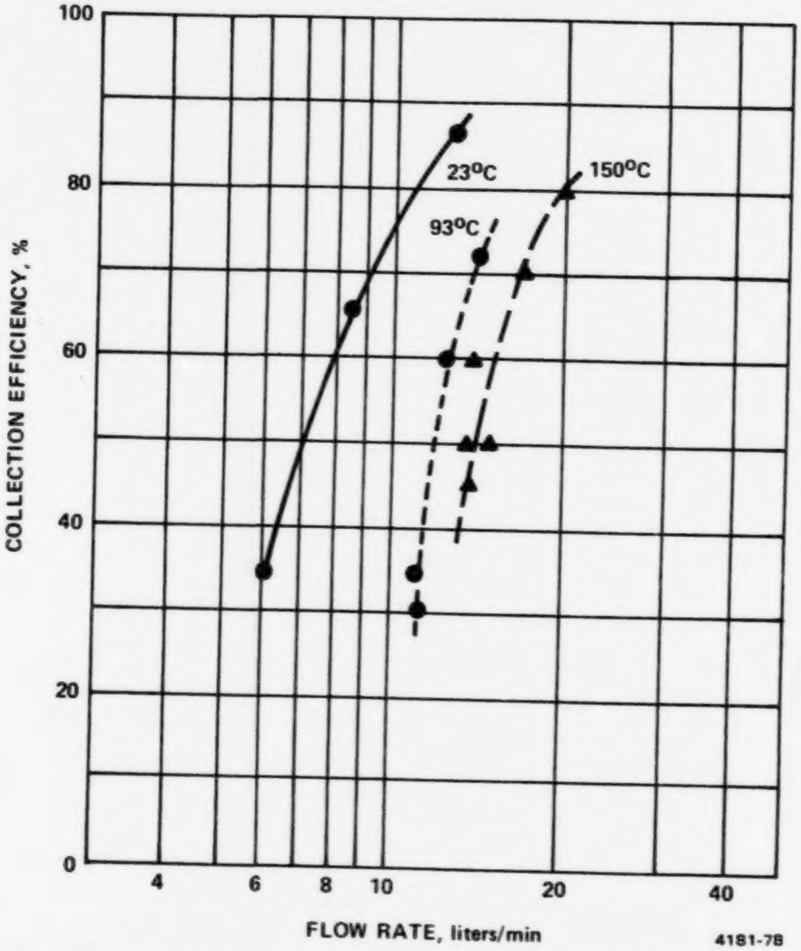

Figure 65. Collection efficiency of Cyclone IX versus flowrate for particles of 15±0.6 μm aerodynamic diameter.

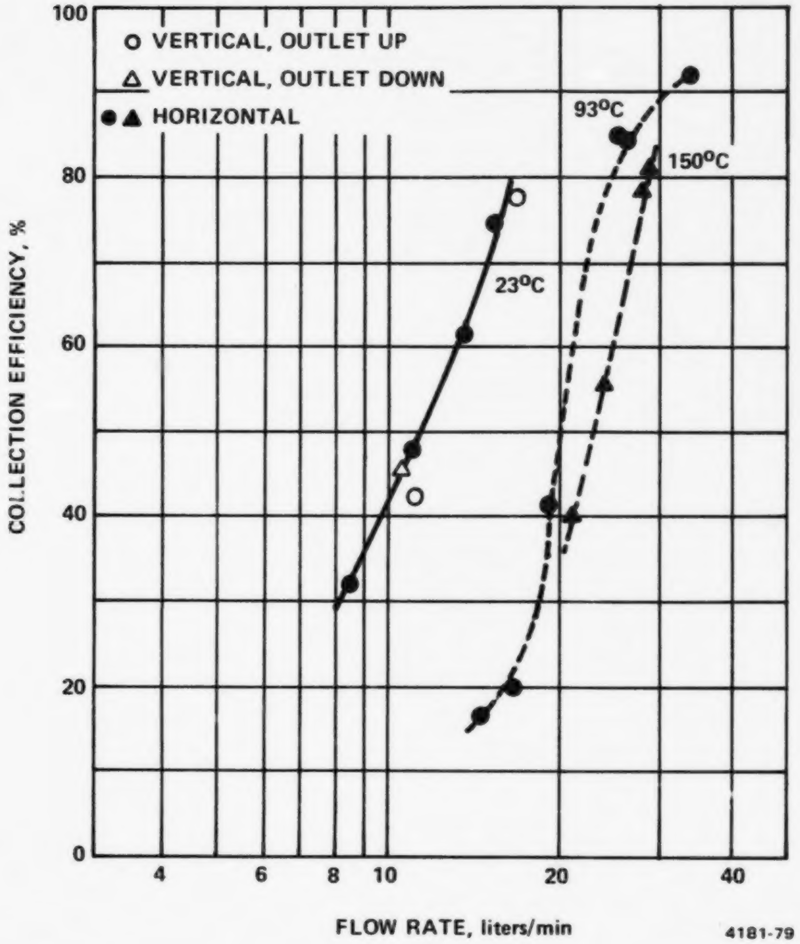

Figure 66. Collection efficiency of Cyclone X versus flowrate for particles of 15±0.6 μm aerodynamic diameter.

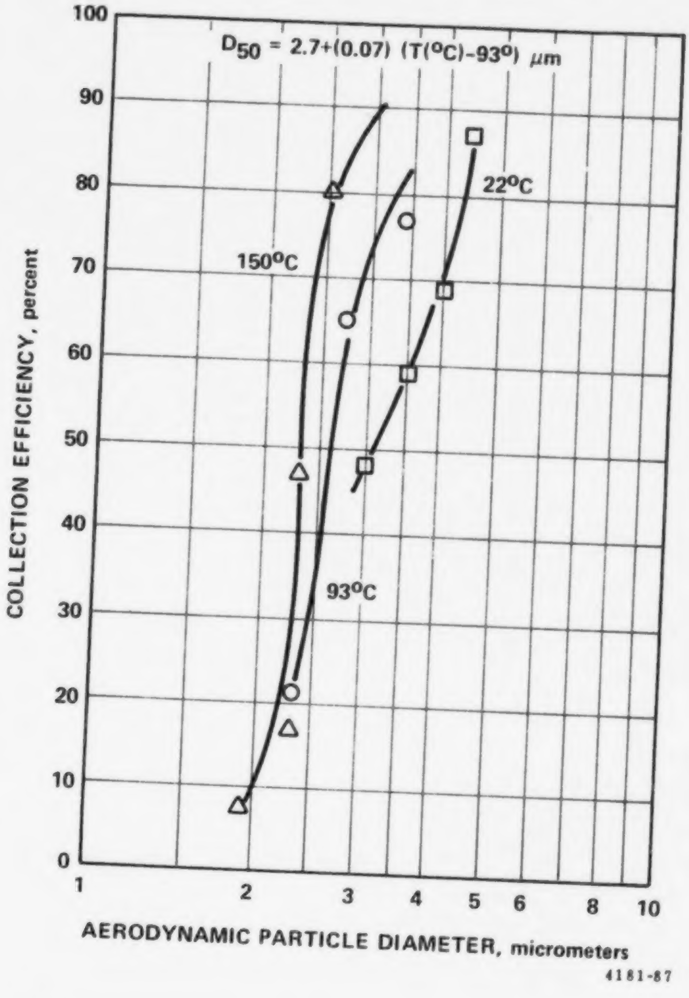

Figure 67. *Collection efficiency versus aerodynamic particle diameter for Cyclone III at 22°C and 11.3 ℓ/min (□), 93°C and 19.8 ℓ/min (○), and 150°C and 22.7 ℓ/min (△).*

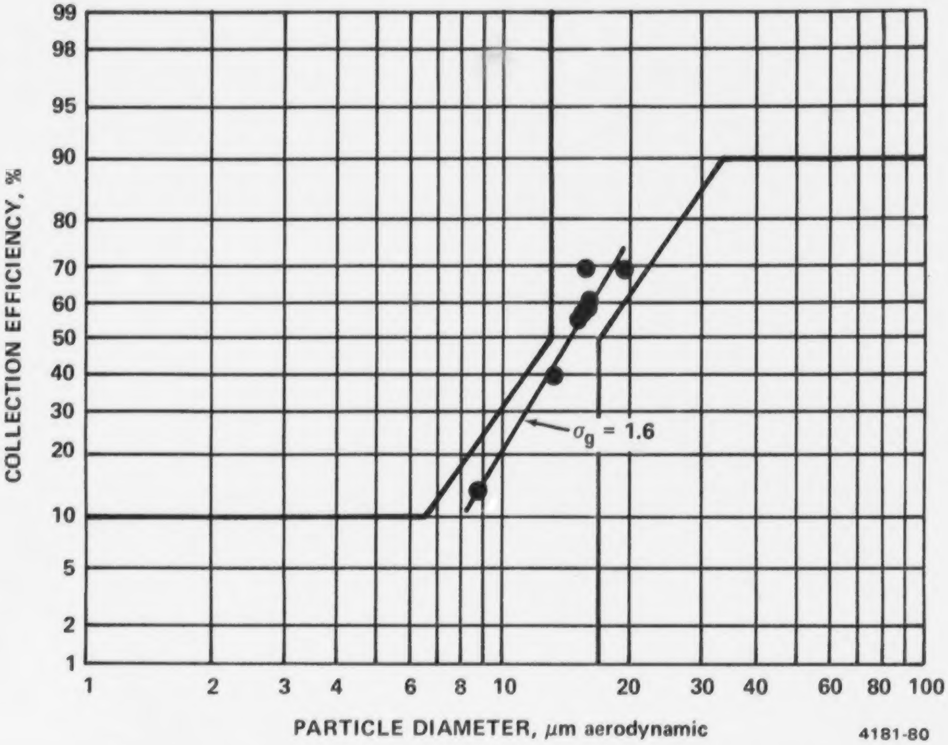

Figure 68. Calibration data for Cyclone IX at 14 ℓ/min and 150°C.

The data reported above define the operating points of cyclones SRI-IX and SRI-X at three discrete values of temperature. When the data are plotted on semi-log coordinates and a smooth line fitted to the points, the following equations of flowrate vs. viscosity result:

For cyclone SRI-X, $Q = (105 \log\mu - 225)\ \ell/\text{min}$ and for cyclone SRI-IX, $Q = (69.5 \log\mu - 150)\ \ell/\text{min}$.

It is not known at present how accurately these equations can be extrapolated to temperatures greater than 150°C.

In order to gain a better qualitative understanding of the mechanisms governing the performance of cyclones, Table 15 was prepared summarizing some of the dimensions and operating parameters of cyclones evaluated at Southern Research Institute. The parameters of greatest interest are the Stokes number St of 15 μm particles in the inlet and the ratio of the settling velocity to the centripetal velocity of 15 μm particles in the cyclone body. The latter is calculated assuming that the air flow in the cyclone body is a jet having the same velocity and diameter as in the inlet. This is obviously a crude approximation, but probably accurate enough to allow a reasonable estimate of the desired ratio.

The settling velocity V_s of unit density spheres is given by the expression (equivalent to Equation 19):

$$V_s = mg\beta \tag{25}$$

where m is the particle mass,

β is the particle mobility, and

g is the acceleration due to gravity.

The centripetal velocity Vc is given by:

$$V_c = \frac{mV_{in}^2}{R}\beta \tag{26}$$

where V_{in} is the gas velocity in the inlet and

R is the cyclone radius.

The desired ratio, then, is:

$$\frac{V_s}{V_c} = \frac{gR}{V_{in}^2} \tag{27}$$

TABLE 15. OPERATING PARAMETERS OF SRI CYCLONES

Cyclone Number	Q, cm^3/sec	D, cm	D_{in}, cm	V_{in}, cm/sec	ΔP, mm H_2O	D_{50} µm	$\sqrt{St}$	gR/V_{in}^2
V	472	1.52	0.30	6670	1800	0.32	0.1	1.6×10^{-5}
IV	472	2.54	0.57	2300	330	0.65	0.1	2.3×10^{-4}
III	472	3.11	0.75	1100	70	1.4	0.1	1.3×10^{-3}
II	472	3.66	1.01	600	40	2.1	0.1	5.0×10^{-3}
I	472	4.47	1.27	370	5	5.4	0.2	1.6×10^{-2}
BRINK	28	1.27	0.51	130	-	13	0.6	4.0×10^{-2}
IX	233(150°C)	5.11	1.53	130	-	15	0.3	0.2
X	190	6.14	1.83	70	-	15	0.2	0.6

Q is the sample flow rate
D is the diameter of the cyclone body
D_{in} is the diameter of the inlet
V_{in} is the gas velocity in the inlet
ΔP is the pressure drop across the cyclone
St is the Stokes number of the 15-µm particles in the inlet
gR/V_{in}^2 is the ratio of the settling velocity to the centripetal velocity in the cyclone body

The values of $\sqrt{St}$ and V_s/V_c can be used to estimate whether or not impaction onto the wall opposite the inlet or particle settling is likely to play a large part in the collection efficiency of a cyclone. If $\sqrt{St}$ is less than about 0.4, then impaction is not likely to occur.[29] If V_s/V_c is very small, then settling is not likely to occur. From Table 15, it can be seen that impaction is probably very significant in the cyclone used with the Brink impactor, while settling probably contributes somewhat to the collection efficiency of cyclones SRI-IX and SRI-X.

SIZE-SELECTIVE INLET FOR THE ANDERSEN HI-VOL SAMPLER

The Andersen Size Selective Inlet was tested using monodisperse aerosols of ammonium fluorescein generated with the vibrating orifice aerosol generator. This device is designed to be a 15 μm aerodynamic diameter inhalable particulate precollector for hi-vol samplers operating at 40 ft^3/min. The tests are only of the second or pure impaction part of the inlet; i.e., the inlet was not tested for the effects of wind speed.

The size selective inlet (SSI) was mounted on top of a standard 40 cfm hi-vol in the laboratory. A flat 8 in. x 10 in. filter collected all particles passing through the SSI. Three tests were performed. Particles generated by the VOAG were directed toward the SSI inlet. The SSI was rotated during the sampling procedure to insure uniform exposure of all portions of the SSI.

Figure 69 shows an exploded view of the SSI and the various surfaces which were washed after each run. These surfaces were:

1. Inlet entrance rim
2. Underside of top cover
3. Top of first plate and bowl sides
4. Bottom of first plate
5. Top of second plate and bowl sides
6. Bottom of second plate and bowl sides
7. Filter

Table 16 shows the test data. The cumulative efficiency shown in the last column does not include the contribution from surface (1) because of probable inconsistencies in the procedure for directing the particles towards the SSI inlet. Results from the tests lay within the proposed IP specification limits.

A STACK DILUTION SAMPLING SYSTEM

A significant problem which arises in the sampling of particulate pollutants in a stack environment is the measurement of

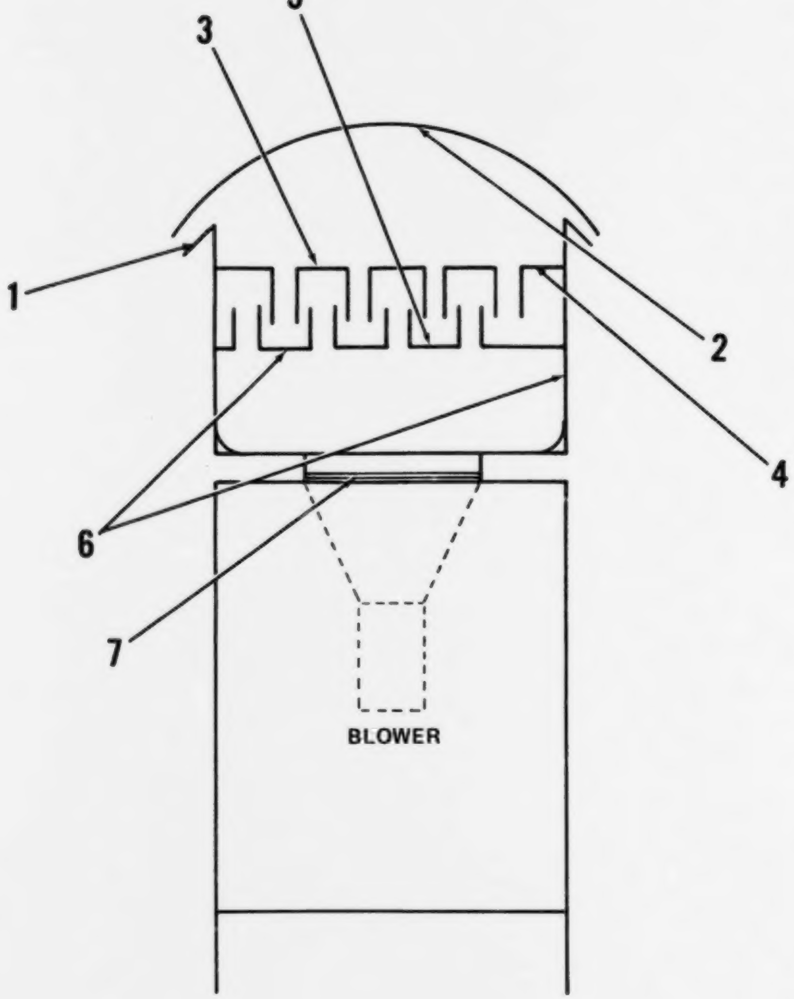

1. INLET ENTRANCE RIM
2. UNDERSIDE OF TOP COVER
3. TOP OF FIRST PLATE AND BOWL SIDES
4. BOTTOM OF FIRST PLATE
5. TOP OF SECOND PLATE AND BOWL SIDES
6. BOTTOM OF SECOND PLATE AND BOWL SIDES
7. FILTER

4181-105

Figure 69. Schematic of size-selective inlet.

TABLE 16. SIZE-SELECTIVE INLET CALIBRATION DATA

		% of Total Mass on Specific Surface							
Run Time(hr)	Particle Size (μm)	Surface 1	2	3	4	5	6	Filter	Efficiency Cumulative 2,3,4,5,6
2.5	16.8	1.98	0.34	10.8	0.09	23.9	7.5	55.4	43.5
2.5	16.7	2.9	1.0	12.4	1.8	27.1	10.2	44.6	54.1
5.0	11.8	3.1	0.02	7.6	0.14	15.4	6.0	67.7	30.2

the particles in the form that they will have after they are emitted into the atmosphere. In particular, it is difficult to characterize primary aerosols formed from condensable vapors in the stack gas as the plume is cooled and diluted by the ambient atmosphere. For example, the original EPA Method 5 attempted to measure the condensable fraction collected at 0°C, with a high probability of condensing water as well. A recently published technique attempts to simulate plume mixing using dilution with clean dry air in the turbulent jet of a dilution ejector pump.[30] This approach, while clearly a great improvement over previous methods, may be criticized in that it uses rapid (0.5 sec), highly turbulent mixing quite different from that in a typical plume. Since the particle size distribution and mass loading of a condensation aerosol are affected by the competing rates of transport, condensation, and adsorption of vapor, the collection conditions of this sampler can be a liability.

In order to provide an independent measure of particles formed from condensable stack vapors, a new sampling system with dilution was developed. The goal of the Southern Research Institute design was to simulate the actual plume formation as closely as possible in a portable instrument suitable for field use while allowing some flexibility in choosing the mixing parameters. In this system, stack gas is extracted and diluted with a standardized "ambient" air. The flow patterns are designed to qualitatively approximate those which occur in an actual plume, with the mixing time of the gases allowed to be as long as practical within reasonable constraints of instrument size and flowrates. A laboratory prototype was constructed and subjected to various diagnostic tests. As a result of the tests on the prototype system, a field diluter instrument was also designed and constructed.

Design and Testing of Laboratory Prototype Sampler

Prototype Design--

A block diagram of the laboratory-scale prototype dilution sampling system is illustrated in Figure 70. The heart of the sampler consists of a Plexiglas cylinder in which simulated stack gas is mixed with filtered ambient air and the resulting aerosol analyzed. The simulated stack gas is introduced through a tube oriented along the axis of the cylinder. Dilution air is introduced through four radially oriented tubes, is diverted along the cylindrical dilution chamber, and passes through a series of fine screens which serve as flow straighteners. The resulting uniform flow of dilution air enters the mixing region in an annulus surrounding the simulated stack sample. In tests using smoke in the sample or dilution air streams, the streams appeared uniform at the point of introduction and provided a good visual representation of the mixing of a plume. Flowrates of both sample and dilution air can be varied; typical conditions are 10 cfm for dilution air and 0.4 cfm for sample air, giving a dilution ratio of 25 and a residence time of about 4 sec.

The diluter is adaptable to a variety of sampling devices for measuring condensed and diluted aerosols. The total flow can be directed into a hi-vol impactor or filter, the particle loading can be examined in situ by optical methods, or portions of the diluted stream can be extracted, further diluted if necessary, and sampled using an electrical aerosol analyzer, an optical counter, or diffusion batteries and a condensation nuclei counter. Tests to characterize the flow, mixing, and condensation in the instrument have used a Climet optical particle counter and a Thermo-Systems Electrical Aerosol Analyzer.

For laboratory experiments, dilution air was taken from the laboratory compressed air supply, which was filtered through an absolute membrane filter, and introduced at ambient temperature and humidity. For some experiments, the air was cooled in an ice bath condenser.

Sample stack gas was simulated using heated, humidity-controlled particle-laden air. Filtered compressed air was passed through a Phoenix SG-20 smoke generator (Phoenix Precision Instruments, Gardiner, NY) to form an aerosol which served as a source of condensation nuclei. A metered portion of this stream was heated and steam was injected, if desired, to adjust the humidity of the sample stream. Experiments have also used either a nebulized salt (sodium chloride) aerosol with or without added moisture, or glycerol smoke, which served as a prototype condensable vapor.

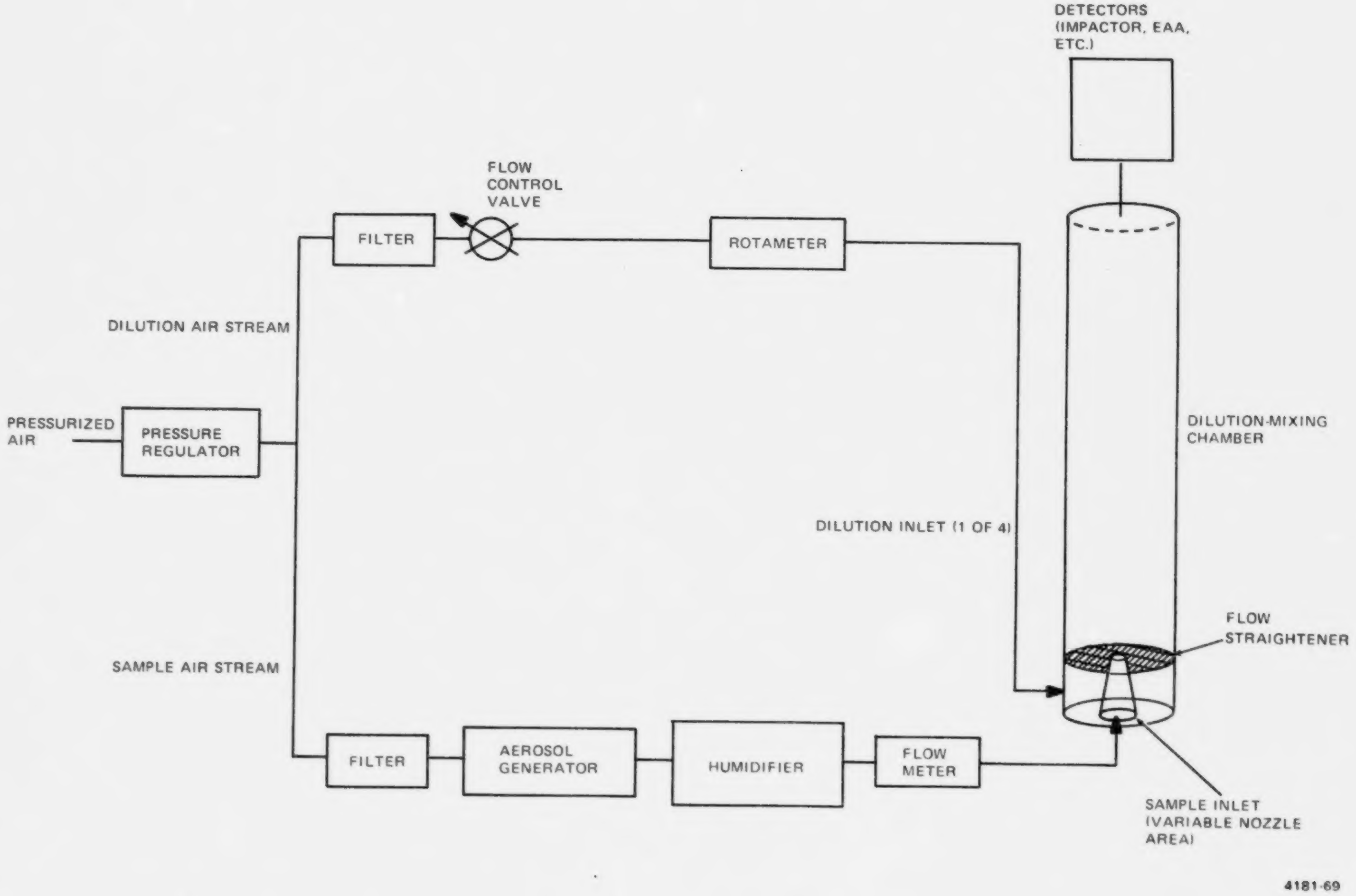
DETECTORS (IMPACTOR, EAA, ETC.)
FLOW CONTROL VALVE
FILTER
ROTAMETER
DILUTION AIR STREAM
PRESSURIZED AIR
PRESSURE REGULATOR
DILUTION-MIXING CHAMBER
DILUTION INLET (1 OF 4)
FLOW STRAIGHTENER
SAMPLE AIR STREAM
FILTER
AEROSOL GENERATOR
HUMIDIFIER
FLOW METER
SAMPLE INLET (VARIABLE NOZZLE AREA)
4181-69

Figure 70. Block diagram of dilution sampling system.

Performance Characterization of Laboratory Prototype Sampler--

In order to assess the suitability of the sampler design for simulating the conditions of real plume formation, several tests were made to investigate the flow and mixing behavior in the diluter. These tests on the laboratory dilution sampler were designed to investigate two characteristics desired in the field version. (1) The sampler must mix the sample gas and dilution air in a reproducible and controlled manner similar to the mixing in actual full-scale plumes. (2) The dilution and cooling of the simulated plume must provide a local environment for condensation which is equivalent to that in a plume.

In an actual plume, the stack gases exhaust into still air with a definite upward momentum and a further tendency to rise due to buoyancy. As the plume rises, transfer of its momentum leads to mixing by entrainment of ambient air and formation of turbulent eddies. By the time the plume momentum has been dissipated and the vapors have been cooled to the local temperature, the stack gases will be diluted by a large but finite factor. Further dilution will occur due to diffusion and meteorological factors, but it may be safely assumed that all condensation has occurred prior to this point.

The dilution sampler attempts to simulate this mixing by injecting the sample gases into a moving stream of dilution air. A small amount of turbulent mixing will occur in the absence of a velocity mismatch. Nevertheless, the most important mixing mechanisms should be the same as in the actual plume. The studies were designed to give a quantitative measure of the degree of mixing in the sampler. A test aerosol was injected in the sample gas stream. At the top of the sampler, a probe was positioned to withdraw a sample from an arbitrary point in the cross section of the diluter tube. The aerosol concentration at this point was measured using an electrical aerosol analyzer or condensation nuclei counter. In this manner a profile of the particle distribution across the diluter could be obtained.

Figure 71 shows the concentration of a salt aerosol across a diameter of the diluter for various sample temperatures. The degree of mixing increases sharply as the temperature of the sample is increased. This effect is expected, since the velocity mismatch is designed to be zero for ambient sample temperatures and proportional to the temperature above the ambient value. As the sample temperature is increased, the transfer of momentum to the dilution air becomes greater and the mixing more thorough. As can be seen in Figure 71, for sample temperatures typical of stack conditions substantial mixing has occurred over the entire diameter of the diluter tube. These results indicate that dilution ratios, local temperatures, and vapor saturation values calculated on the assumption of total mixing will be meaningful.

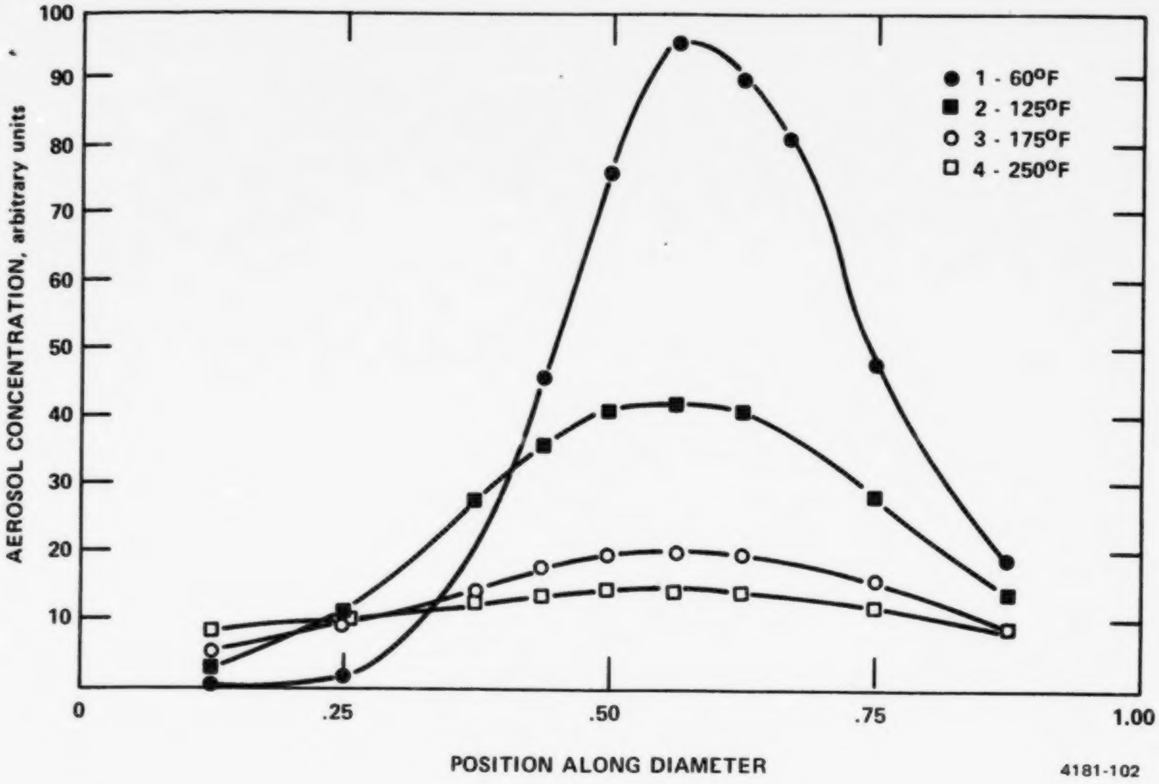

Figure 71. Concentration profile of salt aerosol across diluter.

Profiling tests were also performed using glycerol smoke aerosol. At sample temperatures over about 150°F, a substantial fraction of the original aerosol evaporates in the sample line and recondenses as it is cooled by dilution. Between 200 and 300°F, evaporation is complete and a detached plume of glycerol condensation smoke is observed in the diluter. In this system, as in field samples containing condensable vapors, molecular diffusion could conceivably aid in the mixing process. Results of these tests are illustrated in Figure 72. The dependent variable in this figure is the half-width of the concentration profile relative to the diameter of the diluter tube. As was evident in Figure 71, the half-width of the profile increases with temperature above ambient. Data from the salt aerosol and the glycerol smoke fall along the same curve, indicating that the main mixing mechanism is probably turbulent mixing in macroscopic eddies. This behavior corresponds to what is expected for real plumes.

Attempts were also made to monitor the particle-size distribution of the condensing glycerol aerosol at different sample

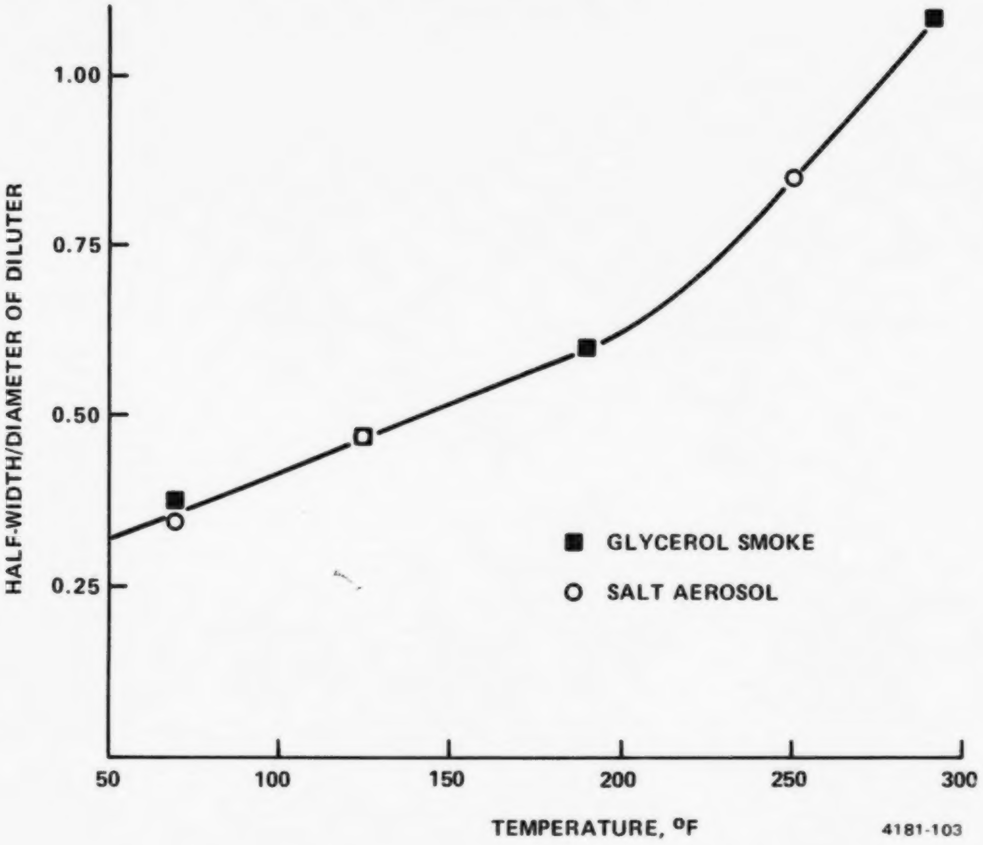

Figure 72. Temperature dependence of cross-section of diluted aerosol plume.

temperatures. For these studies the single point probe was replaced by an averaging probe system using a tube with several holes. After an impactor removed particles larger than 1 μm, particle-size distributions were measured with an electrical aerosol analyzer. Unfortunately, several factors combined to limit the accuracy and reproducibility of these results. First, the signal had an excessive amount of short-term noise due to fluctuations of aerosol concentration reaching the holes in the averaging probe. These fluctuations, caused by the randomness of the turbulent eddies, were partially damped by using a two liter "averaging chamber" in the line to the detector, but longer term fluctuations remained and proved troublesome. Probably most of these residual fluctuations were due to instabilities in the aerosol generator. Due to the nonlinear response of the electrical aerosol analyzer, relative errors are not the same for all channels. Only the data in the 0.05-1 μm size range is reliable. Within this range, semiquantitative comparisons of particle-size distributions under different conditions are feasible.

Particle-size distribution data on glycerol smoke at three temperatures are shown in Figure 73. Figure 73A shows the size distribution of the aerosol as formed by the smoke generator. At higher temperatures the size distribution becomes more nearly monodisperse and the median size becomes greater. This behavior can be explained for the higher temperature data (Figure 73C, 195°F) in terms of condensation of the vapor on residual nuclei. For diffusion-controlled growth under more uniform temperatures and flowrates a monodisperse aerosol would be expected. The residual width of the size distribution may be attributed to the non-uniformity of dilution and cooling rates in the sampler. The 125°F data (Figure 73B) probably reflects a differential evaporation-condensation process in the heating line, as less than 1% of the aerosol mass should be required to saturate air at the sample temperature. In the hot region near the heating line walls, however, evaporation would decrease the size of all particles, followed by condensation in the cooler region near the center of the tube. The behavior at this temperature is strikingly different from that at ambient temperatures and is of some interest for that reason. It has no counterpart in the stack environment, however, and must be considered an artifact of the glycerol smoke test.

The size distribution studies confirm that the diluter is suitable for the study of condensation behavior in laboratory-produced samples and presumably in extracted stack gases. For further evaluation of the prototype dilution sampling system, it was used in a test of a domestic oil-fired furnace at the EPA IERL/RTP facilities. The participation in the test served to demonstrate the sampling system and to obtain data for comparison with the other sampling devices used in the furnace test. In addition, the dilution sampling system provided real-time particle size measurements unavailable from the other devices in the test.

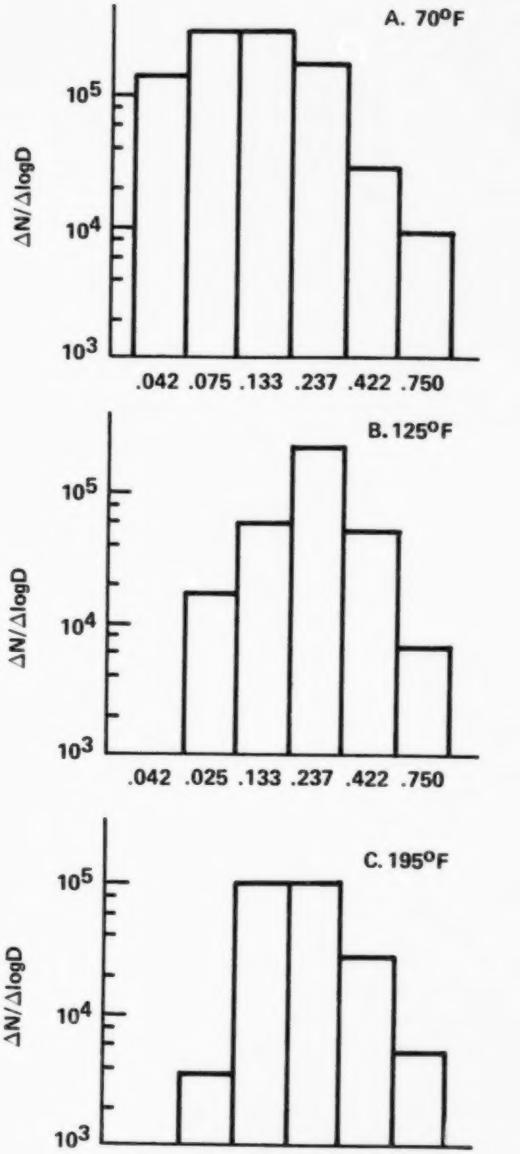

Figure 73. Particle-size distribution of glycerol smoke aerosol.

Domestic Furnace Test--

A modified commercial home furnace burning No. 2 fuel oil was operated under controlled combustion conditions. Between the outlet of the furnace and the barometric damper, probes were inserted for a SASS train, a battery of instruments for flue gas analysis, a smoke tester, and the dilution sampling system. Above the damper were a second SASS train and duplicate flue gas analyzers. Finally, the remaining flow of flue gas plus indraft from the barometric damper was directed into an automotive dilution tunnel and the particulate matter in the diluted stream was collected on an absolute filter. Among the objectives of the test were the characterization of the particulate and organic vapor emissions and the recovery of samples for bioassay.

The dilution sampling system was used in a modified configuration for the oil-fired furnace test. The stack sampling probe was replaced by a simple probe consisting of a short heat-traced stainless steel tube, and the 2-μm cyclone precollector normally on the probe was left off. The sample gas was directed via a 10-ft flexible heated hose through a metering orifice and then into the body of the dilution chamber. The dilution air consisted of filtered room air; although provisions exist on the dilution sampler for humidity and temperature control, these capabilities were not used in the experiment, consistent with the operating conditions of the dilution tunnel. In retrospect, a controlled temperature would have been preferable for consistency of the data. Dilution ratios of approximately 10, 20, and 40 were used during the test.

Approximately 0.5 cfm of the diluted stream was withdrawn into an ultrafine particle sizing system, developed by Southern Research Institute. In this system, the gas stream was further diluted by a factor of about 23 and analyzed with ambient particle-sizing instrumentation. The instruments included a Climet 208A optical particle counter, a Thermo-Systems 3030 Electrical Aerosol Size Analyzer, and an Environment One Rich 100 Condensation Nuclei Counter with or without a parallel-plate diffusion battery. All three instruments are capable of providing near real-time data. Unfortunately, the condensation nuclei counter developed mechanical problems and gave data which may not be reliable, and the optical counter was not suitable for the small particle sizes encountered, so the bulk of useful data was obtained by the Electrical Aerosol Size Analyzer.

The remainder of the diluted sample stream was passed through a Sierra 230 hi-vol impactor modified to give stage D_{50}'s of 0.5, 1, and 2 μm at 15 cfm. Unfortunately, no quantitative inertial sizing could be done since the cellulose substrates could not be weighed accurately with the equipment at hand. Water uptake by the substrates proved to be an insurmountable problem, so finally the stages were removed and the backup filter used to obtain total mass loadings.

The dilution sampling system described above was set up and detailed real-time size data were taken using the Electrical Aerosol Size Analyzer, mostly with the standard dilution ratio of about 20 in the dilution sampler, but also at high (about 40) and low (about 10) dilution ratios. All samples were taken at a constant sample flowrate of 0.78 scfm. The dilution ratio was changed by changing the flowrate of dilution air. For each condition, total particulate matter from four cycles was collected, and a side stream of the filtered sample gas was drawn through an XAD-2 cartridge to measure organic vapors in the diluted stream. In addition, time-resolved measurements using the Ultrafine Sampling System were taken during all combustion cycles.

Results of Dilution Sampling Measurements

Gravimetric Measurements--

As mentioned above, attempts to measure the time-integrated size distribution using the hi-vol impactor failed due to problems with the impactor. Unfortunately, this also prevented measurements of total mass loading, since an unknown but visible fraction of the mass was deposited on the impactor stages. Only on the final test day were the impactor stages omitted and reliable total mass loadings obtained for the three dilutions studied.

Some information can be derived from the earlier runs, however. Measurements taken during 20 cycles indicate a loading of 5.8 mg/nm^3 in the particle-size range less than 0.5 μm, the D_{50} of the last impactor stage. There was visible darkening of the substrates of all three stages used, indicating the presence of particles larger than 2 μm.

On the three runs without the impactor stages, the total mass loadings were measured over four combustion cycles, or 44 minutes of sample time at 0.0275 nm^3/min. In addition, the low dilution series had one 11-minute cycle and 9 minutes sampling after shutdown. The total filter weights were: 9.1 mg, 10.3 mg, and 15.8 mg for standard, high, and low dilution ratios, respectively. After correction for the 0.5 cfm extracted for the ultrafine sizing system, the weights give mass loadings of 7.8 mg/nm^3, 8.7 mg/nm^3, and 11.7 mg/nm^3 for standard, high, and low dilutions, respectively. (Note that these figures refer to the volume of undiluted flue gas). The standard and high dilution values are identical within experimental error. The low dilution value is measurably higher, but is probably corrupted by the inclusion of 9 minutes of sampling of the aerosol from the stagnant flue following the emissions burst at turnoff. Therefore it was tentatively concluded that for the total time-integrated emissions, the total mass loading measured is not demonstrably dependent on dilution ratio in the range from 10 to 40.

There are obvious indications, however, that the dilution and cooling process does affect the aerosol measured. The loadings from the dilution sampler are 25% higher than the 6.6 mg/nm^3 measured by the hot filter of the first SASS train. More striking is the obvious presence of agglomerated particles in the 1-10 μm range, in contrast to the SASS train measurements, which showed nothing in the cyclones that are designed to catch particles over 1 μm.

Temporal Behavior--

Figures 74 and 75 show the time variation of emissions in several size ranges during a typical combustion cycle. The data in these figures were taken during run 23, which was a standard dilution run with the furnace adjusted for a no. 1 smoke spot; however, the general features of the data were the same for both furnace conditions and all dilutions. Although the concentration is measured after dilution, the data are presented in terms of number or mass per unit of the original flue gas, as was done with the time-integrated loadings. This normalization was chosen because the total mass of original particulate matter and condensable vapor per unit volume of flue gas is presumably constant, and dilution should only affect the distribution of this mass among the final aerosol particle sizes. Figure 74 shows the temporal variation of the particle number distribution as measured by the Electrical Aerosol Analyzer. All sizes show a steady increase with burn time except the smallest range measured, which decreases in number. The total number rises steadily to a near maximum and may actually decrease slightly before the end of the burn. Since the fraction of particles in the larger size ranges increases rapidly towards the end of the cycle, the total mass shows a steady, but much more rapid rise, and typically increases by a factor of 2.5 or more in the last five minutes of a combustion cycle while the total particle number increases only about 20%. This can be seen in Figure 75.

Immediately after heater shutdown for the "off" period, one or more large bursts of aerosol were noted as current spikes roughly 10-15 seconds in duration on all channels of the EAA. The appearance of these spikes is exactly coincident with spikes in the carbon monoxide concentration, indicating an origin under conditions of incomplete combustion. The aerosol bursts were too short and insufficiently reproducible for particle-size distribution measurements; however, since measurable currents were seen in the highest channels, it was apparent that sizes of at least 1 μm were included, and that concentrations were many times larger than those measured during the "on" cycle. Unaccountably, no similar burst of emissions was seen at the beginning of the combustion cycle, even though similar levels of soot were noted on the smoke tester, and the gas analyzers suggested similar transient conditions of incomplete combustion. Perhaps the turn-off of the combustion air fan was involved in the higher level of emissions at the end.

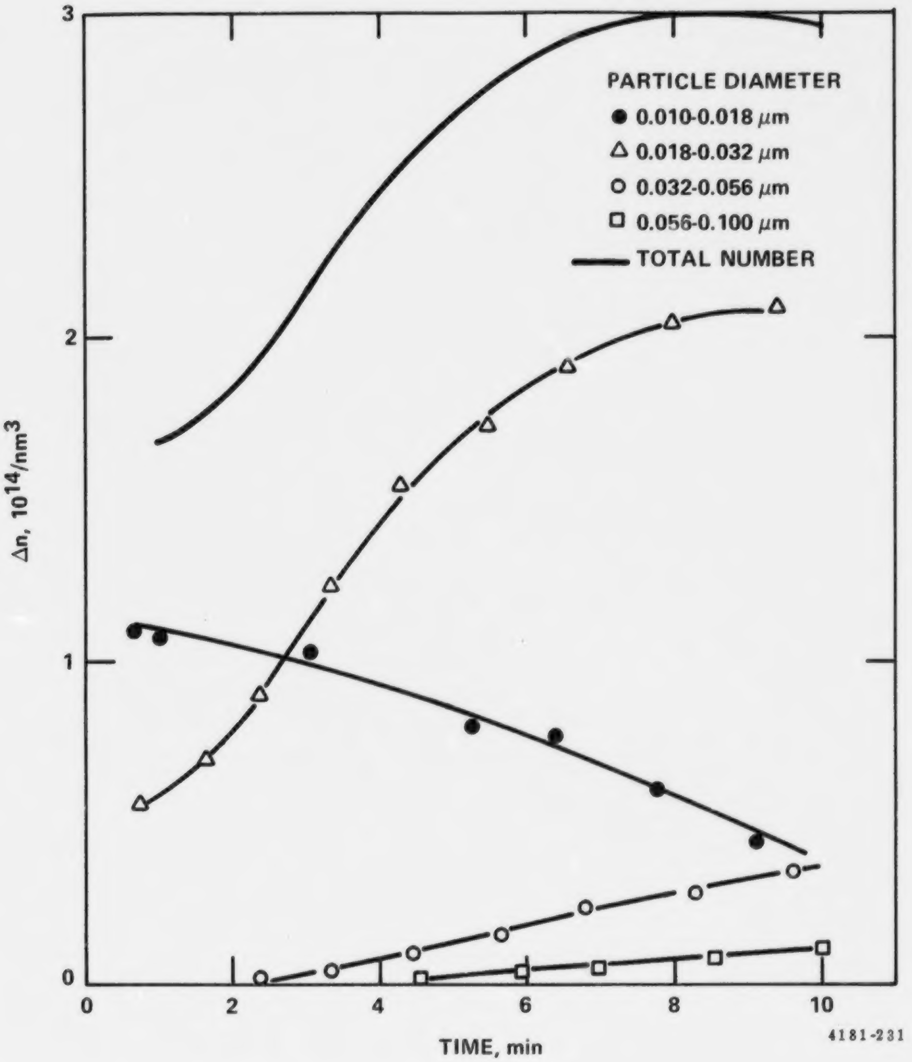

Figure 74. Time variation of particle number concentration per unit flue gas as measured after dilution. Dilution ratio = 19.6 (standard).

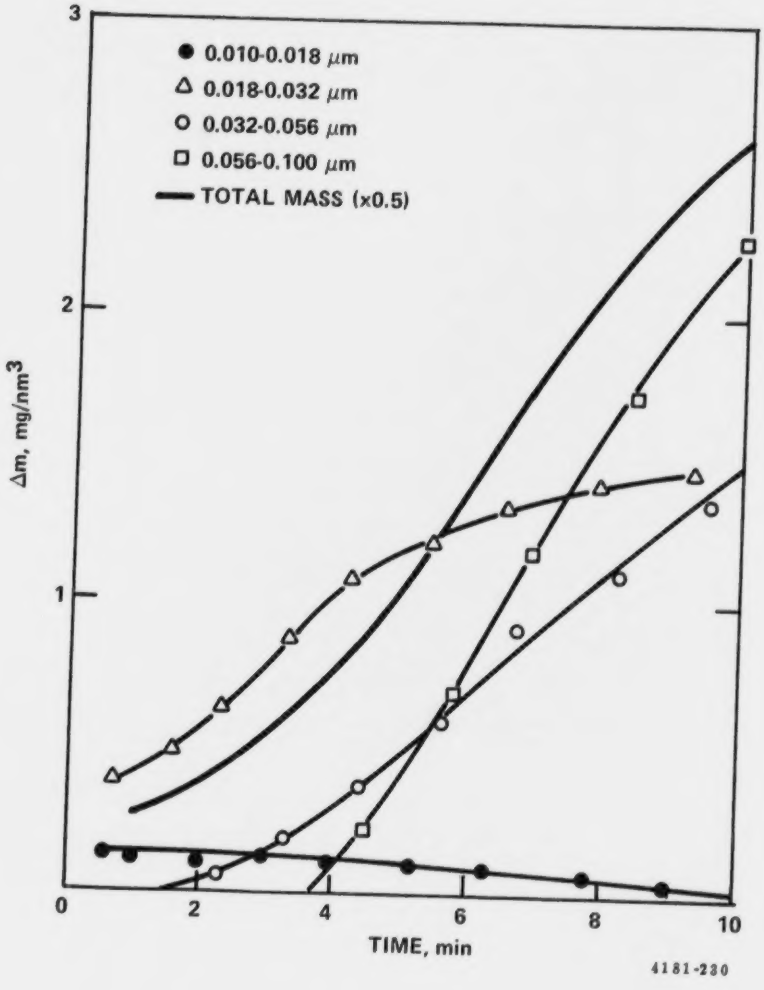

Figure 75. Time variation of particle mass concentration per unit flue gas as measured after dilution. Dilution ratio = 19.6 (standard).

In principle, the particle-size distributions obtained by the electrical mobility measurements could be independently obtained using a series of diffusion battery/condensation nuclei counter measurements. Due to the temporal variation in the furnace test, such measurements would have been difficult to implement or interpret, so the condensation nuclei counter measurements were limited to measurements of the total particle number and the fraction lost in a small parallel-plate diffusion battery. The qualitative behavior of the CN data tends to confirm the EAA number distribution measurements. The measured CN number plotted against time during a combustion cycle looks much like the total number plot in Figure 74 as determined by the aerosol mobility measurements. Furthermore, insertion of a small parallel-plate diffusion battery before the CN counter causes attenuation of the CN number by approximately the fraction predicted from the EAA size distribution. The only disturbing factor is that the CN counter reading is more than an order of magnitude lower than the EAA total number, which is beyond the reasonable calibration error of both instruments. The CN counter appears to have been malfunctioning during the test. The variation of measured concentration with flow was anomalous. There also appeared to be drifts in sensitivity. It was noted that on subsequent cycles with the same operating conditions, the CN number measured at the end of the combustion cycle would occasionally vary by a factor of two without any corresponding variation in the distribution as seen by the EAA. For these reasons, the CN/diffusion battery data have been viewed with some caution.

Likewise, the optical counter was not useful in the configuration used. As is evident from Figure 74, essentially all of the aerosol particles measured by the EAA are smaller than the 0.3 μm detection limit of the optical counter. Larger particles present in lower concentrations were attenuated beyond detectability by the dilution factor necessary for the EAA measurements. Moreover, the 2-μm cyclone precollector prevented measurement of larger particles such as were noted on the impactor substrates.

Effect of Dilution Ratio on Particle Size Distribution--

In order to quantify the effect of dilution ratio on the particle-size distribution of the aerosol in the diluted sample stream, it is necessary to define a reference condition for the time-varying aerosol. This reference point was chosen to be the population which exists eight minutes into the combustion cycle. After eight minutes, many of the combustion conditions (e.g., flue gas composition and temperature, smoke test emissions, and total particle number) have begun to stabilize, yet channel measurements on the EAA may be interpolated without the complication of the transient at the end of the combustion. Once size distributions at eight minutes were determined for each cycle, they were averaged for the cycles at the same dilution conditions.

A histogram showing average size distributions at eight minutes is shown in Figure 76. As before, the mass measurements were normalized to a constant volume of undiluted flue gas. Several features of the data are noteworthy. First, the particles are very small. Considered on a mass basis, the mean particle size is less than 0.075 μm for all dilution conditions. On a number basis, the mean size is less than 0.03 μm. Second, there are signs of bimodality in the data. Under all dilution conditions, the data can be represented as the sum of two modes with mass median diameters of about 0.025 and 0.075 μm. A third observation is that there is a trend toward smaller mean size of the aerosol as the dilution ratio is increased. Finally, the total aerosol mass at eight minutes is the same within the 30-40% experimental error for the three dilution conditions used. This finding is consistent with the time-integrated mass measurements, and is what would be expected if the final temperature is low enough to deplete the bulk of condensable vapors for all dilutions studied.

Conclusions--

The picture that results from these data is that within the dilution limits studied, a constant mass of organic vapors condenses into solid particulate in the diluter. Higher dilution conditions favor a larger number of small particles; less dilution gives fewer but larger particles. This result, along with the higher mass loadings in the diluted stream, as opposed to the SASS measurements, indicates that condensation is indeed taking place in the dilution sampling system.

A condensation mechanism also explains the discrepancy between the SASS train, which saw no particles over 1 μm, the dilution sampler, which indicated particles of that size range in the final emission burst at the end of a combustion cycle, and the smoke tester, which found large soot particles during a combustion cycle as well as at both ends. In the SASS train, operated at 200°C, presumably no condensation could occur. In the dilution sampler, the process of dilution with cooling causes rapid supersaturation and consequent nucleation condensation of some of the less volatile organics (GRAV fraction), resulting in a large number of microscopic particles which rapidly coagulate into particles of the 0.01-0.10 μm size range. It is conceivable that the difference in size distribution with dilution is due entirely to the decreased concentration-residence time product as the dilution air flowrate is increased. In the burst of emissions at the end of a combustion cycle, the rates of condensation and coagulation are both increased sharply, giving rise to large aggregates (>1 μm) in the diluted stream. The difference between the smoke tester and the diluter may possibly be explained as follows. If the bulk of the condensation aerosol consists of unburned hydrocarbons, this fraction may not be as visible in a filter paper spot as the black soot actually measured. In addition, this fraction might condense directly on the walls of the water-cooled smoke tester probe rather than forming an aerosol in the diluted stream. On the other hand, the large soot particles seen on the smoke tester filter paper would not pass through the sampling cyclone of the ultrafine particle sizing system.

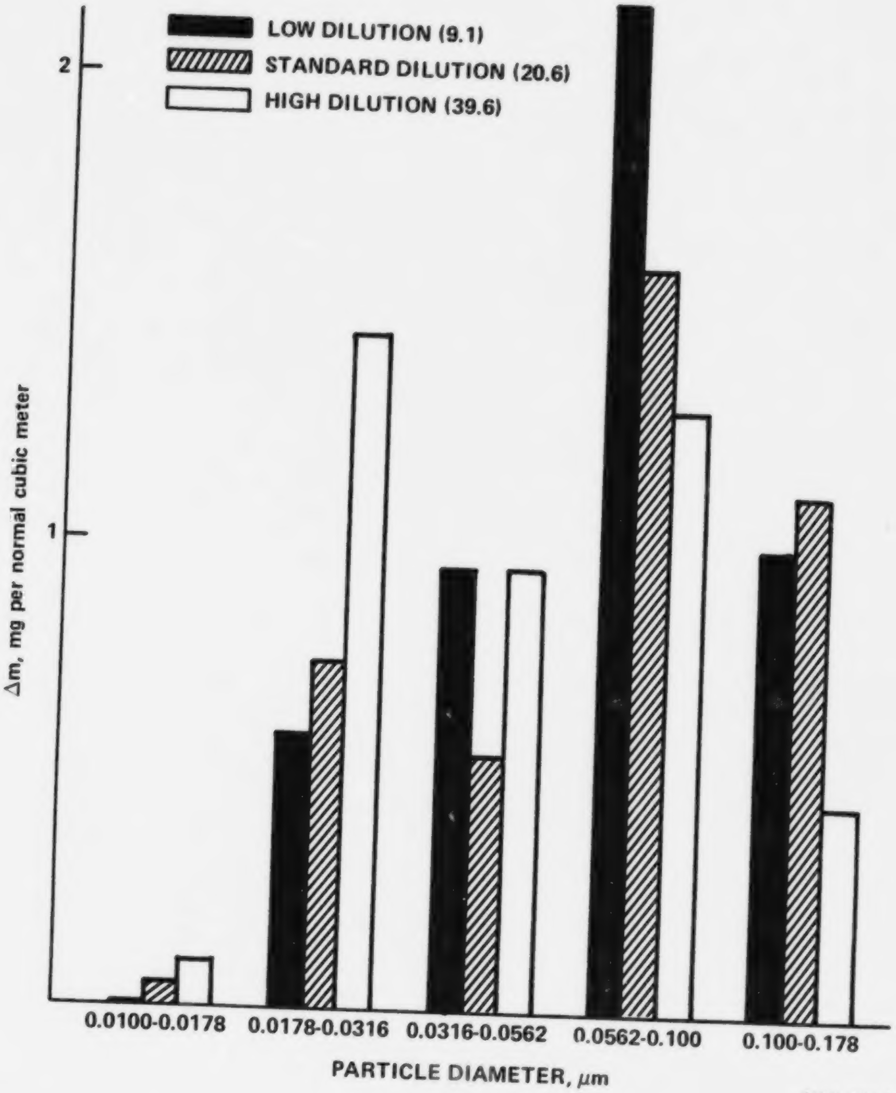

Figure 76. Particle mass concentration per unit flue gas as measured at different dilution ratios. All concentrations measured eight minutes after beginning of combustion cycle.

SECTION 4

OPERATION AND SAMPLING PARAMETERS FOR THE INHALABLE PARTICULATE SAMPLING SYSTEM

This section contains information on (1) modified procedures for the calibration and operation of impactors used for collection in the inhalable particulate size range, (2) the dual-cyclone sampling train designed for collection in this range, and (3) the dilution stack sampling system designed to simulate the conditions of stack plume formation.

CASCADE IMPACTOR CALIBRATION AND OPERATION

In order to measure IP concentrations with cascade impactors, current operating procedures must be modified. The document "Procedures for Cascade Impactor Calibration and Operation in Process Streams" (EPA-600/2-77-004)[31] was modified to incorporate the following new procedures:

(1) Operation with a precollector cyclone having an efficiency curve corresponding to that required of IP samplers
(2) Some refinement of the calibration procedures
(3) A new method for selecting and treating substrates
(4) A new method for selecting the sampling rate and locations
(5) The new data analysis method described above in Section 2.

The revised calibration and operation manual is being published as a separate report.

THE INHALABLE PARTICULATE SAMPLING SYSTEM

An IP Cyclone Sampler has been developed to measure particulate mass with size cuts at 15 μm and 2.5 μm, and a Dilution Stack Sampling System was developed to measure the condensable fraction of stack emissions. The IP Cyclone Sampler is to be used as a precollector for the dilution system, allowing stack gas containing the fine particulate fraction and condensable vapors to be mixed with filtered ambient air in a manner that simulates the dilution/cooling process at the stack/ambient interface. The simulated plume is passed through a hi-vol impactor and/or filter for measurement of condensable mass concentration in the diluted gas stream. This section contains a description of the sampling system and instructions for its preparation and use including sampling, data analysis, and reporting.

The Dual-Cyclone Train

The IP Cyclone Sampler as shown in Figure 77 was designed to have two stages with D_{50}'s of 15 and 2.5 µm at process stream conditions in accordance with the IP specifications. It is operated at a nominal flowrate of 23 ℓ/min (0.8 ft^3/min) at 150°C (300°F). The sampler consists of two cyclones and a backup filter in series, which can be connected directly to an EPA Method 5 or Method 17 sampling train. The backup filter can be a flat filter or, in cases where there is a large percentage of fine particulate matter, a thimble filter. Cyclone SRI-X separates the large-particle fraction from the IP fraction and has a range of nozzles allowing it to sample isokinetically in flues of different gas velocities. Cyclone SRI-III separates the fine particle portion of the IP sample and passes it on to the filter. Thus the fine particulate matter is collected in the filter and the outlet tube of cyclone SRI-III and the IP sample is collected in the outlet tube of cyclone SRI-X and in cyclone SRI-III.

Each IP Cyclone Sampler consists of one each of the following items:

Fabricated Parts:

Drawing Number	Item	Name
4181-31-C-05	501	Cyclone III Shell Inlet
4181-31-C-05	502	Cyclone III Inlet Insert
4181-31-C-06	601	Cyclone III Shell Cap
4181-31-C-06	602	Cyclone III Shell
4181-31-C-07	701	Cyclone III Modified Cap
4181-31-C-09	901	Cyclone III Modified Collection Cup
4181-37-C-10	1001	Cyclone X (Mk2) Collection Cup
4181-37-C-10	1002	Cyclone X (Mk2) Vortex Tube
4181-37-C-11	1101	Cyclone X (Mk2) Body
4181-37-C-12	1201	Cyclone X (Mk2) Nozzle (Set of 11)
4181-37-C-14	1401	Cyclone III Body

Supplier: Dean Tool and Machine Shop
Box 3347
Oxford, Alabama 36203
Phone: (205) 831-4430

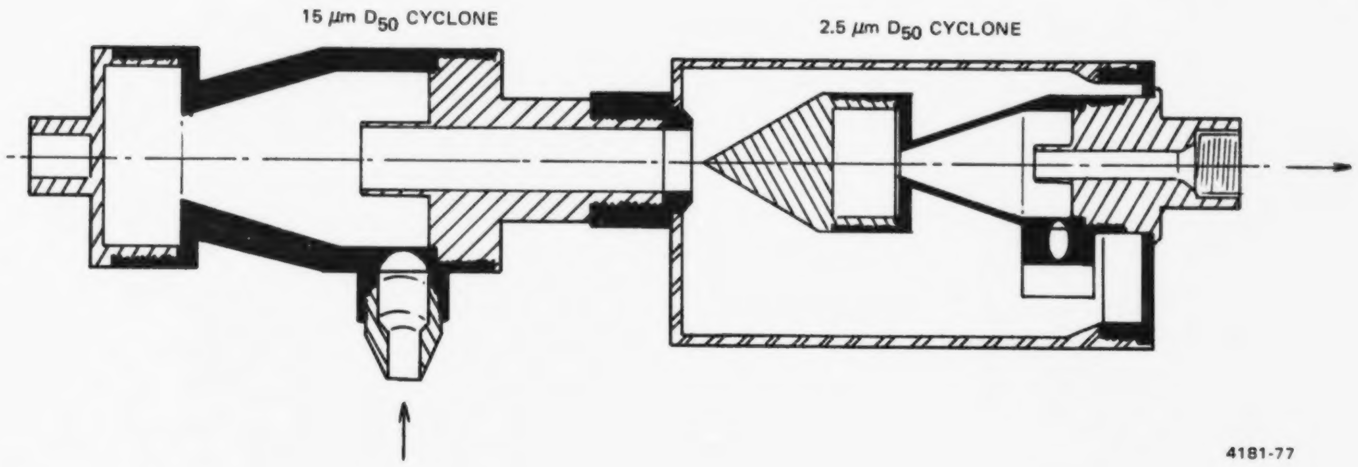
15 µm D50 CYCLONE
2.5 µm D50 CYCLONE
4181-77

Figure 77. Schematic drawing of inhalable particulate sampler.

Seals:

Used On	Quantity	Description	Part Number
Cyclone X Body	2	2.75 inches O.D. x 0.062 inch diameter Inconel X-750 Metal O-Ring	E-O-N-002750 -02-07-1
Cyclone III Body	2	1.375 inches O.D. x 0.062 inch diameter Inconel X-750 Metal O-Ring	E-O-N-001375 -02-07-1
Cyclone X- Cyclone III Connection	1	1.375 inches O.D. x 0.094 inch diameter Inconel X-750 Metal O-Ring	E-O-N-001375 -04-07-1
Cyclone III Shell	1	3.000 inches O.D. x 0.062 inch diameter Inconel X-750 Metal O-Ring	E-O-N-003000 -02-07-1

Supplier: Advanced Products Company
Defco Park Road
North Haven, Connecticut 06473
Phone: (203) 239-3341

Fittings:

One-half inch NPT Hex Nipple, Stainless Steel (316), Quantity: 1, part number SS-8-HN. Connects filter holder to Cyclone III.

Fractional tube adapter to male pipe (NPT), 5/8 inch tube to 1/2-inch pipe, Stainless Steel (316), Quantity: 1, part number SS-10-TA-1-8

Supplier: Cajon Company
32550 Old South Miles Road
Solon, Ohio 44139

Final Filters:

Thimble: 43 mm x 123 mm Stainless Steel Filter Holder
Part number: TH-S/2

Silicon "O" rings - package of six (for TH-S/2)
Part number: TH-1/2

Filter Clamp Band for TH-S/2
Part number: TH-2

Toyo Roshi Co. Fiberglass Thimbles, 43 mm x 123 mm
Part number: 86R (25 thimbles/box)

Supplier: BGI, Incorporated
58 Guinar Street
Waltham, Massachusetts 02154
Phone: (671) 891-9380

__Flat Filter__: 2.5 inches In-Stack Filter Holder, 316 Stainless Steel with 1/2-inch female NPT fittings, 3.0 inches O.D.
Part number: 272

Supplier: Sierra Instruments, Inc.
P.O. Box 909
Carmel Valley, California 93924

2.4 inches Filter Disc, Reeve Angel 923-AH (100/box)

Supplier: Arthur H. Thomas Company
P.O. Box 779
Philadelphia, Pennsylvania 19105

The standard material is 316 stainless steel. Other materials such as titanium (alloy 6Al-4V) or Hastelloy (X) may be used for special applications. Some special applications may require the use of flanges or some other device for connecting the parts other than threads. For those applications it is necessary to know that the internal dimensions are critical. Outside dimensions can vary without affecting the collection characteristics provided that flow into the nozzle is not interrupted. For the same reason, short nozzles should not be used.

The critical (internal) dimensions of a cyclone are illustrated in Figure 78. These are considered to be the critical dimensions because a change in any one of them may affect the operational characteristics of the cyclone (with the exception of H_{cup} and D_{cup} for some designs). The wall thickness of the gas exit tube is not critical as long as it is small compared to the diameter of the tube. The ratio of exit tube wall thickness to I.D. is 0.11 for cyclone SRI-III and 0.08 for cyclone SRI-X. Since there is no cyclone theory that accurately describes how a cyclone's performance changes as the critical dimensions change, it is necessary to keep all the dimensions within close tolerances when manufacturing the sampler. Likewise, it is not known what effect the surface finish has on cyclone performance, so it is advisable to maintain the finish specified in the design drawings.

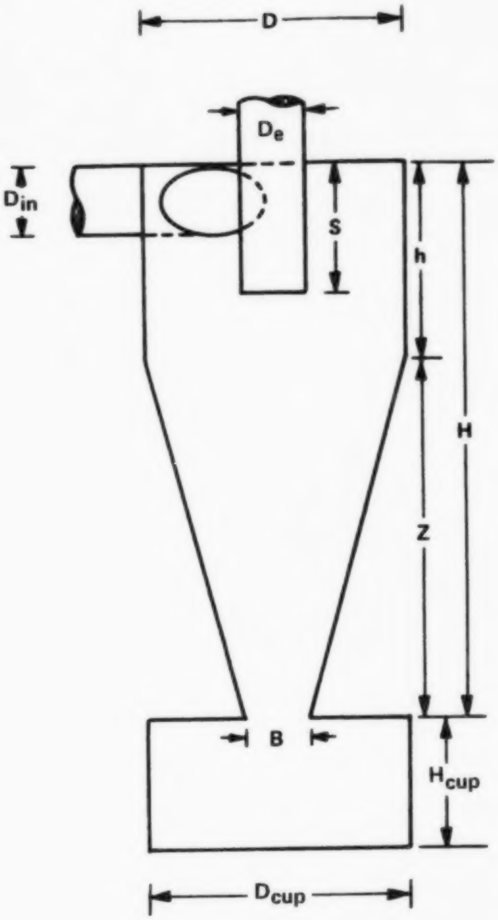

D = DIAMETER OF THE CYLINDER PORTION OF THE CYCLONE, ALSO CALLED THE DIAMETER OF THE CYCLONE
D_{in} = DIAMETER OF THE INLET
D_e = DIAMETER OF THE GAS EXIT
B = DIAMETER OF THE DUST EXIT
H = HEIGHT OF THE CYCLONE
h = HEIGHT OF THE CYLINDER
Z = HEIGHT OF THE CONE
S = INSIDE LENGTH OF THE GAS EXIT TUBE
H_{cup} = HEIGHT OF THE COLLECTION CUP
D_{cup} = DIAMETER OF THE COLLECTION CUP

4181-27

Figure 78. The critical internal dimensions of a cyclone.

The cyclones are designed to provide a leak-free system when used with proper O-rings. The O-rings recommended are made of Inconel X-750; however, other materials may be used. Care should be taken when ordering O-rings. The wrong thickness of O-ring can cause leaks if the O-ring thickness is too small, and can lead to improper alignment if the O-ring is too thick. Thickness of the O-rings for which the sampler was designed is 0.062 inch except for the O-ring in the connection between the cyclone SRI-X vortex tube and the cyclone SRI-III shell which is 0.094 inch.

The final stage of the sampler is an absolute filter. A Method 17 thimble or a flat filter holder may be used. Criteria to be considered in choosing a filter are discussed further in the next section.

The IP Cyclone Sampler was designed to operate with straight nozzles, which increases the total diameter of the system to just under six inches. Use of nozzles shorter than those in the design drawings is not advised.

Cleaning, Inspection, and Assembly--

Before using the sampler, it should be cleaned with a mild detergent, rinsed with water, and dried. The interior surfaces should be inspected for quality of finish and for defects due to corrosion, scouring, or deformation. The O-ring grooves and mating surfaces should be flat and smooth and have no transverse scratches. Certain concentric scratches from machining tools are allowable if they do not affect the leak-seal integrity of the cyclone. The O-rings should also be inspected for dents, cracks, scratches, and deformation. Nicked or bent O-rings should be replaced. The metal O-rings should last several tests, depending on the test conditions, but the pliable O-rings in the thimble holder may need to be replaced after each run. All filter material should be removed from the filter holder between runs. The nozzles should be cleaned and inspected for dents especially on the rim of the nozzle. Large dents that cannot be straightened by hand tools may require re-machining the nozzle rim.

Cyclone SRI-III is encased in a shell which must be disassembled so that all the internal parts can be cleaned. Any part which comes in contact with the sample gas is considered an internal part. For example, the entire Cyclone SRI-III collection cup and body is considered an internal part or surface. The inlet insert for Cyclone SRI-III need not be removed each time if no particles are captured between the inlet and the cyclone body.

The sampler should be assembled as shown in the assembly drawing shown in Figure 77. The proper nozzle and filter holder should be selected and connected to the sampler at the appropriate places. The threads should not be coated with anything, such as thread lubricant, that might contaminate the sample. Before the sampler is used in the field, the threads can be silver plated to prevent galling of the threads. No sealant is needed for the threads on the nozzle: the metal-to-metal seal is sufficient. Teflon pipe tape should be placed on tapered pipe threads such as those on the adapter connecting the final filter to cyclone SRI-III.

Sampling Parameters--

Most of the sampling parameters should be measured by approved EPA reference methods. In general, many of the parameters are the same as for a Method 5 test. Values other than these should be measured accurately and recorded carefully. In particular, the results of a velocity traverse, stack gas temperature measurement, and gas analysis are used to determine the testing parameters such as flowrate and nozzle size.

Gas velocity and analysis--The velocity traverse should be performed in accordance with EPA Method 2. The velocities and temperature in the flue as well as the static pressure in the flue should be measured. An extra effort, if necessary, should be made to obtain the gas velocity at the sampling ports. If possible, velocity fluctuations at those points should be noted and the percent isokineticity estimated. If the velocity fluctuations are so great that ± 20% isokineticity cannot be maintained, then another sampling position should be found, if possible, where the velocity is more stable. A constant flowrate through the sampler must be maintained.

A gas analysis to determine the composition (molecular weight) of the gas, including the amount of water vapor, should be performed using the appropriate EPA reference methods (3, 4, and others as necessary). The molecular weight of the gas can then be accurately determined for viscosity and flowrate calculations and a decision can be made regarding supplemental heating of the sampler. An estimation of the flue gas composition based on previous tests may be acceptable, specifically if the same type of source has been often tested. In such a situation, an estimate of the gas composition for the purpose of determining the gas viscosity is appropriate.

Sampling time--The length of time required to collect an adequate sample is dependent upon the mass loading of the gas, the size distribution of the particles, and the flowrate of the sampler. If the results of a mass test are available, the mass loading can be obtained from them. If not, an estimate should be made based on the pre-test survey or other information. Given the mass concentration, an estimate of the sampling time for initial tests can be obtained from Figure 79. Results from the initial tests can then be used to more accurately establish the optimum sampling time.

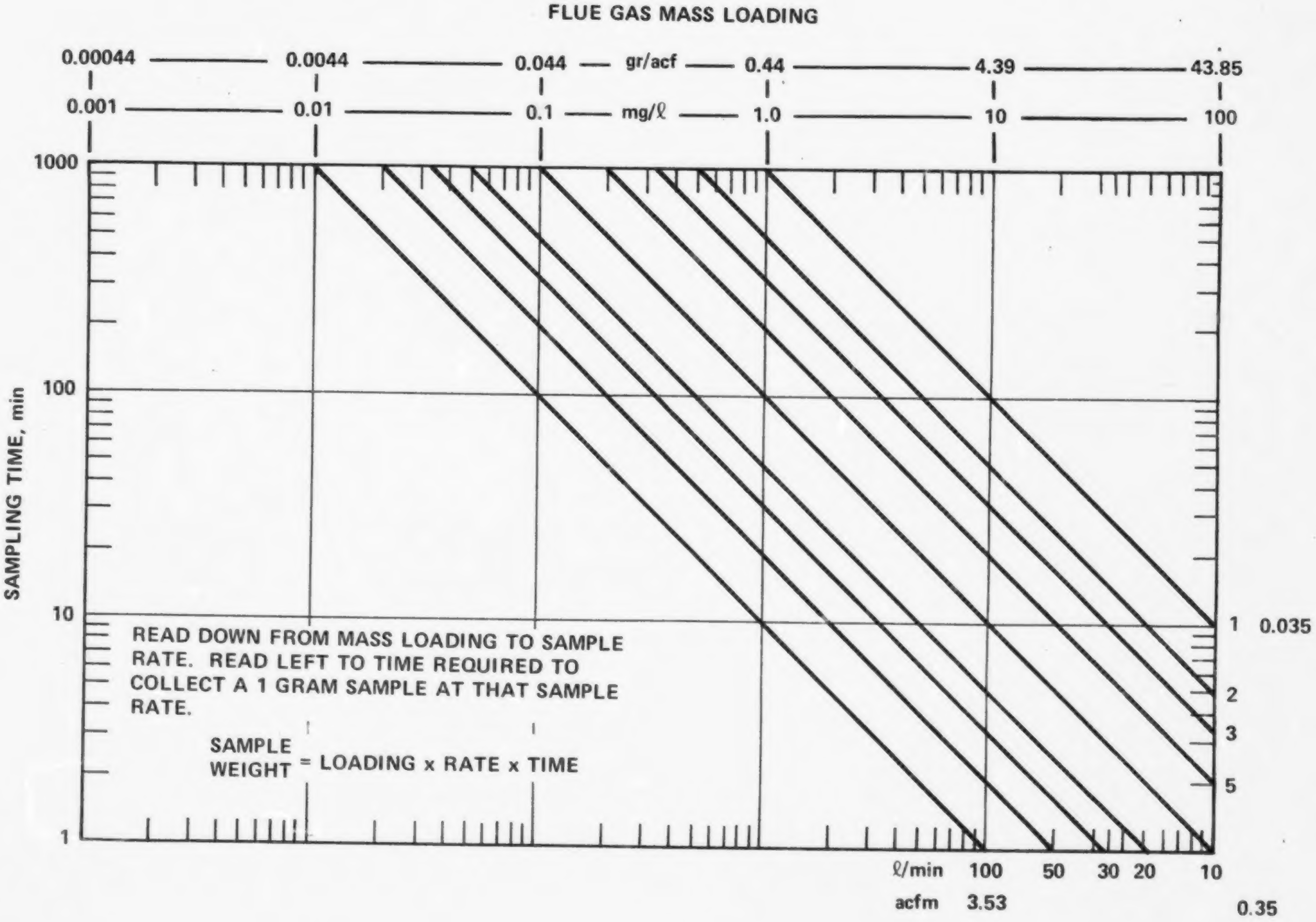

4181-29

Figure 79. Nomograph for selecting proper sampling duration.

Back-up filter--The selection of the back-up filter must be made according to the size distribution of the dust, the mass loading, the flowrate, the amount of sample required, and the type of analysis of the dust which will be made. If a large fraction of the dust is fine particulate, a flat filter will load up before the cyclones have collected an adequate amount of dust. Therefore, a thimble, which has more filtering area, should be used. Similarly, if the mass loading is high, a thimble should be used to allow longer run times so well integrated samples can be obtained. If the mass or the amount of fine particulate is low, a flat filter should be used so that weighing errors will be minimized.

Under some conditions, the material of which the filter fibers are composed will react with constituents in the gas stream (especially sulfur oxides SO_x) and the filter will lose or gain weight. This weight change due to flue gas exposure may be comparable to the weight change due to dust loading. If so, steps must be taken to reduce the weight changes due to flue gas exposure. This can be accomplished in three ways: (1) a filter material which has a small weight change upon flue gas exposure should be used (such as Reeve Angel 934AH), (2) the filter material may be preconditioned by exposing it to the flue gas prior to its initial weighing and use in a sampling test, and (3) the filter material may be preconditioned by exposing it to SO_x in the laboratory prior to its use in a sampling test. Sometimes a combination of (1) and (2) or (1) and (3) will be necessary to sufficiently stabilize the filters against weight changes. Method (3) is carried out by washing the filter with sulfuric acid; the following procedure has been found to be suitable.

Procedure for acid washing filters--

1. Submerge the glass fiber filters to be conditioned in a 1:1 mixture (by volume) of distilled water and reagent grade concentrated sulfuric acid at 100-115°C (212-239°F) and keep them at this temperature for 2 hours. This operation should be carried out in a hood with clean glassware. Any controllable laboratory hotplate is suitable.

If the filters need to be weighted down to keep them submerged, place Teflon disks on the top and bottom of the filter stack. The top disk can be held down with a suitable glass or Teflon weight.

2. After removal of the filters from the acid bath, allow them to cool to room temperature. Then place them in distilled water and rinse them with a continuous water flow of 10-20 ml/min. The filters should be rinsed until the pH of the rinse water, after a few minutes in contact with the filters,

is nearly the same as that of the distilled water, as measured with a pH meter. The importance of thorough washing cannot be overemphasized.

3. After rinsing the filters in distilled water, rinse them in reagent grade 2-propanol (isopropyl alcohol, isopropanol). Submerge them and allow them to remain in it for several minutes. Repeat this step four or five times, each time using fresh 2-propanol.

4. Allow the filters to drain and dry. Spread them out in a clean dry place after they are dry enough to handle.

5. When the filters are quite dry to the touch, bake them in a laboratory oven to vaporize residual moisture or 2-propanol. Bake them at 50 °C (122 °F) for about two hours, at 200 °C (392 °F) for about two hours, and finally at 370 °C (700 °F) for about three hours, to vaporize any residual sulfuric acid. (The filters are now ready for in-situ conditioning.)

As a final check that the acid has been removed, measure the pH of a water extract of the filters. Tear two filters into small pieces, immerse them in about 50 ml of distilled water, stir the water for about 10 minutes, and measure the pH with a pH meter. If the pH is significantly lower than that of the distilled water, then the filters must be baked at 370 °C (700 °F) for several hours more to remove residual sulfuric acid. A high temperature must be used since the boiling point of sulfuric acid is 340 °C (640 °F).

Procedure for in-situ conditioning of filters--Even after acid washing, unwanted weight gains have been observed in some process streams, particularly those at extremely high temperatures and containing relatively large concentrations of sulfur oxides. If such a problem exists, further conditioning is required. Place the filters, loosely packed, in a suitable container preceded by a filter, insert the container in the process stream, and draw filtered gas through the container for 6-24 hours, followed by desiccation and weighing of the filter before use.

Sampling points--Figure 80 shows the locations of the sampling points that are recommended. After the velocity profile has been measured, IP samples should be taken at the locations shown. Four single-point samples should be taken with the IP trains and the mass trains, or the tests repeated with the IP train. Any measurement of total mass concentration that differs from the mean by more than 50% should be considered suspect. The suspect measurement should be compared with the value found by the other train used at the same point. If these values disagree by less than 50%, the deviations are probably due to stratification

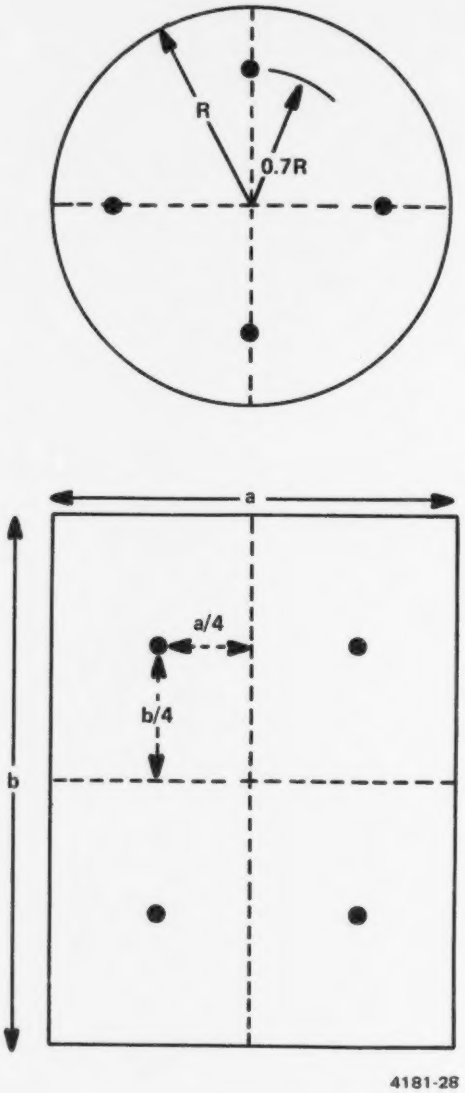
R
0.7R
a
b
a/4
b/4
4181-28

Figure 80. Recommended sampling points for circular and square or rectangular ducts.

of the dust, and all of the data should be retained. In sampling the effluents from variable or cyclical processes, the entire test sequence must be repeated until a good average value of the emissions is obtained. In any event, the sequence should be repeated at least once at each site.

Regardless of the velocity distribution in the flue, the flowrate through the sampler must remain constant. It is desirable to maintain the isokinetic velocity ± 20% or better, throughout the sampling period. Minimum sampling efforts, which are appropriate only for flues with well-developed flow profiles and with no significant concentration stratification, are these: at least two points within a duct should be sampled in each measurement plane, and at least two samples taken at each point. In the event of non-uniform velocity or gradients in mass concentration, the number of samples may need to be increased for reliability.

Selecting the sample flowrate and nozzle--Since the D_{50} of Cyclone SRI-X must be 15 μm aerodynamic but depends on the viscosity of the gas and the flowrate through the cyclone, the sample flowrate will be determined by the viscosity of the gas. Figure 81 illustrates the relationship between the flowrate and viscosity for Cyclone SRI-X to obtain a D_{50} of 15 μm. Using the results of the gas analysis, the viscosity can be calculated; otherwise the following equation can be used: $\mu = (174.4 + 0.406T(°C)) \times 10^{-6}$ poise. The sampling flowrate is then determined from Figure 81. The flowrate can be used with the gas velocity to select the appropriate nozzle using Figure 82. Only straight nozzles should be used. The D_{50} of Cyclone SRI-III can be estimated from previous calibration curves. (See Figure 60.)

Leak testing--Before use, the sampler should be leak tested. Immediately after assembly, the operator should perform a leak test on the sampler. This can be performed in the lab with a minimum amount of equipment. Leak tests should also be made at operating temperature - after the Inconel O-rings have thermally expanded. This expansion will generally help to seal the cyclones.

It is suggested that the cyclones be checked for leaks at the same time the mass trains are checked.

Sampling--

There can be no substitute for trained and experienced personnel to operate the IP Cyclone Sampler. The same care should be taken with the sampler during testing as is required for Method 5 and cascade impactor operation. Essentially, the sampler should be operated the same way as in Method 5 except for the sampling points and the need to maintain a constant flowrate.

The IP Cyclone Sampler is still in the prototype stage of development and has not been used extensively in field applications. It is expected that better, and more detailed, operating

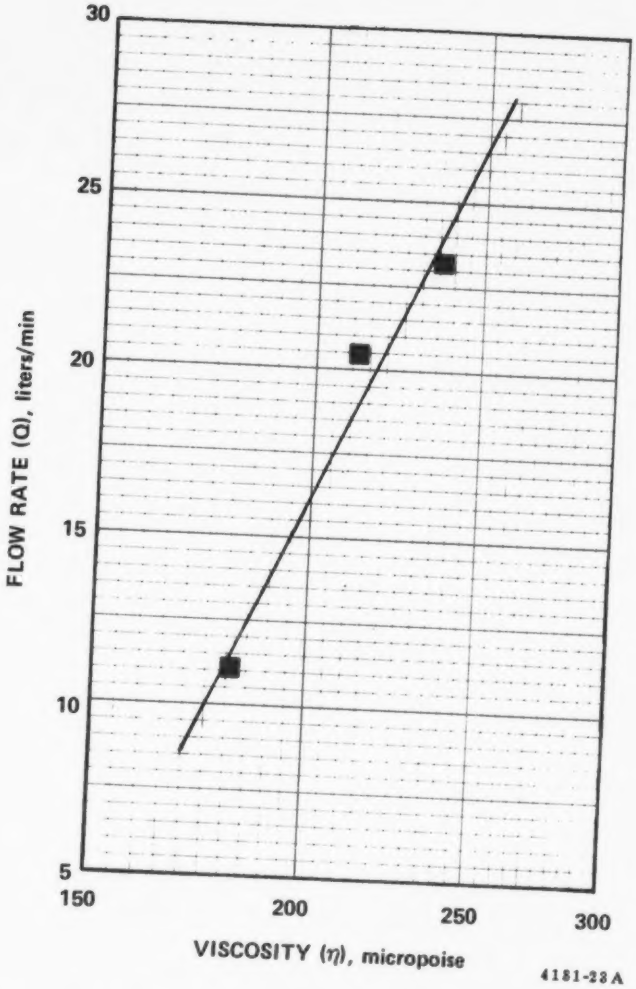

Figure 81. *Gas flowrate versus viscosity at D_{50} = 15 μm aerodynamic diameter for IP cyclone SRI-X.*

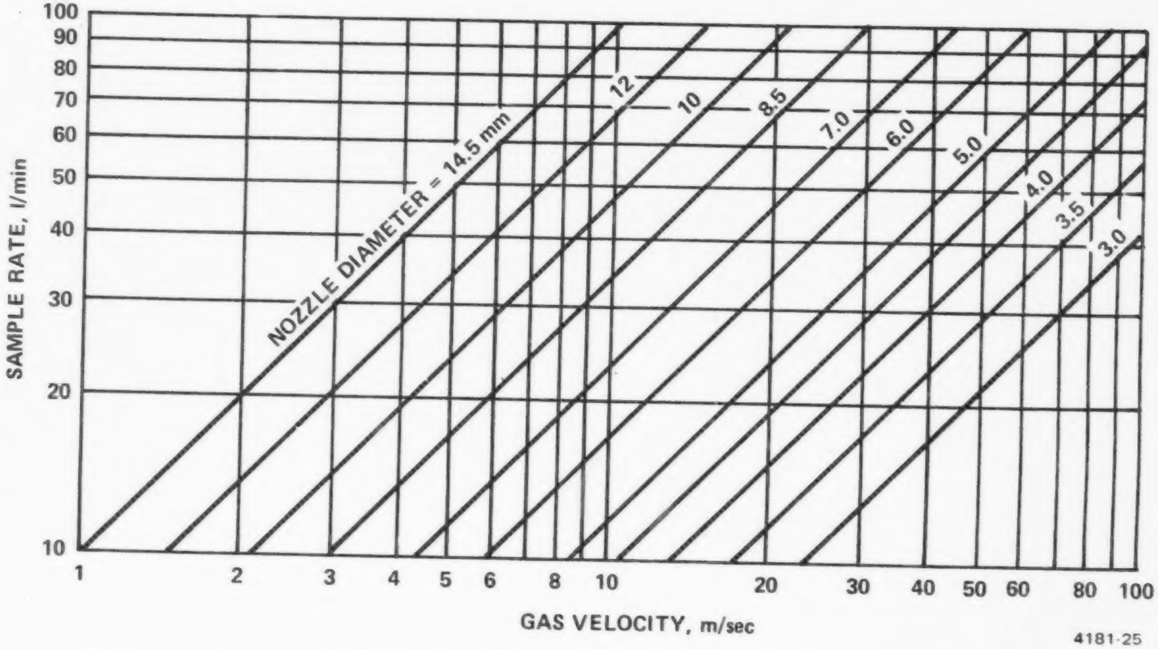

Figure 82. Nomograph for selecting nozzles for isokinetic sampling, using cyclone samplers.

procedures will be developed as this experience is gained. Potential problem areas include possible reentrainment from overloading Cyclone SRI-III at high mass loadings and long run times, extremely long run times at flues with low mass loadings and loss of particles during the unloading process.

Flowrate--During the run, the predetermined flowrate must be maintained to ensure stable cut points. Any attempt to modulate flow to provide isokinetic sampling will destroy the utility of the data by changing the cut points of the cyclones. As the final filter collects particulate, the pressure drop across it will increase, lowering the sample flowrate. The flowrate should be monitored and adjusted when necessary.

Traversing--During traversing (moving to a new point or new port) all motion should be smooth and brief to avoid bumping or vibrating the sampler. When removing or inserting the sampler, care must be taken not to scrape the nozzle on the port wall. Also, the sampler should not be allowed to bump against the far inside wall of the flue.

Orientation--The IP Cyclone Sampler is designed to operate in any orientation with equally accurate results. However, when the sampler is operated in the upright position (the backup filter above Cyclone SRI-III which is above Cyclone SRI-X), the flow should not be terminated until the sampler is in the HORIZONTAL position. Otherwise some dust might fall from one stage of the sampler into another and thus be measured where it is not collected. After the flow has been terminated, the sampler can be transported to the lab in the horizontal position with the nozzle plugged or covered to avoid contamination or loss of the samples.

Data logging--In addition to the sampling parameters and process information usually recorded in a Method 5 test, the operator of the IP Cyclone Sampler should also record the sampler identification, sampler orientation, filter identification, gas viscosity, and the sampler flowrate.

Sample Retrieval and Weighing--

Unloading the sampler--After the sampler has cooled down to nearly ambient temperature and brought into the lab, it is "unloaded" by removing the catch of particulate matter. Great care is needed to insure that all of the particulate matter is recovered and transferred to the proper sample containers. The following procedure has been found to be suitable.

First, remove sample collected in Cyclone SRI-X. With the nozzle plugged, turn the sampler from a horizontal position to a position 45° from the horizontal. Cyclone SRI-X should be lower than the backup filter. Holding the sampler in this position, carefully unscrew the body of Cyclone SRI-X from the cap. Holding the body underneath the cap, brush the particles adhering to the bottom of the cap and the outside of the gas exit tube into the cyclone body. A no. 7 camels hair artists' brush (or the small nylon brush made for cleaning electric shavers) is suggested. Rotate the cyclone so that the nozzle is pointing upward at 30-45° from the horizontal and brush the particles caught inside the nozzle down into the cyclone. Rotate the cyclone back to an upright position and use a downward, pushing motion to brush the particles on the inside walls of the body of the cyclone down into the collection cup. Carefully detach the collection cup from the body and, holding the body over the cup, brush the particles adhering to the underside of the body into the cup. At this point, all of the particles caught by Cyclone SRI-X should be in the cup. If a cup insert is used, remove it with a pair of tweezers for desiccation and weighing. If not, transfer the sample by pouring and brushing to a pre-weighed container.

Cyclone SRI-III should still be in the 45°-from-horizontal position, with the backup filter higher than the cyclone. Very carefully, unscrew the shell of Cyclone SRI-III and, holding it over a sample container, brush the dust down into the container from the shell, the cyclone, and the inside of the exit tube and connecting pieces of Cyclone SRI-X. Then, holding the container underneath, brush off the dust clinging to the outside of the Cyclone SRI-III body and collection cup and the now exposed part of the cap. After all this dust has been removed, slowly unscrew the Cyclone SRI-III body from the cap. Hold the body upright and brush all the particles down into the collection cup. Remember to brush the dust out of the inlet. Then slowly remove the collection cup from the body and transfer its contents to the sample container. Finally, hold the sample container underneath the vortex tube and brush the dust on the outside of the exit tube and the underside of the vortex tube into the container.

Now turn the connecting tubing and filter so that the Cyclone SRI-III cap is directly above the filter. Brush the dust collected on the inside of the gas exit tube and the connecting tubing down onto the filter. When all the internal surfaces directly upstream of the filter have been brushed clean, remove the filter and place it in a proper sample container for desiccation and weighing.

In some cases it may also be necessary to wash the internal nozzle and cyclone surfaces with a solvent, such as methylene chloride, into a preweighed bottle or aluminum cup. If the dust is hard and dry, the particles can be brushed off into the weighing container; if the particles are sticky or wet, some type of washdown procedure should be used. Use a solvent that is considerably more volatile than the particulate matter. Cover the sample container loosely and allow the solvent to evaporate completely before desiccation and weighing. Desiccation is complete when consecutive weighings (two hours apart) of the sample yield the same values. In a sealed container of a desiccant like silica gel, desiccation takes about 24 hours.

Drying and weighing--Each of the particulate containers must be dried to a constant weight, with two hour checks used to establish the uniformity of the weights. Samples of hard, non-volatile particles are often dried in a convection oven at a temperature of 212°F, kept in a desiccator until cooled to room temperature, weighed, and then check-weighed two hours later. Volatile particles present special problems which have to be dealt with according to the particulate characteristics and sampling goals. One technique for particles which are volatile at elevated temperatures is to desiccate them 24 hours before weighing. Whatever the technique used, constant weight of the samples after further drying is the criterion to be met. Record the results of the weighings and any notes in a notebook and keep it with the run sheets.

Data Analysis and Reports--

Data taken in various inhalable particulate studies should be readily comparable and independent of the sampling team. The data should therefore be presented in identical format.

Calculation of mass concentration--The total mass loading or total concentration is found by dividing the total mass collected, M, by the volume of gas sampled (product of the sample flowrate, Q, and the sampling duration, t). Similarly, the inhalable particulate concentration is calculated by dividing the mass collected in Cyclone SRI-III and the filter by the volume of gas sampled, and the fine particulate concentration is found by dividing the mass on the filter by the gas volume. The product of the sample flowrate at stack conditions and the sampling duration gives the total actual volume of gas that was sampled. The equation below is used to calculate the equivalent volume of gas at standard (normal) temperature (20°C) and pressure (760 torr) and at dry conditions (water vapor diluted), V_{dry}.

$$V_{dry} = Qt \frac{\text{Stack Pressure x } 293°\text{K}}{\text{Stack Temperature x } 760 \text{ torr}} \text{ x } (1-f_{H_2O})$$

where f_{H_2O} is the fraction of water vapor present in the gas. The mass concentration at "normal" conditions is thus found by dividing the mass by V_{dry}. The results should be summarized in a format like that below:

PARTICULATE MASS CONCENTRATION

(Example)

	Actual Conditions		Normal Conditions		Cumulative	Cumulative %
	mg/m^3	gr/ft^3	mg/nm^3	gr/ft^3	%	Including Condensables
Total	1.6×10^5	0.30	2.5×10^5	0.46	100.0	60
IP (<15 μm)	1.5×10^5	0.27	2.2×10^5	0.41	52.5	54.5
FP (<2.5 μm)	2.7×10^4	0.05	4.1×10^4	0.08	8.0	--
FP (<2.5 μm, including condensables)	4.2×10^4	0.08	6.4×10^4	0.12	--	11.9

IP is inhalable particulate, FP is fine particulate

Cyclone calibration data--In each report, calibration curves showing the collection efficiency and D_{50} cut point for the type of cyclone that was used should be included. Any extrapolation from these curves to the actual field test conditions should be recorded with explanatory notes. Likewise, the filter material that was used should be identified fully and any conditioning or acid treatment should be described. The particle retention characteristics, in the form of calibration curves or manufacturer's data, should also be reported. If a chemical analysis of the filter is performed, then the background elemental analyses should also be reported. This information can be obtained from the manufacturer or, better, determined by the laboratory on clean filters.

Reporting data--Each report should include all the parameters of each test. In general, the data required are those required by Method 5. Specifically, the following items should be reported:

- Gas viscosity
- Sample flowrate at actual and normal conditions
- Mass collected in each stage of the sampler
- D_{50} cut point of each cyclone for each test
- Particle density
- Sampling duration
- Percent isokinetic gas flow at each point sampled.

A simple report outline might follow the scheme of the one below:

I. Conclusions
II. Recommendations
III. Introduction
IV. Plant/Process Description
V. Sampling Strategy
VI. Mass Train Data (if applicable)
VII. Cascade Impactor Data (if applicable)
VIII. IP Sampler Data
IX. Appendices
X. References

The Dilution Stack Sampling System

Design and Operating Procedures--

A diagram of the major components of the Stack Dilution Sampling System is shown in Figure 83. In operation, gases from the process stream are drawn through the IP Cyclone Sampler, in which particles with aerodynamic diameter greater than 15 μm and those in the range 2.5-15 μm are removed in two stages. The stack gas containing the fine particle fraction (<2.5 μm) and condensable vapors passes through the heat-traced probe and flexible sample line and is introduced axially into the bottom of the cylindrical dilution chamber. At this point the stack gas is mixed with dilution air to form a simulated plume which flows upward through the dilution chamber, through a standard 20 cm x 25 cm (8 in. x 10 in.) hi-vol filter which collects the fine particulate and any new particulate formed by condensation. The diluted stream is exhausted by a 1 HP blower or optionally by a standard hi-vol blower.

Dilution air is drawn from the ambient through a blower and forced through an ice bath condenser. In this condenser, the air is cooled to 5-8°C, depending on the flow and ambient temperature. More significantly, the dilution humidity is reduced to about 0.57% by volume, corresponding to saturated air at the ice point. After the condenser, the air is reheated as required to reach 21°C (70°F) at the dilution chamber inlet, filtered through an HEPA-type absolute filter, and introduced into the dilution chamber. The dilution air enters through a single tangential inlet at the base of the dilution chamber and passes through a set of flow-straightening screens into the annular region surrounding the sample gas inlet. The ratio of the areas of the two inlets is such that for sample gas at room temperature the velocities of the sample and dilution streams are equal. Sample gas at stack temperature will be injected at a higher velocity proportional to the thermal expansion of the heated gas stream. This was judged the best simulation of a buoyant plume injected into stagnant air.

System Description--

The geometric and flow specifications have been set by several constraints. The sample flowrate is set by the flow requirements of the IP Cyclone Sampler. Ideally, to approximate the conditions found in actual plumes, the dilution ratio should be high (approaching 10^3-10^4) and the mixing times long (tens of seconds). The actual dilution conditions represent a compromise dictated by limitations on the size of a portable field instrument. Geometric and flow specifications are as follows:

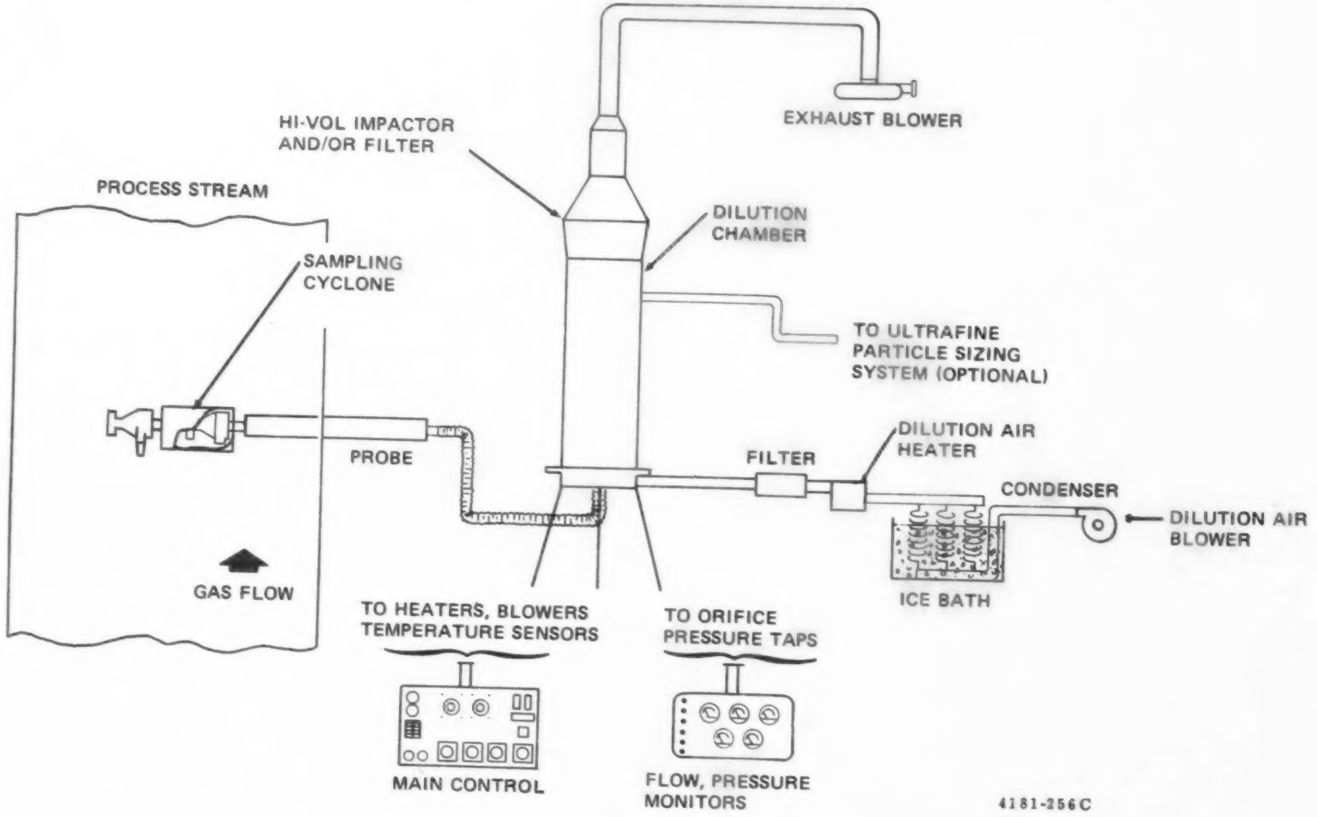
HI-VOL IMPACTOR AND/OR FILTER
EXHAUST BLOWER
PROCESS STREAM
DILUTION CHAMBER
SAMPLING CYCLONE
TO ULTRAFINE PARTICLE SIZING SYSTEM (OPTIONAL)
DILUTION AIR HEATER
PROBE
FILTER
CONDENSER
DILUTION AIR BLOWER
ICE BATH
GAS FLOW
TO HEATERS, BLOWERS TEMPERATURE SENSORS
TO ORIFICE PRESSURE TAPS
MAIN CONTROL
FLOW, PRESSURE MONITORS
4181-256C

Figure 83. Diagram of Stack Dilution Sampling System.

Active length of dilution tube: 1.22 m (4 ft)
Total height of sampler: 1.8-2.1 m (6-7 ft)
I.D. of dilution tube: 21.3 cm (8.4 in.)
I.D. of sample inlet tube: 4.27 cm (1.68 in.)
Active dilution volume: 43.6 ℓ (1.54 ft^3)
Sample flow: 17 nℓ/min (0.6 ft^3/min-determined by cyclone cut point)
Dilution flow: 425 nℓ/min (15 ft^3/min)
Dilution factor: 25
Residence time: 6.2 sec
Sample velocity: 25 cm/sec at 150°C
Dilution air velocity: 19.8 cm/sec at 21°C

Since the effect of varying dilution air temperature and humidity cannot be easily predicted for all typical process streams, standard conditions of 0.57% moisture by volume at 21°C (corresponding to about 24% RH at 70°F) were chosen. This relatively dry dilution air should not be subject to water condensation for normal stack samples, yet is more realistic than totally dry air.

Sample probe and heated hose--The sample probe and heated hose assemblies are shown in Figure 84. The probe is a heat-traced stainless steel assembly consisting of a core of 5/8-in. tubing wrapped with high-temperature heating tape, glass-fiber insulation, and a stainless steel outer jacket. The heating tape covers only the final 4 ft of the probe which extends outside the stack. Thermocouples monitor the temperature of the process stream, of the inner tube walls, and of the gas sampled between the probe and the hose. The heated hose is a commercially available, heat-traced, flexible sample hose with a 1/2-in. O.D. Teflon core, a nichrome wire heating element, specially installed RTD and thermocouple temperature sensors, glass-fiber insulation, and a weather-resistant outer coating. The hose is rated for operation below 200°C.

Dilution air line--The dilution air line, pictured in Figure 85, consists of a portable blower, a high-flow condenser, air heater (consisting of a coil heating element), an HEPA-type absolute filter, and a flow metering orifice, all joined by flexible tubing. The purpose of the line is to provide a high flow of filtered air with controlled temperature and humidity. Dilution air temperature is monitored downstream of the condenser and in the base of the dilution chamber. The cooling-reheating process provides a means of reducing the humidity to the specified value, and also allows temperature control over a wide range of ambient conditions. Very dry ambient air may have to be prehumidified to reach the proper level, but such conditions should not commonly occur except in sub-freezing weather.

Dilution chamber inlet--The dilution chamber inlet assembly shown in Figure 86 determines the mixing conditions of the sample

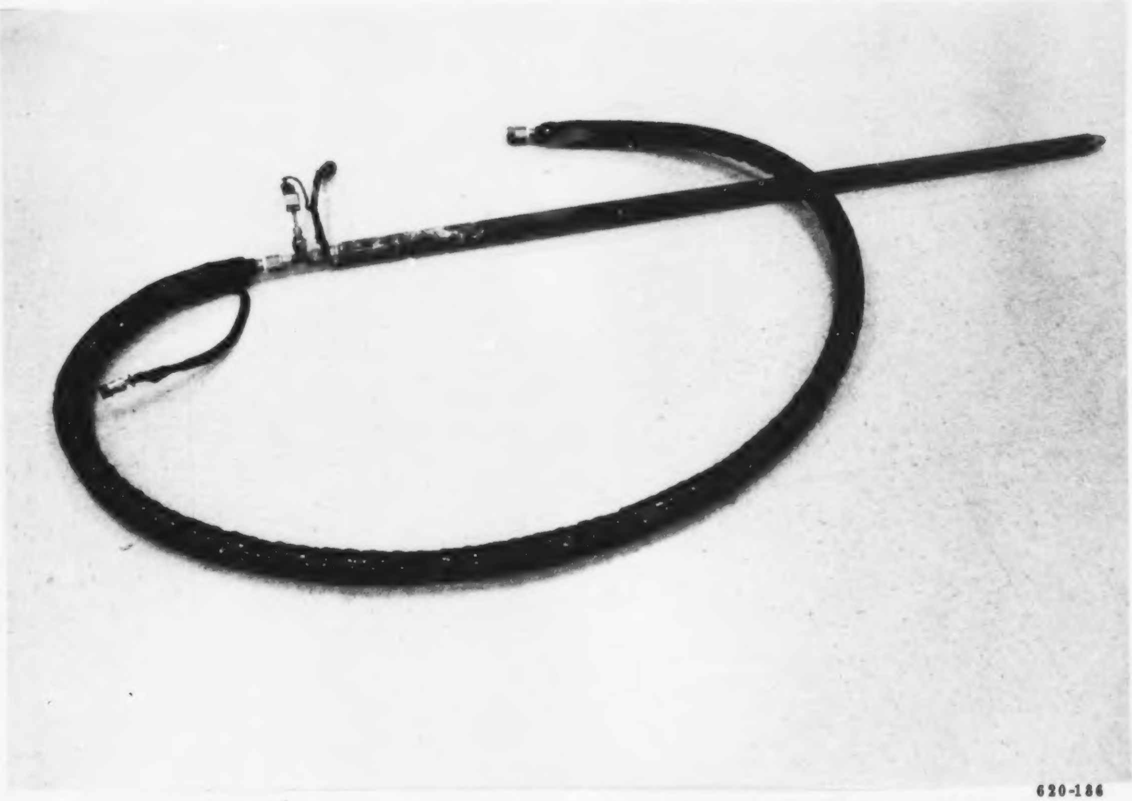
620-186

Figure 84. Sample probe and heated hose for the Dilution Stack Sampling System.

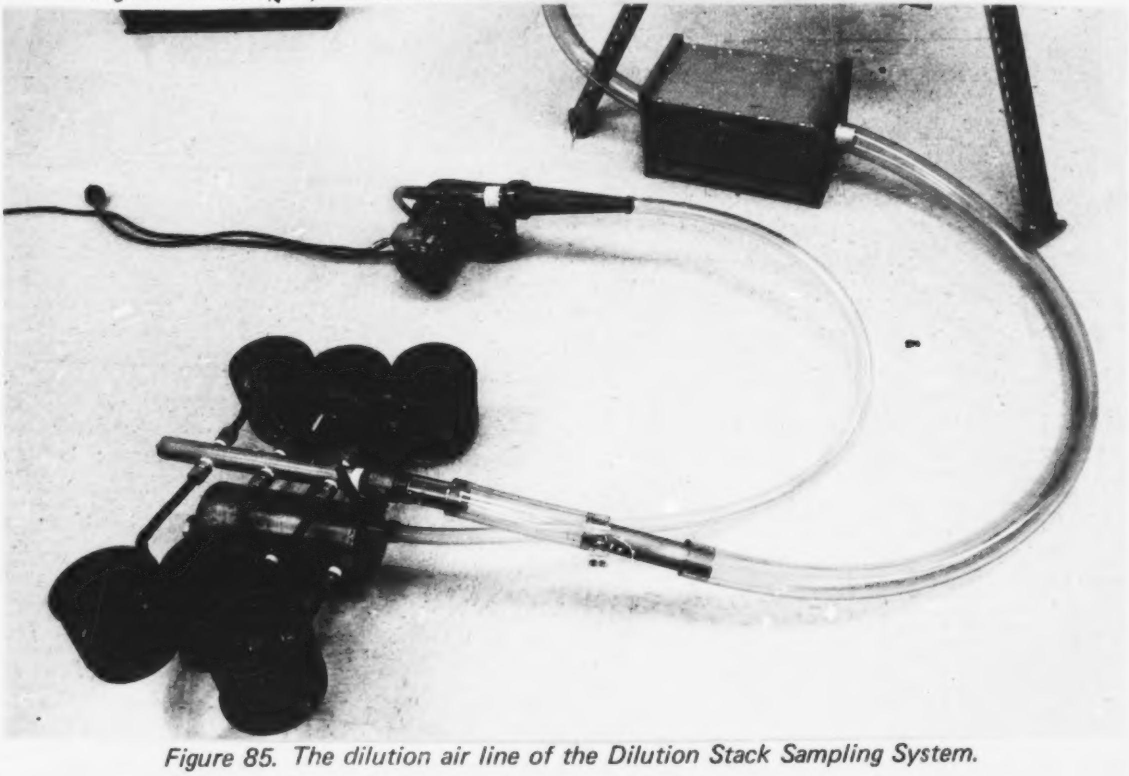

Figure 85. The dilution air line of the Dilution Stack Sampling System.

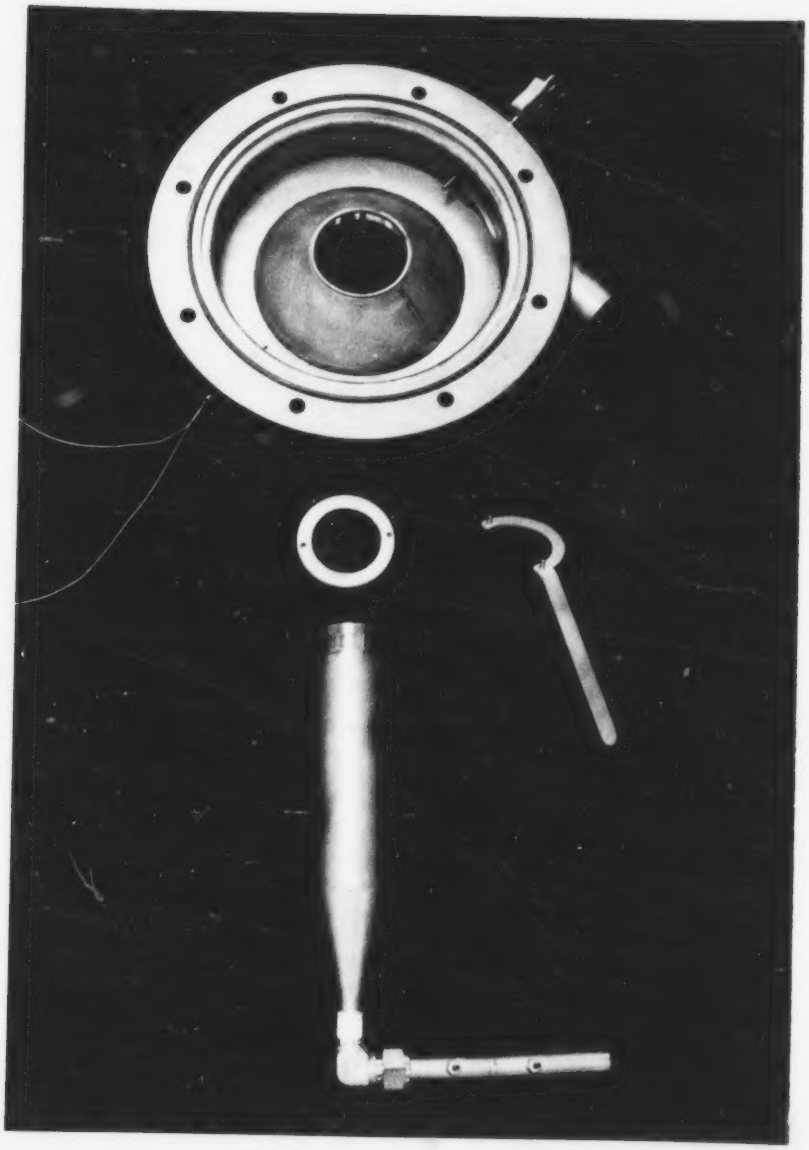

620-188

Figure 1. Inlet assembly of the dilution chamber of the stack dilution sampling system.

gas and dilution air streams. The sample inlet is heated and offers no flow restriction. The temperature of the inlet tube is monitored at two points. The dilution air section is thermally isolated from the sample gas inlet by a spacer of glass-reinforced Teflon in order to minimize preheating of the dilution air or cooling of the top of the sample inlet tube, which might lead to condensation on the tube walls. The dilution air is injected tangentially; the shape of the dilution chamber inlet and the fine mesh flow straightening screens combine to minimize the vortex effect and provide a nearly-uniform dilution air velocity profile.

Dilution chamber body--The dilution chamber itself is simply a long tube in which the mixing and cooling process occurs. Provisions have been made to extract a small sample (10-30 ℓ/min) for sizing with optical, electrical mobility, or diffusional means. The top of the dilution chamber body adapts to a square flange for mounting the hi-vol filter or impactor assembly.

Hi-vol filter and impactor assembly--The hi-vol filter and impactor assembly are shown in Figure 87. In the figure, the impactor base plate and one impaction stage are mounted on the hi-vol filter holder. For standard operation, measurements would include only filter measurements of total particulate mass loadings in the diluted stream.

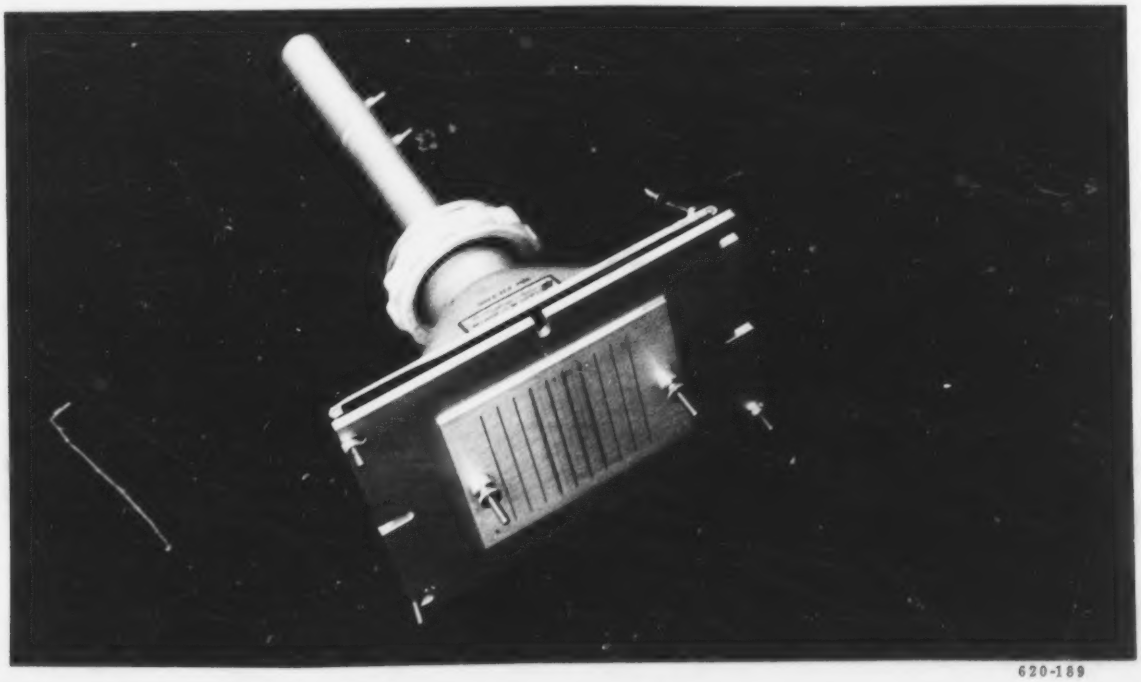

620-189

Figure 87. Hi-vol filter and impactor assembly of the Stack Dilution Sampling System.

Instrument packages--Figure 88 shows the Pressure and Flow Measurement Module, which is the smaller of the two suitcase-mounted instrument packages. In this module, magnahelic pressure gages monitor the pressure differential in the dilution chamber with respect to ambient, the pressure drop across the impactor and/or filter, and the flow through orifices in the sample, dilution air, and exhaust lines.

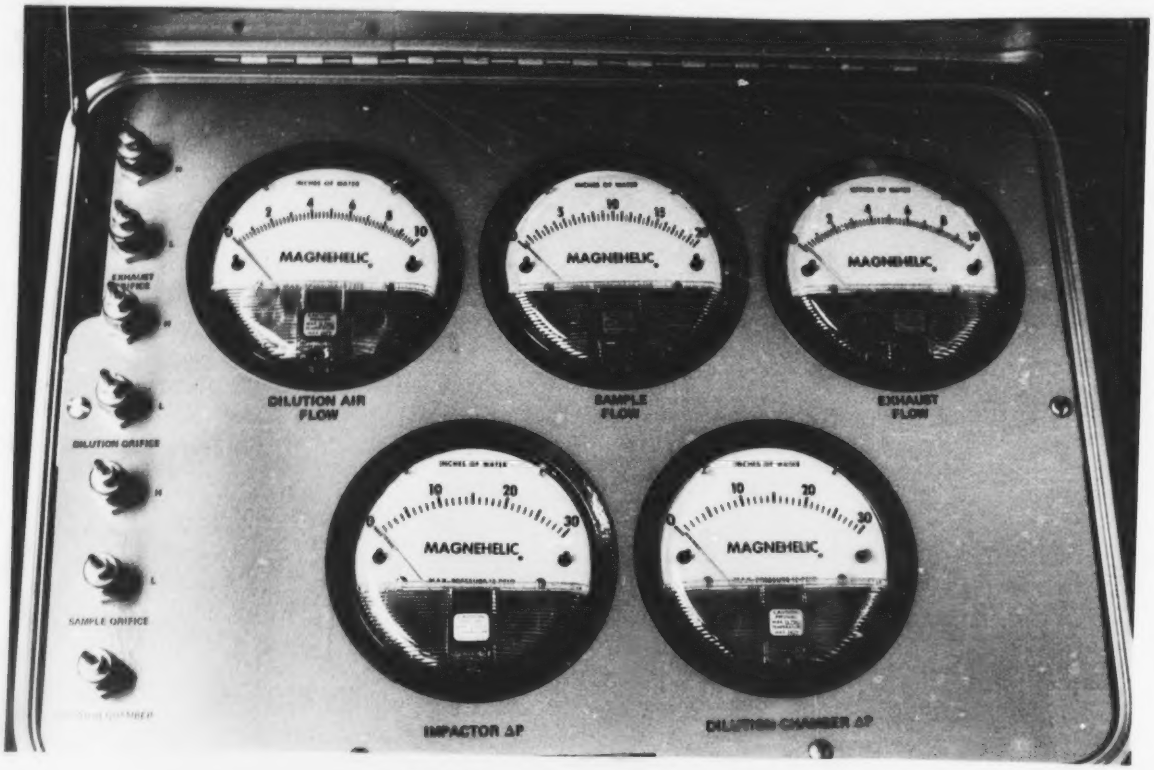
EXHAUST ORIFICE
DILUTION ORIFICE
SAMPLE ORIFICE
MAGNEHELIC
MAGNEHELIC
MAGNEHELIC
MAGNEHELIC
MAGNEHELIC
DILUTION AIR FLOW
SAMPLE FLOW
EXHAUST FLOW
IMPACTOR ΔP
DILUTION CHAMBER ΔP

Figure 88. Pressure and flow measurement module.

The Heater and Flow Control Module contains all electrical connections to the Stack Dilution Sampling System (Figure 89). Powered by two independent 110V, 20A power lines, the package contains proportional temperature controls for the probe, heated hose, sample inlet, and dilution air reheat. A digital thermocouple readout monitors temperatures at various points in the system, and variable auto transformers supply power to the dilution and exhaust blowers.

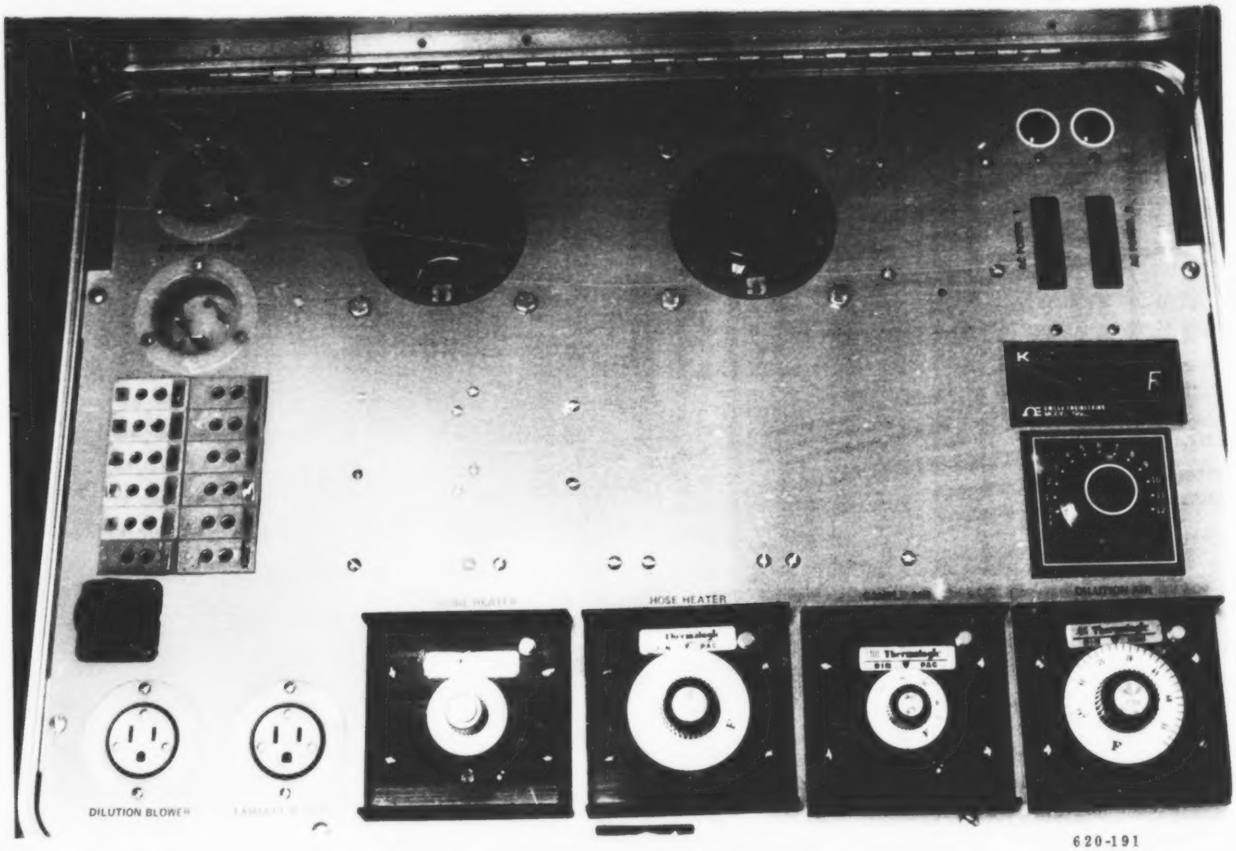

Figure 89. Heater and flow control module.

Assembly--

The dilution chamber, dilution air line, probe, and hose should be assembled as shown in Figures 83-87. Since the interconnections are made with standard tube fittings or with 1.5-in. I.D. flexible tubing, assembly is relatively straightforward, and only details which may not be obvious are presented below. The assembly of the IP Cyclone Sampler is described in the preceding section of this report. Electrical and thermocouple connections to the control module are straightforward, since all connectors are either numbered, color-coded, or unique to the mating component. Likewise, pressure taps leading the pressure/flow monitor module are clearly labeled.

Setup at a typical site would proceed as follows. The dilution chamber body is set up in the optimum location near the sampling port. The dilution chamber base is assembled as shown in Figure 86, using the special tool shown to screw in the Teflon insulating spacer. The flow straightening screens and retaining gasket are positioned in the base, the O-ring inserted and the base bolted to the mating flange in the dilution chamber. Since the orientation of the dilution air inlet is not important, it should be positioned in a direction convenient for setup of the dilution air line. The heated hose and probe should be attached to the sample gas inlet, and the dilution air line set up in the order shown in Figure 85. While the interconnection tubing lengths for the dilution air line are not specified, it is preferable that they be kept short in order to minimize pressure drop and warming of the chilled dilution air. If the heating tape and insulation have not been installed on the sample gas inlet tube, they should be installed at this time, taking care that the insulation extends over the connector to the heated hose. The IP cyclone sampler should be prepared according to the cyclone sampler procedures manual and attached to the probe with the appropriate fittings. For normal operation, the extraction tube for fine particle sampling is removed and fitting capped.

Since the hi-vol filter assembly is operated in an upsidedown configuration, the filter must be mounted with some care. For systems which have the optional hi-vol impactor, it is most convenient to use the impactor base plate as a retainer even though no impactor stages are used. Alternatively, a hi-vol filter hold-down frame, such as the Sierra 305-2017, may be used as a support for the filter. The filter holder is removed from the apparatus, the filter mounted, and the impactor base plate (or hold-down frame) secured above the filters as shown in Figure 87. The assembly can then be mounted on the dilution chamber using a second rubber gasket. Finally, the exhaust orifice tube and exhaust line can be connected.

Sampling Parameters--

Most of the sampling parameters should be measured by approved EPA reference methods. Many of the parameters are the same as for a Method 5 test. Values other than these should be measured accurately and recorded carefully. In particular, the results of a velocity traverse, stack gas temperature measurement, and gas analysis are used to determine testing parameters such as flowrate and nozzle size for the cyclone train. Stack temperature and moisture content will determine the final moisture content of the diluted stream and may in some cases preclude normal operation due to water condensation in the dilution chamber. Ambient temperature and humidity may likewise require adjustment in operation.

Temperature and moisture content of stack gas and ambient air--While the standard dilution air humidity was deliberately chosen to be rather low (corresponding to a dew point of 0°C) situations might arise which make testing at the standard humidity difficult or unfeasible. One such situation might arise if the process stream has such a high moisture content that condensation of water occurs in the dilution chamber. When process streams of typical compositions are diluted by air of the composition used in the Stack Dilution Sampling System, the relative humidity of the diluted stream reaches a maximum at relatively low dilution factors of 2-5. Thus, transient condensation of water plume might occur in the dilution chamber followed by evaporation prior to the hi-vol filter. This effect would be detrimental to system operation if the water fog persists at the full dilution, causing the filter to blind rapidly. Such blinding would occur in the rather unlikely case of a stack gas consisting of over 33% moisture by volume. If such a stream is encountered measurements with the Stack Dilution Sampling System must be modified by completely drying the dilution air with desiccant columns and/or increasing the dilution air flow and thus the dilution ratio.

A more likely complication might occur if the dew point of the ambient air is lower than 0°C. This would certainly be the case in subfreezing weather conditions; it could also occur under warmer but extremely dry conditions. In such circumstances it will not be possible to maintain the standard dilution air humidity without some preliminary humidification. If such low humidity conditions are encountered, values of ambient temperature and humidity should be recorded every hour during the sampling cycle and notation made on the data sheets that the dilution air humidity is expected to be low. While the effects of such lower humidity on the condensation process are not completely understood, the differences in the data obtained are expected to be minimized.

Sampling time--Even in the absence of condensable matter, the proportion of particulate in the fine particle fraction (<2.5 μm) passed by the cyclone samplers is expected to be high enough that the filter is adequately loaded before sufficient sample is collected in the cyclones. In general, measurement of the cyclone contents is important, so sampling time will be determined by the need for an adequate sample in the cyclone train. Some guidelines for estimating the sampling time are given in the previous section on operation of the IP Sampler. If only the condensable and fine particle fractions are of interest, the sample run can be terminated when a substantial increase in pressure drop across the filter is noted.

Gas velocity, temperature, and analysis--Since the flowrate of the cyclone sample is dependent upon the viscosity of the stack gas, and since the nozzle selected for this sampler depends on the stack velocity, these parameters must be measured carefully. The procedures for measurement of stack parameters and selection of sample nozzle and flowrate are outlined in detail in the previous section of this report on operation of the IP Sampler.

Filter and substrate selection--Under some conditions, the material of which the hi-vol filters (or impactor substrates) are composed will react with constituents in the gas stream (especially SO_x) and the filter will gain or lose weight due primarily to sulfate formation. This problem is common in in-stack sampling and has been noted in ambient hi-vol sampling as well. The diluted stack gas represents an intermediate situation more similar to ambient than in-stack sampling. Difficulties due to sulfate formation are expected to be avoided by a suitable choice of filter material. Candidate glass fiber materials are Reeve Angel 934AH or Schleicher and Schuell 30, both of which exhibit low weight gain at stack conditions. Alternatively, some glass fiber filters, such as Gelman Spectrograde, exhibit low weight gain at ambient temperatures even though they are unsuitable for in-stack use. Other filter materials, such as fibrous quartz, Teflon, or cellulose, may be suitable for specialized applications, especially when chemical analysis of the particulate matter is planned. However, for accurate gravimetric determinations these materials are generally inferior to glass fiber filters and are not recommended for general use.

Desiccation and weighing of filters and substrates should be performed with the care customary for Method 5 and cascade impactor tests.

Sampling--

As for a Method 5 or cascade impactor operation, the Stack Dilution Sampling System operation requires great care in all phases. Operation of the system will be similar to the operation of the IP Cyclone Sampler without dilution; the previous section of this report contains information regarding operation of the IP Sampler.

The Stack Dilution Sampling System is still in the prototype stage of development and has not been used extensively in field applications. It is expected that better and more detailed operating procedures will be developed as this experience is gained. Potential problems include difficulty in flow measurement and control, difficulties with port access and portability due to the size of the instrument, loss of particulate to the walls or by re-evaporation from the hi-vol filter, and unwanted interaction between the collected particulate matter and the gas stream.

Flowrate--As mentioned above, the sample flowrate is predetermined by the requirements of the cyclone sampler. The diluted flowrate is fixed at its standard value of 425 normal liters per minute in order to maintain a reproducible aerodynamic pattern in the dilution chamber. In addition, when the optional hi-vol impactor is used, the diluted flowrate must remain constant to insure stable cut points for the impactor stages. Both sample and diluted flowrates may tend to change due to drift in the two blower system or loading of the hi-vol filter. Both flowrates should be monitored and adjusted as necessary.

Sampling points--Because of the size of the Stack Dilution Sampling System, it may not be possible to sample at several points in a duct. It is recommended that a port be chosen at a spot in the duct where stratification of particulate matter is not expected, and that this lack of stratification be confirmed by measurements with mass trains or with the IP train without dilution. Measurements with the Stack Dilution Sampling System should be made at two representative points in the duct where undiluted IP or mass train measurements have been made. At least two samples should be taken at each port. In the event of non-uniform velocity or gradients in mass concentration, the number of samples may have to be increased to obtain reliable results. In sampling the effluents from variable or cyclical processes, the test sequence must be repeated until a good average of the emissions is obtained.

Data logging--The operator should record the sampling parameters and process information appropriate for the IP Cyclone Sampler. In addition, the exhaust, sample, and dilution air flowrates and pressure drops in the system should be logged, along with readings of the temperature at all monitoring points in the system, and the temperature and relative humidity of the ambient air.

Size analysis of diluted aerosol--While the standard operating procedure for the Stack Dilution Sampling System calls only for measurement of total particulate mass in the diluted sample, it may be desirable for some studies to know the particle size distribution in the diluted gas stream. For this purpose, the dilution chamber was designed to accept a Sierra Model 230 High Volume Cascade Impactor through which the entire diluted flow passes prior to the hi-vol filter. Operation of the Stack Dilution Sampling System in this configuration requires only a few modifications to the normal operating conditions. The impactor stages 3-6 will be mounted on the impactor base plate prior to loading the filter. The stages and substrates are secured to the mounting posts on the base plate by the knurled mounting screws. While some attention must be paid to proper alignment of the substrates and slotted stages, the procedure is straightforward. As mentioned above, it is important that the diluted flowrate should be maintained at its specified value in order to maintain constant stage D_{50}'s. At the diluted flowrate of 425 ℓ/min, the nominal D_{50} values for stages 3-6 are 2.4, 1.6, 0.84, and 0.47 μm, respectively.

In order to allow study of submicron particles formed in the dilution/cooling process, provision has been made to extract a portion of the diluted stream for subsequent size analysis using electrical mobility, diffusional, or optical size analysis. The extraction probe can be inserted in the bored-through tube fitting at the top of the dilution chamber. Approximately 10-30 ℓ/min can be withdrawn without excessive losses for particles below 1 μm. The extracted stream may have to be further diluted for use with the sensitive sizing instruments mentioned above.

Sample Retrieval and Weighing--

After the end of a sample run, the hi-vol filter (and substrates, if applicable) and the cyclone catches should be removed with care, dried, and weighed. The hi-vol filter assembly should be removed as a unit from the dilution chamber body. The filter and substrates should then be removed, taking care to avoid tearing or loss of filter material. Detailed proceedings for unloading the IP Cyclone Sampler are found in the previous section on IP Sampler operation.

Data Analysis and Reports--

The data taken with the Stack Dilution Sampling System should be reported with that taken using the IP Cyclone Sampler. The reporting procedures are like those for the Dual Cyclone Operation Section of this report.

REFERENCES

1. Johnson, J. W., G. I. Clinard, L. G. Felix, and J. D. McCain. A Computer-Based Cascade Impactor Data Reduction System. U.S. Environmental Protection Agency Report EPA-600/7-78-042 (NTIS PB 285433), Southern Research Institute, Birmingham, AL, March 1978. 601 pp.

2. McCain, J. D., G. I. Clinard, L. G. Felix, and J. W. Johnson. A Data Reduction System for Cascade Impactors. U.S. Environmental Protection Agency Report EPA-600/7-78-132a (NTIS PB 283173), Southern Research Institute, Birmingham, AL, July 1978. 44 pp.

3. Scheid, Francis. Numerical Analysis. McGraw-Hill, New York, 1968. p. 65.

4. Smith, F. H. The Effects of Nozzle Design and Sampling Techniques on Aerosol Measurements. EPA-650/2-74-070, U.S. Environmental Protection Agency, Research Triangle Park, North Carolina, 1974. 89 pp.

5. U.S. Environmental Protection Agency. Standards of Performance for New Stationary Sources. Federal Register 42 (160): 41776-41782, 1977.

6. Smith, W. B., P. R. Cavanaugh, and R. R. Wilson, Jr. Technical Manual: A Survey of Equipment and Methods for Particulate Sampling in Industrial Process Streams. U.S. Environmental Protection Agency Report EPA-600/7-78-043 (NTIS PB 282501), Southern Research Institute, Birmingham, AL, March 1978. 280 pp.

7. Blake, D. E. Source Assessment Sampling System: Design and Development. EPA-600/7-78-018, U.S. Environmental Protection Agency, Research Triangle Park, North Carolina, 1978. 221 pp.

8. Elder, J. C., L. G. Littlefield, M. I. Tillery, and H. J. Ettinger. Preliminary Design of a Prototype Particulate Stack Sampler. Los Alamos Scientific Laboratory Informal Report LA-7286-MS, 1978. 17 pp.

9. Ringwall, C. G. Compact Sampling System for Collection of Particulates from Stationary Sources. EPA-650/2-74-029, U.S. Environmental Protection Agency, Research Triangle Park, North Carolina, 1974. 108 pp.

10. Smith, W. S., and E. W. Stewart. Field Evaluation of an Autoisokinetic Stack Particulate Sampling System. EPA-600/2-77-035, U.S. Environmental Protection Agency, Research Triangle Park, North Carolina, 1977. 58 pp.

11. Miller, F. J., D. E. Gardner, J. A. Graham, R. E. Lee, Jr., W. E. Wilson and J. D. Bachmann. Size Considerations for Establishing a Standard For Inhalable Particles. J. Air Pollut. Control Assoc. 29(6):610-615, 1979.

12. Corn, M. and F. Stein. Reentrainment of Particles from a Plume Surface. Amer. Ind. Hyg. Assoc. J. 26:325, 1965.

13. Rao, A. K., and K. T. Whitby. Non-ideal Collection Characteristics of Single Stage Cascade Impactors. Amer. Ind. Hyg. Assoc. J. 38:174, 1977.

14. Cushing, J. M., J. D. McCain, and W. B. Smith. Experimental Determination of Sizing Parameters and Wall Losses of Five Source-Test Cascade Impactors. Environ. Sci. Technol. 13:726, 1979.

15. Smith, W. B., R. R. Wilson, Jr., and D. B. Harris. A Five-Stage Cyclone System for In-Situ Sampling. Environ. Sci. Technol. 13:1387, 1979.

16. Yule, T. J., and C. G. Broniarek. An Experimental Study of Virtual Impactors. In: Proceedings, Advances in Particle Sampling and Measurement (Daytona Beach, FL, Oct. 1979), Wallace B. Smith, Ed. U.S. Environmental Protection Agency Report EPA-600/9-80-004, Southern Research Institute, Birmingham, AL, Jan. 1980. pp. 1-21.

17. Fuchs, N. A. The Mechanics of Aerosols. Pergamon, New York, 1964. p. 110.

18. Stein, F., W. A. Esmen, and M. Corn. The Shape of Atmospheric Particles in Pittsburgh Air. Atmos. Environ. 3:443, 1969.

19. Rimberg, D., and J. W. Thomas. Comparison of Particle Size of Latex Aerosols by Optical and Gravity Settling Methods. J. Colloid Interface Sci. 32:101, 1970.

20. Corn, M., F. Stein, Y. Hammad, S. Manekshaw, W. Bell, S. J. Penkola, and R. Freedman. Physical and Chemical Characteristics of 'Respirable' Coal Mine Dust. Ann. N. Y. Acad. Sci. 200:17, 1972.

21. Medical Research Council Panels, cited by R. J. Hamilton and W. H. Walton. The Selective Sampling of Respirable Dust. In: C. N. Davies, ed. Inhaled Particles and Vapors, Pergamon Press, Oxford, 1961.

22. Mercer, T. T. Aerosol Technology in Hazard Evaluation. Academic Press, New York, 1973, Chapter 8.

23. Natanson, G., cited in N. A. Fuchs, The Mechanics of Aerosols, Pergamon Press, New York, 1964. p. 112.

24. Rusanov, A. A. Determination of the Basic Properties of Dust and Gases. In: Ochistka Dymovykh Gasov v Promyshlennoy Energetike (Cleaning Stack Gases in Industrial Power Engineering), A. A. Rusanov, I. I. Urbakh, and A. P. Anastasiadi, eds. "Energiya," Moscow, 1969.

25. Hochstrasser, J.M. The Investigation and Development of Cyclone Dust Collector Theories for Application to Miniature Cyclone Presamplers. Ph.D. Thesis, University of Cincinnati, Cincinnati, 1976.

26. Lippmann, M., and T. L. Chan. Cyclone Sampler Performance. Staub Reinhalt. Luft 39:7-12, 1979.

27. John, W. G., P. Reischl, and J. J. Wesolowski. Size-Selective Monitoring Techniques for Particulate Matter in California Air. AIHL/SP-12. Final Report, California Air Resources Board Contract No. A5-00487, 1978.

28. Chan, T. L., and M. Lippmann. Particle Collection Efficiencies of Air Sampling Cyclones: An Empirical Theory. Environ. Sci. Technol. 11:377-382, 1977.

29. Marple, V. A. A Fundamental Study of Inertial Impactors. Ph.D. Thesis, University of Minnesota, Mechanical Engineering Department, Minneapolis, Particle Technology Laboratory Publication 144, 1970. 243 pp.

30. Heinsohn, R. J., J. W. Davis, G. W. Anderson, and E. A. Kopetz, Jr. The Design and Performance of the Stack Sampling System with Dilution. Presented at the 69th Annual Air Pollution Control Association Meeting, Portland, Oregon, June 1976.

31. Harris, D. Bruce. Procedures for Cascade Impactor Calibration and Operation in Process Streams. U.S. Environmental Protection Agency Report, EPA-600/2-77-004. January 1977.

APPENDIX A

MODIFICATIONS TO CIDRS CUMULATIVE MASS CURVE FITTING PROGRAMS FOR INHALABLE PARTICULATE DETERMINATION

PROGRAM CONVERSION AND PROGRAM LISTINGS

The primary purpose of developing the OSCFIT subroutine in its proposed form is, of course, to expand the range of accuracy of the cumulative mass size distribution as calculated by the CIDRS series of programs. Another consideration in its development was the ease of conversion from the original CIDRS programs. For those who have already converted the CIDRS programs to a form compatible with their computer systems, the OSCFIT subroutine minimizes the changes to be made. Only changes in the program SPLIN1 are necessary. In the revised SPLIN1, calling variables for the OSCFIT subroutine are defined, OSCFIT is called defining the cumulative mass distribution beyond the first stage D_{50} in a functional form, and the spline fitting technique continues as in the original SPLIN1 program.

To simplify the program conversion, Table A-1 lists the specific lines of SPLIN1 which are to be replaced followed by a brief comment on the change. Listings of the original SPLIN1 version (Table A-2) and of the new SPLIN1 version (Table A-3) follow with the changed lines boxed and labeled according to the index of Table A-1. Also given here is a listing of the OSCFIT subroutine in Table A-4. Calling arguments are defined in SPLIN1 and also in the OSCFIT subroutine. Section 2 of the report contains a description of the program development.

TABLE A-1. CONVERSIONS FROM ORIGINAL SPLIN1 TO PROPOSED SPLIN1

Conversion Index	New line(s) of SPLIN1	Replaces former line(s) of SPLIN1	Comments
A	227	200	Correction of error made in comment cards of original CIDRS report from "(1+4) point" to "(1+3) point." Action in program is not changed.
B	267-287	237-243	Commend cards describing hyperbola fit are replaced with description of osculating polynomial fit.
C	288-289	244-245	Variable name HYPL (hyperbola length). is changed to OSCL (osculating polynominal length). This is the area over which the osculating polynomial fits. OSCL=HYPL.
D	291-302	247-252	Coefficients B_1 and B_2 for a hyperbola over the fitted region are replaced by the variables needed by subroutine OSCFIT and the call to OSCFIT. OSCFIT then returns 3rd order polynomial coefficients B_1, B_2, B_3, and B_4, and the zero slope point ZSPT.
E	313-321	262	Values of log (mass concentration) along the hyperbola are replaced by values of mass concentration along the oscullating polynomial length and then converted to log (mass concentration). Log (mass concentration) is defined as the log of maximum concentration for diameters $\geq$ zero slope diameter, ZSPT.

TABLE A-1 (continued)

Conversion index	New line(s) of SPLIN1	Replaces former line(s) of SPLIN1	Comments
F	331	270	In new SPLIN1, the spline fitting routine is begun two intervals back from the original SPLIN1 program so that the SPLIN1 fit over these last two intervals before the first D_{50} will "feel the effect" of the osculating polynomial points. (This is an improvement over letting the extrapolated polynomial points beyond the first stage D_{50} guide the fit as in the original SPLIN1 version.)

TABLE A-2. ORIGINAL SPLIN1 LISTING

```
C     MAIN PROGRAM SPLIN1
C***********************************************************************
C*
C*      PROGRAM SPLIN1 FITS LOG10(CUMULATIVE MASS LOADING) VS LOG10(D50)
C*      WITH A SERIES OF OVER LAPPING, CONTINUOUS 2ND DEGREE POLYNOMIALS.
C*      BOTH THE POLYNOMIALS AND THEIR 1ST DERIVATIVES ARE CONTINUOUS.
C*
C***********************************************************************
C
      INTEGER VV
      DOUBLE PRECISION DLOG10,XNDPEN(10),YO(10)
      DOUBLE PRECISION XINC,YINC
      DIMENSION ID(80),DPC(8),CUMG(8),DMDLD(9),GEOMD(9),DNDLD(9)
      DIMENSION X(53),Y(53),A(16),B(4),COE(50,3),COE1(50,3)
      DIMENSION X1(53),Y1(53)
      DIMENSION FILSPL(2),FILNAM(2)
      DIMENSION AA(9),BB(3)
      EQUIVALENCE (X,X1),(Y,Y1),(COE,COE1)
      DATA FILNAM/'KMC00','1BIN'/
      DATA FILSPL/'FILSP','LBIN'/
      CALL DEFINE(10,251,101,FILNAM,I10,0,0,0)
      CALL DEFINE(11,507,100,FILSPL,I10,0,0,0)
C
C     RECORD 101 CONTAINS GENERAL INFORMATION PERTAINING
C     TO ALL RUNS. NRUN=NO. OF RUNS (2 RECORDS FOR EACH RUN)
C      ISFIN = LAST RECORD NUMBER CONTAINING INDIVIDUAL RUN DATA
C      IN FILE 10.
      READ(10'101)NRUN
      ISFIN = NRUN*2
C
C      KREAD = 0 - MAKE FIT TO ALL SETS OF CUM. MASS LOADING VS D50
C      VALUES OF FILE. KREAD NOT = 0 - READ IN SETS TO BE FITTED.
C
      READ(2,1)KREAD
C
C      NN = NUMBER OF SUBINTERVALS TO BE SET UP IN LAST INTERVAL
C      BETWEEN D50 OF 1ST STAGE AND DMAX.
C      N = NUMBER OF SUBINTERVALS TO BE SET UP BETWEEN EACH PAIR OF
C      D50'S UP TO D50 OF 1ST STAGE.  N=3 TO N=6 PERMITTED.
C
  307 NN=5
      RR=NN
      N=6
      R=N
      DO 400 INDEX=1,ISFIN
      IAV=INDEX
C
C      IF KREAD NOT = 0, READ RECORD NO. IAV FOR DATA TO BE FITTED.
C      ALSO, IF KREAD NOT = 0, LEAVE LAST CARD BLANK TO STOP.
C
      IF(KREAD)310,310,2
    2 READ(2,1)IAV
      IF(IAV.EQ.0)STOP
C
C      VALUES TO BE USED FROM READING OF RECORD ARE:
C        NFIT - NUMBER OF CUMULATIVE MASS LOADING VS. D50 POINTS (+1
C               FOR TOTAL MASS LOADING VS. MAXIMUM DIAMETER) TO BE
C               FITTED.
C       XNDPEN(I),I=1,NFIT - SET OF D50 VALUES AND MAXIMUM DIAMETER.
C       YO(I),I=1,NFIT - SET OF MASS LOADING VALUES.
```

```
C       OTHER VALUES READ HERE ARE NOT USED.
C
  310 READ(10'IAV)IS,NFIT,GRNAM,ID,RHO,TKS,POA,FGH2O,DSMA,DMAX,
     1DPC,CUMG,DMDLD,GFOMD,DNDLD,CYC3,MC3,M00,MS,VV,
     2(XNDPEN(I),I=1,NFIT),(YO(I),I=1,NFIT)
C
C       NFIT1 = NUMBER OF CUMULATIVE MASS LOADING VS. D50 POINTS
C       (EXCLUDES TOTAL LOADING VS. DMAX).
C       NPT = TOTAL NUMBER OF POINTS USED FOR FITTING BETWEEN (AND
C       INCLUDING) MAXIMUM PARTICLE SIZE AND D50 OF LAST STAGE.
C
      NFIT1=NFIT-1
      NPT=((NFIT1-1)*N)+NN+1
      NFIT2=NFIT-2
C
C       THIS **DO 100** LOOP FITS A 2ND DEGREE POLYNOMIAL TO 3
C       LOG10(CUMULATIVE MASS LOADING) VS. LOG10(D50) POINTS ON EACH
C       TRAVERSE, IE.:
C       LOG10 OF (XNDPEN(1),YO(1)),(XNDPEN(2),YO(2)),(XNDPEN(3),YO(3));
C         **  ** (XNDPEN(2),YO(2)),(XNDPEN(3),YO(3)),(XNDPEN(4),YO(4));
C       ;.........................................................;
C         **  ** (XNDPEN(NFIT2),YO(NFIT2)),(XNDPEN(NFIT1),YO(NFIT1)),
C       (XNDPEN(NFIT),YO(NFIT))
C       IF THE FITTING POLYNOMIAL HAS NON-NEGATIVE SLOPE AT BOTH
C       LOG10(XNDPEN(I),YO(I)) AND LOG10(XNDPEN(I+1),YO(I+1)), THE
C       FITTING COEFFICIENTS ARE USED BETWEEN THESE 2 POINTS TO DEFINE
C       3 INTERMEDIATE POINTS EVENLY SPACED ON LOG10 SCALE. IF THERE IS A
C       NEGATIVE SLOPE AT EITHER OF THESE 2 POINTS, A STRAIGHT LINE FIT
C       BETWEEN THE POINTS IS USED TO DEFINE THE 3 INTERMEDIATE POINTS.
C       THE VECTORS X1 AND Y1 REPRESENT LOG10 OF ORIGINAL CUM. MASS
C       LOADING VS. D50 POINTS AND THE FABRICATED INTERMEDIATE POINTS.
C
C       THE NUMBER OF POINTS REPRESENTED BY THE X1, Y1 VECTORS IS
C       (NFIT2*4)+1+2. THERE ARE (NFIT2*4)+1 POINTS BETWEEN POINTS AT
C       LOG10(D50) OF LAST STAGE AND LOG10(D50) OF 1ST STAGE INCLUSIVE.
C       2 MORE ARE EXTRAPOLATED BEYOND LOG10(D50) OF 1ST STAGE.
C
      DO 100 I=1,NFIT2
      JJ=N-1
      IF(NFIT2-I)90,80,80
   80 JJ=N+2
   90 M=(I-1)*N+1
      X1(M)=DLOG10(XNDPEN(I))
      Y1(M)=DLOG10(YO(I))
      XINC=(DLOG10(XNDPEN(I+1))-DLOG10(XNDPEN(I)))/N
C
C       SIMQ SOLVES N SIMULTANEOUS LINEAR EQUATIONS, AX = B. HERE
C       N = 3. THE MATRIX OF COEFFICIENTS, A, IS DESTROYED IN THE
C       COMPUTATION. THE VECTOR OF ORIGINAL CONSTANTS, B, IS REPLACED
C       BY THE FINAL SOLUTION VALUES, VECTOR X. COEFFICIENT MATRIX A AND
C       CONSTANT VECTOR B ARE DEFINED IN THIS LOOP.
C
      DO 1100 II=1,3
      MM=I-1+II
      B(II)=DLOG10(YO(MM))
      K=3*(II-1)
      DO 1100 J=1,3
      M3=I-1+J
 1100 A(K+J)=DLOG10(XNDPEN(M3))**(II-1)
      KS=0
      CALL STMQ(A,B,3,KS)
C
C       USE STRAIGHT LINE FIT, NOT POLY FIT, IF NEGATIVE SLOPE AT EITHER
C       END OF ORIGINAL INTERVAL.
C
      DO 1119 J=1,2
      SLOPE=B(2)+2.0*B(3)*DLOG10(XNDPEN(I+J-1))
      IF(SLOPE)1104,1119,1119
 1104 B(2)=(DLOG10(YO(I+1)/YO(I)))
     1/(DLOG10(XNDPEN(I+1)/XNDPEN(I)))
      B(1)=DLOG10(YO(I))-B(2)*DLOG10(XNDPEN(I))
      B(3)=0.0
      GO TO 1120
 1119 CONTINUE
 1120 DO 100 J=1,JJ
      K=M+J
      X1(K)=DLOG10(XNDPEN(I))+J*XINC
      Y1(K)=B(1)+B(2)*X1(K)+B(3)*X1(K)**2
  100 CONTINUE
C
C       FIT THE FIRST 3 (X,Y) POINTS WITH A 2ND DEGREE POLYNOMIAL IN
C       ORDER TO DEFINE SLOPE AT (X(1),Y(1)). (NOTE - (X1,Y1) POINTS ARE
C       EQUIVALENT TO (X,Y) POINTS!!!)
C
  104 DO 110 I=1,3
      K=3*(I-1)
      DO 110 J=1,3
      M=1+(J-1)*N
  110 A(K+J)=X(M)**(I-1)
      DO 115 I=1,3
      M=1+(I-1)*N
  115 B(I)=Y(M)
      KS=0
      CALL STMQ(A,B,3,KS)
C
C       CHECK THE SLOPE OF THIS CURVE FIT AT THE FIRST POINT, IF IT IS
C       NEGATIVE, ADD A POINT ON THE OTHER SIDE OF POINT 1 FROM THE
C       2ND POINT A DISTANCE (X(2)-X(1)) FROM X(1). THE Y COORDINATE
C       VALUE IS SET = TO Y(1). THE POLYNOMIAL FIT THROUGH THIS POINT,
C       (X(1),Y(1)), AND (X(2),Y(2)) MUST HAVE POSITIVE SLOPE AT
C       (X(1),Y(1)).
C
      SLOPE=B(2)+2.0*B(3)*X(1)
      IF(SLOPE)4,19,19
    4 DO 5 I=1,3
    5 A(I)=1
      A(4)=X(1)-(X(N+1)-X(1))
      A(7)=(A(4))**2
      DO 10 I=1,2
      K=3*I
      DO 10 J=2,3
      M=1+((J-2)*N)
   10 A(K+J)=X(M)**I
      B(1)=Y(1)
      DO 15 I=2,3
      M=1+((I-2)*N)
   15 B(I)=Y(M)
      KS=0
      CALL STMQ(A,B,3,KS)
   19 DO 20 I=1,3
   20 COF(1,I)=B(I)
C
C       II = FIRST INTERVAL FOR WHICH FITTING COEFFICIENTS ARE DEFINED.
C       INTS1 = LAST INTERVAL WHERE POLYNOMIAL FITS WERE USED TO FABRI-
C       CATE INTERMEDIATE POINTS. THE UPPER BOUNDARY OF THIS INTERVAL
C      IS LOG10(XNDPEN(NFIT1),YO(NFIT1)) HERE.
C
      II=1
      INTS1=NPT-NN-1
C
C       THIS LOOP FINDS THE FITTING COEFFICIENTS FOR EACH INTERVAL. THE
C       3 EQUATIONS ARE SOLVED FOR 3 UNKNOWN COEFFICIENT VALUES FOR THE
C      FITTING 2ND DEGREE POLYNOMIAL. THE EQUATIONS EXPRESS 3
C      CONDITIONS FOR THE FIT:
C         1.  THE FITTING POLYNOMIALS OF THE 2 JOINING INTERVALS ARE
C             CONTINUOUS AT THE MUTUAL BOUNDARY POINT.
C         2.  THE FIRST DERIVATIVES SAME ARE CONTINUOUS AT THE
C             MUTUAL BOUNDARY POINT.
C         3.  THE FITTING POLYNOMIAL OF THIS I TH INTERVAL (FITTING
C             BETWEEN POINTS I AND I+1) GOES THROUGH THE (I+4)TH POINT,      Ⓐ
C             I.E. A POINT OUTSIDE THE INTERVAL. FITTING ROUTINE ''LOOKS
C             AHEAD'' TO LET COMING POINTS INFLUENCE CURVE DIRECTION.
C
   23 DO 50 I=II,INTS1
      JJ=1
      B(1)=0.0
      DO 25 J=2,3
      K=I-1
      IF(I.EQ.1)K=I
   25 B(1)=B(1)+(J-1)*(COF(K,J))*X(I)**(J-2)
      B(2)=COF(K,1)
      DO 30 J=2,3
   30 B(2)=B(2)+COF(K,J)*X(I)**(J-1)
      B(3)=Y(I+3)
      DO 35 J=1,3
      L=1+(J-1)*3
   35 A(L)=(J-1)*X(I)**(J-2)
      DO 40 J=1,3
      K=J-1
      KK=3*K
   40 A(KK+2)=X(I)**K
      DO 43 J=1,3
      K=J-1
      KK=3*K
   43 A(KK+3)=X(I+3)**K
      KS=0
      CALL SIMQ(A,B,3,KS)
C
C       SAVE THE FITTING COEFFICIENT VECTOR B WHICH FITS OVER INTERVAL
C       I AS COF.
C
      DO 45 J=1,3
      COF(I,J)=B(J)
   45 CONTINUE
   50 CONTINUE
      IF(JJ.EQ.(NPT-1))GO TO 55
C
C      THE LAST SERIES OF INTERVALS FOR WHICH FITTING COEFFICIENTS ARE
C      TO BE DEFINED LIES BETWEEN LOG10(XNDPEN(NFIT1),YO(NFIT1)) AND
C      LOG10(XNDPEN(NFIT),YO(NFIT)). THE POINTS ARE DEFINED ALONG       Ⓑ
```

```
C       AN HYPERBOLA BETWEEN THESE 2 POINTS OF THE FORM LOG10(Y) =
C       B(1) + B(2) / X.                                          Ⓑ cont.
C
      HYPL=DLOG10(XNDPEN(NFIT))-DLOG10(XNDPEN(NFIT1))
      XINC=HYPL/RR                                                Ⓒ
      M=(NFIT1-1)*N+1
      XSUB1=1.D0/XNDPEN(NFIT1)
      YSUB1=Y1(M)
      XSUB2=1.D0/XNDPEN(NFIT)                                     Ⓓ
      YSUB2=DLOG10(YO(NFIT))
      B(2)=(YSUB2-YSUB1)/(XSUB2-XSUB1)
      B(1)=YSUB1-B(2)*XSUB1
C
C       THE NUMBER OF POINTS TO BE USED ALONG THE HYPERBOLA IS NN+2 = 8+2.
C       THE 2 ADDED POINTS ARE EXTRAPOLATED VALUES BEYOND
C       LOG10(XNDPEN(NFIT),YO(NFIT)).
C
      N3=NN+2
      DO 1150 I=1,N3
      J=M+I
      X1(J)=X1(M)+I*XINC
      Y1(J)=B(1)+B(2)*(1.0/(10.0**X1(J)))                         Ⓔ
 1150 CONTINUE
C
C       REDEFINE **DO 50** LOOP INDEX BEGINNING AND END. BEGINNING
C       INTERVAL II IS FIRST INTERVAL OF HYPERBOLA, BEGINS AT D50 OF 1ST
C       STAGE. LAST INTERVAL, INTS1, ENDS WITH DMAX. RETURN TO TOP OF
C       LOOP TO FIND FITTING POLYNOMIAL COEFFICIENTS OVER THESE INTERVALS.
C
      II=NPT-NN                                                   Ⓕ
      INTS1=NPT-1
      GO TO 23
C
C       INT = NUMBER OF INTERVALS FOR WHICH FITTING COEFFICIENTS HAVE
C       BEEN DEFINED.
C
   55 INT=NPT-1
C
C       FILE NUMBER OF FITTED POINTS, THE INTERVAL BOUNDARY POINT
C       VALUES, AND FITTING COEFFICIENTS FOR EACH INTERVAL.
C
      WRITE(11'IAV)NPT,(X1(I),I=1,NPT),(Y1(I),I=1,NPT),
     1((COE1(I,J),J=1,3),I=1,INT)
  400 CONTINUE
    1 FORMAT (3I2)
      END
```

TABLE A-3. NEW SPLIN1 LISTING

```
C     MAIN PROGRAM SPLIN1                                               SPLI   1
C***********************************************************************SPLI   2
C*                                                                     *SPLI   3
C*     PROGRAM SPLIN1 FITS LOG10(CUMULATIVE MASS LOADING) VS LOG10(D50)*SPLI   4
C*     WITH A SERIES OF OVERLAPPING, CONTINUOUS 2ND DEGREE POLYNOMIALS*SPLI   5
C*     BOTH THE POLYNOMIALS AND THEIR 1ST DERIVATIVES ARE CONTINUOUS.  *SPLI   6
C*                                                                     *SPLI   7
C***********************************************************************SPLI   8
      INTEGER VV                                                        SPLI   9
      DOUBLE PRECISION DLOG10,XNDPEN(10),YD(10)                         SPLI  10
      DOUBLE PRECISION XINC,YINC                                        SPLI  11
      DIMENSION ID(80),DPC(8),CUMG(8),DMDLD(9),GEOMD(9),DNDLD(9)        SPLI  12
      DIMENSION X(53),Y(53),A(16),B(4),COE(50,3),COE1(50,3)             SPLI  13
      DIMENSION X1(53),Y1(53)                                           SPLI  14
      DIMENSION FILSPL(2),FILNAM(2)                                     SPLI  15
      DIMENSION AA(2),BB(3)                                             SPLI  16
      EQUIVALENCE (X,X1),(Y,Y1),(COE,COE1)                              SPLI  18
      DATA FILNAM/'KMC00','1BIN'/                                       SPLI  19
      DATA FILSPL/'FILSP','LBIN'/                                       SPLI  20
C                                                                       SPLI  22
      CALL DEFINE(10,251,101,FILNAM,I10,0,0,0)                          SPLI  23
      CALL DEFINE(11,507,100,FILSPL,I11,0,0,0)                          SPLI  24
C***********************************************************************SPLI  26
C*                                                                     *SPLI  27
C*      ISFIN = LAST RECORD NUMBER CONTAINING INDIVIDUAL RUN DATA      *SPLI  28
C*      IN FILE 10.                                                    *SPLI  29
C*     (RECORD 101 CONTAINS GENERAL INFORMATION PERTAINING TO ALL RUNS.)*SPLI  30
C*                                                                     *SPLI  31
C*                                                                     *SPLI  32
C*      KREAD = 0 - MAKE FIT TO ALL SETS OF CUM. MASS LOADING VS D50   *SPLI  33
C*      VALUES OF FILE. KREAD NOT = 0 - READ IN SETS TO BE FITTED.     *SPLI  34
C*                                                                     *SPLI  35
C*                                                                     *SPLI  36
C*     ISFIN NUMBER OF RECORDS WHICH CONTAIN CUMULATIVE MASS LOADINGS  *SPLI  37
C*     VS. D50 SETS.                                                   *SPLI  38
C*                                                                     *SPLI  39
C***********************************************************************SPLI  40
      READ(10'101) NRUN                                                 SPLI  42
      ISFIN=NRUN*2                                                      SPLI  43
      READ(2,1)KREAD                                                    SPLI  44
C***********************************************************************SPLI  45
C*                                                                     *SPLI  46
C*      NN = NUMBER OF SUBINTERVALS TO BE SET UP IN LAST INTERVAL      *SPLI  47
C*      BETWEEN D50 OF 1ST STAGE AND DMAX.                             *SPLI  48
C*      N = NUMBER OF SUBINTERVALS TO BE SET UP BETWEEN EACH PAIR OF   *SPLI  49
C*      D50'S UP TO D50 OF 1ST STAGE.                                  *SPLI  50
C*                                                                     *SPLI  51
C***********************************************************************SPLI  52
  307 NN=8                                                              SPLI  53
      PR=NN                                                             SPLI  54
      N=4                                                               SPLI  55
      R=N                                                               SPLI  56
      DO 400 INDEX=1,ISFIN                                              SPLI  57
      IAV=INDEX                                                         SPLI  58
C***********************************************************************SPLI  59
C*                                                                     *SPLI  60
C*       IF KREAD NOT = 0, READ RECORD NO. IAV FOR DATA TO BE FITTED.  *SPLI  61
C*       ALSO, IF KREAD NOT = 0, LEAVE LAST CARD BLANK TO STOP.        *SPLI  62
C*                                                                     *SPLI  63
C***********************************************************************SPLI  64
```

```
      IF(KREAD)310,310,2                                                SPLI  65
    2 READ(2,1)IAV                                                      SPLI  66
      IF(IAV.EQ.0)STOP                                                  SPLI  67
C***********************************************************************SPLI  68
C*                                                                     *SPLI  69
C*      VALUES TO BE USED FROM READING OF RECORD ARE:                  *SPLI  70
C*        NFIT - NUMBER OF CUMULATIVE MASS LOADING VS. D50 POINTS (+1  *SPLI  71
C*               FOR TOTAL MASS LOADING VS. MAXIMUM DIAMETER) TO BE    *SPLI  72
C*               FITTED.                                               *SPLI  73
C*        XNDPEN(I),I=1,NFIT - SET OF D50 VALUES AND MAXIMUM DIAMETER. *SPLI  74
C*        YO(I),I=1,NFIT - SET OF MASS LOADING VALUES.                 *SPLI  75
C*      OTHER VALUES READ HERE ARE NOT USED.                           *SPLI  76
C*                                                                     *SPLI  77
C***********************************************************************SPLI  78
  310 READ(10'IAV)IS,NFIT,GRNAM,ID,RHO,TKS,POA,FGH2O,DSMA,DMAX,         SPLI  79
     1DPC,CUMG,DMDLD,GEOMD,DNDLD,CYC3,MC3,MOO,MS,MF,VV,                 SPLI  80
     2(XNDPEN(I),I=1,NFIT),(YO(I),I=1,NFIT)                             SPLI  81
C***********************************************************************SPLI  86
C*                                                                     *SPLI  87
C*      NFIT1 = NUMBER OF CUMULATIVE MASS LOADING VS. D50 POINTS       *SPLI  88
C*      (EXCLUDES TOTAL LOADING VS. DMAX).                             *SPLI  89
C*      NPT = TOTAL NUMBER OF POINTS USED FOR FITTING BETWEEN (AND     *SPLI  90
C*      INCLUDING) MAXIMUM PARTICLE SIZE AND D50 OF LAST STAGE.        *SPLI  91
C*                                                                     *SPLI  92
C***********************************************************************SPLI  93
  313 NFIT1=NFIT-1                                                      SPLI  94
      NPT=((NFIT1-1)*N)+NN+1                                            SPLI  95
      NFIT2=NFIT-2                                                      SPLI  96
C***********************************************************************SPLI  97
C*                                                                     *SPLI  98
C*      THIS ''DO 100'' LOOP FITS A 2ND DEGREE POLYNOMIAL TO 3         *SPLI  99
C*      LOG10(CUMULATIVE MASS LOADING) VS. LOG10(D50) POINTS ON EACH   *SPLI 100
C*      TRAVERSE, IE.:                                                 *SPLI 101
C*      LOG10 OF (XNDPEN(1),YO(1)),(XNDPEN(2),YO(2)),(XNDPEN(3),YO(3)); *SPLI 102
C*        ''  '' (XNDPEN(2),YO(2)),(XNDPEN(3),YO(3)),(XNDPEN(4),YO(4)); *SPLI 103
C*      :.........................................................; *SPLI 104
C*        ''  '' (XNDPEN(NFIT2),YO(NFIT2)),(XNDPEN(NFIT1),YO(NFIT1)),  *SPLI 105
C*      (XNDPEN(NFIT),YO(NFIT))                                        *SPLI 106
C*      IF THE FITTING POLYNOMIAL HAS NON-NEGATIVE SLOPE AT BOTH       *SPLI 107
C*      LOG10(XNDPEN(I),YO(I)) AND LOG10(XNDPEN(I+1),YO(I+1)), THE     *SPLI 108
C*      FITTING COEFFICIENTS ARE USED BETWEEN THESE 2 POINTS TO DEFINE *SPLI 109
C*      3 INTERMEDIATE POINTS EVENLY SPACED ON LOG10 SCALE,IF THERE IS A*SPLI 110
C*      NEGATIVE SLOPE AT EITHER OF THESE 2 POINTS, A STRAIGHT LINE FIT *SPLI 111
C*      BETWEEN THE POINTS IS USED TO DEFINE THE 3 INTERMEDIATE POINTS. *SPLI 112
C*      THE VECTORS X1 AND Y1 REPRESENT LOG10 OF ORIGINAL CUM. MASS    *SPLI 113
C*      LOADING VS. D50 POINTS AND THE FABRIGATED INTERMEDIATE POINTS. *SPLI 114
C*                                                                     *SPLI 115
C*      THE NUMBER OF POINTS REPRESENTED BY THE X1, Y1 VECTORS IS      *SPLI 116
C*      (NFIT2*4)+1+2. THERE ARE (NFIT2*4)+1 POINTS BETWEEN POINTS AT  *SPLI 117
C*      LOG10(D50) OF LAST STAGE AND LOG10(D50) OF 1ST STAGE INCLUSIVE. *SPLI 118
C*      2 MORE ARE EXTRAPOLATED BEYOND LOG10(D50) OF 1ST STAGE.        *SPLI 119
C*                                                                     *SPLI 120
C***********************************************************************SPLI 121
      DO 100 I=1,NFIT2                                                  SPLI 122
      JJ=N-1                                                            SPLI 123
      IF(NFIT2-I)90,80,80                                               SPLI 124
   80 JJ=N+2                                                            SPLI 125
   90 M=(I-1)*N+1                                                       SPLI 126
      X1(M)=DLOG10(XNDPEN(I))                                           SPLI 127
      Y1(M)=DLOG10(YO(I))                                               SPLI 128
      XINC=(DLOG10(XNDPEN(I+1))-DLOG10(XNDPEN(I)))/R                    SPLI 129
C***********************************************************************SPLI 130
C*                                                                     *SPLI 131
C*     SIMQ SOLVES N SIMULTANEOUS LINEAR EQUATIONS, AX = B. HERE       *SPLI 132
C*     N = 3. THE MATRIX OF COEFFICIENTS, A, IS DESTROYED IN THE       *SPLI 133
C*     COMPUTATION. THE VECTOR OF ORIGINAL CONSTANTS, B, IS REPLACED   *SPLI 134
C*     BY TH FINAL SOLUTION VALUES, VECTOR X. COEFFICIENT MATRIX A AND *SPLI 135
C*     CONSTANT VECTOR B ARE DEFINED IN THIS LOOP.                     *SPLI 136
C*                                                                     *SPLI 137
C***********************************************************************SPLI 138
      DO 1100 II=1,3                                                    SPLI 139
      MM=I-1+II                                                         SPLI 140
      B(II)=DLOG10(YO(MM))                                              SPLI 141
      K=3*(II-1)                                                        SPLI 142
      DO 1100 J=1,3                                                     SPLI 143
      M3=I-1+J                                                          SPLI 144
 1100 A(K+J)=DLOG10(XNDPEN(M3))**(II-1)                                 SPLI 145
      KS=0                                                              SPLI 146
      CALL SIMQ(A,B,3,KS)                                               SPLI 147
C***********************************************************************SPLI 148
C*                                                                     *SPLI 149
C*     USE STRAIGHT LINE FIT, NOT POLY FIT, IF NEGATIVE SLOPE AT EITHER*SPLI 150
C*     END OF ORIGINAL INTERVAL.                                       *SPLI 151
C*                                                                     *SPLI 152
C***********************************************************************SPLI 153
      DO 1119 J=1,2                                                     SPLI 154
      SLOPE=B(2)+2.0*B(3)*DLOG10(XNDPEN(I+J-1))                         SPLI 155
      IF(SLOPE)1104,1119,1119                                           SPLI 156
 1104 B(2)=(DLOG10(YO(I+1)/YO(I)))                                      SPLI 157
     1/(DLOG10(XNDPEN(I+1)/XNDPEN(I)))                                  SPLI 158
      B(1)=DLOG10(YO(I))-B(2)*DLOG10(XNDPEN(I))                         SPLI 159
      B(3)=0.0                                                          SPLI 160
      GO TO 1120                                                        SPLI 161
 1119 CONTINUE                                                          SPLI 162
 1120 DO 100 J=1,JJ                                                     SPLI 163
      K=M+J                                                             SPLI 164
      X1(K)=DLOG10(XNDPEN(I))+J*XINC                                    SPLI 165
      Y1(K)=B(1)+B(2)*X1(K)+B(3)*X1(K)**2                               SPLI 166
  100 CONTINUE                                                          SPLI 167
C***********************************************************************SPLI 168
C*                                                                     *SPLI 169
C*     FIT THE FIRST 3 (X,Y) POINTS WITH A 2ND DEGREE POLYNOMIAL IN    *SPLI 170
C*     ORDER TO DEFINE SLOPE AT (X(1),Y(1)). (NOTE - (X1,Y1) POINTS ARE*SPLI 171
C*     EQUIVALENT TO (X,Y) POINTS!!!)                                  *SPLI 172
C*                                                                     *SPLI 173
C***********************************************************************SPLI 174
  104 DO 110 I=1,3                                                      SPLI 175
      K=3*(I-1)                                                         SPLI 176
      DO 110 J=1,3                                                      SPLI 177
      M=1+(J-1)*N                                                       SPLI 178
  110 A(K+J)=X(M)**(I-1)                                                SPLI 179
      DO 115 I=1,3                                                      SPLI 180
      M=1+(I-1)*N                                                       SPLI 181
  115 B(I)=Y(M)                                                         SPLI 182
      KS=0                                                              SPLI 183
      CALL SIMQ(A,B,3,KS)                                               SPLI 184
C***********************************************************************SPLI 185
C*                                                                     *SPLI 186
C*     CHECK THE SLOPE OF THIS CURVE FIT AT THE FIRST POINT. IF IT IS  *SPLI 187
C*     NEGATIVE, ADD A POINT ON THE OTHER SIDE OF POINT 1 FROM THE     *SPLI 188
```

```
C*     2ND POINT A DISTANCE (X(2)-X(1)) FROM X(1). THE Y COORDINATE    *SPLI 189
C*     VALUE IS SET = TO Y(2). THE POLYNOMIAL FIT THROUGH THIS POINT,  *SPLI 190
C*     (X(1),Y(1)), AND (X(2),Y(2)) MUST HAVE POSITIVE SLOPE AT        *SPLI 191
C*     (X(1),Y(1)).                                                    *SPLI 192
C*                                                                     *SPLI 193
C***********************************************************************SPLI 194
      SLOPE=B(2)+2.0*B(3)*X(1)                                          SPLI 195
      IF(SLOPE)4,19,19                                                  SPLI 196
    4 DO 5 I=1,3                                                        SPLI 197
    5 A(I)=1.                                                           SPLI 198
      A(4)=X(1)-(X(N+1)-X(1))                                           SPLI 199
      A(7)=(A(4))**2                                                    SPLI 200
      DO 10 I=1,2                                                       SPLI 201
      K=3*I                                                             SPLI 202
      DO 10 J=2,3                                                       SPLI 203
      M=1+((J-2)*N)                                                     SPLI 204
   10 A(K+J)=X(M)**I                                                    SPLI 205
      B(1)=Y(1)                                                         SPLI 206
      DO 15 I=2,3                                                       SPLI 207
      M=1+((I-2)*N)                                                     SPLI 208
   15 B(I)=Y(M)                                                         SPLI 209
      KS=0                                                              SPLI 210
      CALL SIMQ(A,B,3,KS)                                               SPLI 211
   19 DO 20 I=1,3                                                       SPLI 212
   20 COF(1,I)=B(I)                                                     SPLI 213
C***********************************************************************SPLI 214
C*                                                                     *SPLI 215
C*     II = FIRST INTERVAL FOR WHICH FITTING COEFFICIENTS ARE DEFINED, *SPLI 216
C*     INTS1 = LAST INTERVAL WHERE POLYNOMIAL FITS WERE USED TO FABRI- *SPLI 217
C*     CATE INTERMEDIATE POINTS. THE UPPER BOUNDARY OF THIS INTERVAL   *SPLI 218
C*     ISLOG10(XNDPEN(NFIT1),YO(NFIT1)) HERE.                          *SPLI 219
C*                                                                     *SPLI 220
C***********************************************************************SPLI 221
      II=1                                                              SPLI 222
      INTS1=NPT-NN-1                                                    SPLI 223
C***********************************************************************SPLI 224
C*                                                                     *SPLI 225
C*     THIS LOOP FINDS THE FITTING COEFFICIENTS FOR EACH INTERVAL. THE *SPLI 226
C*     3 EQUATIONS ARE SOLVED FOR 3 UNKNOWN COEFFICIENT VALUES FOR THE *SPLI 227
C*     FITTING 2ND DEGREE POLYNOMIAL. THE EQUATIONS EXPRESS 3          *SPLI 228
C*     CONDITIONS FOR THE FIT:                                         *SPLI 229
C*       1.  THE FITTING POLYNOMIALS OF THE 2 JOINING INTERVALS ARE    *SPLI 230
C*           CONTINUOUS AT THE MUTUAL BOUNDARY POINT.                  *SPLI 231
C*       2.  THE FIRST DERIVATIVES SAME ARE CONTINUOUS AT THE          *SPLI 232
C*           MUTUAL BOUNDARY POINT.                                    *SPLI 233
C*       3.  THE FITTING POLYNOMIAL OF THIS I TH INTERVAL (FITTING    *SPLI 234
C*           BETWEEN POINTS I AND I+1) GOES THROUGH THE (I+3)RD POINT, *SPLI 235  ←Ⓐ
C*           I.E. A POINT OUTSIDE THE INTERVAL. FITTING ROUTINE ''LOOKS*SPLI 236
C*           AHEAD'' TO LET COMING POINTS INFLUENCE CURVE DIRECTION.   *SPLI 237
C*                                                                     *SPLI 238
C***********************************************************************SPLI 239
   23 DO 50 I=II,INTS1                                                  SPLI 240
      JJ=I                                                              SPLI 241
      B(1)=0.0                                                          SPLI 242
      DO 25 J=2,3                                                       SPLI 243
      K=I-1                                                             SPLI 244
      IF(I.EQ.1)K=I                                                     SPLI 245
   25 B(1)=B(1)+(J-1)*(COF(K,J))*X(I)**(J-2)                            SPLI 246
      B(2)=COF(K,1)                                                     SPLI 247
      DO 30 J=2,3                                                       SPLI 248
   30 B(2)=B(2)+COF(K,J)*X(I)**(J-1)                                      SPLI 249
      B(3)=Y(I+2)                                                         SPLI 250
      DO 35 J=1,3                                                         SPLI 251
      L=1+(J-1)*3                                                         SPLI 252
   35 A(L)=(J-1)*X(I)**(J-2)                                              SPLI 253
      DO 40 J=1,3                                                         SPLI 254
      K=J-1                                                               SPLI 255
      KK=3*K                                                              SPLI 256
   40 A(KK+2)=X(I)**K                                                     SPLI 257
      DO 43 J=1,3                                                         SPLI 258
      K=J-1                                                               SPLI 259
      KK=3*K                                                              SPLI 260
   43 A(KK+3)=X(I+2)**K                                                   SPLI 261
      KS=0                                                                SPLI 262
      CALL SIMQ(A,B,3,KS)                                                 SPLI 263
C***********************************************************************SPLI 264
C*                                                                     *SPLI 265
C*     SAVE THE FITTING COEFFICIENT VECTOR B WHICH FITS OVER INTERVAL  *SPLI 266
C*     I AS COF.                                                       *SPLI 267
C*                                                                     *SPLI 268
C***********************************************************************SPLI 269
      DO 45 J=1,3                                                         SPLI 270
      COE(I,J)=B(J)                                                       SPLI 271
   45 CONTINUE                                                            SPLI 272
   50 CONTINUE                                                            SPLI 273
      IF(JJ.EQ.(NPT-1))GO TO 55                                           SPLI 274
C***********************************************************************SPLI 275
C*                                                                     *SPLI 276
C*     THE LAST SERIES OF INTERVALS FOR WHICH FITTING COEFFICIENTS ARE *SPLI 277
C*     TO BE DEFINED LIES BETWEEN LOG10(XNDPEN(NFIT1),YO(NFIT1)) AND   *SPLI 278
C*     LOG10(XNDPEN(NFIT),YO(NFIT)). THE POINTS ARE DEFINED BY AN OSCU-*
C*     LATING POLYNOMIAL DEFINED IN OSCFIT GIVEN:                      *
C*       1. THE LOG VALUE OF THE FIRST D50 AND THE VALUE OF CUMULATIVE *
C*       MASS < THIS D50 CALCULATED FROM SPLINE FIT, (XLLD50,YLD50).   *
C*       2. THE DERIVATIVE OF CUMULATIVE MASS WITH RESPECT TO LOG      *
C*       DIAMETER AT POINT DESCRIBED ABOVE, DMDLD0.                    *
C*       3. THE LOG OF THE MAXIMUM PARTICLE DIAMETER AND THE TOTAL     *
C*       ACCUMULATED MASS CONCENTRATION, (XLDMAX,YMAX).                *
C*       4. THE DERIVATIVE OF CUMULATIVE MASS WITH RESPECT TO LOG      *   ←Ⓑ
C*       DIAMETER AT POINT DESCRIBED ABOVE, 0.0.                       *
C*     OSCFIT RETURNS THE LOG DIAMETER AT WHICH ZERO FIRST DERIVATIVE  *
C*     BEGINS, ZSPT, I.E. D(CUMULATIVE MASS)/D(LOG DIAMETER)=0.0 FOR   *
C*     LOG DIAMETER < OR = ZSPT. IT ALSO RETURNS THE FITTING COEFFI-   *
C*     CIENTS B(1), B(2), B(3), B(4) FOR CUMULATIVE MASS VS. LOG       *
C*     DIAMETER BETWEEN POINTS DESCRIBED IN 1. AND 3. ABOVE.           *
C*                                                                     *SPLI 282
C***********************************************************************SPLI 283
      OSCL=DLOG10(XNDPEN(NFIT))-DLOG10(XNDPEN(NFIT1))
      XINC=OSCL/RR                                                            ←Ⓒ
      NN=(NFIT1-1)*N+1                                                    SPLI 286
      XLLD50=DLOG10(XNDPEN(NFIT1))
      XLDMAX=DLOG10(XNDPEN(NFIT))
      NLD50=NPT-NN
      YLD50=10.0**Y1(NLD50)
      DEL1=COE(INTS1,2)+COE(INTS1,3)*2.*XLLD50
      PPP=COF(INTS1,1)
      DO 505 L=2,3
  505 PPP=PPP+COF(INTS1,L)*XLLD50**(L-1)                                      ←Ⓓ
      DMDLD0=DEL1*(10.0**PPP)*2.302585
      YMAX=YO(NFIT)
      CALL OSCFIT(XLLD50,YLD50,XLDMAX,YMAX,OMDLD0,0.0,ZSPT,
     1B(1),B(2),B(3),B(4))                                              Ⓓ
C***********************************************************************SPLI 293  con't.
C*      THE NUMBER OF POINTS TO BE USED ALONG THE OSCULATING POLYNOMIAL *
C*      IS NN+2 = 8+2 THE 2 ADDED POINTS ARE EXTRAPOLATED VALUES BEYOND *
C*      LOG10(XNDPEN(NFIT),Y0(NFIT)).
C*                                                                     *SPLI 297
C*                                                                     *SPLI 298
C***********************************************************************SPLI 299
      N3=NN+2                                                           SPLI 300
      DO 1150 I=1,N3                                                    SPLI 301
      J=M+I                                                             SPLI 302
      X1(J)=X1(M)+I*XINC                                                SPLI 303
      IF(X1(J).LE.ZSPT)GO TO 550
      Y1(J)=PLOG10(Y0(NFIT))
      GO TO 1150
  550 CONTINUE
      Y1(J)=B(1)
      DO 1148 K=2,4
 1148 Y1(J)=Y1(J)+B(K)*X1(J)**(K-1)                                     Ⓔ
      Y1(J)=ALOG10(Y1(J))
 1150 CONTINUE
C***********************************************************************SPLI 305
C*                                                                     *SPLI 306
C*      REDEFINE "DO 50" LOOP INDEX BEGINNING AND END. BEGINNING       *SPLI 307
C*      INTERVAL II BEGINS TWO (X1,Y1) POINTS BEFORE D50 OF FIRST      *SPLI 308
C*      STAGE. LAST INTERVAL, INTS1, ENDS WITH DMAX. RETURN TO TOP OF  *
C*      LOOP TO FIND FITTING POLYNOMIAL COEFFICIENTS OVER THESE        *SPLI 310
C*      INTERVALS.                                                     *SPLI 311
C*                                                                     *SPLI 312
C***********************************************************************SPLI 313
      II=NPT-NN-2                                                      *SPLI 314
      INTS1=NPT-1                                                       Ⓕ
      GO TO 23                                                          SPLI 316
C***********************************************************************SPLI 317
C*                                                                     *SPLI 318
C*      INT = NUMBER OF INTERVALS FOR WHICH FITTING COEFFICIENTS HAVE  *SPLI 319
C*      BEEN DEFINED.                                                  *SPLI 320
C*                                                                     *SPLI 321
C***********************************************************************SPLI 322
   55 INT=NPT-1                                                        *SPLI 323
C***********************************************************************SPLI 324
C*                                                                     *SPLI 325
C*      FILE NUMBER OF FITTED POINTS, THE INTERVAL BOUNDARY POINT      *SPLI 326
C*      VALUES, AND FITTING COEFFICIENTS FOR EACH INTERVAL.            *SPLI 327
C*                                                                     *SPLI 328
C***********************************************************************SPLI 329
      WRITE(11'IAV)NPT,INT,(X1(I),I=1,NPT),(Y1(I),I=1,NPT),            *SPLI 330
     1((COF1(I,J),J=1,3),I=1,INT)                                       SPLI 331
  400 CONTINUE                                                          SPLI 332
      STOP                                                              SPLI 333
    1 FORMAT (3I2)                                                      SPLI 336
      END                                                               SPLI 337
                                                                        SPLI 345
```

TABLE A-4. SUBROUTINE OSCFIT LISTING

```
      SUBROUTINE OSCFIT(X0,Y0,X1,Y1,YP0,YP1,XIN,A4,A3,A2,A1)            OSCFIT01
C***********************************************************************
C*
C*     THIS SUBROUTINE GENERATES THE COEFFICIENTS OF A FIRST ORDER     *
C*     OSCULATING PULYNOMIAL OF DEGREE THREE TO APPROXIMATE Y(X) OVER  *
C*     THE INTERVAL X0.LE.X.LE.X1  .                                   *
C*     INPUTTED VALUES ARE :                                           *
C*        X0  : THE VALUE OF X AT THE LOWER LIMIT                      *
C*        Y0  : THE VALUE OF Y(X) AT X EQUAL THE LOWER LIMIT           *
C*        YP0 : THE VALUE OF THE FIRST DERIVATIVE DY/DX AT X=X0        *
C*        X1  : THE VALUE OF X AT THE UPPER LIMIT                      *
C*        Y1  : THE VALUE OF Y(X) AT X EQUAL THE UPPER LIMIT           *
C*        YP1 : THE VALUE OF THE FIRST DERIVATIVE DY/DX AT X=X1        *
C*                                                                     *
C*     OUTPUTTED VALUES ARE :                                          *
C*        X1N : THE NEW UPPER LIMIT (LARGEST VALUE) OF X IN THE INTERVAL
C*              X0.LE.X1N.LE.X1 SUCH THAT THE APPROXIMATING FUNCTION   *
C*              P(X) IS ALWAYS GREATER THAN OR EQUAL TO ZERO (I.E.
C*              NEVER NEGATIVE).                                       *
C*        A1  : THE COEFFICIENTS OF THE BEST FIT CUBIC EQUATION IN THE *
C*        A2    OSCULATING SENSE PASSING THROUGH Y0 AND Y1 AND MATCHING*
C*        A3    THE SLOPES YP0 AND YP1 AT THESE POINTS.. NOTE THAT IF  *
C*        A4    X1N.LT.X1 THE CALLING PROGRAM SHOULD DEFINE P(X)=Y1    *
C*              (I.E. A CONSTANT) AND DP(X)/DX = YP1 (ALSO A CONSTANT) *
C*              IN THE INTERVAL X1N.LE.X.LE.X1 .                       *
C*                                                                     *
C*     THE GENERATED APPROXIMATING POLYNOMIAL IS GIVEN BY:             *
C*                                                                     *
C*        P(X) = A1*(X**3) + A2*(X**)2 + A3*(X) + A4                   *
C*                                                                     *
C***********************************************************************
      REAL K1,K2,K3,K4,K5,K6                                            OSCFIT02
C***********************************************************************
C*
C*     N IS A COUNTER OF THE NUMBER OF TIMES THRU THE ITERATIVE LOOP   *
C*     STEP IS THE INITIAL BACKWARD STEP SIZE IN X FOR THE BACKWARD    *
C*     SUCCESSIVE APPROXIMATION OF X1N THE NEW UPPER LIMIT IN X        *
C*     STEP1 IS THE FORWARD STEP SIZE USED TO DETERMINE IF THE         *
C*     POLYNOMIAL HAS A NEGATIVE SLOPE ANYWHERE WITHIN                 *
C*     THE RANGE OF X VALUES.  STEP1 IS ALWAYS TAKEN AS                *
C*     (UPPER LIMIT - LOWER LIMIT)/99.                                 *
C*                                                                     *
C***********************************************************************
      N=0                                                               OSCFIT03
      STEP=1.0E-1                                                       OSCFIT04
      XX1=X1                                                            OSCFIT05
      DELX=X1-X0                                                        OSCFIT06
      STEP1=DELX/99.                                                    OSCFIT07
   10 N=N+1                                                             OSCFIT08
      DEL1=X0-XX1                                                       OSCFIT09
      DEL2=-DEL1                                                        OSCFIT10
      DEL1S=DEL1**2                                                     OSCFIT11
      DEL2S=DEL2**2                                                     OSCFIT12
      DEL1C=DEL1S*DEL1                                                  OSCFIT13
      DEL2C=DEL2S*DEL2                                                  OSCFIT14
      K1=Y0/DEL1S                                                       OSCFIT15
      K2=-2.*Y0/DEL1C                                                   OSCFIT16
      K3=Y1/DEL2S                                                       OSCFIT17
      K4=-2.*Y1/DEL2C                                                   OSCFIT18
      K5=YP0/DEL1S                                                      OSCFIT19
      K6=YP1/DEL2S
      A1=K2+K4+K5+K6                                                    OSCFIT20
      A2=(K1+K3-(2.*XX1+X0)*(K2+K5)-(2.*X0+XX1)*(K4+K6))                OSCFIT21
      A3=((K2+K5)*((XX1**2)+2.*X0*XX1)+(K4+K6)*((X0**2)+2.*X0*XX1))     OS369T22
     1-2.*K1*XX1-2.*K3*X0                                               OSCFIT23
      A4=(K1*(XX1**2)+K3*(X0**2)-X0*(XX1**2)*(K2+K5))-(X0**2)*XX1*(K4   OSCFIT24
     1+K6)                                                              OSCFIT25
C***********************************************************************OSCFIT26
C*    ******************************************************************
C*        THE DO LOOP ENDING AT 100 EVALUATES THE FIRST DERIVATIVE OF THE *
C*        APPROXIMATING POLYNOMIAL TO SEE IF IT PREDICTS A NEGATIVE VALUE *
C*        IN THE RANGE X0.LE.X.LE.XX1  WHERE XX1.LE.X1   .  IF A NEGATIVE *
C*        VALUE IS FOUND THE UPPER LIMIT XX1 WILL BE REDUCED BY THE CURRENT
C*        VALUE OF STEP AND A NEW SET OF COEFFICIENTS IS CALCULATED FOR   *
C*        THIS REDUCED RANGE.  IF NO NEGATIVE VALUE IS FOUND AND N=1 THEN *
C*        THE BEST FIT EQUATION HAS BEEN FOUND AND OSCFIT RETURNS TO THE  *
C*        CALLING PROGRAM.  IF N IS NOT 1 THEN XX1 MAY BE TOO SMALL SO GO *
C*        BACK TO XX1 VALUE JUST PRIOR TO CURRENT ONE AND SEARCH WITH A   *
C*        STEP VALUE 1/10 AS LARGE AS BEFORE.  THIS PROCESS CONTINUES UNTIL
C*        EITHER (1) A CORRECT VALUE OF XX1 IS FOUND OR (2) STEP IS SMALLER
C*        THAN SOME PREDETERMINED VALUE (HERE 1.0E-06), WHEN EITHER       *
C*        OCCURS THE SUBROUTINE THEN RETURNS THE LAST VALUES OF THE       *
C*        COEFFICIENTS TO THE CALLING PROGRAM.                            *
C*                                                                        *
C***********************************************************************  *
      ******************************************************************
      X=X0-STEP1
      DO 100 I=1,100                                                    OSCFIT27
      X=X+STEP1                                                         OSCFIT28
      IF(X.GT.XX1) GO TO 100                                            OSCFIT29
      YP=3.*A1*(X**2)+2.*A2*X+A3                                        OSCFIT30
      IF (YP.LT.0.) GO TO 110                                           OSCFIT31
  100 CONTINUE                                                          OSCFIT32
      GO TO 120                                                         OSCFIT33
  110 XX1=XX1-STEP                                                      OSCFIT34
      GO TO 10                                                          OSCFIT35
  120 IF(N.EQ.1) GO TO 140                                              OSCFIT36
      XX1=XX1+STEP                                                      OSCFIT37
      STEP=STEP/10.                                                     OSCFIT38
      IF(ABS(STEP).LT.1.0E-06) GO TO 130                                OSCFIT39
      GO TO 10                                                          OSCFIT40
  130 CONTINUE                                                          OSCFIT41
       XX1=XX1-1.*STEP                                                  OSCFIT42
  140 CONTINUE                                                          OSCFIT43
      X1N=XX1                                                           OSCFIT44
      RETURN                                                            OSCFIT45
      END                                                               OSCF9T50
                                                                        OSCFIT51
```

APPENDIX B

FINAL REPORT

SRI Contract No. N0014

(Acct. No. 3858-13)

"Modeling of SRI Impactor Data"

MODELING OF SRI IMPACTOR DATA AND CALCULATION OF IP CONCENTRATION

Prepared by

A. Kapadia, D. Y. H. Pui, and K. T. Whitby

Submitted by

K. T. Whitby, Professor and Chief
Environmental Division
Mechanical Engineering Department
University of Minnesota
Minneapolis, Minnesota 55455

October, 1979

Particle Technology Laboratory Publication No. 403

ABSTRACT

The SRI impactor data for emissions from several different stationary sources have been analyzed using a modal analysis technique, in which the data are fitted with multi-component log-normal distributions. The technique is used because the available data do not contain sufficient size classification information in the upper particle size limit of 10 to 100 μm. This information is needed in order to estimate the inhalable particulate (IP) concentration, i.e., all particles below 15 μm aerodynamic diameter, for these source aerosols. By using a simplex minimization method, the present technique projects the entire size distribution by fitting the available portion of the size distsribution with log-normal distributions. It has previously been applied successfully to atmospheric aerosols (Whitby, 1978). This study shows that the technique can indeed be extended to the source aerosols and work reasonable well. The conditions under which the technique applies are discussed.

The size distributions thus obtained are integrated with the proposed IP sampler curve. The resulting IP concentrations are presented, together with their sensitivity to the assumed modal parameters of the size distributions. The effects of varying the sampler cut size and the sharpness of cut on the IP concentrations are included. The calculations indicate that the present specifications for the performance curve of the IP sampler, $D_{50} = 15 \pm 2$ μm and $\sigma_{gD} = 1.0 - 1.7$, are adequate because the resulting IP concentrations change by less than ±20% within the tolerance of the performance curve.

TABLE OF CONTENTS

Page

Abstract i

Contents ii

List of Figures. iv

I. INTRODUCTION 1
  A. Background 1
  B. Estimation of Inhalable Particulate (IP) Concentration . . 3
  C. Log-Normal Function for Aerosol Size Distribution 4

II. ANALYSIS TECHNIQUE 7
  A. Minimization Procedures. 7
  B. Estimation of IP Concentration 11
  C. Sample Data Analysis 11
    1. Aerosol at the inlet of control device 12
    2. Aerosol at the outlet of control device. 12
  D. Sensitivity Analysis 15
    1. Modal parameters 15
      a. Variation of σ_g. 15
      b. Variation of MMD_2. 18
    2. Effect of IP sampler curve on IP concentration 21
      a. Variation of σ_{gD} 21
      b. Variation of D_{50} 21

III. RESULTS AND DISCUSSION 23
  A. Coal-Fired Boiler, Hot Side ESP Inlet (NGP-13) 23
  B. Coal-Fired Boiler, Cold Side ESP Inlet (JBI-13). 32
  C. Copper Smelter, Hot Side ESP Inlet (AJOI-3, AJOI-5). . . . 41

TABLE OF CONTENTS (cont.)

Page

IV. SUMMARY AND RECOMMENDATIONS. 51

A. Summary. 51

B. Recommendations. 52

References 53

APPENDIX A. COMPUTER PROGRAM FOR IMPACTOR DATA MODELING AND IP CONCENTRATION CALCULATION. 54

LIST OF FIGURES

No.	Title	Page
I.1	Modeling of aerosols at the inlet and outlet of an electrostatic precipitator: (a) inlet aerosol, (b) electrostatic precipitator penetration, and (c) output aerosol.	5
I.2	Modeling of aerosols at the inlet and outlet of a scrubber: (a) input aerosol, (b) scrubber penetration, and (c) output aerosol.	6
II.1	Graphical representation of the search method in the simplex minimization procedure.	9
II.2	Modeling of impactor data for a coal-fired power plant obtained at the inlet of an electrostatic precipitator. . .	13
II.3	Modeling of impactor data for a coal-fired power plant obtained at the outlet of an electrostatic precipitator. . .	14
II.4	Effect of assumed σ_{g2} of the inlet aerosol and σ_{gD} of the sampler curve on the IP concentration estimate.	16
II.5	Effect of assumed σ_{g2} of the outlet aerosol and σ_{gD} of the sampler curve on the IP concentration estimate.	17
II.6	Effect of assumed MMD_2 of the inlet aerosol and σ_{gD} of the sampler curve on the IP concentration estimate.	19
II.7	Effect of assumed MMD_2 of the outlet aerosol and σ_{gD} of the sampler curve on the IP concentration estimate.	20
II.8	Effect of IP sampler curve cut size on the estimated IP concentration for the inlet data.	22
III.1	Modal fitting of impactor data from coal-fired boiler, hot side ESP inlet (NGP-13, $\rho = 1.0$).	24
III.2	Effect of assumed aerosol σ_{g2} and sampler σ_{gD} on the IP concentration estimate (NGP-13, $\rho = 1.0$).	25
III.3	Effect of assumed aerosol MMD_2 and sampler σ_{gD} on the IP concentration estimate (NGP-13, $\rho = 1.0$).	26
III.4	Effect of sampler D_{50} on the IP concentration estimate (NGP-13, $\rho = 1.0$).	27
III.5	Modal fitting of impactor data from coal-fired boiler, hot side ESP inlet (NGP-13, $\rho = 2.41$).	28

LIST OF FIGURES (cont.)

No.	Title	Page
III.6	Effect of assumed aerosol σ_{g2} and sampler σ_{gD} on the IP concentration estimate (NGP-13, $\rho = 2.41$).	29
III.7	Effect of assumed aerosol MMD_2 and sampler σ_{gD} on the IP concentration estimate (NGP-13, $\rho = 2.41$).	30
III.8	Effect of sampler D_{50} on the IP concentration estimate (NGP-13, $\rho = 2.41$).	31
III.9	Modal fitting of impactor data from coal-fired boiler, cold side ESP inlet (JBI-13, $\rho = 1.0$).	33
III.10	Effect of assumed aerosol σ_{g2} and sampler σ_{gD} on the IP concentration estimate (JBI-13, $\rho = 1.0$).	34
III.11	Effect of assumed aerosol MMD_2 and sampler σ_{gD} on the IP concentration estimate (JBI-13, $\rho = 1.0$).	35
III.12	Effect of sampler D_{50} on the IP concentration estimate (JBI-13, $\rho = 1.0$).	36
III.13	Modal fitting of impactor data from coal-fired boiler, cold side ESP inlet (JBI-13, $\rho = 2.34$).	37
III.14	Effect of assumed aerosol σ_{g2} and sampler σ_{gD} on the IP concentration estimate (JBI-13, $\rho = 2.34$).	38
III.15	Effect of assumed aerosol MMD_2 and sampler σ_{gD} on the IP concentration estimate (JBI-13, $\rho = 2.34$).	39
III.16	Effect of sampler D_{50} on the IP concentration estimate (JBI-13, $\rho = 2.34$).	40
III.17	Modal fitting of impactor data from copper smelter, hot side ESP inlet (AJOI-3).	43
III.18	Effect of assumed aerosol σ_{g2} and sampler σ_{gD} on the IP concentration estimate (AJOI-3).	44
III.19	Effect of assumed aerosol MMD_2 and sampler σ_{gD} on the IP concentration estimate (AJOI-3).	45
III.20	Effect of sampler D_{50} on the IP concentration estimate (AJOI-3).	46
III.21	Modal fitting of impactor data from copper smelter, hot side ESP inlet (AJOI-5).	47

LIST OF FIGURES (cont.)

No.	Title	Page
III.22	Effect of assumed aerosol σ_{g2} and sampler σ_{gD} on the IP concentration estimate (AJOI-5)	48
III.23	Effect of assumed aerosol MMD_2 and sampler σ_{gD} on the IP concentration estimate (AJOI-5)	49
III.24	Effect of sampler D_{50} on the IP concentration estimate (AJOI-5)	50

I. INTRODUCTION

This is the final report on SRI Contract No. N0014, entitled "Modeling of SRI Impactor Data". A progress report, PTL No. 391, was submitted in May, 1979. It described the analysis technique used in the impactor data reduction together with the sample data analysis for two sets of in-stack data. The present report extends the analysis technique to other SRI data (Section IV). In addition, a computer program developed for this study is included in Appendix A.

A. Background

Atmospheric aerosols have been found to encompass almost six decades of size, from clusters on the order of 10 Å to particles on the order of 100 μm in size. Further study of atmospheric aerosols has shown that the combination of different generation mechanisms with different classification mechanisms produces modes or sub-range groupings often having more or less homogeneous physical and chemical properties. Condensational mechanisms produce particles primarily less than 1 or 2 μm in size. On the other hand, mechanical processes produce particles from about 1 μm up. Aerosol growth dynamics often operate to limit condensation-sized aerosols to less than 1 μm and to limit the amount of mass transfer between the smaller fine particles and the coarse particles.

Furthermore, it has been found convenient to characterize these groupings by additive log-normal distributions called modes. In particular, we have found that three modes--one with a number geometric size peak around .01 μm, called the nuclei mode; a second one with a number peak around .07 μm, called the accumulation mode; and a coarse particle mode peaking in the 5 to 20 μm range--are sufficient to characterize atmospheric distributions well.

Since it was known that the same formation and classification mechanisms must operate in stationary sources that produce particulates, with different concentrations and size limits, it seems reasonable to apply the same modal analysis techniques developed for atmospheric aerosols to the stationary source aerosols.

The analysis is based on a number of assumptions mostly derived from the atmospheric aerosol analysis experience findings and assumption as follows:

1) Three additive log-normal distributions are usually an adequate characterization for the aerosol.
2) Geometric standard deviations of these additive log-normal distributions are usually on the order of 2. This is small enough so that the modes do not overlap to the point where they cannot be separated by analysis techniques such as the simplex program used for the data analysis of this report.
3) Classification techniques, such as those introduced by the gas cleaners or by settling, tend to modify the geometric standard deviations of the modes and the means of the modes, but do not change the shape of the modes enough so that they can still be fitted quite well by a log-normal distribution.

The usual method of size distribution analysis for source particulate testing has been the cascade impactor. The cascade impactor yields fairly good size distribution information in the few tenths of a μm to 10 μm range, but generally the aerosol between the cut size of the last stage and the filter is not characterized well, nor is the size distribution from 10 μm and up. In practice, this means that the nuclei mode, which is essentially all on the filter, is not going to be characterized very well by size, nor is the coarse mode if its size is larger than 10 μm. The coarse particle mode also may not be characterized well because impactor stages which operate above 10 μm have not been too practical.

However, from work on atmospheric aerosols, when the size distribution is not known in enough detail over the entire particle size range, good estimates of the total mass in the nuclei and coarse particle modes can be made by partial fitting to the available portion of the size distribution. The work done for this project is an extension of the analysis to stack data.

B. Estimation of Inhalable Particulate (IP) Concentration

Currently EPA has under consideration the specification of an inhalable particulate sampler which would have a cut size of 15 ± 2 μm and a geometric standard deviation of the classification efficiency curve in the range from 1.0 to 1.7. The idea is to use this pre-classifier on samplers so that the sample passing would presumably be that which could be inhaled by a normal human being. One question is how sensitive the mass passing through such a sampler would be to the cut size and the slope of the IP classification curve. Therefore, we investigated this by integrating the IP curve with geometric standard deviations varying from 1 for the perfect classification, to IP curves with a σ_g of 1.7. These were integrated with a typical size distribution ahead of the gas cleaner and a typical one after the gas cleaner. Not surprisingly, these results show that the mass passing from the IP classifier is not very sensitive to the slope of the efficiency curve, but is quite sensitive to the cut point. This indicates that for such a sampler, much greater variations on the slope could be tolerated than in the cut point.

The investigation of the variation of the assumed σ_g of the coarse particle mode showed that it too can be varied over quite a range when fitting coarse particle mode without seriously affecting the IP results.

C. Log-Normal Function for Aerosol Size Distribution

Atmospheric aerosols have been modeled successfully by Whitby (1978) using a three-component or a trimodal log-normal distribution for particles in the size range of 0.002 μm to 60 μm. The three-component log-normal distribution is used in the present study to model the aerosol at the inlet and the outlet of a control device. It is reasonable to assume that the aerosol at the inlet of the control device can be modeled by a multi-component log-normal distribution, but no *a priori* assumption regarding the aerosol at the outlet of the control device can be made. To demonstrate the feasibility of modeling the outlet aerosol by the multi-component log-normal distribution, the following calculations were made.

The histogram in Figure I.1a shows a typical mass distribution measured at the inlet of the control device. Figure I.1b shows the efficiency of an electrostatic precipitator (McCain et al., 1975), and the histogram in Figure I.1c is the calculated aerosol at the outlet of the precipitator obtained by taking the product of Figures I.1a and I.1b. The histograms of both the inlet and the outlet aerosols were fitted by bimodal log-normal distributions. As can be seen from the figures, the aerosol can be modeled satisfactorily by multi-component log-normal distribution. It should be noted here that the χ^2 values are of the same order of magnitude for both the inlet and the outlet aerosols. Similar results were found when the calculations were done using a scrubber efficiency (McCain, 1978). The resulting calculations are shown in Figure I.2.

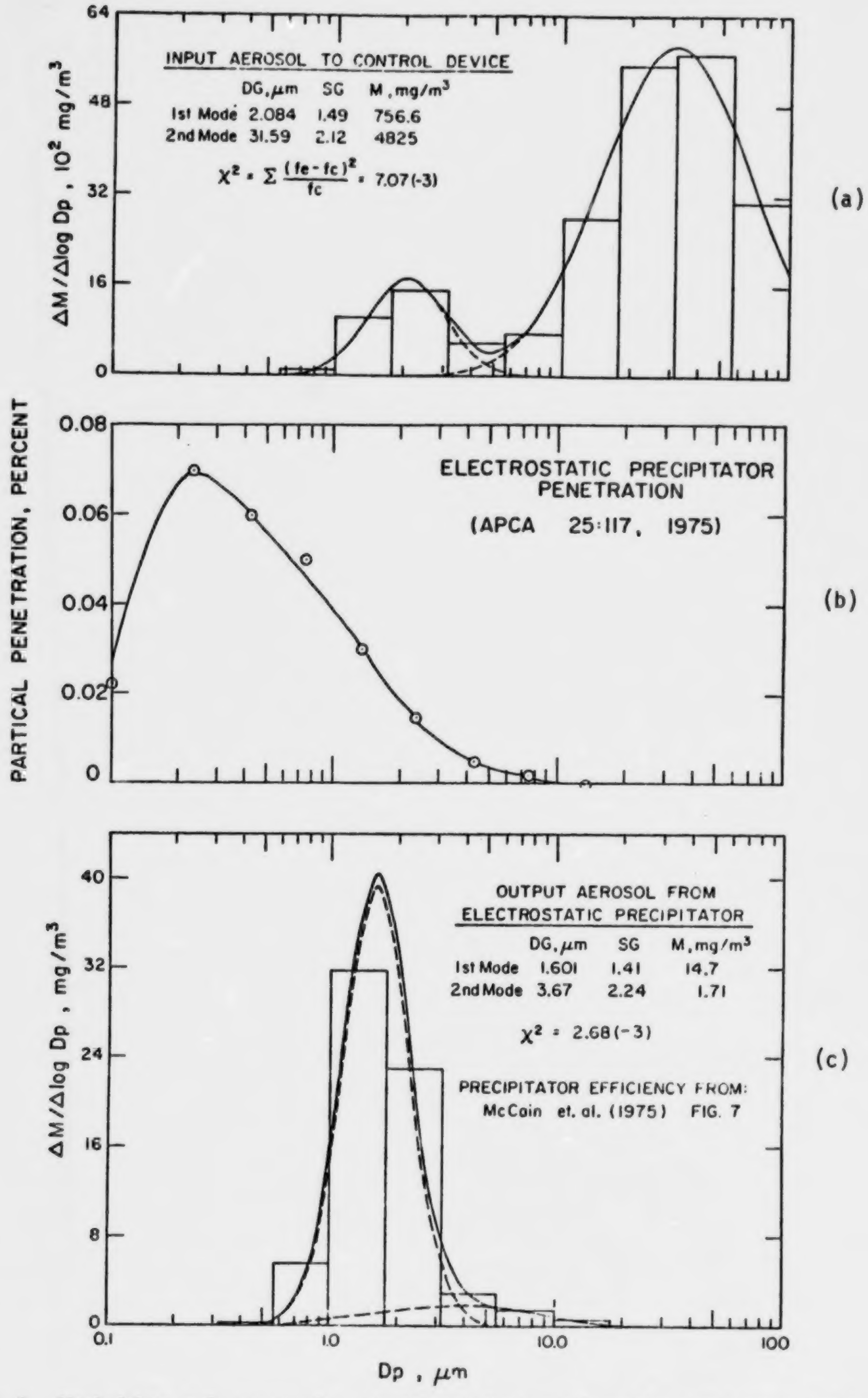

Figure I.1 Modeling of aerosols at the inlet and outlet of an electrostatic precipitator: (a) inlet aerosol, (b) electrostatic precipitator penetration, and (c) output aerosol.

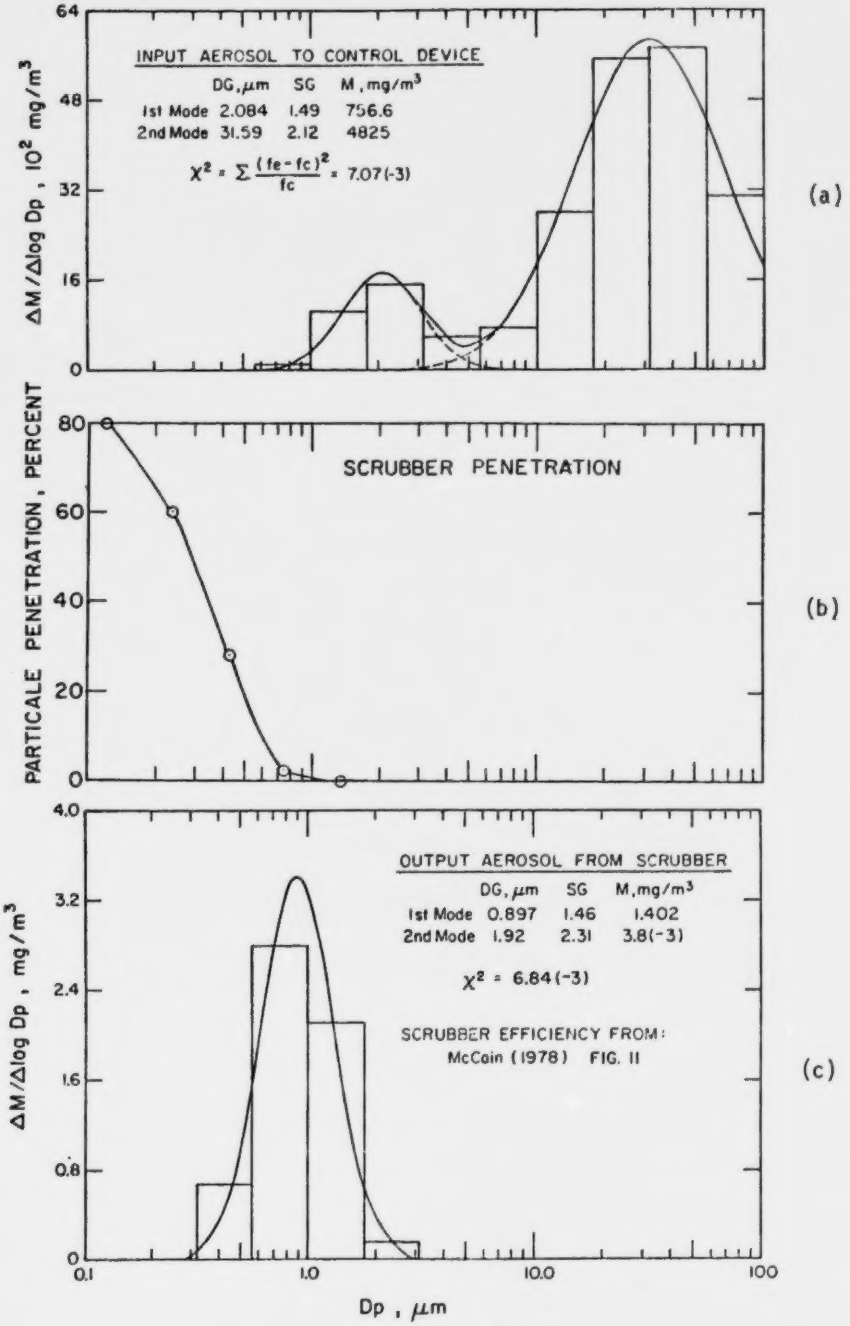

Figure I.2 Modeling of aerosols at the inlet and outlet of a scrubber: (a) input aerosol, (b) scrubber penetration, and (c) output aerosol.

II. ANALYSIS TECHNIQUE

Several procedures for fitting functions with non-linear coefficients are available. Bevington (1969) and Daniel and Wood (1971) describe several numerical methods for non-linear curve fitting. Raabe (1978) has recently applied a non-linear curve fitting method to obtain the modal parameters of aerosol size distributions. In the present study, a multi-component (up to three) log-normal distribution was fitted to impactor data from stack sampling measurements. It should be noted here that no correction for bounce and cross-sensitivity were made to the raw data before the fitting procedure was carried out.

A. Minimization Procedures

The fitting procedure used in the present study is based on the simplex minimization method developed by Nelder and Mead (1965).

In order to use this method, the following three requirements have to be specified: (a) the form of the solution which can be specified by several parameters (trimodal log-normal distribution), (b) the minimization procedure which gives the set of parameters that best fit the data, and (c) the function to be minimized (hereafter referred to as the objective function).

In this method, a function of m variables is minimized using a direct search method. For a function of m variables, a general simplex of m+1 vertices, denoted by P_j, j=1,2,....m+1 is initially formed and the objective function evaluated at each of the vertices. The value of the objective function at P_j is denoted by y_j. The vertex which has the highest value of the objective function (P_h) is then replaced by another point.

To determine the new point, first the centroid ($\overline{P}$) of the remaining points (i.e., P_j, j=1,2....m+1, $j \neq h$) is calculated and the location of the next point is determined by one of the three operations: reflection, expansion, or contraction.

The coordinates of P^* determined by reflection are given by

$$P^* = (1 + \alpha)\overline{P} - \alpha\, P_h \qquad \text{(II.1)}$$

where α is a positive constant. Thus, P^* lies on the far side of $\overline{P}$ from P_h, and on the line joining $\overline{P}$ and P_h. If y^* (value of the objective function at P^*) is between y_h and y_l (highest and lowest value of the objective function evaluated at the vertices of the simplex), P_h is replaced by P^*, and a new simplex formed and the process restarted.

To show the process graphically, consider a two-variable function which is to be fitted. Let the two variables be X_1 and X_2. In Figure II.1, P_1, P_2, and P_3 form the initial simplex and assume that P_3 is P_h. The point $\overline{P}$ will then lie on the line joining P_1 and P_2 and P^* on the line joining P_3 and $\overline{P}$.

If P^* produces a new minimum, i.e., $y^* < y_l$, an expansion is attempted and P^{**} located. The coordinates of P^{**} are determined by

$$P^{**} = \gamma P^* + (1 + \gamma)\overline{P} \qquad \text{(II.2)}$$

and in Figure II.1, $\gamma = (P^{**}\overline{P})/(P^*\overline{P})$, where γ is greater than unity. If y^{**} is less than y^*, P^* is replaced by P^{**}, a new simplex formed, and the process restarted. Otherwise, P_h is replaced by P^*.

On the other hand, a contraction is carried out, giving P^{***}, when reflection fails. The location of P^{***} is determined by

$$P^{***} = \beta P_h + (1 - \beta)\overline{P} \qquad \text{(II.3)}$$

with the contraction coefficient β taking values between 0 and 1. In Figure II.1, $(P^{***}\overline{P})/(P_h/\overline{P})$ equals β. P^{***} replaces P_h, unless $y^{***} > \min(y_h, y^*)$, i.e., the contraction point is worse than the better of P_h and P^*. When contraction fails, all the P_i's are replaced by $(P_i + P_l)/2$, and the process restarted.

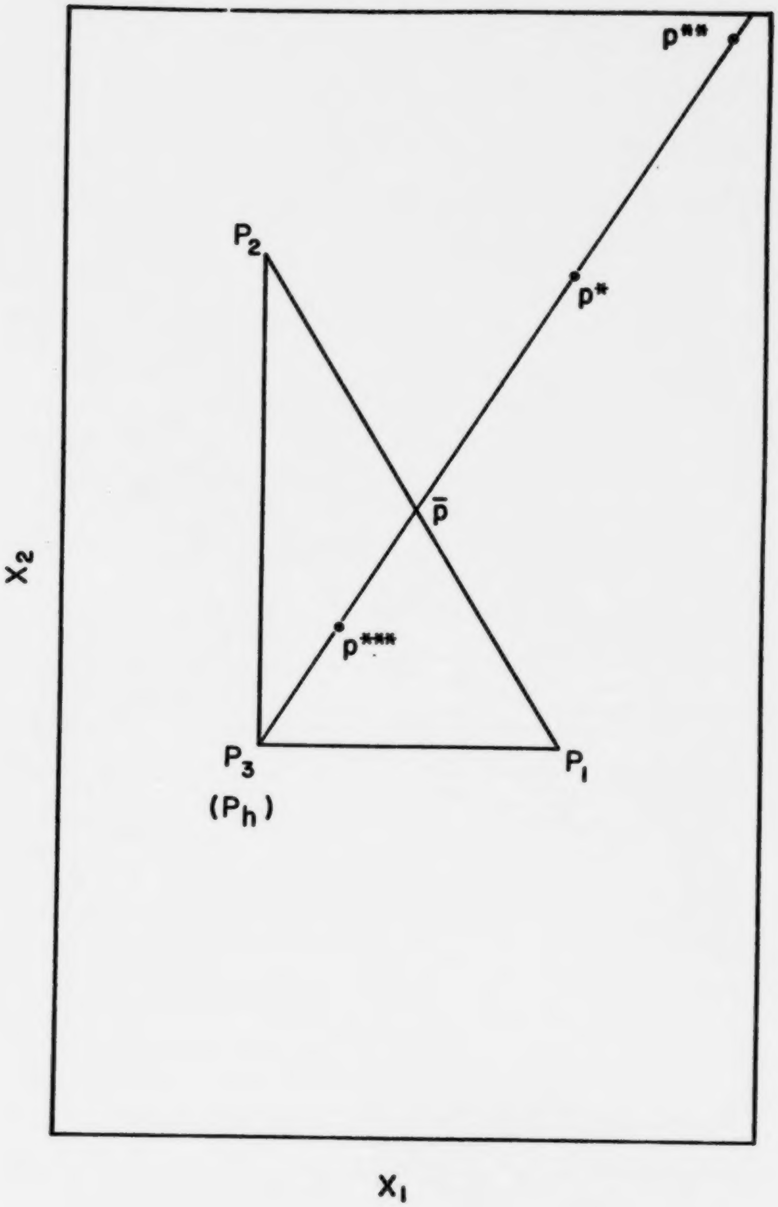

p**
P2
p*
p̄
X2
p***
P3
(Ph)
P1
X1

Figure II.1 Graphical representation of the search method in the simplex minimization procedure.

In this manner, the simplex continuously adapts itself to the landscape and contracts in the neighborhood of a minimum. The search process is halted when dimensions of the simplex become smaller than certain set values. In the present work, $\alpha = 1.0$, $\gamma = 0.5$, and $\beta = 2.0$ were chosen as recommended by Nelder and Mead (1965). It should be noted here that the minimum may not necessarily be a global minimum, but only a local minima. In order to ensure that it is a global minima, either the minimization process should be repeated with different starting simplices, or the solution can be taken as reasonably close to the global optimum if the value of the objective function is acceptable.

Three forms of the objective function were tested: the modified chi-square, χ^2_m, given by Equation (II.4); the normal χ^2 function, given by Equation (II.5); and the weighted least square, WLS, given by Equation (II.6)

$$\chi^2_m = \frac{1}{MT} \sum \frac{(\Delta M_i' - \Delta M_i)^2}{(\Delta M_1' + \Delta M_1)/2} \qquad \text{(II.4)}$$

$$\chi^2 = \frac{(MT' - MT)^2}{MT'} + \sum \frac{\left(\frac{\Delta M_i'}{\Sigma_j \Delta M_j'} - \frac{\Delta M_i}{\Sigma_j \Delta M_j}\right)^2}{\Delta M_i'/\Sigma_j \Delta M_j'} \qquad \text{(II.5)}$$

$$WLS = \frac{(MT' - MT)^2}{MT} + \sum \frac{\left(\frac{\Delta M_i'}{\Sigma_j \Delta M_j'} - \frac{\Delta M_i}{\Sigma_j \Delta M_j}\right)^2}{\sigma_i^2} \qquad \text{(II.6)}$$

where $\Delta M_i'$ is the calculated mass based on the trimodal log-normal distribution parameter; ΔM_i is the measured mass on the ith impactor stage; MT and MT' are the measured and calculated total mass; and σ_i is the uncertainty in the measured concentration. The σ_i depends on the instrumental uncertainty and the stability of the measured aerosol. As no _a priori_ estimate of σ_i is available, it is assumed that the σ_i^2 is proportional to the normalized concentration.

The proportionality constant is assumed to be unity for minimization purposes, as only the relative values WLS are of interest.

From the analysis of two sets of impactor data, the normal chi-square appears to give a better fit than the modified chi-square in the lower size limit of the distribution. Subsequent study by Kapadia (1979) shows that the WLS is capable of giving better results than the normal chi-square. Therefore, all the fitting results in Section III were obtained using the WLS as the objective function.

B. Estimation of IP Concentration

Equation (II.7) gives the estimate of the IP concentration, once the optimum set of parameters for the three-component log-normal distribution are determined,

$$IP = \int SDC(D_{50}, \sigma_{gD}) \cdot f_M(D_p)\, d \ln D_p \qquad (II.7)$$

where $SDC(D_{50}, \sigma_{gD})$ is the function representing the sampler curve with D_{50} as the cut size and σ_{gD} as the spread of the sampling characteristic, and $f_M^*(D_p)$ is the optimized three-component log-normal distribution which best fits the differential mass data for the impactors.

C. Sample Data Analysis

Two sets of data have been selected from the SRI report to the Electric Power Research Institute (EPRI FP-792). The data were obtained from a coal-fired power plant equipped with an electrostatic precipitator. Set A gives the aerosol mass distribution measured at the inlet of the control device, and Set B gives the mass distribution at the outlet of the control device. These sets of impactor data compare favorably with the electrical aerosol analyzer data in the size range where they overlapped, i.e., between 0.1 μm to 1.0 μm.

1. Aerosol at the inlet of control device

The inlet data were obtained by SRI using a modified Brink cascade impactor. The impactor has seven stages (S0-S6), an in-line cyclone precollector, and a back-up filter. Following the recommendation of J. D. McCain, we have combined the cyclone mass with S0 mass and also neglected the back-up filter mass. The reason for combining cyclone mass and S0 mass is due to the uncertainty in the cyclone cut size. The back-up filter mass was not used because of the impactor bounce problem. The histogram of the impactor data is shown in Figure II.2. The EAA data are also included, and they are plotted with hatched lines. In the present study, only the cascade impactor data were used in the analysis. The EAA data are shown here for comparison purposes.

The impactor data were fitted with a bimodal log-normal distribution using the simplex minimization procedures described above. The resulting modal parameters and fitted curves are shown in Figure II.2. Good fitting is obtained in the first mode. In the second mode, the fitted curve covers only two histogram intervals. Section IID describes the sensitivity analysis for this mode, giving the IP concentration as a function of σ_g and mass median diameter.

2. Aerosol at the outlet of control device

The outlet data were obtained by SRI using an Andersen Model III stack sampler. The S1 and S2 masses were combined because of the close proximity of their cut sizes. The back-up filter mass was included in the analysis, and a particle diameter of 0.01 μm was used for the lower interval boundary. The maximum diameter of particles collected by the sampler for both the inlet and the outlet data was determined by SRI using a microscope. The histogram of the impactor data is shown in Figure II.3. The EAA data in the shaded area are included for comparison purposes.

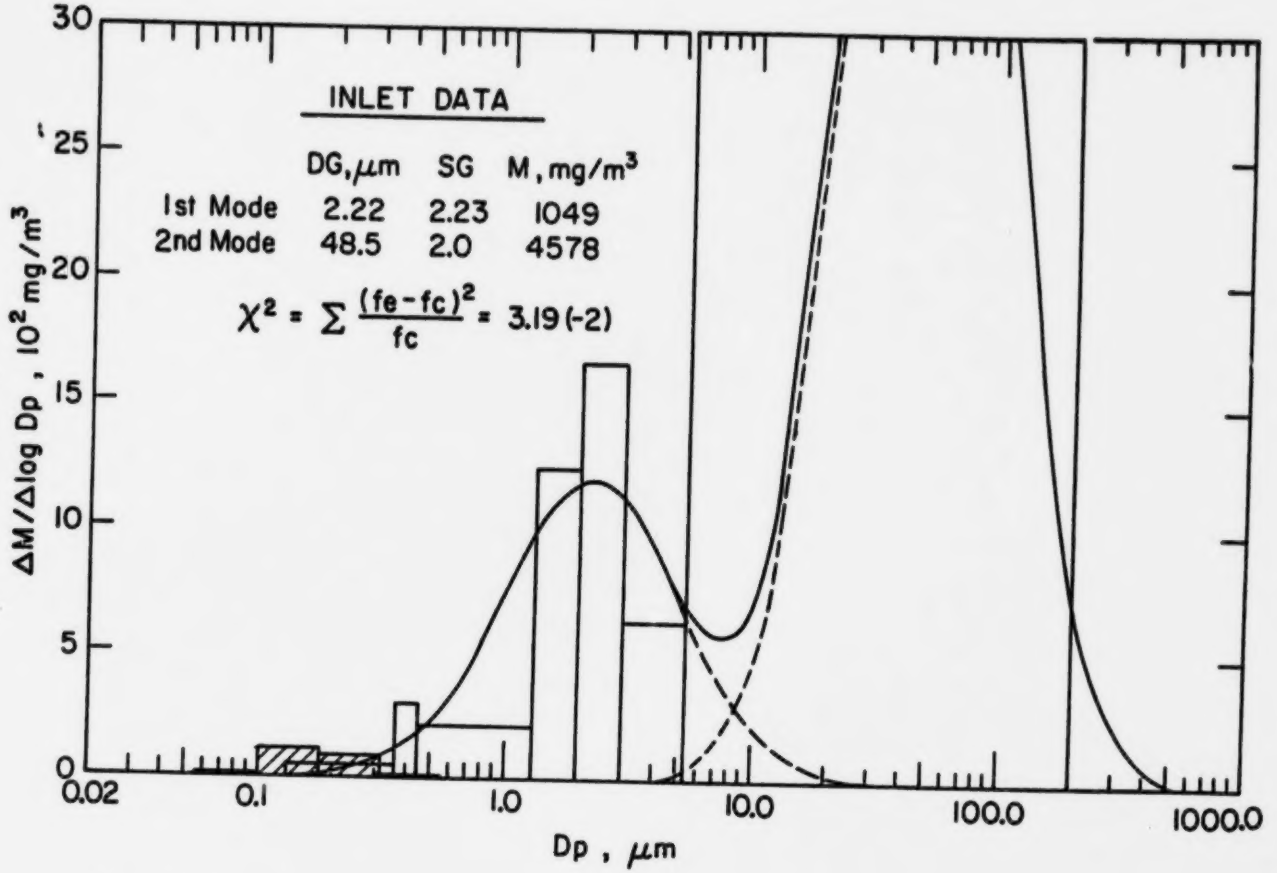

Figure II.2 Modeling of impactor data for a coal-fired power plant obtained at the inlet of an electrostatic precipitator.

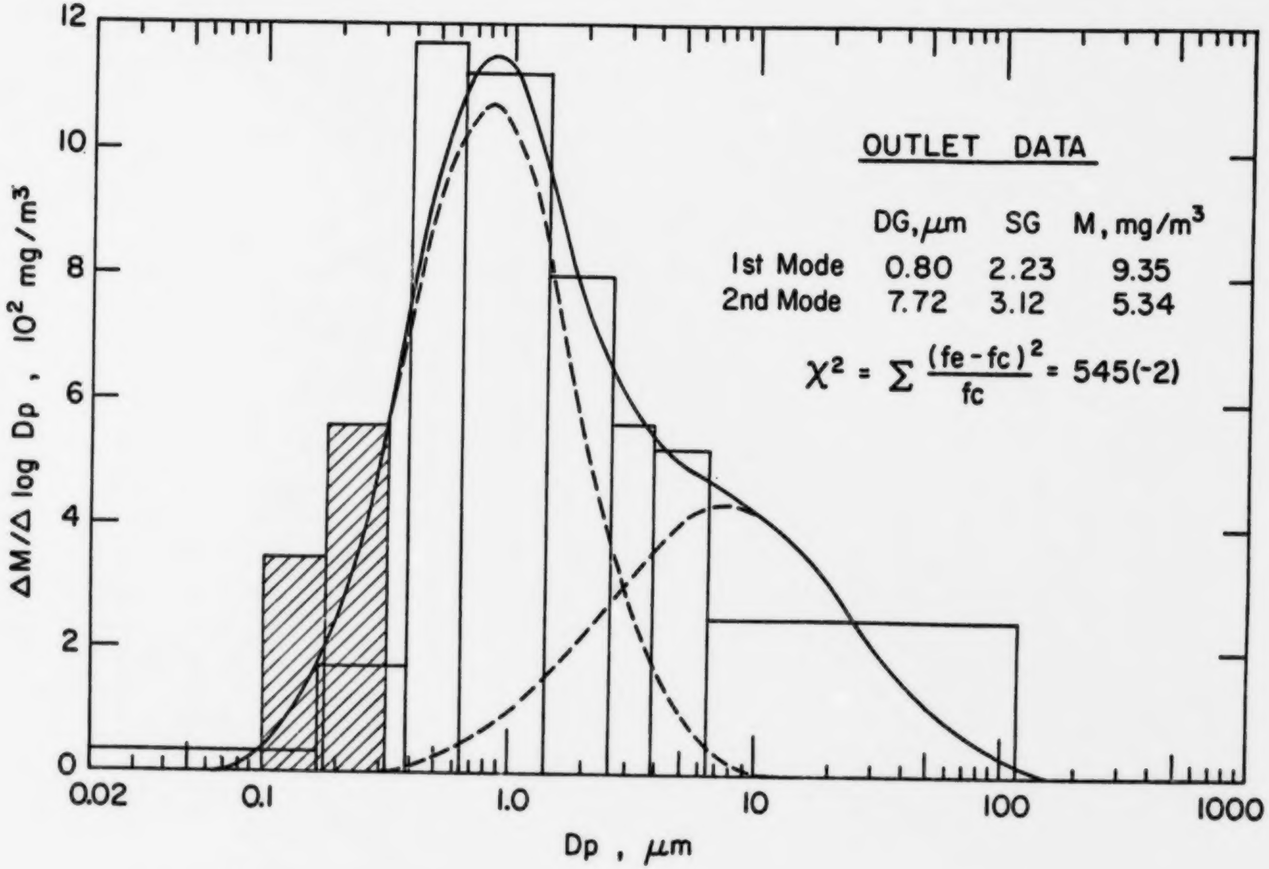

Figure II.3 Modeling of impactor data for a coal-fired power plant obtained at the outlet of an electrostatic precipitator.

The impactor data were fitted with a bimodal log-normal distribution using the simplex minimization procedure. The resulting modal parameters and fitted curves are shown in Figure II.3. It can be seen that the outlet data can be fitted satisfactorily with the bimodal log-normal distribution. The sensitivity analysis for the second mode were also done and are given in the next section.

D. Sensitivity Analysis

One of the main objectives of this study is to develop an analysis technique for estimating the inhalable particulate (IP) concentration from the existing in-stack data. The accuracy of the estimated IP concentration depends on the accuracy of the impactor data modeling and the criteria used for the IP sampler curve. The analysis below shows the sensitivity of the estimated IP concentration to the variation of the fitted parameters of the impactor data and the characteristics of the IP sampler curve.

1. Modal parameters

a. Variation of σ_g

Figures II.4 and II.5 give the variation of IP concentration as a function of the geometric standard deviation of the second mode, σ_{g2}, for the inlet data (Figure II.2) and the outlet data (Figure II.3), respectively. The IP concentration is obtained by keeping the σ_{g2} constant during the minimization process. The χ^2 of the fitted distribution is also plotted in the same figure to indicate the goodness of fit. The two curves for the IP concentration are for $\sigma_{gD} = 1.0$ and $\sigma_{gD} = 1.7$ with $D_{50} = 15.0$ µm. The discussion for the IP sampler curve is given in Section II2.

Figure II.4 shows that, for the inlet data, the total mass below 15 µm for the sampler curve with $\sigma_{gD} = 1.0$, M-15, changes by less than 20% as the geometric standard deviation for the second mode, σ_{g2}, varies from 1.0 to 2.0.

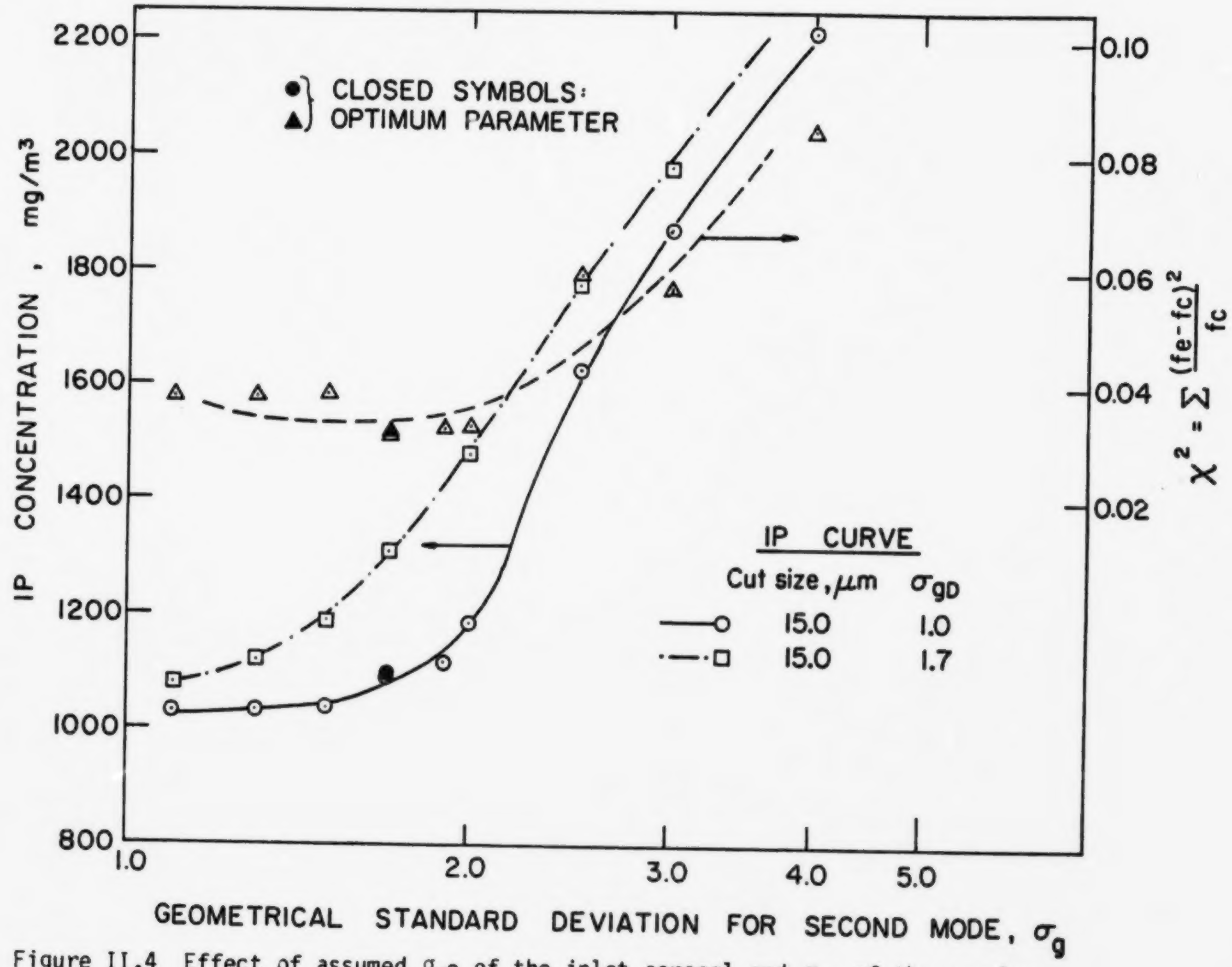

Figure II.4 Effect of assumed σ_{g2} of the inlet aerosol and σ_{gD} of the sampler curve on the IP concentration estimate.

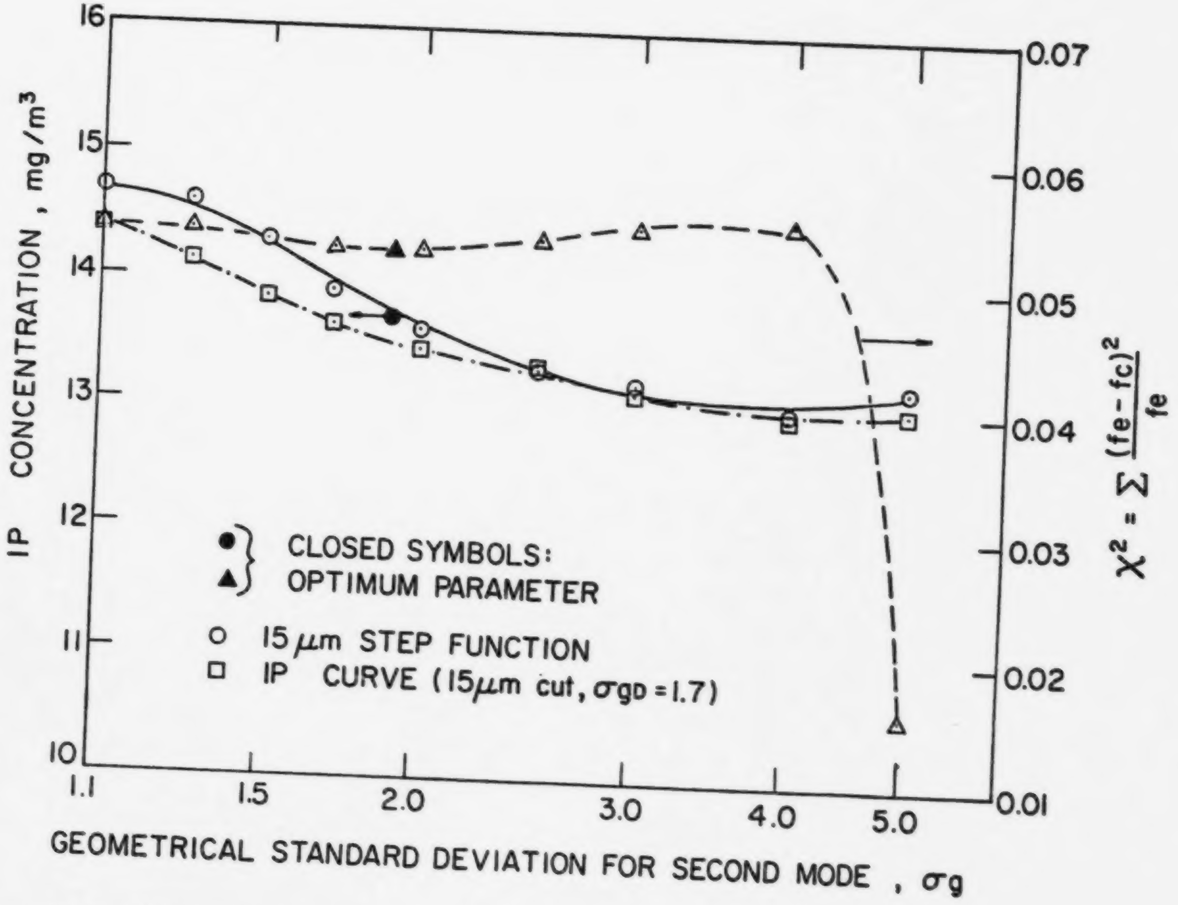

Figure II.5 Effect of assumed σ_{g2} of the outlet aerosol and σ_{gD} of the sampler curve on the IP concentration estimate.

The IP concentration for a sampler curve with D_{50} = 15.0 μm and σ_{gD} = 1.7 changes by about 40% in the same range of σ_{g2}. These curves indicate that for a sampler with a narrow cut-off characteristic and assuming that the σ_{g2} of the inlet aerosol size distribution is below 2.0, the IP concentration can be determined to an accuracy of 20% for the sample data used. The closed symbols in the figure indicate optimum parameters obtained by setting all six modal parameters as variables during fitting procedures. The parameters are seen to locate very close to the minimum χ^2 value. The geometric standard deviation for the second mode was found to be 1.7, giving an M-15 value of 1100 mg/m^3.

For the outlet data, Figure II.5 shows that the M-15 and IP concentration vary by less than 15% over a wide range of σ_{g2}, from 1.1 to 5.0. Therefore, the IP concentration can be estimated with good accuracy for the sample outlet data.

b. Variation of MMD_2

Figures II.6 and II.7 give the variation of IP concentration as a function of the mass median diameter of the second mode, MMD_2, for the inlet data and the outlet data, respectively. The IP concentration is obtained by keeping the MMD_2 constant during the minimization process. The χ^2 of the fitted distribution is also plotted in the same figure.

Figure II.6 shows that, for the inlet data, the IP concentration is a strong function of the MMD_2. This figure, together with Figure II.4, indicates that additional information concerning the second mode will be needed in order to obtain a good estimated IP concentration for the inlet data.

For the outlet data, Figure II.7 shows that the M-15 and IP concentration vary by less than 20% over a wide range of MMD_2, from 2.0 to 40.0 μm. This figure, together with Figure II.5, indicates that for the outlet data, the IP concentration can be estimated with good accuracy.

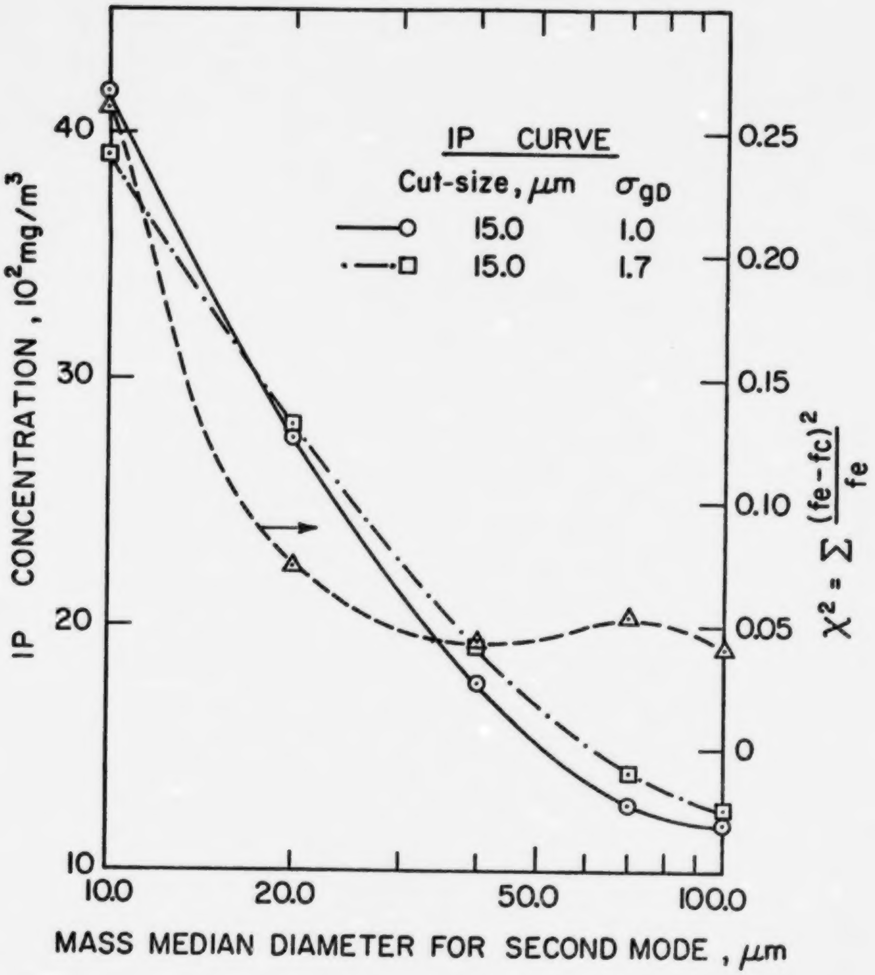

Figure II.6 Effect of assumed MMD_2 of the inlet aerosol and σ_{gD} of the sampler curve on the IP concentration estimate.

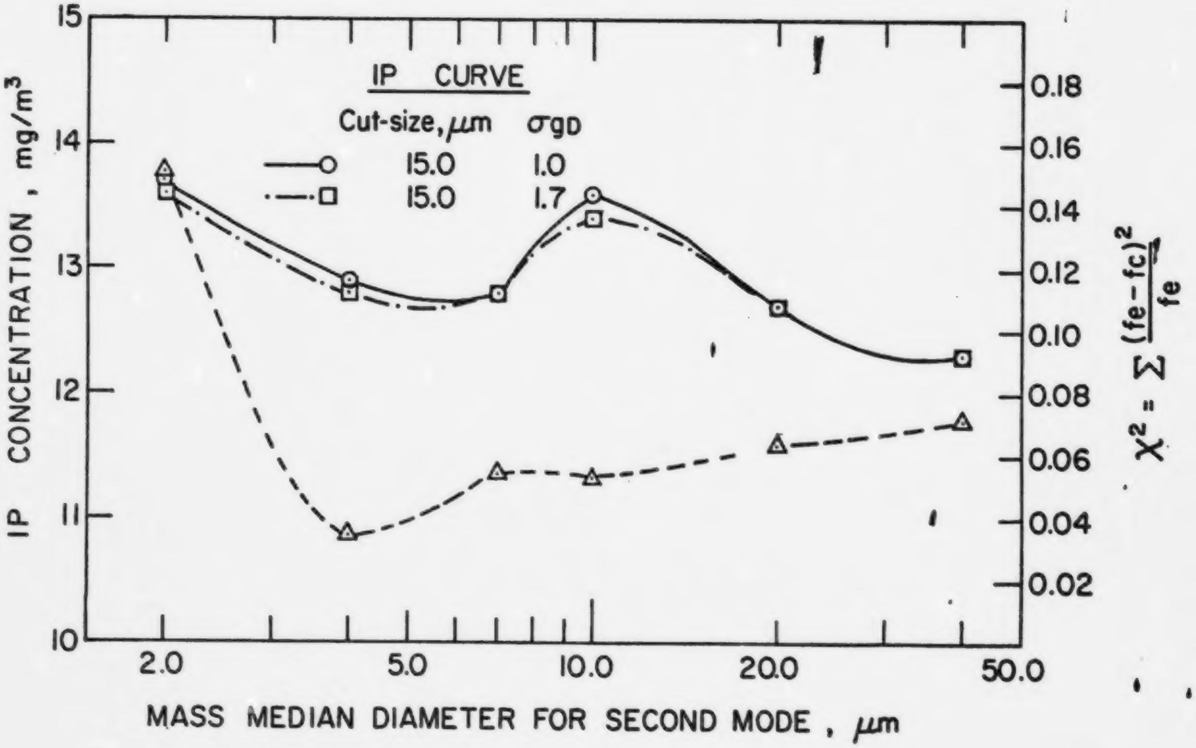

Figure II.7 Effect of assumed MMD_2 of the outlet aerosol and σ_{gD} of the sampler curve on the IP concentration estimate.

2. Effect of IP sampler curve on IP concentration

a. Variation of σ_{gD}

Figures II.4 through II.7 give the IP concentration for two IP sampler curves: (1) D_{50} = 15.0 μm and σ_{gD} = 1.0, or M-15, and (2) D_{50} = 15.0 μm and σ_{gD} = 1.7. As seen in the figures, the IP concentration is not strongly affected by the σ_{gD}. The IP concentration varies by less than 5% for the outlet data and by less than 15% for the inlet data.

b. Variation of D_{50}

The variation of IP concentration as a function of cut size of IP sampler curve is shown in Figure II.8. The ordinate gives the ratio of IP concentration at various cut sizes to the concentration at 15 μm cut size. As expected, the ratio depends strongly on the cut size. Such a curve is useful in setting the permitted variability in the cut size parameter.

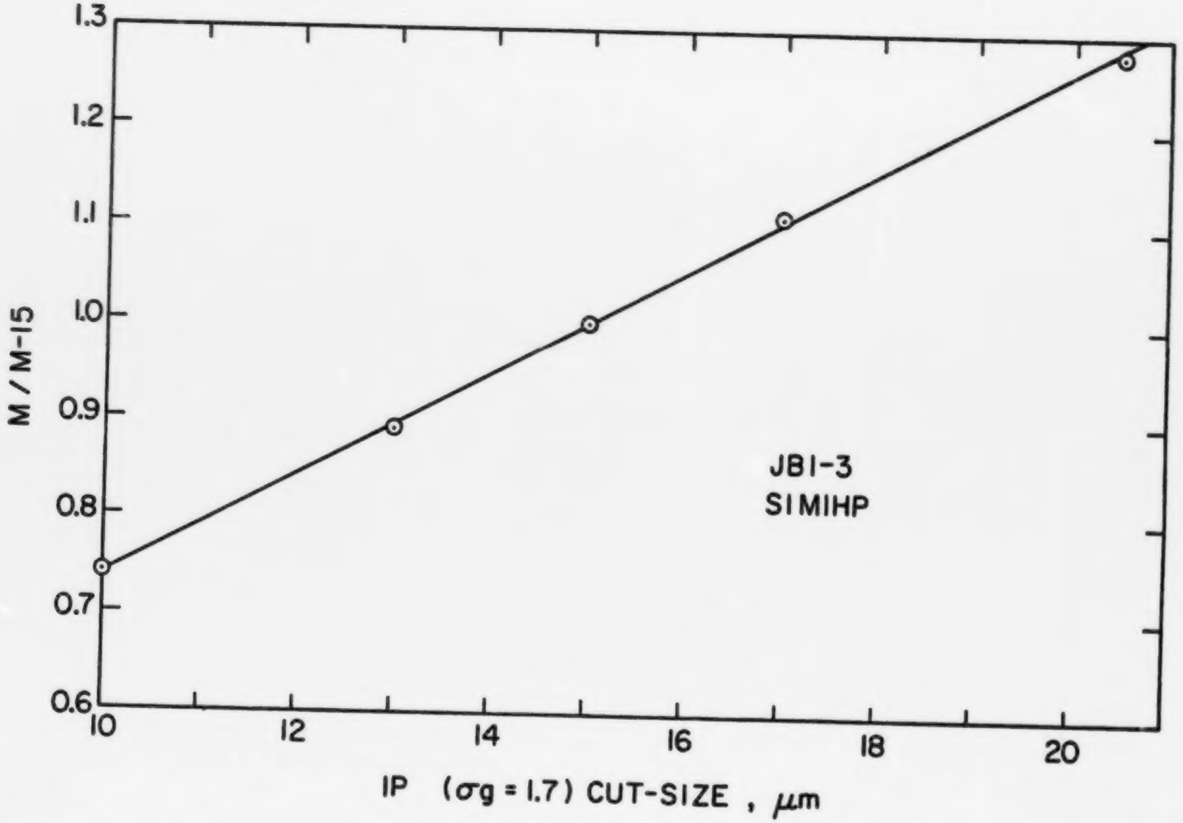

Figure II.8 Effect of IP sampler curve cut size on the estimated IP concentration for the inlet data.

III. RESULTS AND DISCUSSION

Three pairs of SRI impactor data have been selected for the analysis. The data were taken at the inlets of control devices for two pulverized coal boilers and a copper smelter. For the pulverized coal boilers, each pair consists of the same set of impactor data except calculated with two different assumed particle densities. The density difference results in a change in the impactor cut size, giving a somewhat different particle size distribution. The analysis of the data therefore provides some information on the effect of the assumed particle density on the estimated IP concentration.

The analysis here follows the formats of Section II.C and II.D, which include the fitted modal parameters and the sensitivity of the IP concentration to the variation of the coarse particle size and deviation, as well as the performance curve of the IP sampler.

A. Coal-Fired Boiler, Hot Side ESP Inlet (NGP-13)

The results of the modal fitting and the IP concentration calculation are shown in Figures III.1 through III.4 for an assumed particle density of 1.0 g/cm^3, and in Figures III.5 through III.8 for an assumed particle density of 2.41 g/cm^3.

The important findings to be noted are:

1. The impactor data can be fitted satisfactorily with a bimodal log-normal distribution.
2. Because the mass concentration of the second mode is not substantially higher than that of the first mode, the estimated IP concentration consequently is not very sensitive to the variation of the geometrical standard deviation and the mass median diameter of the second mode, the coarse particle mode.

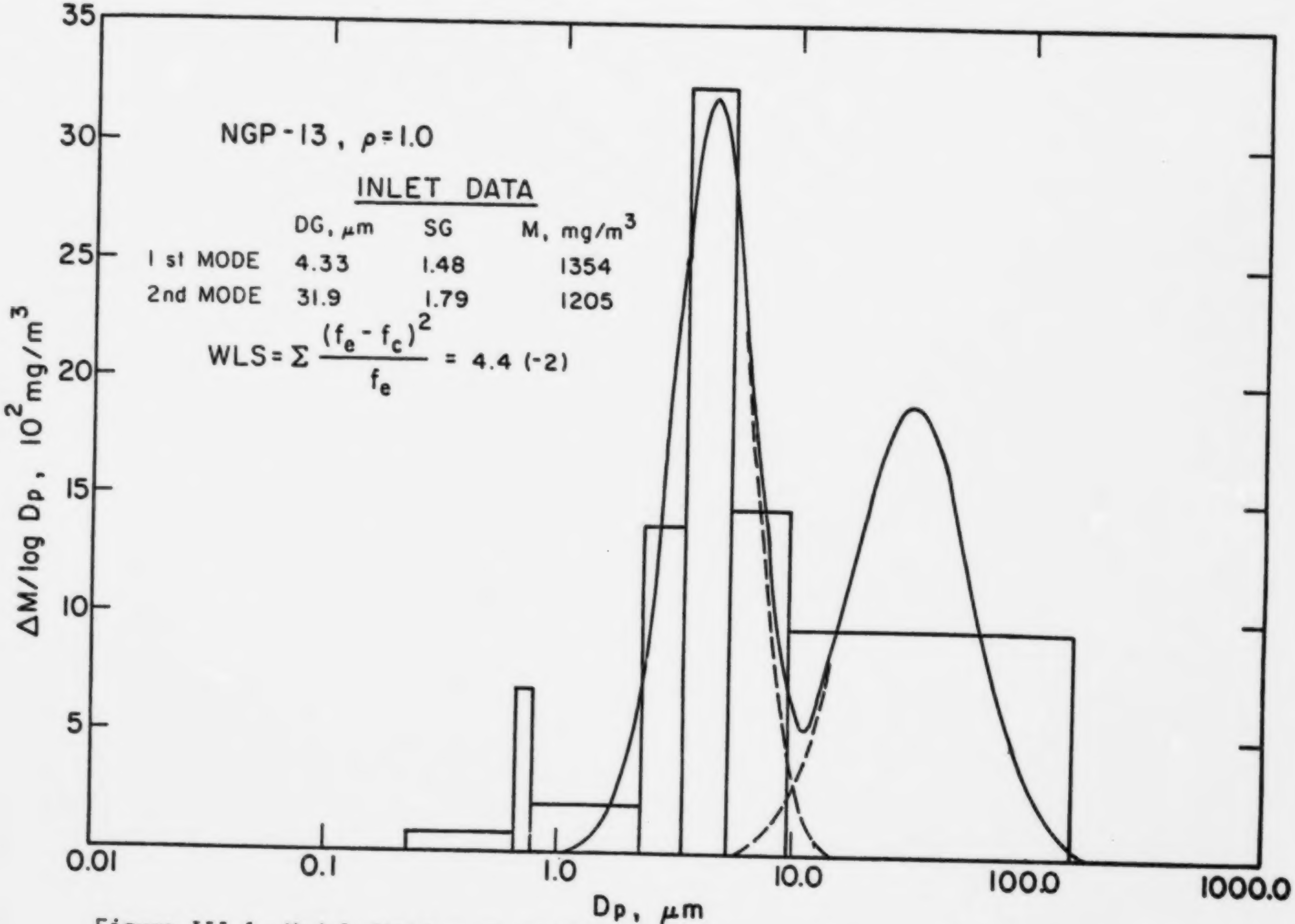

Figure III.1 Modal fitting of impactor data from coal-fired boiler, hot side ESP inlet (NGP-13, $\rho = 1.0$).

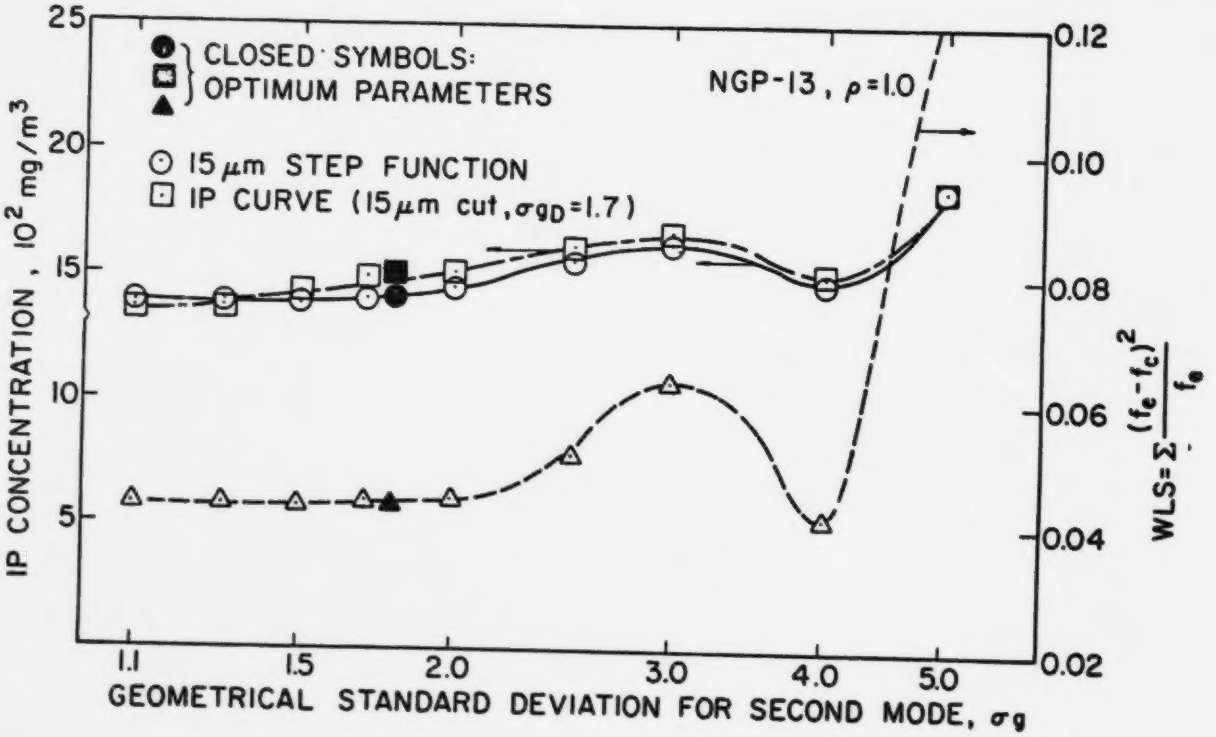

Figure III.2 Effect of assumed aerosol σ_{g2} and sampler σ_{gD} on the IP concentration estimate (NGP-13, ρ = 1.0).

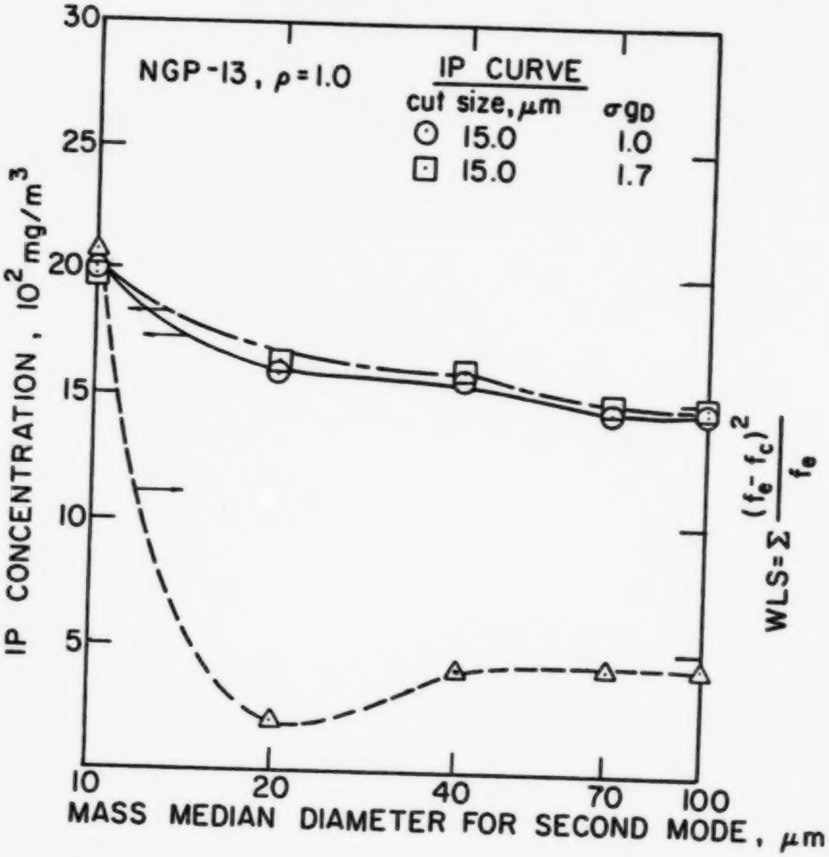

Figure III.3 Effect of assumed aerosol MMD_2 and sampler σ_{gD} on the IP concentration estimate (NGP-13, ρ = 1.0).

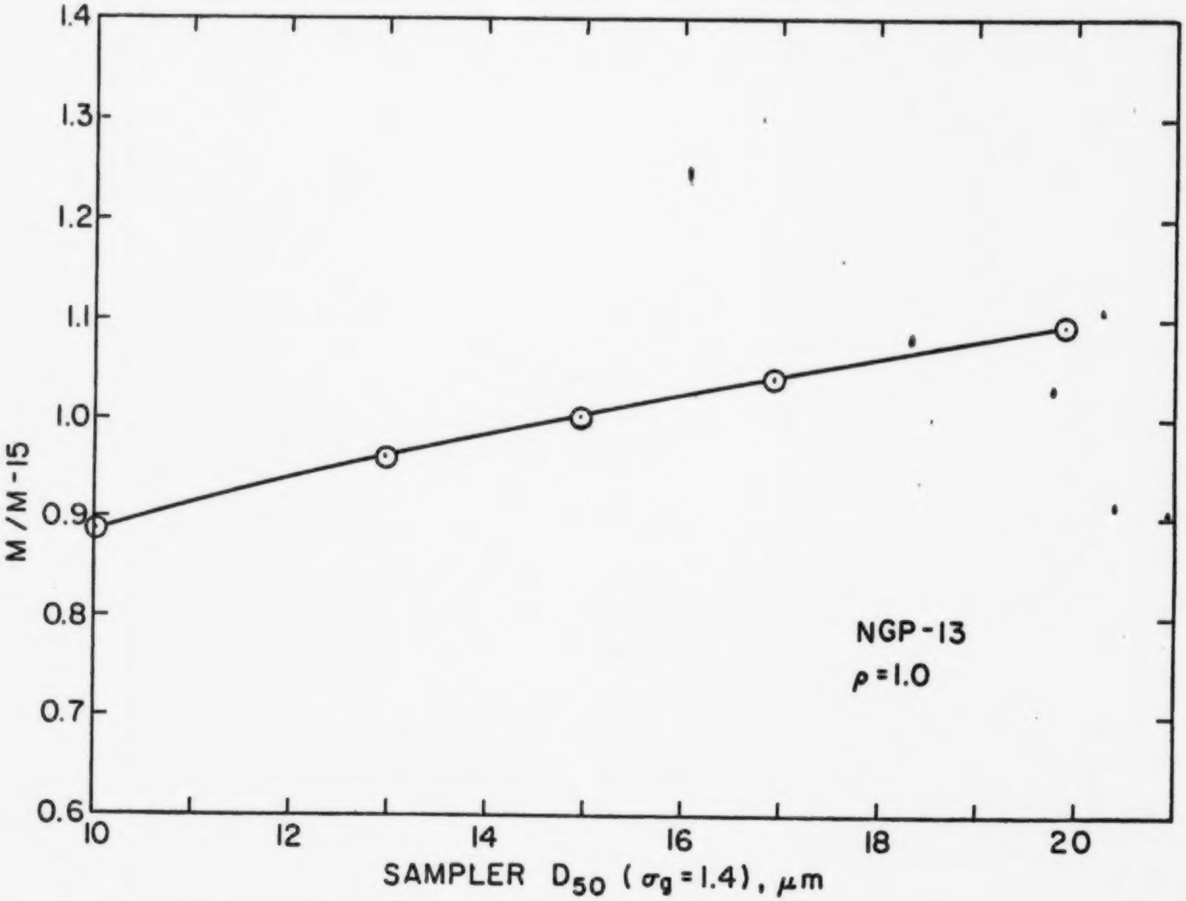

Figure III.4 Effect of sampler D_{50} on the IP concentration estimate (NGP-13, ρ = 1.0).

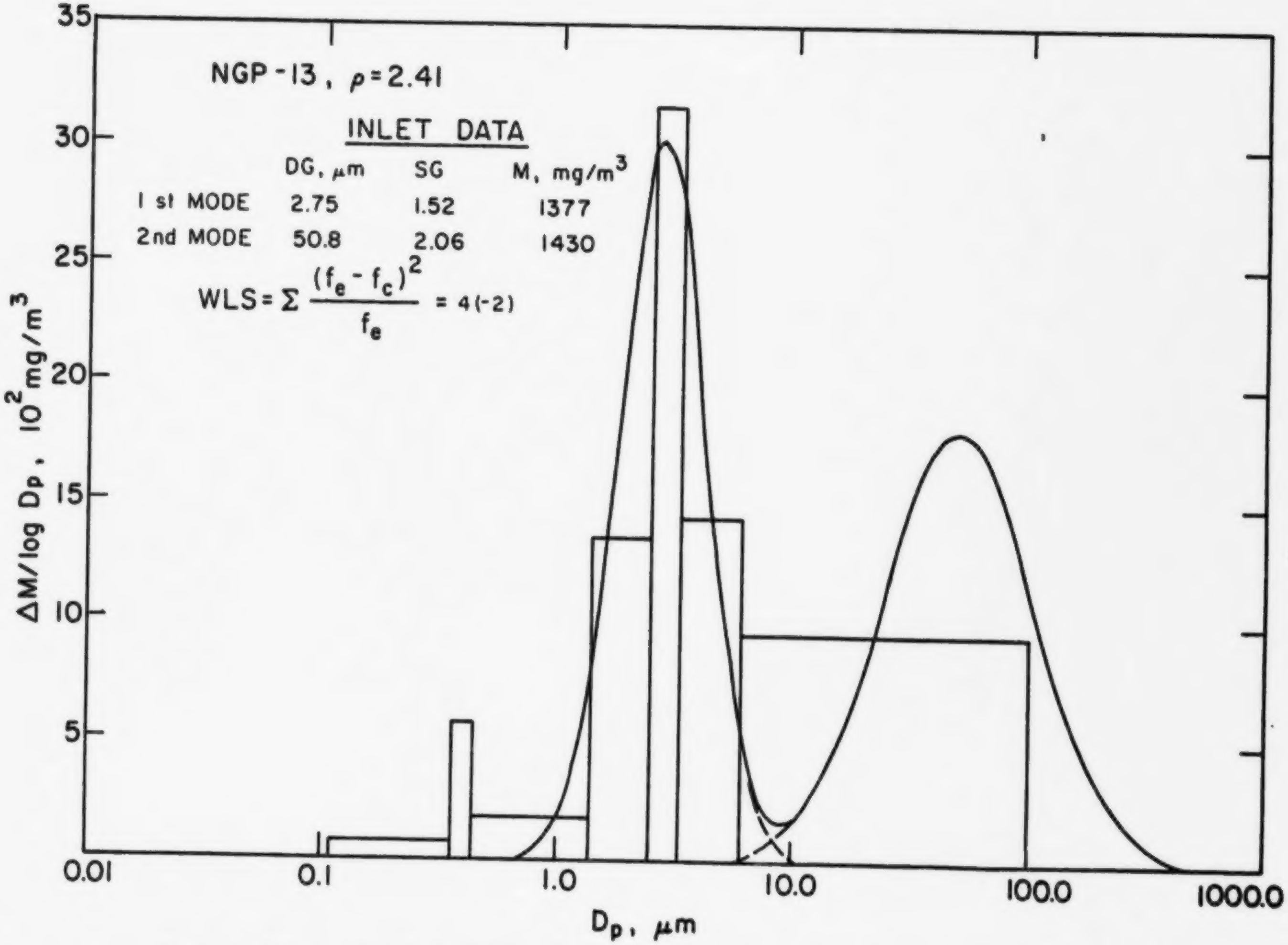

Figure III.5 Modal fitting of impactor data from coal-fired boiler, hot side ESP inlet (NGP-13, $\rho = 2.41$).

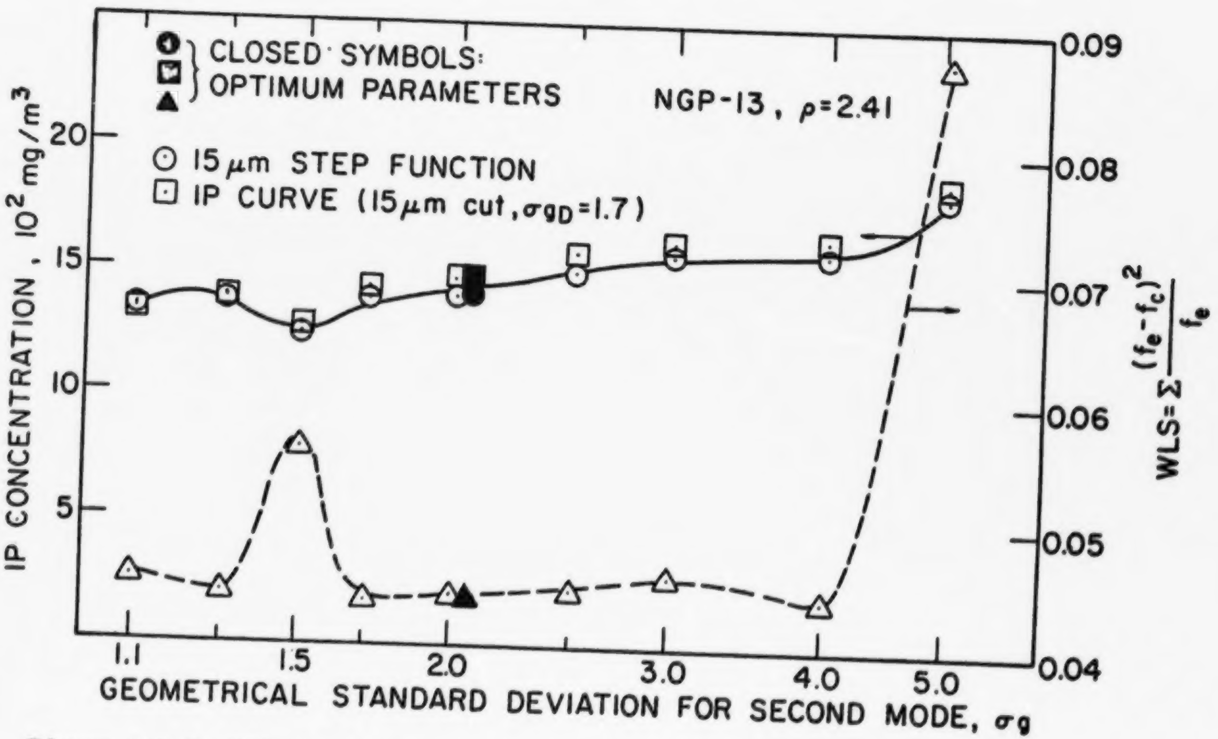

Figure III.6 Effect of assumed aerosol σ_{g2} and sampler σ_{gD} on the IP concentration estimate (NGP-13, ρ = 2.41).

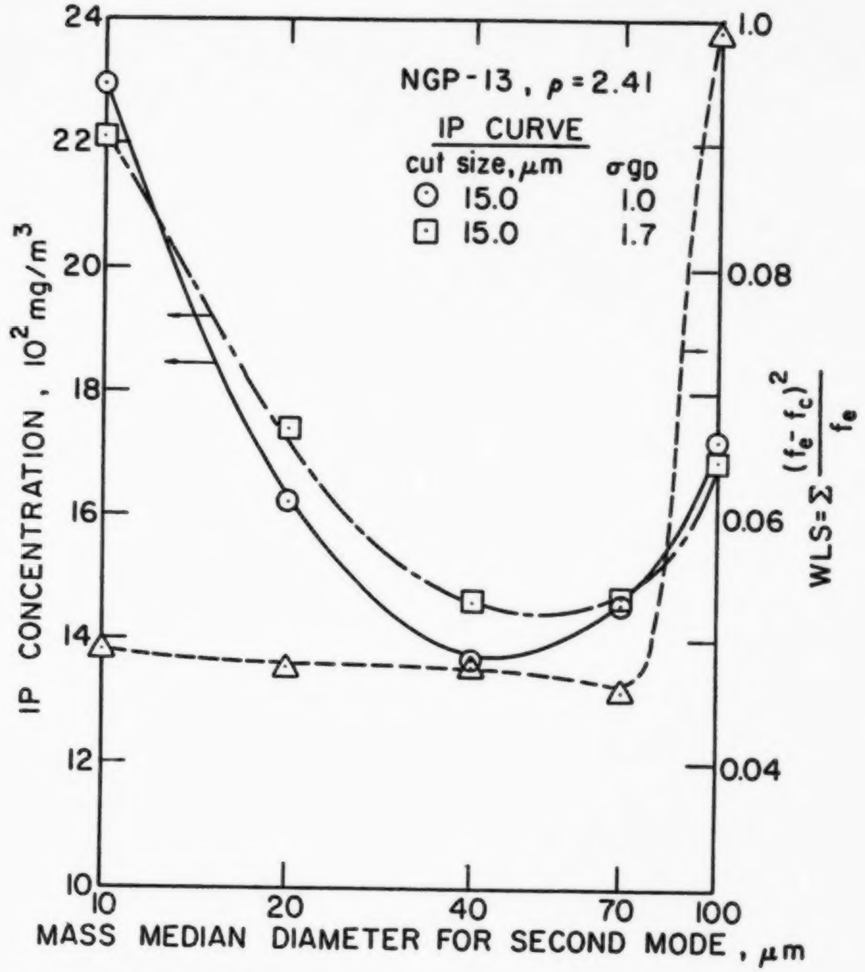

Figure III.7 Effect of assumed aerosol MMD_2 and sampler σ_{gD} on the IP concentration estimate (NGP-13, ρ = 2.41).

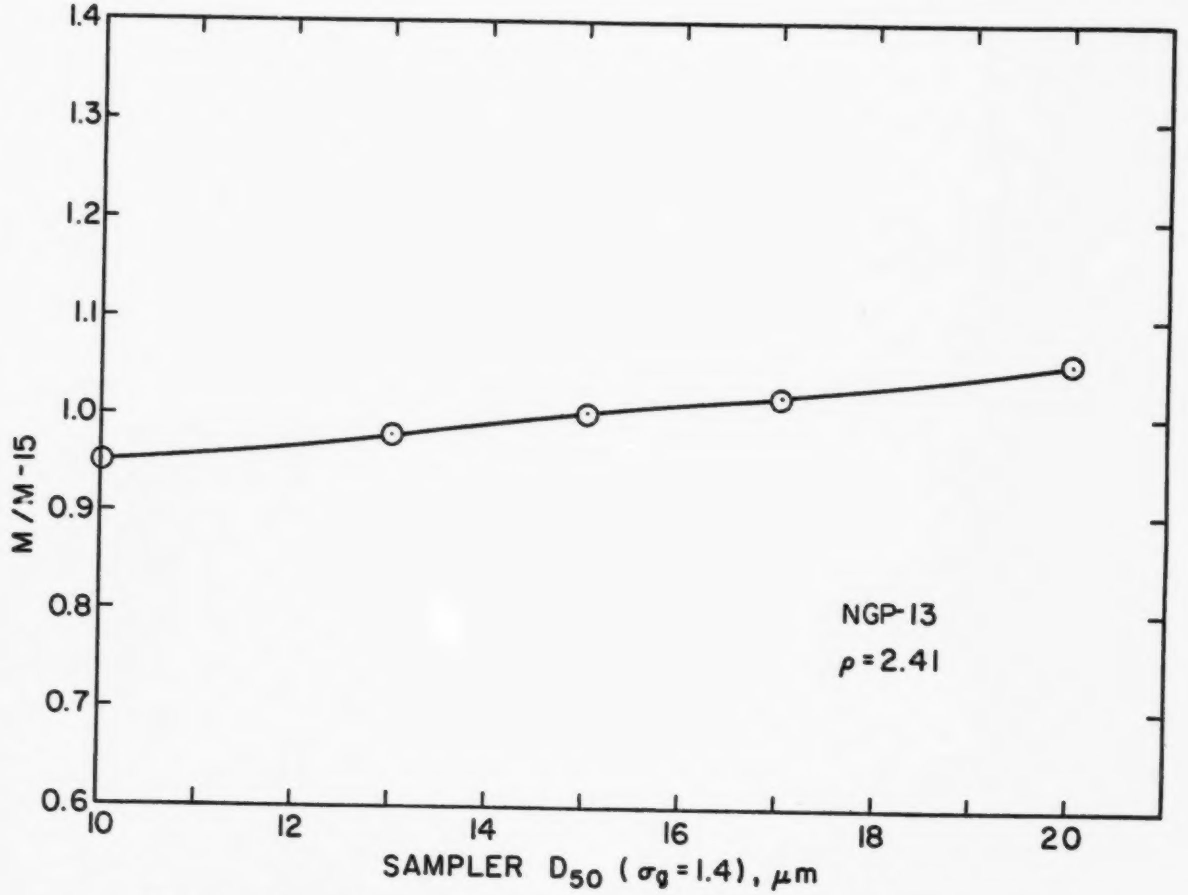

Figure III.8 Effect of sampler D_{50} on the IP concentration estimate (NGP-13, ρ = 2.41).

3. The estimated IP concentration is not strongly affected by the slope of the sampler collection curve, σ_{gD}. It varies by less than 7% as the σ_{gD} varies from 1.0 for a perfect sampler to 1.7, the worst allowed by the IP performance curve.
4. More variation in the estimated IP concentration is shown as the cut size of the IP sampler, D_{50}, varies. However, within the specified limits of the performance curve, 13 to 17 μm, there is only a difference of ±5% in the IP concentration.
5. The particle size distribution changes when a different assumed particle density for the impactor data is used. However, the density change does not appear to affect greatly the estimated IP concentration for these data. The IP concentrations shown in Figures III.2, III.3, III.6, and III.7 all have a value of about 1500 mg/m^3 in the vicinity of the minimum WLS value.

B. Coal-Fired Boiler, Cold Side ESP Inlet (JBI-13)

The results of the modal fitting and the IP concentration calculation are shown in Figures III.9 through III.12 for an assumed particle density of 1.0 g/cm^3, and in Figures III.13 through III.16 for an assumed particle density of 2.34 g/cm^3. The coarse particle concentration is nearly ten times higher than the fine particle concentration, in contrast to the data above where the two concentrations are about equal.

The important findings to be noted are:

1. The impactor data can be fitted satisfactorily with a bimodal log-normal distribution.
2. The estimated IP concentration is sensitive to the variation of the geometrical standard deviation and the mass median diameter

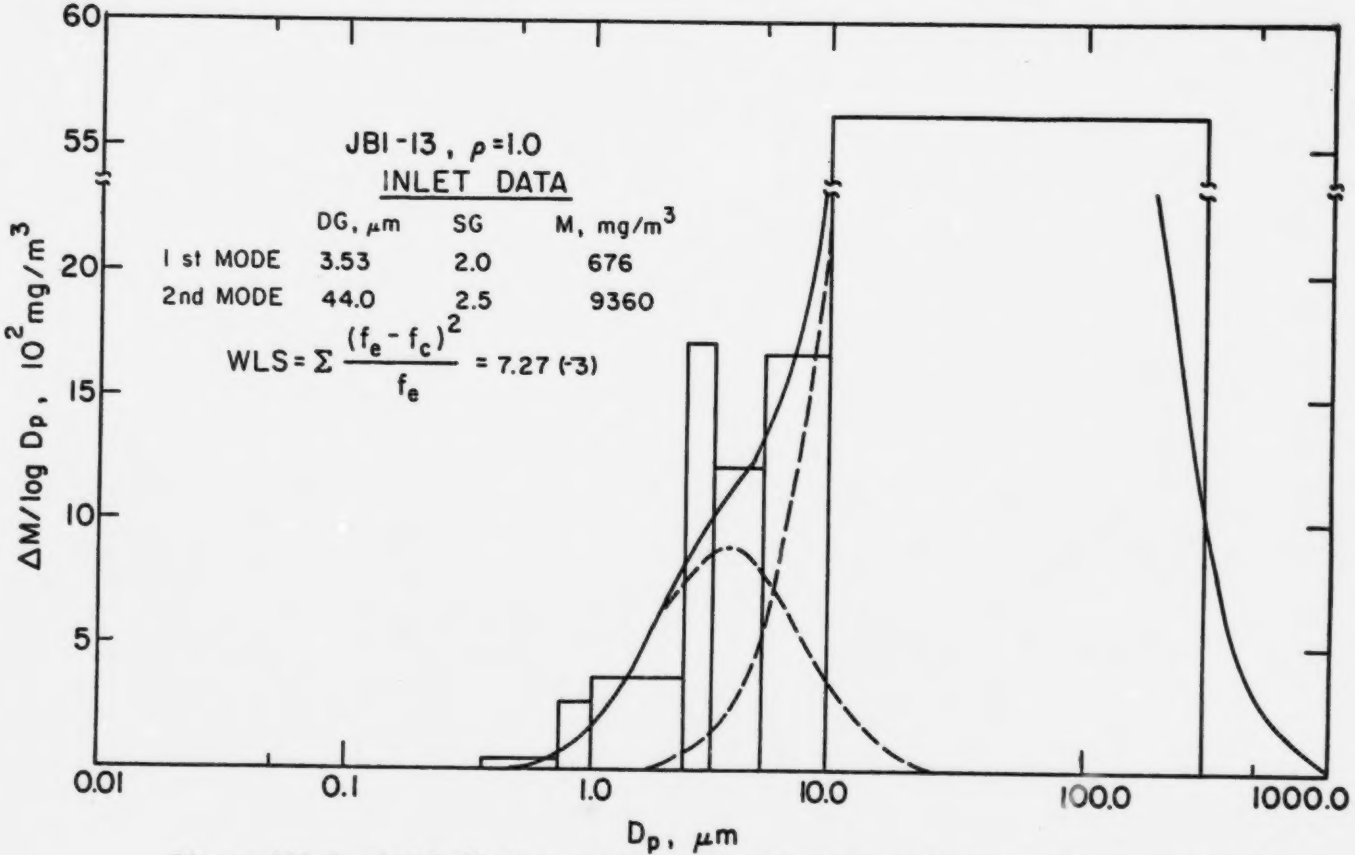

Figure III.9 Modal fitting of impactor data from coal-fired boiler, cold side ESP inlet (JBI-13, $\rho = 1.0$).

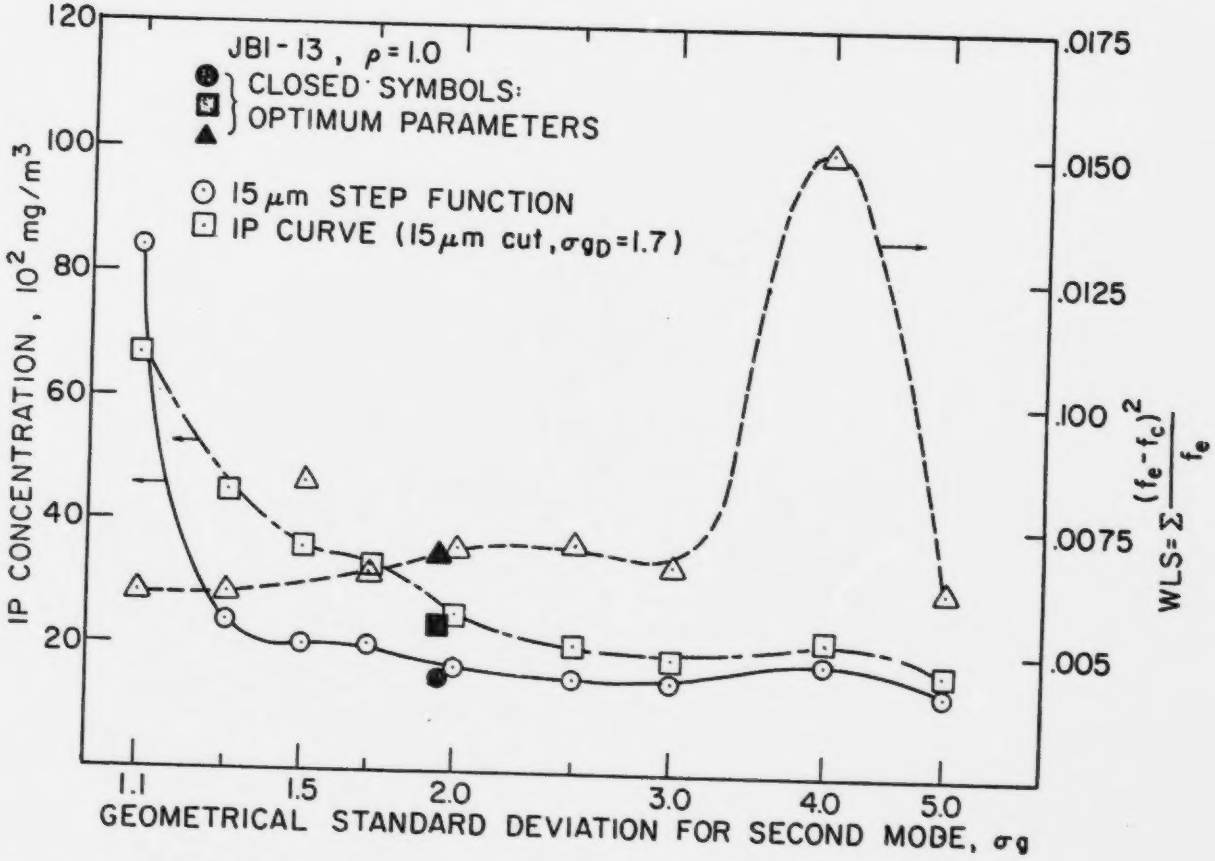

Figure III.10 Effect of assumed aerosol σ_{g2} and sampler σ_{gD} on the IP concentration estimate (JBI-13, ρ = 1.0).

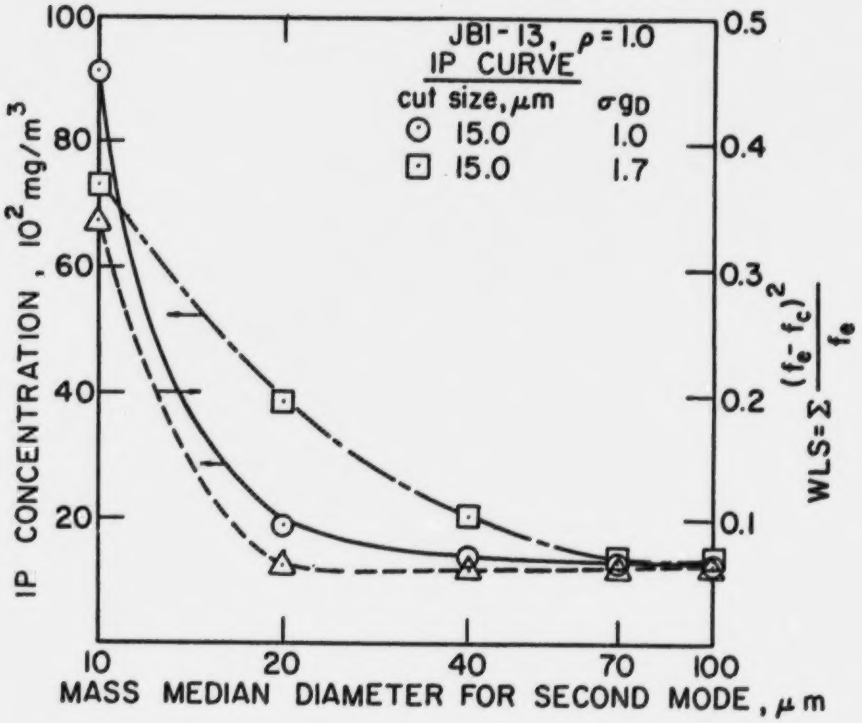

Figure III.11 Effect of assumed aerosol MMD_2 and sampler σ_{gD} on the IP concentration estimate (JBI-13, ρ = 1.0).

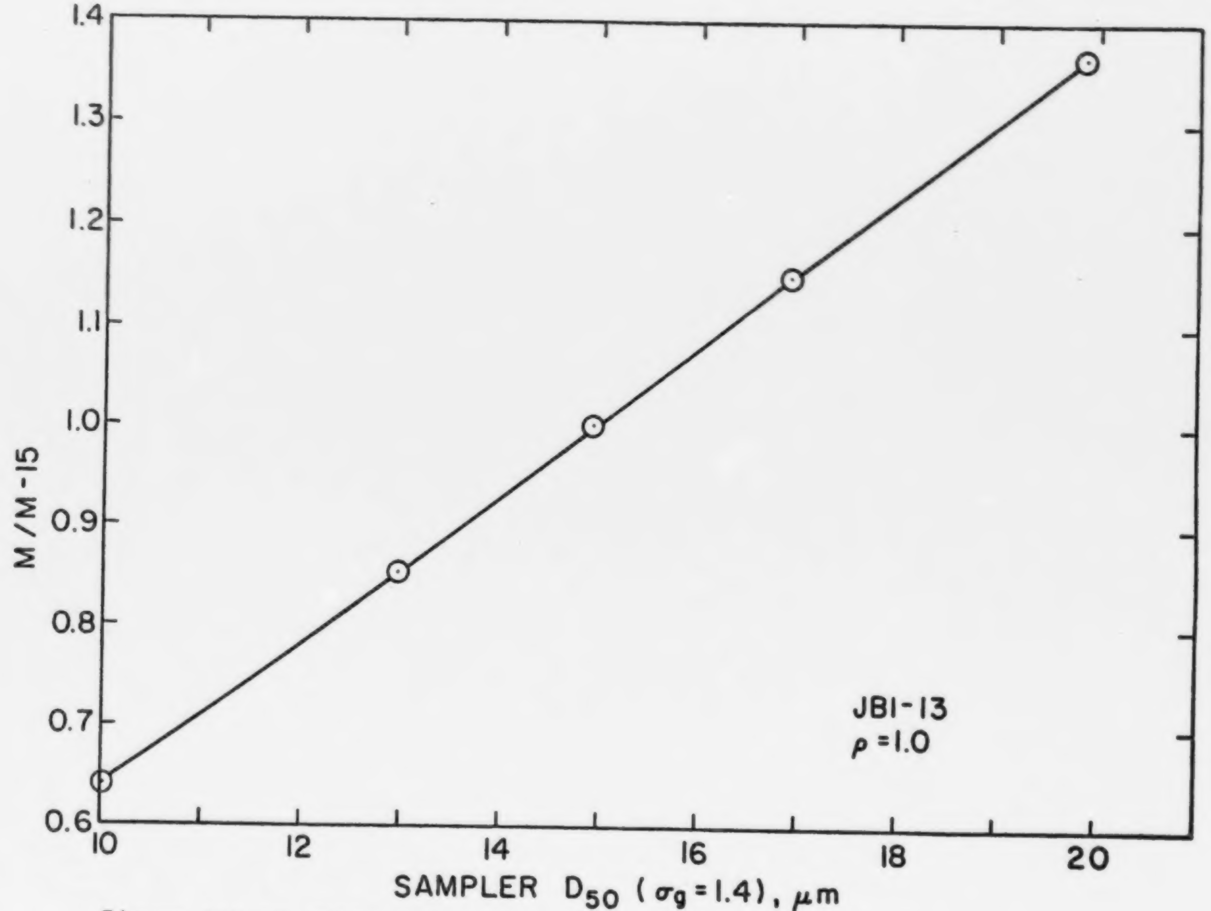

Figure III.12 Effect of sampler D_{50} on the IP concentration estimate (JBI-13, ρ = 1.0).

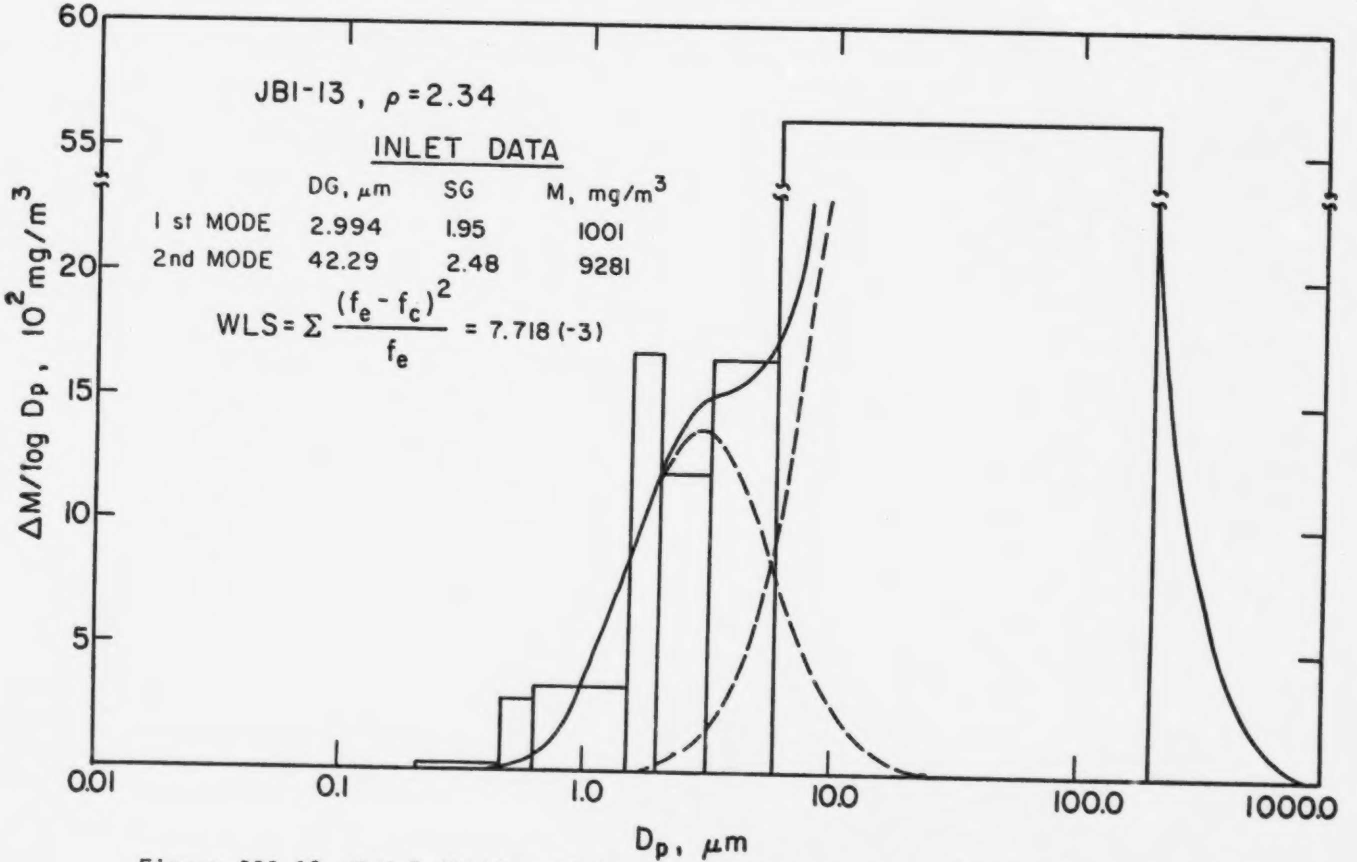

Figure III.13 Modal fitting of impactor data from coal-fired boiler, cold side ESP inlet (JBI-13, ρ = 2.34).

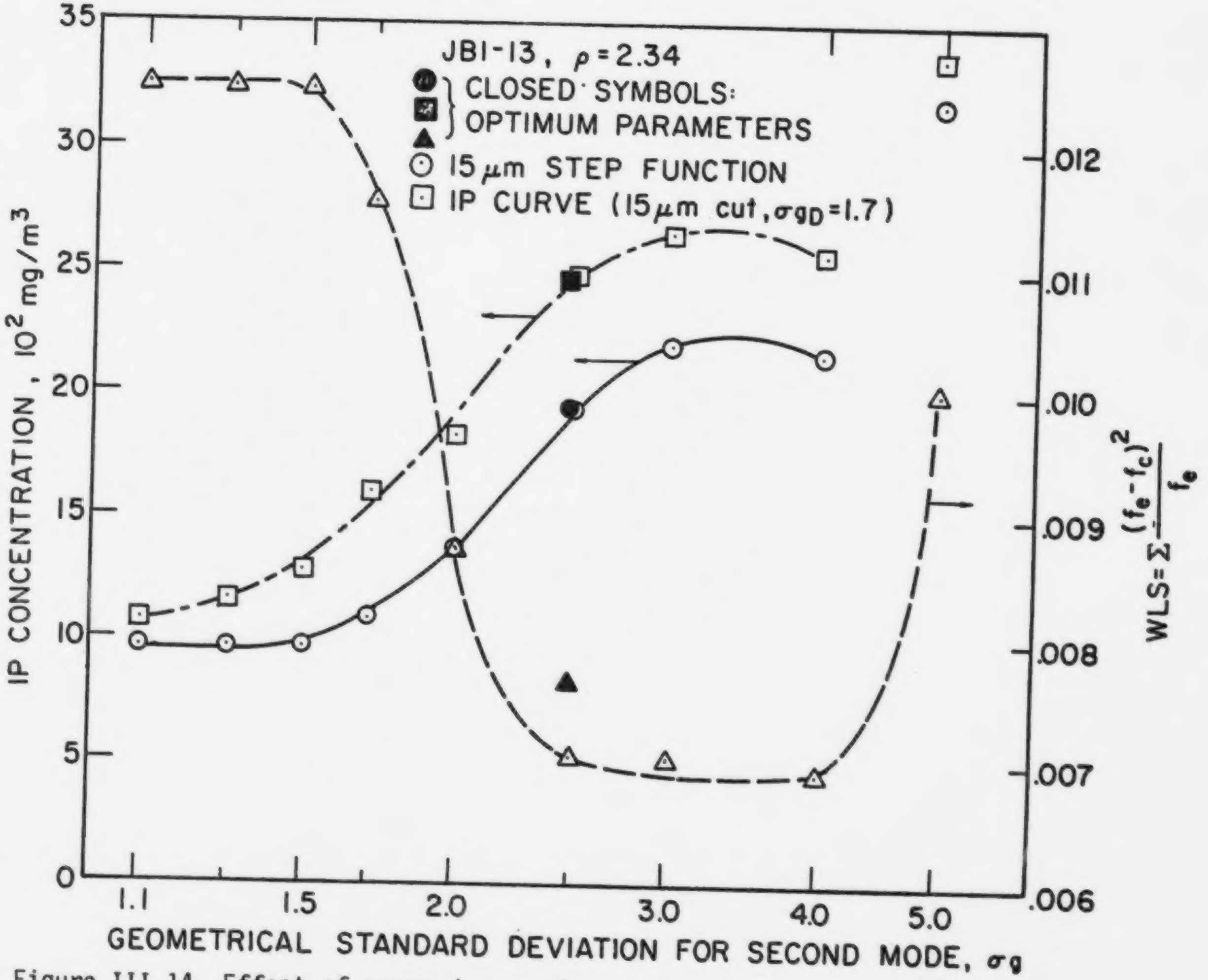

Figure III.14 Effect of assumed aerosol σ_{g2} and sampler σ_{gD} on the IP concentration estimate (JBI-13, ρ = 2.34).

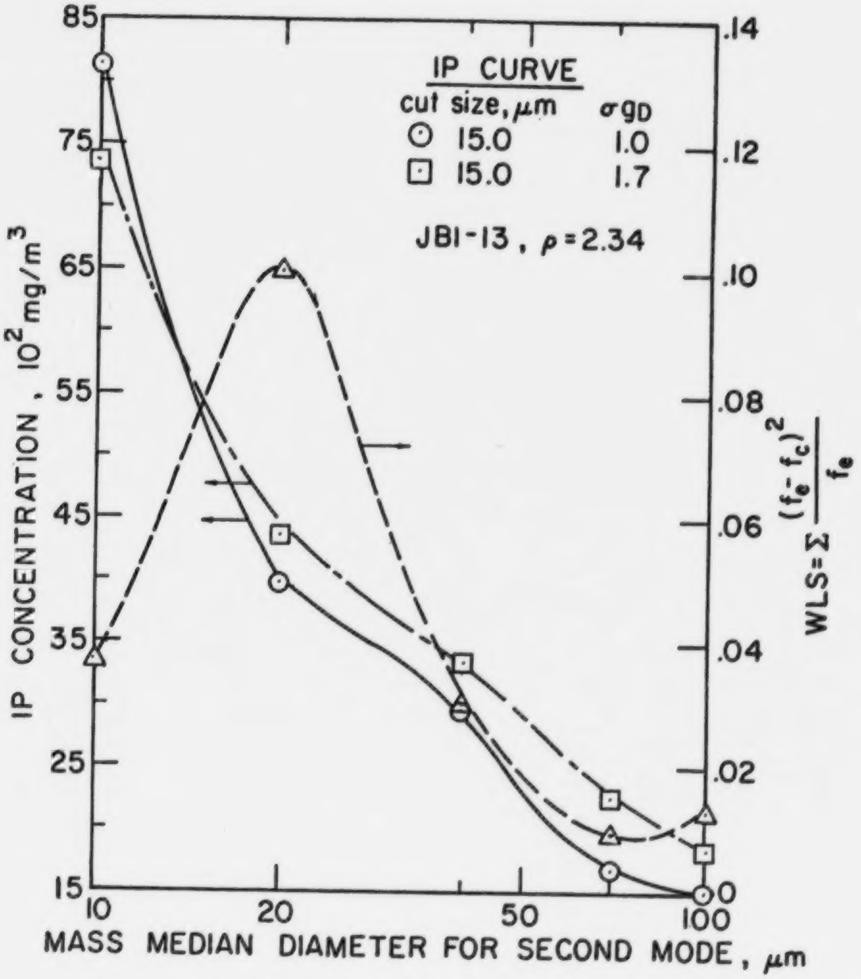

Figure III.15 Effect of assumed aerosol MMD_2 and sampler σ_{gD} on the IP concentration estimate (JBI-13, ρ = 2.34).

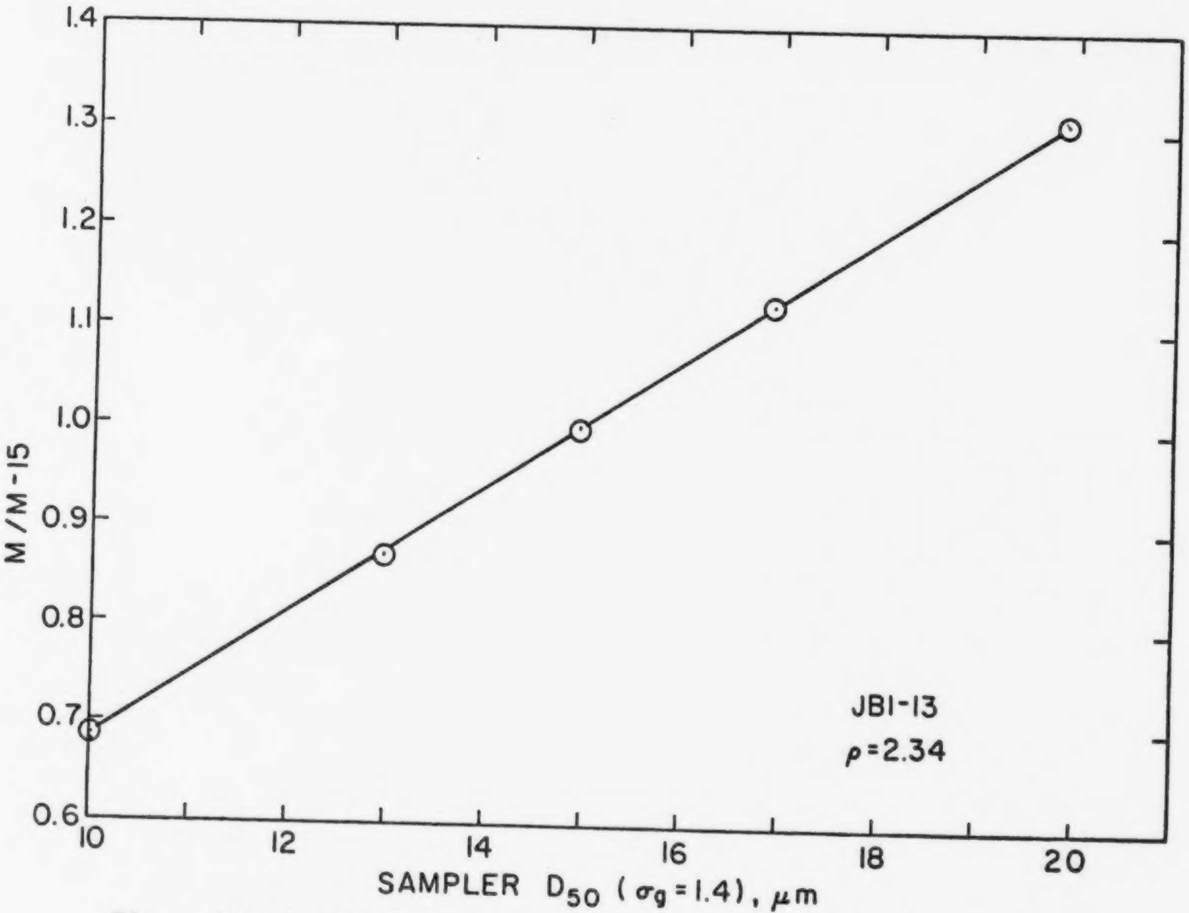

Figure III.16 Effect of sampler D_{50} on the IP concentration estimate (JBI-13, ρ = 2.34).

2. (cont.)

   of the coarse particle mode. A factor of three difference in the IP concentration is observed as the σ_{g2} and the MMD_2 vary from 1.1 to 5.0 and from 10 to 100 μm, respectively. This is due to the much higher concentration for the coarse particle mode compared to the fine particle mode. The results suggest that, for this aerosol, additional information is needed for the coarse particle mode in order to accurately determine the IP concentration.

3. The estimated IP concentration is affected by the slope of the sampler collection curve. However, in the vicinity of the minimum WLS value, the difference in the IP concentration for a sampler with σ_{gD} of 1.0 and 1.7 is not too great, the maximum being about 20%.

4. As the cut size of the IP sampler varies, a larger variation is found in the estimated IP concentration. Within the specified limits of the performance curve of 13 to 17 μm, the estimated IP concentration changes by about ±15%.

5. Although the particle size distribution changes with different assumed particle densities, the change does not appear to affect greatly the estimated IP concentration. In the vicinity of the minimum WLS value, the IP concentration in Figures III.10, III.11, III.14, and III.15 all have a value of about 2000 mg/m^3.

C. Copper Smelter, Hot Side ESP Inlet (AJOI-3, AJOI-5)

Two sets of data have been selected for copper smelter emissions. AJOI-3 represents an average mass loading run, and AJOI-5 is the lowest mass loading run. An assumed particle density of 3.58 g/cm^3 is used for both sets of data. The results of the modal fitting and IP concentration calculation are shown in Figures III.17 through III.20 for Run No. AJOI-3 and in Figures III.21 through III.24 for Run No. AJOI-5.

The important findings to be noted are:

1. The impactor data can be fitted reasonably well with a bimodal log-normal distribution.
2. The estimated IP concentration is sensitive to the variation of the geometrical standard deviation and the mass median diameter of the coarse particle mode for the high mass loading run, AJOI-3, and less sensitive for the low mass loading run, AJOI-5.
3. The estimated IP concentration is not strongly affected by the slope of the sampler collection curve, σ_{gD}, the maximum concentration difference for a σ_{gD} range of 1.0-1.7 being about 10%.
4. A larger variation in IP concentration is found as the cut size of the IP sampler varies. However, within the specified limits of the performance curve of 13 to 17 μm, the estimated IP concentration changes by less than ±10%.

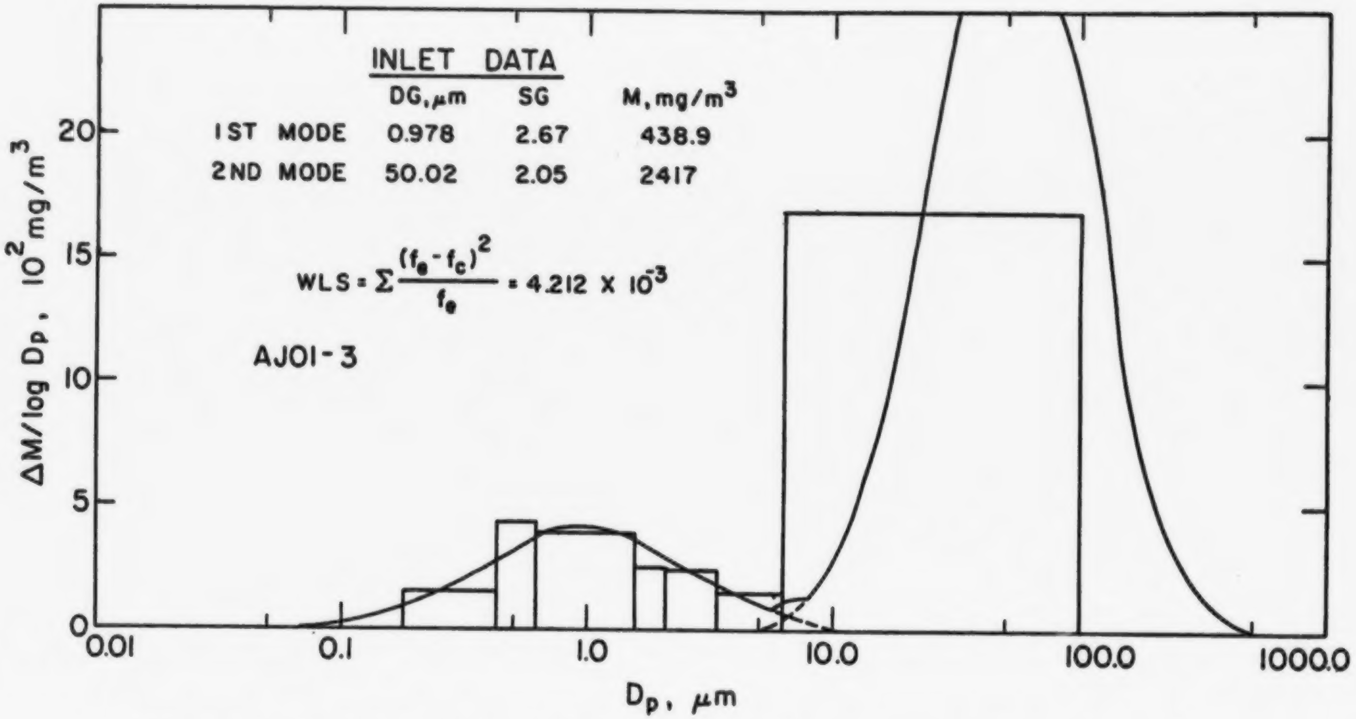

Figure III.17 Modal fitting of impactor data from copper smelter, hot side ESP inlet (AJOI-3).

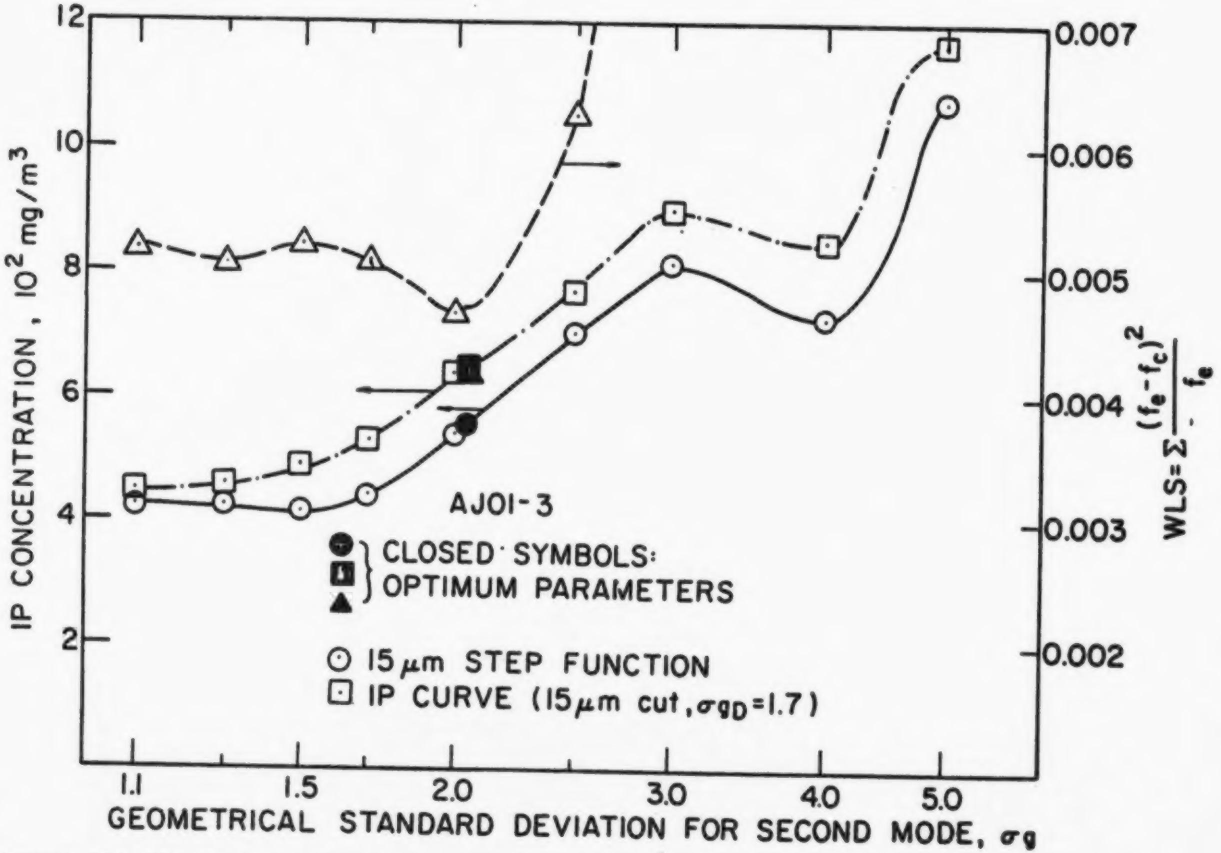

Figure III.18 Effect of assumed aerosol σ_{g2} and sampler σ_{gD} on the IP concentration estimate (AJOI-3).

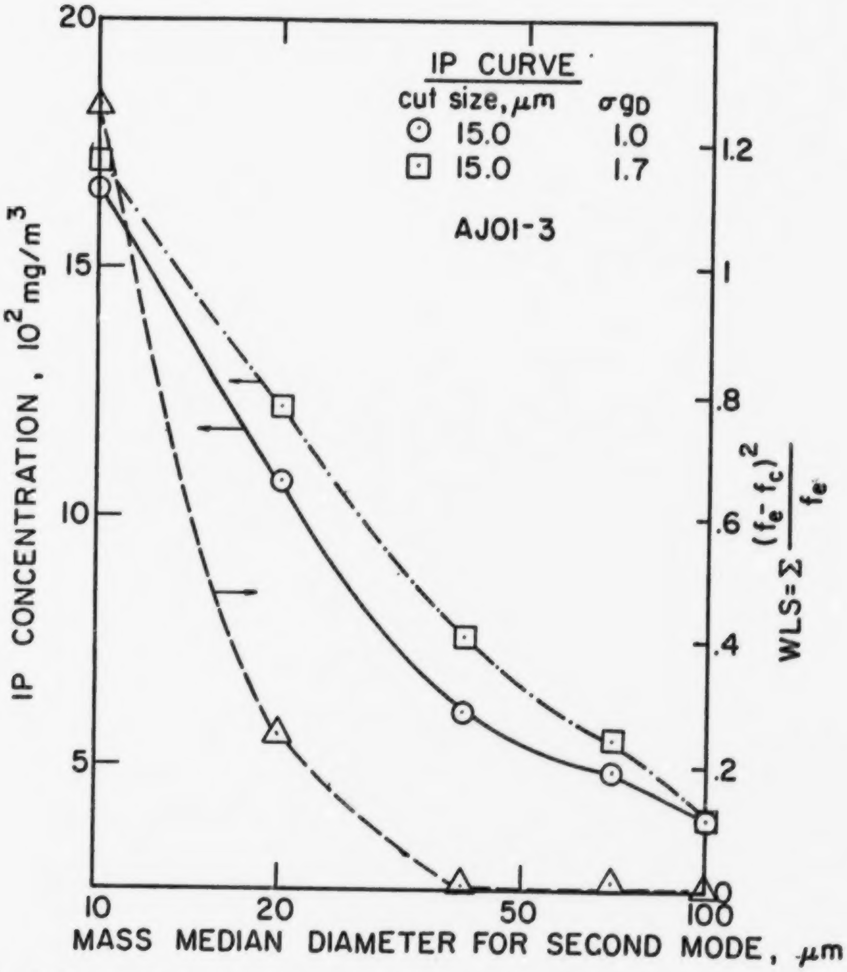

Figure III.19 Effect of assumed aerosol MMD_2 and sampler σ_{gD} on the IP concentration estimate (AJ0I-3).

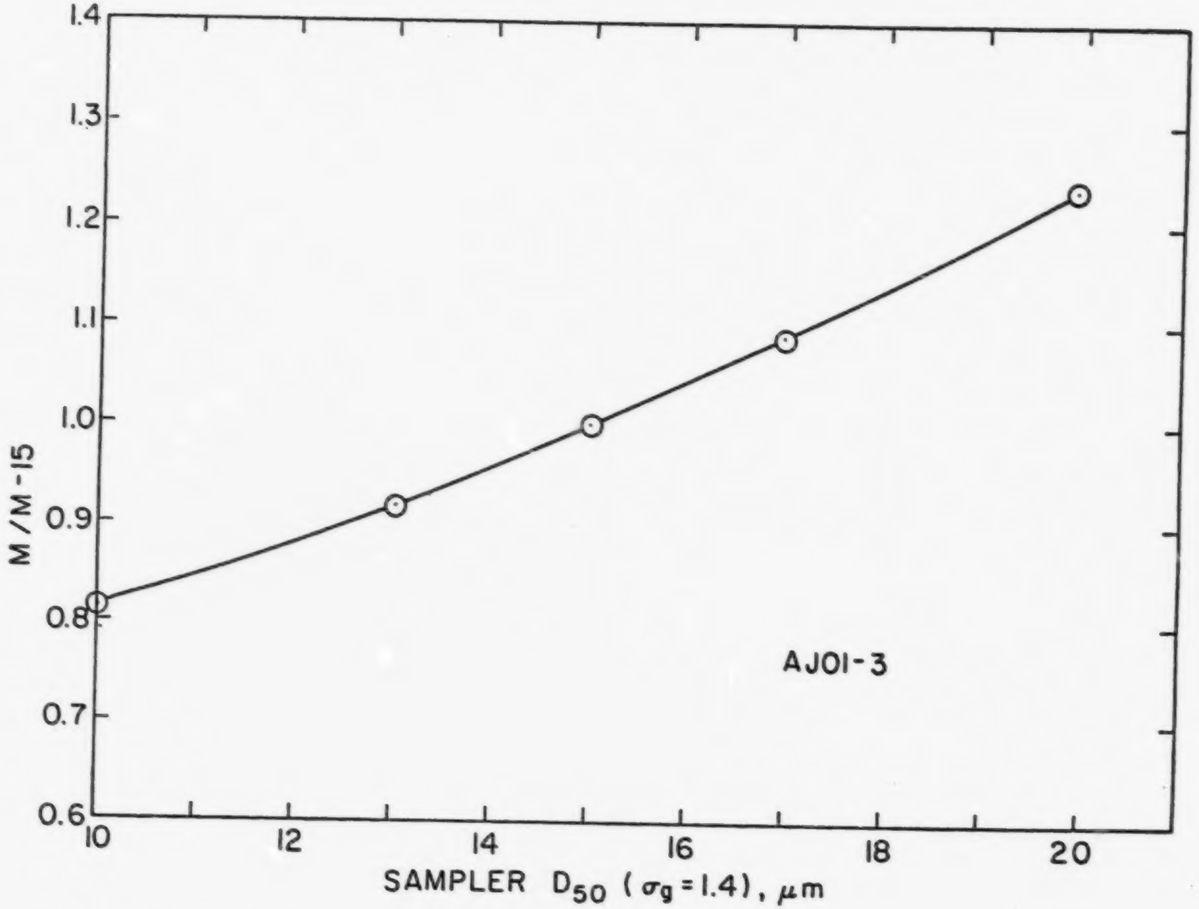

Figure III.20 Effect of sampler D_{50} on the IP concentration estimate (AJOI-3).

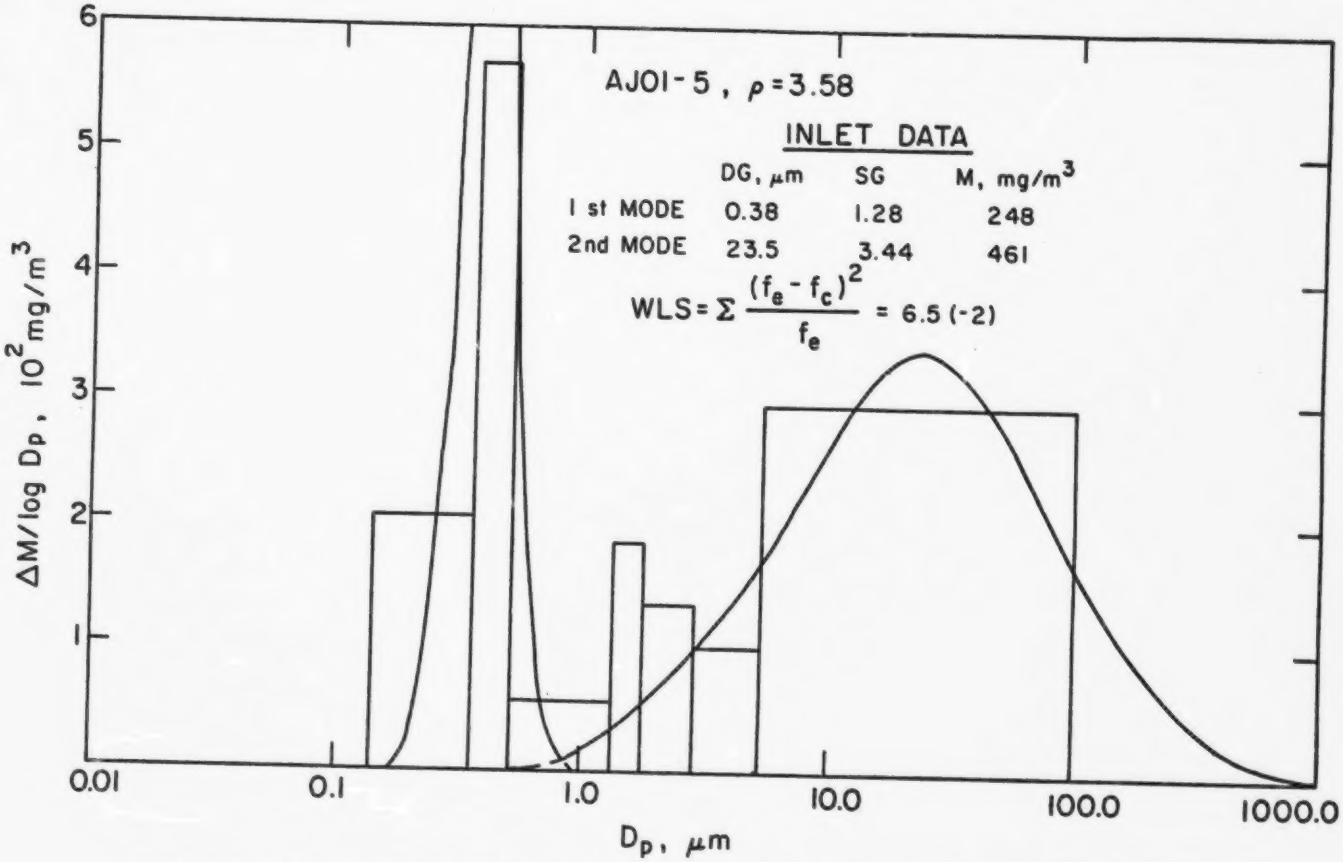

Figure III.21 Modal fitting of impactor data from copper smelter, hot side ESP inlet (AJOI-5).

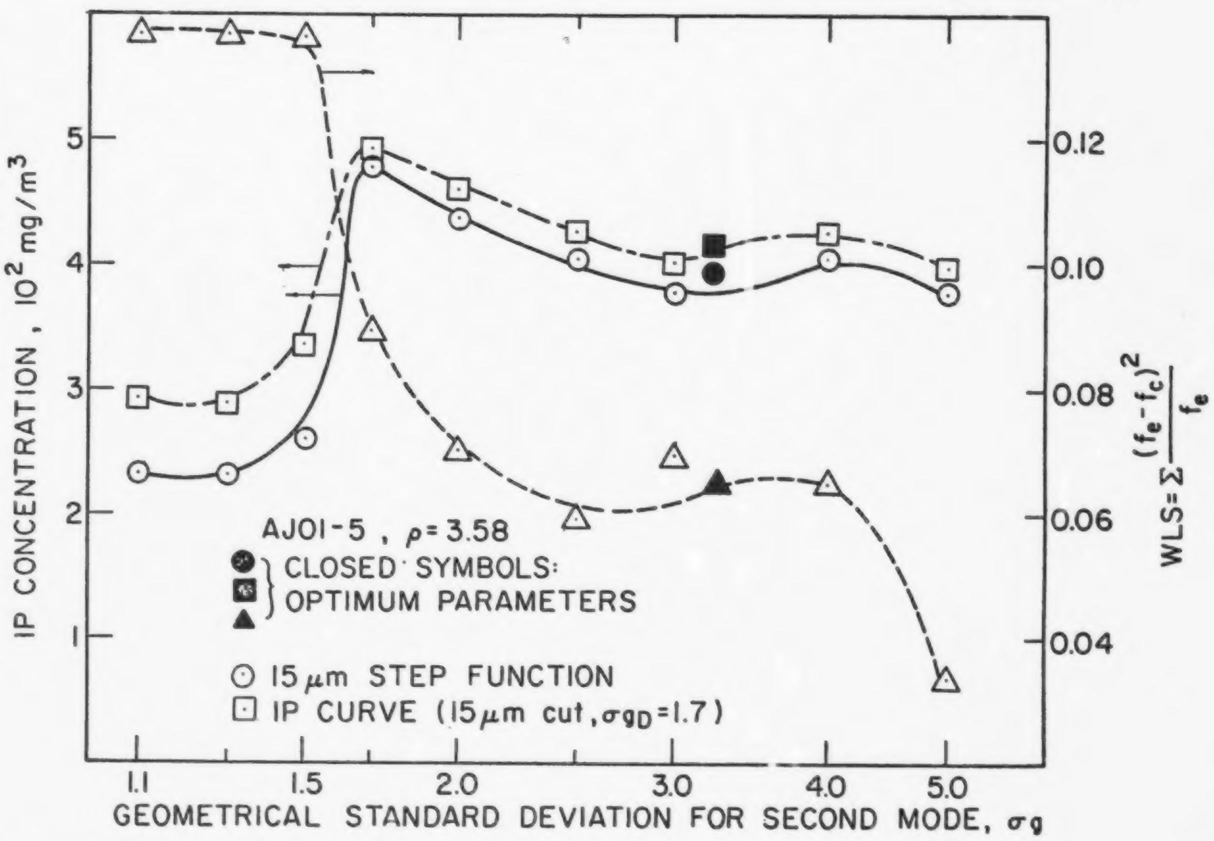

Figure III.22 Effect of assumed aerosol σ_{g2} and sampler σ_{gD} on the IP concentration estimate (AJOI-5).

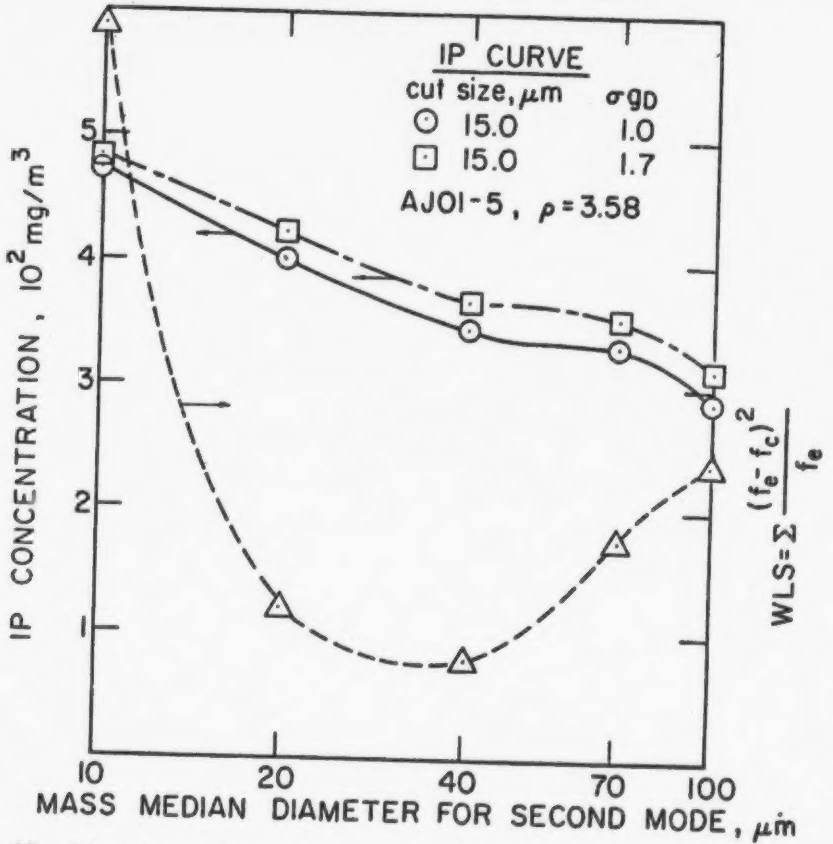

Figure III.23 Effect of assumed aerosol MMD_2 and sampler σ_{gD} on the IP concentration estimate (AJ0I-5).

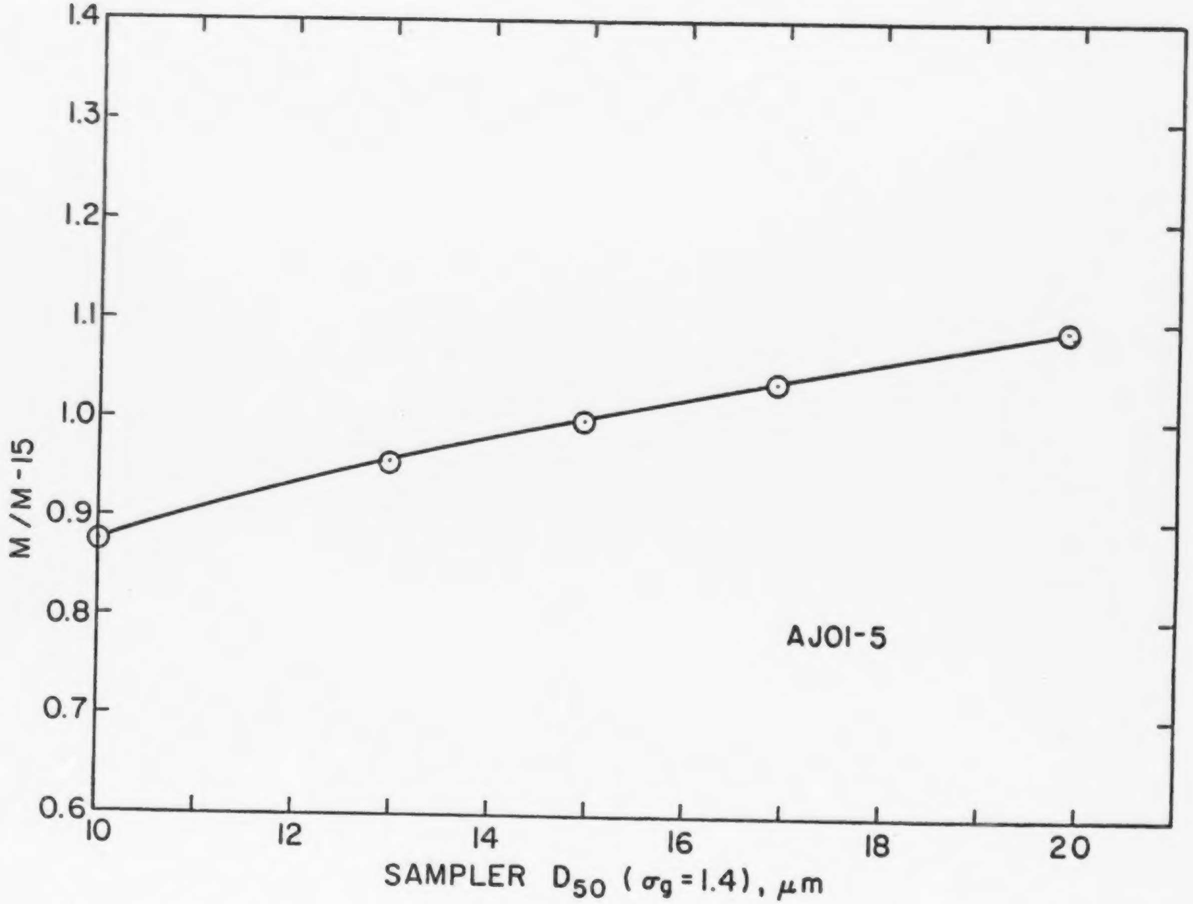

Figure III.24 Effect of sampler D_{50} on the IP concentration estimate (AJOI-5).

IV. SUMMARY AND RECOMMENDATIONS

A. Summary

1. Aerosols at the inlet as well as at the outlet of the control device in a stack can be modeled satisfactorily by using multi-component log-normal distributions.
2. The SRI impactor data analyzed in this study can be fitted with a bimodal, log-normal distribution. The modal parameters of the first mode, the fine particle mode, can be determined with good accuracy. For the second mode, the coarse particle mode, the modal parameters are obtained through partial fitting to two or three stages of impactor data. These parameters are consequently less accurate and are sensitive to the assumed mass median diameter and the geometrical standard deviation. Sensitivity analysis of these parameters was therefore performed to examine their effect on the estimated IP concentration.
3. The present analysis technique gives a good estimate, ±20%, of the IP concentration when the coarse particle concentration is in the same order of magnitude as the fine particle concentration. This situation is encountered in all of the outlet data and about half of the inlet data analyzed here. When the coarse particle concentration is much higher than the fine particle concentration, the estimated IP concentration is sensitive to the variation of the geometrical standard deviation and the mass median diameter. However, by properly selecting the calculated IP concentration using minimum objective function value as an indicator, it is possible to estimate the IP concentration to within a factor of two or better.

4. The IP concentration is affected more by the cut size, D_{50}, than the sharpness of cut, σ_{gD}, of the sampler curve. The present specifications for the performance curve of the IP sampler, $D_{50} = 15 \pm 2$ μm and $\sigma_{gD} = 1.0 - 1.7$, are found to be adequate because the resulting IP concentration changes by less than ±20% within the tolerance of the performance curve.
5. For a coal-fired boiler, two sets of impactor data have been analyzed using two different assumed densities, namely, 1 and 2.41 gm/cm^3. Although the particle size distribution changes with different assumed densities, the change does not appear to affect greatly the estimated IP concentration for the limited data analyzed here.

B. Recommendations

1. While the present analysis technique gives a reasonable estimate of the IP concentration, the accuracy can be greatly improved if additional size classification information is available in the size range of 10-100 μm. This information is especially needed for sampling situations in which the coarse particle concentration is significantly higher than the fine particle concentration. It can be obtained by adding one or two classification stages in the sampling device or by the microscopic determination of the σ_g of the measured aerosol.
2. The accuracy of the estimated IP concentration depends on the quality of the impactor data. It is therefore desirable to investigate further the non-ideal behavior of the impactor, such as the effect of particle bounce, wall loss, and cross-channel interference on the particle size distribution, in order to better determine the IP concentration.

REFERENCES

Bevington, P. R. Data Reduction and Error Analysis for the Physical Sciences. McGraw-Hill, New York, 1969.

Daniel, C. and F. S. Wood. Fitting Equations to Data. Wiley-Interscience, New York, 1971.

Kapadia, A. Data Reduction Techniques for Aerosol Size Distribution Measuring Instruments: Electrical Aerosol Analyzer and Diffusion Battery. Ph.D. Thesis, Mechanical Engineering Department, University of Minnesota, Minneapolis, Minnesota, 1980.

McCain, J. D. CEA Variable-Throat Venturi Scrubber Evaluation. EPA-600/7-78-094, U. S. Environmental Protection Agency, Research Triangle Park, North Carolina, 1978.

McCain, J. D., J. P. Gooch and W. B. Smith. Results of Field Measurements of Industrial Particulate Sources and Electrostatic Precipitator Performance. J. Air Pollut. Control Assoc. 25(2):117-121, 1975.

Raabe, O. G. A General Method for Fitting Size Distributions to Multi-Component Aerosol Data using Weighted Least-Squares. Environ. Sci. Technol. 12(10): 1162-1167, 1978.

Whitby, K. T. The Physical Characteristics of Sulfur Aerosols. Atmos. Environ. 12:135-159, 1978.

APPENDIX A

Computer Program for Impactor Data Modeling and IP Concentration Calculation

Program MODSIM is developed for impactor data fitting and IP concentration calculation. The input parameters are the particle boundaries and concentrations, the mask values used to determine whether the desired distribution is a unimodal, bimodal, or trimodal distribution, and an initial estimate of parameters which characterize the distribution. The objective function to be minimized can be chosen to be either normal chi-square, modified chi-square, or weighted least square, as defined in Section IIA. The program uses a simplex method to minimize the objective function which is calculated by comparing the input particle concentration to the calculated particle concentration. In addition, the fitted distribution is integrated with the sampler classification curve of an input cut-off size, D_{50}, and geometrical standard deviation, σ_{gD}. The output gives a set of parameters for a log-normal distribution which has a minimum objective function value, the histogram of the fitted distribution, and the sampler concentration.

In the following pages, the sample input and output data, as well as the program listing, are included.

SAMPLE INPUTS

```
 RUN MODSIM
    ENTER DATA DESCRIPTION (60 CHARACTERS MAXM)
    (NOTE: THE TITLE SHOULD CONTAIN AMONG OTHER THINGS THE
    WEIGHTING OF THE DISTRIBUTION, AND THE UNITS OF THE
    CONCENTRATION VARIABLE)

SAMPLE RUN

    ENTER NO. OF DATA POINTS ---MAX OF 20

8

    ENTER PARTICLE BOUNDARIES
.18,.35,.75,1.2,2.2,6,15,30,100.0

    ENTER DATA
.251,.512,.949,1.625,3.633,9.487,21.213,54.772

    ENTER 9 MASK VALUES
    1 TO KEEP THE PARAMETER CONSTANT
    0 TO KEEP THE PARAMETER VARIABLE
    THE ORDER OF THE VARIABLES IS
    DPG1, SG1, TOTAL1, DPG2, SG2, TOTAL2, DPG3, SG3, TOTAL3


1,1,1,0,0,0,0,0,0

    ENTER INITIAL ESTIMATES FOR
    DPG1,SG1,TOTAL1,DPG2,SG2,TOTAL2,DPG3,SG3,TOTAL3
 005,2,0,2.2,1.7,100,40,2.5,75.0
          CHOOSE DESIRED OBJECTIVE FUNCTION (ENTER 1,2,OR 3)
                1--NORMAL CHI SQUARED FUNCTION
                2--WHITBYS MODIFIED CHI SQUARED FUNCTION
                3--WEIGHTED LEAST SQUARED FUNCTION
3
    INHALABLE PARTICULATE MATTER CALCULATION
    ENTER D50 , SG
    OR ----HIT RETURN TO SKIP
15,1.4
    INHALABLE PARTICULATE MATTER CALCULATION
    ENTER D50 , SG
    OR ----HIT RETURN TO SKIP


          CHOOSE COURSE OF ACTION  (ENTER 0,1,2,OR 3)
                0--STOP PROGRAM
                1--USE FINAL VALUES OF PARAMETERS AS INITIAL ESTIMATES
                2--ENTER NEW INITIAL ESTIMATES
                3--USE DIFFERENT OBJECTIVE FUNCTION


TT2  --  STOP
>
```

SAMPLE OUTPUTS

```
SAMPLE RUN


OBJECTIVE FUNCTION: WEIGHTED LEAST SQUARES

BEGINNING OBJECTIVE FUNCTION VALUE =        5. 886E+01
FINAL OBJECTIVE FUNCTION VALUE =        2. 221E-02
FUNCTION COMPUTATIONS = 145


INITIAL ESTIMATES
   MODE1
DG1=0. 0050              MODE2
SG1=2. 00             DG2= 2. 200              MODE3
TOTAL1=0. 000E-01     SG2=1. 70             DG3= 40. 00
                      TOTAL2=1. 000E+02     SG3=2. 50
                                            TOTAL3=7. 500E+01

FINAL VALUES OF THE PARAMETERS
   MODE1
DG1=0. 0050              MODE2
SG1=2. 00             DG2= 3. 275              MODE3
TOTAL1=0. 000E-01     SG2=1. 69             DG3= 42. 54
                      TOTAL2=5. 514E+00     SG3=2. 21
                                            TOTAL3=1. 011E+02


                            INPUT DISTRIBUTION                  FITTED DISTRIBUTION
   DP        DPG         DATA    D(DATA)/D(LOGDP)          FDATA      D(FDATA)/D(LOGDP)
  0. 180
             0. 251     2. 510E-01     8. 691E-01         6. 010E-05     2. 081E-04
  0. 350
             0. 512     5. 120E-01     1. 547E+00         1. 410E-02     4. 261E-02
  0. 750
             0. 949     9. 490E-01     4. 649E+00         1. 422E-01     6. 968E-01
  1. 200
             1. 625     1. 625E+00     6. 173E+00         1. 093E+00     4. 154E+00
  2. 200
             3. 633     3. 633E+00     8. 338E+00         4. 258E+00     9. 772E+00
  6. 000
             9. 487     9. 487E+00     2. 384E+01         9. 541E+00     2. 398E+01
 15. 000
            21. 213     2. 121E+01     7. 047E+01         2. 382E+01     7. 912E+01
 30. 000
            54. 772     5. 477E+01     1. 048E+02         5. 354E+01     1. 024E+02
100. 00


INHALABLE PARTICULATE MATTER
D50 =   15. 000        SG =    1. 400        TOTAL IPM MASS= 1. 702E+01
```

PROGRAM LISTING

```
C
C
C       MODSIM.FTN IS A SIMPLEX MINIMIZATION PROGRAM FOR THE SRI
C       IMPACTOR DATA
C
C
        COMMON X(9), XMAX(9), XMIN(9), DELTAX(9), MASK(9),
        1DELMIN(9), DATA(20), CDAT1(21), CDAT2(21),
        2CDAT3(21), BDS(21), DPI(20), NBAR, TOTL,
        3ALDAT(20), ALCDAT(20), BCHISQ, FCHISQ,NF,CTOTL
        DIMENSION TITLE(15),CALDAT(40), X1(9)
        DATA Y/'YES'/
        CALL ASSIGN (3,'SRI.INP')
        CALL ASSIGN(6,'LP:')
C
C       INPUT TITLE
C
220     WRITE (5,10)
10      FORMAT (5X,'ENTER DATA DESCRIPTION (60 CHARACTERS MAXM)',/
        1,5X,'(NOTE: THE TITLE SHOULD CONTAIN AMONG OTHER THINGS THE',/
        2,5X,'WEIGHTING OF THE DISTRIBUTION, AND THE UNITS OF THE',/
        3,5X,'CONCENTRATION VARIABLE)',/)
        READ (5,20) TITLE
20      FORMAT (15A4)
C
C       INPUT DATA
C
        WRITE (5,30)
30      FORMAT (/5X,'ENTER NO. OF DATA POINTS
        1---MAX OF 20',/)
        READ (5,40) NBAR
C
C       READ SIR.INP
C
D       READ (3,25) XMAX, XMIN,DELTAX, DELMIN
D25     FORMAT (4(9F10.0))
40      FORMAT (I2)
        IF (NBAR-10) 42,42,49
42      WRITE(5,45)
45      FORMAT(/5X,'ENTER PARTICLE BOUNDARIES')
        NBAR1=NBAR+1
        READ (5,46) (BDS(J), J=1,NBAR1)
46      FORMAT(20F10.0)
        WRITE(5,43)
43      FORMAT(/5X,'ENTER DATA')
        READ(5,44) (DATA(J), J=1,NBAR)
44      FORMAT(10F10.0)
        GO TO 89
49      WRITE(5,70)
70      FORMAT(/5X, 'ENTER FIRST TEN PARTICLE BOUNDARIES',/)
        READ(5,71) (BDS(J), J=1,10)
71      FORMAT(15F10.0)
        NBAR1=NBAR+1
        WRITE(5,75)
```

```
75      FORMAT(/5X,'ENTER REST OF PARTICLE BOUNDARIES',/)
        READ(5,80) (BDS(J), J=11,NBAR1)
80      FORMAT(15F10.0)
        WRITE (5,50)
50      FORMAT (/5X, 'ENTER  FIRST TEN DATUM',/)
        READ (5,60) (DATA(J), J=1,10)
60      FORMAT (20F10.0)
        WRITE (5,51)
51      FORMAT (/5X, 'ENTER REST OF DATUM',/)
        READ (5,61) (DATA(J), J=11,NBAR)
61      FORMAT(20F10.0)
        WRITE (5,70)
C
C       ENTER MASK
C
89      WRITE (5,90)
90      FORMAT (/5X, 'ENTER 9 MASK VALUES',/, 5X, '1 TO KEEP THE',
        1' PARAMETER CONSTANT',/5X, '0 TO KEEP THE PARAMETER VARIABLE',
        2,/5X,'THE ORDER OF THE VARIABLES IS', /5X, 'DPG1, SG1,
        3 TOTAL1, DPG2, SG2, TOTAL2, DPG3, SG3,
        4 TOTAL3',/)
        READ (5,100) MASK
100     FORMAT (9I2)
C
C
C
C       INITIAL ESTIMATES
C
C
D       WRITE (5, 140)
D140    FORMAT (/5X, 'ENTER YES IF YOU WANT TO INPUT THE INITIAL',
D       1'ESTIMATES',/)
D       READ (5, 150) FLAG
D150    FORMAT (I3)
D       IF (FLAG.EQ.Y) GO TO 160
D       GO TO 170
160     WRITE (5, 180)
180     FORMAT(/5X,'ENTER INITIAL ESTIMATES FOR',/,5X,'DPG1,SG1,TOTAL1
        1,DPG2,SG2,TOTAL2,DPG3,SG3,TOTAL3')
        READ (5, 190)X1
190     FORMAT (9F10.0)
        GO TO 193
191     DO 192 J=1,9
192     X1(J)=X(J)
193     DO 195 J =1,9
195     X(J) = X1(J)
196     DO 197 J=1,9
197     DELMIN(J)=DELMIN(J)*X(J)
D       WRITE (6,199)DELTAX,DELMIN,XMAX,XMIN,TOTL,BDS,DATA
D       WRITE(5,201) NBAR
D201    FORMAT(5X,I3)
D199    FORMAT(9(3X,F10.3))
```

```
C
C
C       CALCULATE DATA/DLOGD, TOTL
C
C
        TOTL=0.0
        DO 110 J=1,NBAR
        A=ALOG10 (BDS(J+1)/BDS(J))
        ALDAT(J)=DATA(J)/A
        TOTL=TOTL+DATA(J)
110     CONTINUE
C
C
C
        GO TO 1100
170     CALL ESTIN
1100    CALL STEPIT(MFLAG)
C
C
C
C       CALULATE CDATA/DLOGD,CTOTL
C
        DO 1300 J=1,NBAR
        AAA=ALOG10(BDS(J+1)/BDS(J))
        CALDAT(J)=ALCDAT(J)/AAA
1300    CONTINUE
C
C
245     CALL FINLPLT(X1,MFLAG,TITLE,CALDAT)
        DO 250 J=1,9
        DELTAX(J)=0.0
250     DELMIN(J)=0.03
        WRITE(5,200)
200     FORMAT(/10X,'CHOOSE COURSE OF ACTION  (ENTER 0,1,2,OR 3)',/,15X
        1,'0--STOP PROGRAM',/,15X
        2,'1--USE FINAL VALUES OF PARAMETERS AS INITIAL ESTIMATES',/
        3,15X,'2--ENTER NEW INITIAL ESTIMATES',/15X
        3,'3--USE DIFFERENT OBJECTIVE FUNCTION',/,5X)
        READ (5,251) IFLAG
251     FORMAT(I2)
        GO TO (191,160,193) IFLAG
240     STOP
        END
```

```
C
C       OBJCT.FTN IS THE OBJECTIVE FUNCTION USED TO FIT A
C       TRIMODAL LOGNORMAL CURVE TO THE INPUT DATA.
C
        SUBROUTINE OBJCT(NV,CHISQ,MFLAG)
        COMMON X(9), XMAX(9), XMIN(9), DELTAX(9), MASK(9),
        1DELMIN(9), DATA(20), CDAT1(21), CDAT2(21),
        2CDAT3(21), BDS(21), DPI(20), NBAR, TOTL,
        3ALDAT(20), ALCDAT(20), BCHISQ, FCHISQ,NF,CTOTL
        GO TO (700,800,900) MFLAG
C       IF MFLAG=1 THE NORMAL CHI SQUARED FUNCTION IS USED
C       IF MFLAG=2 WHITBYS MODIFIED CHI SQUARED FUNCTION IS USED
C       IF MFLAG=3 THE WEIGHTED LEAST SQUARED FUNCTION IS USED
C
C
C
C
C       WHITBYS MODIFIED CHI SQUARED
800     DO 10 J=1,NV
        IF(MASK(J)) 10,20,10
20      IF (X(J)-XMAX(J)) 30,30,40
30      IF (X(J)-XMIN(J)) 40,10,10
10      CONTINUE
        CHISQ=0.0
        CALL ALOND(CDAT1,X(1),X(2),X(3))
        CALL ALOND(CDAT2,X(4),X(5),X(6))
        CALL ALOND(CDAT3,X(7),X(8),X(9))
D       WRITE(6,100) CDAT1,CDAT2,CDAT3,X
D100    FORMAT(10(2X,1PE10.3),/)
        DO 50 J=1,NBAR
        A=ALOG10(BDS(J+1)/BDS(J))
        ALCDAT(J)=(CDAT1(J)+CDAT2(J)+CDAT3(J))
        A=ALCDAT(J)-DATA(J)
        B=(ALCDAT(J)+DATA(J))/2.0
        CHISQ=CHISQ+((A**2)/B) /TOTL
50      CONTINUE
        GO TO 60
40      CHISQ=1.0E20
60      NF=NF+1
        GO TO 262
C
C
C       WEIGHTED LEAST SQUARES FUNCTION
900     DO 110 J=1,NV
        IF (MASK(J)) 110,120,110
120     IF (X(J)-XMAX(J)) 130,130,140
130     IF (X(J)-XMIN(J)) 140,110,110
110     CONTINUE
        CHISQ=0.0
        CALL ALOND(CDAT1,X(1),X(2),X(3))
        CALL ALOND(CDAT2,X(4),X(5),X(6))
        CALL ALOND(CDAT3,X(7),X(8),X(9))
        CTOTL=0.0
        DO 170 J=1,NBAR
```

```
170   CTOTL=CTOTL+CDAT1(J)+CDAT2(J)+CDAT3(J)
      DO 150 J=1,NBAR
      ALCDAT(J)=(CDAT1(J)+CDAT2(J)+CDAT3(J))
      A=ALCDAT(J)/CTOTL-DATA(J)/TOTL
      CHISQ=CHISQ+(A**2)/(DATA(J)/TOTL+1.0E-20)
150   CONTINUE
      CHISQ=CHISQ+((CTOTL-TOTL)**2)/TOTL
      GO TO 160
140   CHISQ=1.0E20
160   NF=NF+1
      GO TO 262
C
C
C     NORMAL CHI SQUARED FUNCTION
700   DO 210 J=1,NV
      IF(MASK(J)) 210,220,210
220   IF(X(J)-XMAX(J)) 230,230,240
230   IF(X(J)-XMIN(J)) 240,210,210
210   CONTINUE
      CHISQ=0.0
      CALL ALOND(CDAT1,X(1),X(2),X(3))
      CALL ALOND(CDAT2,X(4),X(5),X(6))
      CALL ALOND(CDAT3,X(7),X(8),X(9))
      CTOTL=0.0
      DO 270 J=1,NBAR
270   CTOTL=CTOTL+CDAT1(J)+CDAT2(J)+CDAT3(J)
      DO 250 J=1,NBAR
      ALCDAT(J)=(CDAT1(J)+CDAT2(J)+CDAT3(J))
      A=ALCDAT(J)/CTOTL-DATA(J)/TOTL
      CHISQ=CHISQ+(A**2)/(ALCDAT(J)/CTOTL+1.0E-20)
250   CONTINUE
      CHISQ=CHISQ+((CTOTL-TOTL)**2)/CTOTL
      GO TO 260
240   CHISQ=1.0E20
260   NF=NF+1
262   RETURN
      END
      BLOCK DATA




      COMMON X(9), XMAX(9), XMIN(9), DELTAX(9), MASK(9),
     1DELMIN(9), DATA(20), CDAT1(21), CDAT2(21),
     2CDAT3(21), BDS(21), DPI(20), NBAR, TOTL,
     3ALDAT(20), ALCDAT(20), BCHISQ, FCHISQ,NF
      DATA DELTAX/0.0,0.0,0.0,0.0,0.0,0.0,0.0,0.0,0.0/
      DATA DELMIN/0.03,0.03,0.03,0.03,0.03,0.03,0.03,0.03,0.03/
      DATA XMAX/1.0,5.0,1000.,10.0,5.0,10000.,1000.0,5.0,100000./
      DATA XMIN/0.001,1.1,0.0,.01,1.1,0.0,.1,1.1,0.0/
      END
```

```
        BLOCK DATA
        COMMON X(9), XMAX(9), XMIN(9), DELTAX(9), MASK(9),
        1DELMIN(9), DATA(20), CDAT1(21), CDAT2(21),
        2CDAT3(21), BDS(21), DPI(20), NBAR, TOTL,
        3ALDAT(20), ALCDAT(20), BCHISQ, FCHISQ,NF
        DATA DELTAX/0. 0,0. 0,0. 0,0. 0,0. 0,0. 0,0. 0,0 . 0,0. 0/
        DATA DELMIN/0. 03,0. 03,0. 03,0. 03,0. 03,0. 03,0. 03,0. 03,0. 03/
        DATA XMAX/1. 0,5. 0,1000. ,10. 0,5. 0,10000. ,1000. 0,5. 0,100000. /
        DATA XMIN/0. 001,1. 1,0. 0,. 01,1. 1,0. 0,. 1,1. 1,0. 0/
        END
```

```
C
C       SUBROUTINE ALOND CALCULATES AREA UNDER LOGNORMAL DISTRIBUTION
C
        SUBROUTINE ALOND (CDAT, AMEAN, SIGMA, CONI)
        COMMON X(9), XMAX(9), XMIN(9), DELTAX(9), MASK(9),
        1DELMIN(9), DATA(20), CDAT1(21), CDAT2(21),
        2CDAT3(21), BDS(21), DPI(20), NBAR, TOTL,
        3ALDAT(20), ALCDAT(20), BCHISQ, FCHISQ,NF,CTOTL
        DIMENSION CDAT (20)
        XMEAN= ALOG (AMEAN)
        XSIGMA = ALOG (SIGMA)
        DO 10 J= 1,NBAR
        A=(ALOG (BDS(J)) - XMEAN) / XSIGMA
        B =( ALOG (BDS(J+1)) - XMEAN) / XSIGMA
        CDAT (J) = APROX (A,B)*CONI
10      CONTINUE
        RETURN
        END

C        THIS IS AN APPROXIMATION FOR THE CUMULATIVE
C        NORMAL DISTRIBUTION FUNCTION. REF. ABRAMOWITZ
C        AND STEGUN: MATHEMATICAL HANDBOOK.
         FUNCTION APROX(A,B)
         X1=ABS(A)
         X2=ABS(B)
         IF(X1) 10,20,10
10        PX1=P(X1)
         GO TO 30
20        PX1=0. 5
30        IF(X2) 35,40,35
35        PX2=P(X2)
         GO TO 45
40        PX2=0. 5
45        SIN=A*B
         IF(SIN)60,50,50
50        APROX=ABS(PX2-PX1)
         GO TO 70
60        APROX=1. 0-(PX2+PX1)
70        RETURN
         END
```

```
C         THIS FUNCTION IS USED WITH APROX
          FUNCTION P(X)
          DIMENSION B(6)
          DATA B/0.319381530,-0.356543782,1.781477937,-1.821255978,
         11.330274429,0.2316419/
          T=1.0/(1.0+B(6)*X)
          P=Z(X)*(B(1)*T+B(2)*T**2+B(3)*T**3+B(4)*T**4+B(5)*T**5)
          RETURN
          END
C         THIS FUNCTION IS USED WITH APPROX
          FUNCTION Z(X)
          PI=3.1415927
          S2PI=SQRT(2.0*PI)
          ARG=X**2/2.0
          IF(ARG-87.0) 10,20,20
10         A=EXP(ARG)
          Z=1.0/(S2PI*A)
          RETURN
20         Z=0.0
          RETURN
          END
C        THIS SUBROUTINE CALCULATES THE FRACTION BETWEEN GIVEN BOUNDS
C
         SUBROUTINE CNUMS(CNUM,ANMD,SIGMA,TOTL)
         DIMENSION CNUM(40)
         BD1=.001
         DPMULT=1.3335214
         XANMD=ALOG(ANMD)
         XSIGMA=ALOG(SIGMA)
         DO 10 J=1,40
         A=(ALOG(BD1)-XANMD)/XSIGMA
         B=(ALOG(BD1*DPMULT)-XANMD)/XSIGMA
         BD1=BD1*DPMULT
10       CNUM(J)=APROX(A,B)*TOTL
         RETURN
         END
C        THIS SUBROUTINE CALCULATES THE IHP FRAC FOR A UNIMODAL DIST.
C
         SUBROUTINE AIHP(XIHP,XNMD,XSIG)
         DIMENSION XIHP(40)
         DPI=.00115478
         DPMULT=1.3335214
         XANMD=ALOG(XNMD)
         XSIGMA=ALOG(XSIG)
         DO 10 J=1,40
         A=(ALOG(DPI)-XANMD)/XSIGMA
         X1=ABS(A)
         IF(X1) 20,30,20
20       XIHP(J)=P(X1)
         GO TO 40
30       XIHP(J)=0.5
40       IF(A .LT. 0.0) XIHP(J)=1.0-XIHP(J)
10       DPI=DPI*DPMULT
         RETURN
         END
```

```
      SUBROUTINE STEPIT(MFLAG)
C
C  MINIMIZES A PIECEWISE CONTINUOUS FUNCTION SUBJECT TO ARBITRARY
C  CONSTRAINTS OF INEQUALITY.
C  J. A. NELDER AND R. MEAD, THE COMPUTER JOURNAL 7 (1965) 308
C
C
C
       COMMON X(9), XMAX(9), XMIN(9), DELTAX(9), MASK(9),
       1DELMIN(9), DATA(20), CDAT1(21), CDAT2(21),
       2CDAT3(21), BDS(21), DPI(20), NBAR, TOTL,
       3ALDAT(20), ALCDAT(20), BCHISQ, FCHISQ,NF,CTOTL
      DIMENSION CHI(10),Z(10,9),ZBAR(9),ZSTAR(9)
C
C
       WRITE(5,20)
20     FORMAT(10X,'CHOOSE DESIRED OBJECTIVE FUNCTION (ENTER 1,2,OR 3)',/
       1,15X,'1--NORMAL CHI SQUARED FUNCTION',/
       2,15X,'2--WHITBYS MODIFIED CHI SQUARED FUNCTION',/
       3,15X,'3--WEIGHTED LEAST SQUARED FUNCTION')
       READ (5,25) MFLAG
25     FORMAT (I3)
      NFLAT=1
       CHISQ=0.0
       NV=9
      NFMAX=500
   40 HUGE=0.5E 38
      ALPHA=1.0
      BETA=0.5
      GAMMA=2.0
C
   50 DO 130 J=1,NV
      IF(MASK(J))130,60,130
   60 IF((X(J)+DELTAX(J))-X(J))100,70,100
   70 IF(X(J))90,80,90
   80 DELTAX(J)=0.01
      GO TO 100
   90 DELTAX(J)=0.10*X(J)
  100 IF(XMAX(J)-XMIN(J))110,110,120
  110 XMAX(J)=HUGE
      XMIN(J)=-HUGE
  120 X(J)=AMAX1(XMIN(J),AMIN1(XMAX(J),X(J)))
  130 CONTINUE
```

```
C
C
C   CALCULATE INITIAL P(I) AND Y(I).
C
  220 NVA=0
      NF=0
      J=1
  230 IF(MASK(J))270, 240, 270
  240 NVA=NVA+1
      DO 250 K=1, NV
  250 Z(NVA, K)=X(K)
      Z(NVA, J)=Z(NVA, J)+DELTAX(J)
      XS=X(J)
      X(J)=Z(NVA, J)
        CALL OBJCT(NV, CHISQ, MFLAG)
  260 X(J)=XS
      CHI(NVA)=CHISQ
  270 J=J+1
      IF(J-NV)230, 230, 280
  280 IF(NVA)290, 290, 310
  290 DO 300 J=1, NV
  300 MASK(J)=0
      GO TO 50
  310 NVP=NVA+1
      DO 320 J=1, NV
  320 Z(NVP, J)=X(J)
C
C
        CALL OBJCT(NV, CHISQ, MFLAG)
  390 CHI(NVP)=CHISQ
        BCHISQ=CHISQ
  440 JL=NVP
C
C   DETERMINE H AND L.
C
  450 JH=JL
      DO 490 J=1, NVP
      IF(CHI(J)-CHI(JH))470, 470, 460
  460 JH=J
  470 IF(CHI(J)-CHI(JL))480, 490, 490
  480 JL=J
  490 CONTINUE
        IF(JH-JL) 560, 500, 560
  500 IF(NFLAT)540, 540, 1200
  540 JH=1
      IF(JL-1)560, 550, 560
  550 JH=2
C
C   CALCULATE PBAR.
C
  560 DO 600 J=1, NV
      IF(MASK(J))600, 570, 600
  570 ZBAR(J)=0.0
      DO 590 K=1, NVP
      IF(K-JH)580, 590, 580
  580 ZBAR(J)=ZBAR(J)+Z(K, J)
  590 CONTINUE
      ZBAR(J)=ZBAR(J)/FLOAT(NVA)
  600 CONTINUE
```

```
C
C  ATTEMPT A REFLECTION.
C  FORM P*
C
      DO 620 J=1,NV
      IF(MASK(J))620,610,620
  610 X(J)=(1.0+ALPHA)*ZBAR(J)-ALPHA*Z(JH,J)
  620 ZSTAR(J)=X(J)
         CALL OBJCT(NV,CHISQ,MFLAG)
  630 CHISTR=CHISQ
      IF(CHISQ-CHI(JL))690,730,730
C
C  THE REFLECTION SUCCEEDED.   ATTEMPT AN EXPANSION.
C  FORM P**
C
  690 DO 710 J=1,NV
      IF(MASK(J))710,700,710
  700 X(J)=GAMMA*X(J)+(1.0-GAMMA)*ZBAR(J)
  710 CONTINUE
         CALL OBJCT(NV,CHISQ,MFLAG)
  720 IF(CHISQ-CHISTR)1100,790,790
C
C  THE REFLECTION FAILED.
C
  730 DO 750 J=1,NVP
      IF(J-JH)740,750,740
  740 IF(CHISQ-CHI(J))790,750,750
  750 CONTINUE
      IF(CHISQ-CHI(JH))810,830,830
C
C
C  REPLACE P(JH) BY P*
C
  790 DO 800 J=1,NV
  800 Z(JH,J)=ZSTAR(J)
      CHI(JH)=CHISTR
      GO TO 1120
C
  810 DO 820 J=1,NV
  820 Z(JH,J)=X(J)
      CHI(JH)=CHISQ
C
C  ATTEMPT A CONTRACTION.
C  FORM P**
C
  830 DO 850 J=1,NV
      IF(MASK(J))850,840,850
  840 X(J)=BETA*Z(JH,J)+(1.0-BETA)*ZBAR(J)
  850 CONTINUE
         CALL OBJCT(NV,CHISQ,MFLAG)
  860 IF(CHISQ-CHI(JH))1100,960,960
```

```
C
C  THE CONTRACTION FAILED.
C  REPLACE ALL P(I) BY (P(I)+P(JL))/2.0 , GUARDING THE ROUNDING.
C
  960 JS=JL
      DO 1060 J=1,NVP
      IF(J-JL)970,1060,970
  970 DO 1020 K=1,NV
      IF(MASK(K))1020,980,1020
  980 IF(Z(J,K)-Z(JL,K))990,1000,990
  990 X(K)=(Z(J,K)+Z(JL,K))/2.0
      IF(X(K)-Z(J,K))1010,1000,1010
 1000 X(K)=Z(JL,K)
 1010 Z(J,K)=X(K)
 1020 CONTINUE
         CALL OBJCT(NV,CHISQ,MFLAG)
 1030 IF(CHISQ-CHI(JS))1040,1050,1050
 1040 JS=J
 1050 CHI(J)=CHISQ
 1060 CONTINUE
      JL=JS
      GO TO 1120
C
C
C  REPLACE P(JH) BY P* OR P**
C
 1100 DO 1110 J=1,NV
 1110 Z(JH,J)=X(J)
      CHI(JH)=CHISQ
C
C  TEST FOR CONVERGENCE.
C
 1120 DO 1150 J=1,NV
      IF(MASK(J))1150,1130,1150
 1130 ZMAX=Z(1,J)
      ZMIN=Z(1,J)
      DO 1140 K=2,NVP
      ZMAX=AMAX1(ZMAX,Z(K,J))
 1140 ZMIN=AMIN1(ZMIN,Z(K,J))
      IF((ZMAX-ZMIN)-ABS(DELMIN(J)))1150,1150,1260
 1150 CONTINUE
C
1180     IF(CHI(JH)-CHI(JL))1190,1200,1200
1190     JL=JH
 1200 DO 1210 J=1,NV
 1210 X(J)=Z(JL,J)
         CALL OBJCT(NV,CHISQ,MFLAG)
         FCHISQ=CHISQ
 1250 RETURN
C
1260     CONTINUE
 1270 IF(NF-NFMAX)450,450,1180
      END
      SUBROUTINE ESTIN
      COMMON X(9), XMAX(9), XMIN(9), DELTAX(9), MASK(9),
      1DELMIN(9), DATA(20), CDAT1(21), CDAT2(21),
      2CDAT3(21), BDS(21), DPI(20), NBAR, TOTL,
      3ALDAT(20), ALCDAT(20), BCHISQ, FCHISQ, NF
      A=1.0
      RETURN
      END
```

```
C
C
C          FINLPLT.FTN IS FOR OUTPUTING THE DATA

           SUBROUTINE FINLPLT (X1,MFLAG,TITLE,CALDAT)
           COMMON X(9), XMAX(9), XMIN(9), DELTAX(9), MASK(9),
           1DELMIN(9), DATA(20), CDAT1(21), CDAT2(21),
           2CDAT3(21), BDS(21), DPI(20), NBAR, TOTL,
           3ALDAT(20), ALCDAT(20), BCHISQ, FCHISQ,NF,CTOTL
           DIMENSION TITLE(15),ABDS(21),X1(9),XIHP(40),CNUM(40),CALDAT(40)
           WRITE(6,10) TITLE
  10       FORMAT (1H1,4X,15A4,//)
           GO TO (201,202,203) MFLAG
  201      WRITE(6,205)
  205      FORMAT(5X,'OBJECTIVE FUNCTION:NORMAL CHI SQUARED',/)
           GO TO 38
  202      WRITE(6,206)
  206      FORMAT(5X,'OBJECTIVE FUNCTION:WHITBYS MODIFIED CHI SQUARED',/)
           GO TO 38
  203      WRITE(6,207)
  207      FORMAT (5X,'OBJECTIVE FUNCTION:WEIGHTED LEAST SQUARES',/)
  38       NBAR1=NBAR+1
           WRITE (6,40) BCHISQ, FCHISQ, NF
  40       FORMAT(5X,'BEGINNING OBJECTIVE FUNCTION VALUE = ',5X,1PE10.3,/
           1,5X,'FINAL OBJECTIVE FUNCTION VALUE = ',5X,1PE10.3,/
           2,5X,'FUNCTION COMPUTATIONS =',I4,//)
           WRITE(6,45)
  45       FORMAT(/5X,'INITIAL ESTIMATES',/,8X,'MODE1',14X,'MODE2',15X
           1,'MODE3')
           WRITE(6,50)X1(1),X1(4),X1(7),X1(2),X1(5),X1(8),X1(3),X1(6),
           1X1(9)
  50       FORMAT(5X,'DG1=',F6.4,10X,'DG2=',F6.3,10X,'DG3=',F6.2,/
           15X,'SG1=',F4.2,12X,'SG2=',F4.2,12X,'SG3=',F4.2,/
           35X,'TOTAL1=',1PE9.3,4X,'TOTAL2=',1PE9.3,4X,'TOTAL3=',1PE9.3,/)
           WRITE(6,55)
  55       FORMAT(/5X,'FINAL VALUES OF THE PARAMETERS',/,8X,'MODE1',14X
           1,'MODE2',15X,'MODE3')
           WRITE(6,50)X(1),X(4),X(7),X(2),X(5),X(8),X(3),X(6),X(9)
           WRITE(6,70)
```

```
70      FORMAT(//,27X,'INPUT DISTRIBUTION',11X,'FITTED DISTRIBUTION',
        1,/,8X,'DP',5X,'DPG',7X,'DATA',3X,'D(DATA)/D(LOGDP)'
        2,5X,'FDATA',3X,'D(FDATA)/D(LOGDP)')
        DO 80 J=1,NBAR
        ABDS(J)=SQRT(BDS(J+1)*BDS(J))
        WRITE(6,90) BDS(J)
90      FORMAT(5X,F6.3)
        WRITE(6,100)ABDS(J),DATA(J),ALDAT(J),ALCDAT(J),CALDAT(J)
100     FORMAT(13X,F6.3,4X,1PE9.3,3X,1PE9.3,7X,1PE9.3,4X,1PE9.3)
80      CONTINUE
        WRITE(6,90) BDS(NBAR1)
        BDS1=BDS(1)
        BDS2=BDS(2)
        BDS(1)=.001
        BDS(2)=15.0
        CALL ALOND(CDAT1,X(1),X(2),X(3))
        CALL ALOND(CDAT2,X(4),X(5),X(6))
        CALL ALOND(CDAT3,X(7),X(8),X(9))
        CDAT1(1)=CDAT1(1)+CDAT2(1)+CDAT3(1)
        BDS(1)=BDS1
        BDS(2)=BDS2
        JJ=0
106     WRITE(5,107)
107     FORMAT(5X,'INHALABLE PARTICULATE MATTER CALCULATION'
        1,/,5X,'ENTER D50 ,  SG',/,5X,'OR ----HIT RETURN TO SKIP')
        READ (5,109) AIHPMN,AIHPSG
109     FORMAT (2F10.0)
        IF (AIHPMN) 190,190,112
112     IF (AIHPSG) 190,190,110
110     IF (JJ .EQ. 1) GO TO 118
        WRITE(6,103)
103     FORMAT(//,5X,'INHALABLE PARTICULATE MATTER')
        JJ=1
118     TIHP=0.0
        CALL AIHP(XIHP,AIHPMN,AIHPSG)
D       WRITE(6,120) XIHP
D120    FORMAT(5X,'IHP FRACTION',/4(10(3X,F6.4),/))
        DO 130 K=1,7,3
        CALL CNUMS(CNUM,X(K),X(K+1),X(K+2))
D       WRITE(6,140) CNUM
D140    FORMAT(5X,'NUM.FRAC.',/4(10(3X,1PE9.3),/))
        DO 150 J=1,40
150     TIHP=TIHP+CNUM(J)*XIHP(J)
130     CONTINUE
        WRITE(6,160) AIHPMN,AIHPSG,TIHP
160     FORMAT(5X,'D50 = ',F7.3,5X,'SG = ',F7.3,5X,'TOTAL IPM MASS='
        1 ,1PE10.3)
188     GO TO 106
190     CONTINUE
        RETURN
        END
```

APPENDIX C

DESIGN DRAWINGS OF THE INHALABLE PARTICULATE SAMPLING TRAIN

Figure C-1 Cyclone III Shell Inlet.
Figure C-2 Cyclone III Inlet Insert.
Figure C-3 Cyclone III Shell Cap.
Figure C-4 Cyclone III Shell.
Figure C-5 Cyclone III Modified Cap.
Figure C-6 Cyclone III Modified Collection Cup.
Figure C-7 Cyclone X (Mk2) Collection Cup.
Figure C-8 Cyclone X (Mk2) Vortex Tube.
Figure C-9 Cyclone X (Mk2) Body.
Figure C-10 Cyclone X (Mk2) Nozzles (Set of 11).
Figure C-11 Cyclone III Body.

ASSY.	ITEM	QUAN.	NAME	DESCRIPTION	MATERIAL
	501	1	SHELL INLET, 1 1/2" Aluminum Hex Bar, 1.100" Long		
	502	1	INLET INSERT, .800 square, .649 [illegible]		

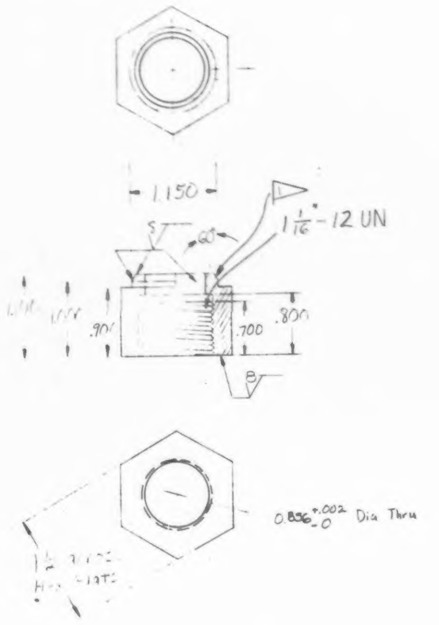
1.150
1 1/16" - 12 UN
60°
.900
1.000
1.100
.700
.800
0.856 +.002 -0 Dia Thru
1 1/2 [illegible] Hex Flats

SHELL INLET, CYCLONE III (501)

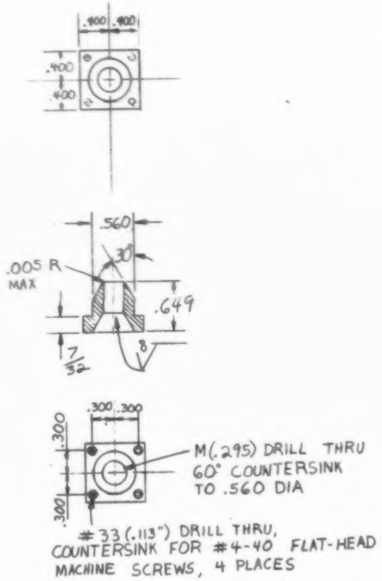
.400 .400
.400
.400
.560
30°
.005 R MAX
.649
7/32
.300 .300
.300
.300

M(.295) DRILL THRU
60° COUNTERSINK
TO .560 DIA

#33(.113") DRILL THRU,
COUNTERSINK FOR #4-40 FLAT-HEAD
MACHINE SCREWS, 4 PLACES

INLET INSERT, CYCLONE III (502)

▷ ALL FILLETS & ROUNDS 1/16" R UNLESS
OTHERWISE NOTED

DATE	REVISIONS	ZONE	NO.

TOLERANCES UNLESS OTHERWISE NOTED		
FRACTIONS	± 1/32	± 1/64
DECIMALS	± .010	±.002
ANGLES	± 1°	
FINISH		
APPROVED		
CHECKED		
DRAWN	K BASSON	

SOUTHERN RESEARCH INSTITUTE
BIRMINGHAM, ALABAMA 35205

TITLE SRI CYCLONE IX

INLET PARTS

SCALE FULL
DATE 4-12-79
DWG. NO. 4181-31-C-05

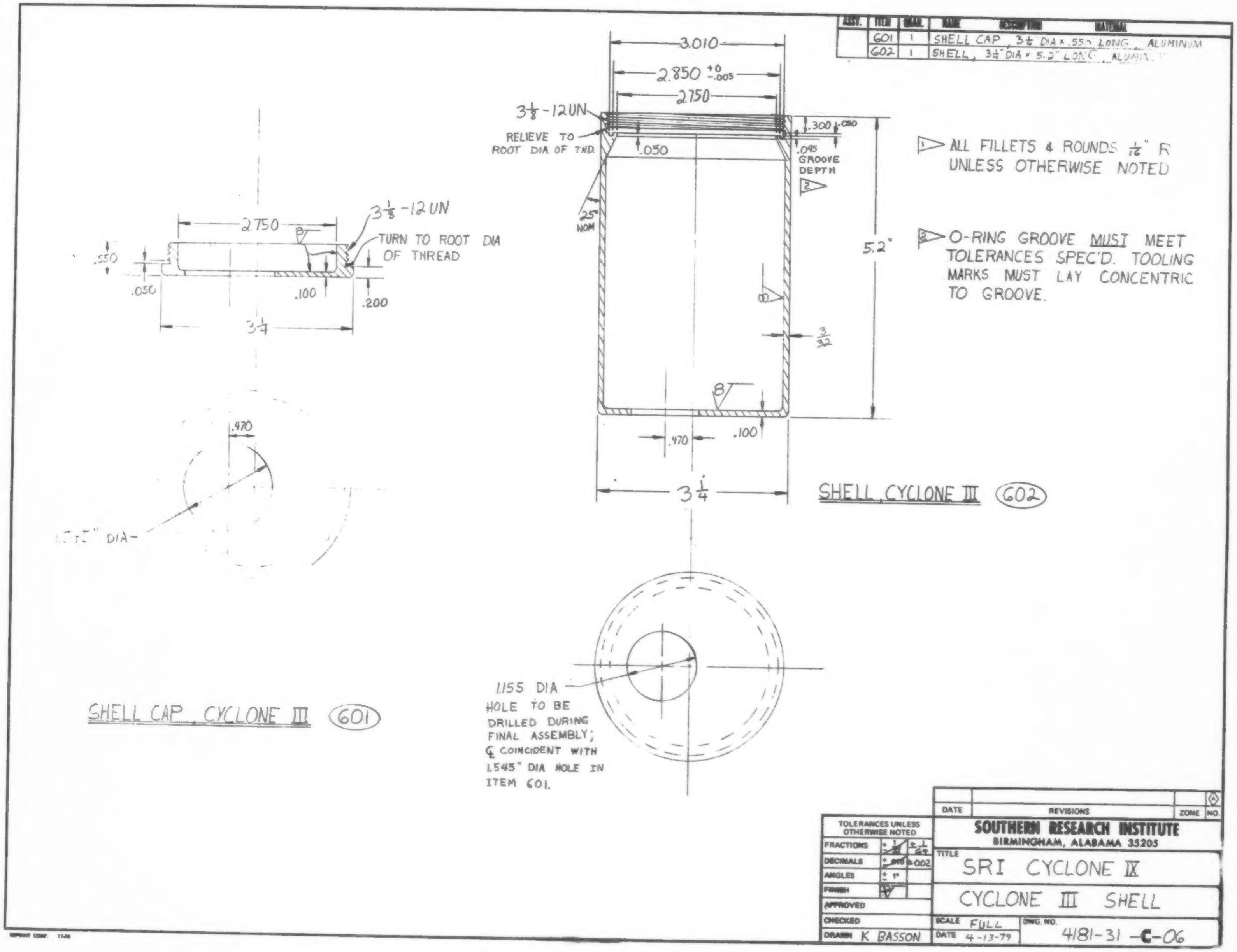
ASSY. | ITEM | QUAN. | NAME | DESCRIPTION | MATERIAL
601 | 1 | SHELL CAP, 3¼" DIA × .550 LONG, ALUMINUM
602 | 1 | SHELL, 3¼" DIA × 5.2" LONG, ALUMINUM
3.010
2.850 +0 -.005
2.750
3⅛-12UN
RELIEVE TO ROOT DIA OF THD.
.050
.300
.050
.045 GROOVE DEPTH
2
25° NOM
5.2"
3/32
.470
.100
3¼
1
ALL FILLETS & ROUNDS 1/16" R UNLESS OTHERWISE NOTED
2
O-RING GROOVE MUST MEET TOLERANCES SPEC'D. TOOLING MARKS MUST LAY CONCENTRIC TO GROOVE.
SHELL, CYCLONE III (602)
2.750
3⅛-12UN
TURN TO ROOT DIA OF THREAD
.550
.050
.100
.200
3¼
.470
1.545" DIA
SHELL CAP, CYCLONE III (601)
1.155 DIA
HOLE TO BE DRILLED DURING FINAL ASSEMBLY; ℄ COINCIDENT WITH 1.545" DIA HOLE IN ITEM 601.
DATE | REVISIONS | ZONE | NO.
TOLERANCES UNLESS OTHERWISE NOTED
FRACTIONS ± 1/32 ± 1/64
DECIMALS ± .010 ± .002
ANGLES ± 1°
FINISH
APPROVED
CHECKED
DRAWN K BASSON
SOUTHERN RESEARCH INSTITUTE
BIRMINGHAM, ALABAMA 35205
TITLE SRI CYCLONE IX
CYCLONE III SHELL
SCALE FULL
DATE 4-13-79
DWG. NO. 4181-31-C-06

ASSY.	ITEM	QUAN.	NAME	DESCRIPTION	MATERIAL
	701	1	MODIFIED CAP, 1 $\frac{11}{16}$" DIA × 2.300" LONG		[illegible]

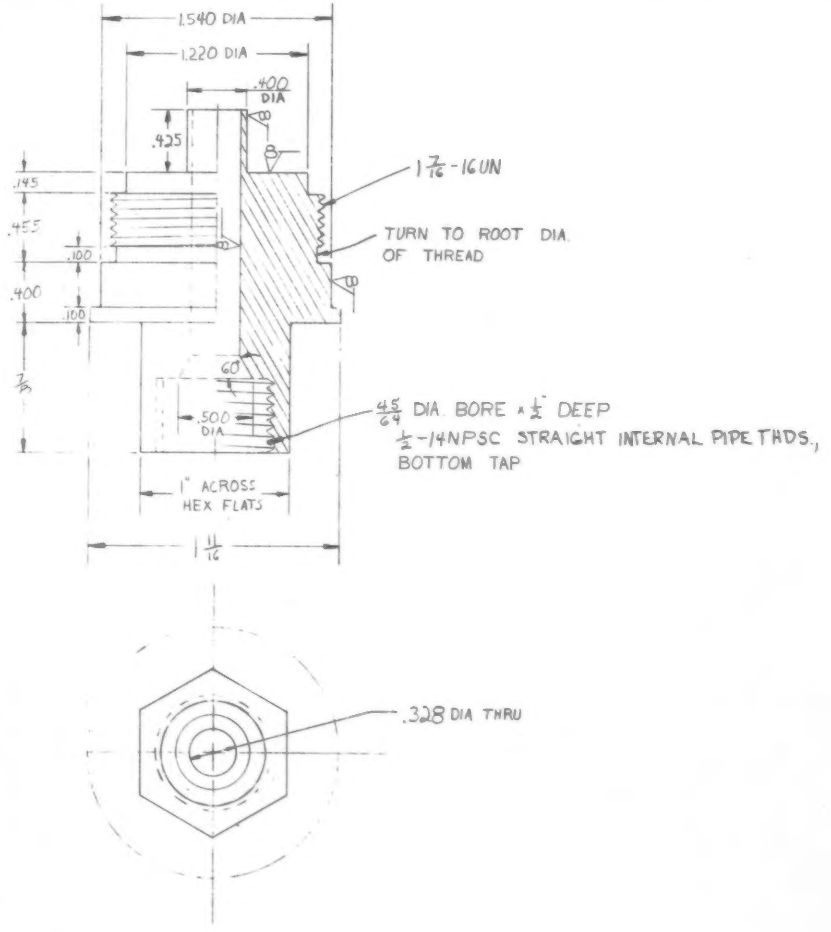
1.540 DIA
1.220 DIA
.400 DIA
.425
.145
.455
.100
.400
.100
7/8
1 $\frac{7}{16}$-16UN
TURN TO ROOT DIA. OF THREAD
60°
.500 DIA
$\frac{45}{64}$ DIA. BORE × $\frac{1}{2}$" DEEP
$\frac{1}{2}$-14NPSC STRAIGHT INTERNAL PIPE THDS., BOTTOM TAP
1" ACROSS HEX FLATS
1 $\frac{11}{16}$
.328 DIA THRU

MODIFIED CAP CYCLONE III (701)

1▷ ALL FILLETS & ROUNDS $\frac{1}{16}$" R UNLESS OTHERWISE NOTED

DATE	REVISIONS	ZONE	NO.

TOLERANCES UNLESS OTHERWISE NOTED		
FRACTIONS	~~± 1/32~~	± 1/64
DECIMALS	~~± .010~~	±.002
ANGLES	± 1°	
FINISH	32 ∇	
APPROVED		
CHECKED		
DRAWN	K BASSON	

SOUTHERN RESEARCH INSTITUTE
BIRMINGHAM, ALABAMA 35205

TITLE SRI CYCLONE IX

CYCLONE III MODIFIED CAP

SCALE 2:1
DATE 4-13-79
DWG NO. 4181-31 -C-07

ASSY.	ITEM	QUAN.	NAME DESCRIPTION MATERIAL
	901	1	COLLECTION CUP, 1.540 DIA x 2.175 LONG, ALUMINUM
	902	1	NOZZLE, .840 DIA x 1.242 LONG, ALUMINUM
	903	1	" " " "
	904	1	" " " "
	905-915		NOZZLE, .840 DIA x 1.242" LONG, ALUM, SEE CHART FOR I.D

▷1 ALL FILLETS & ROUNDS 1/16 R UNLESS OTHERWISE NOTED

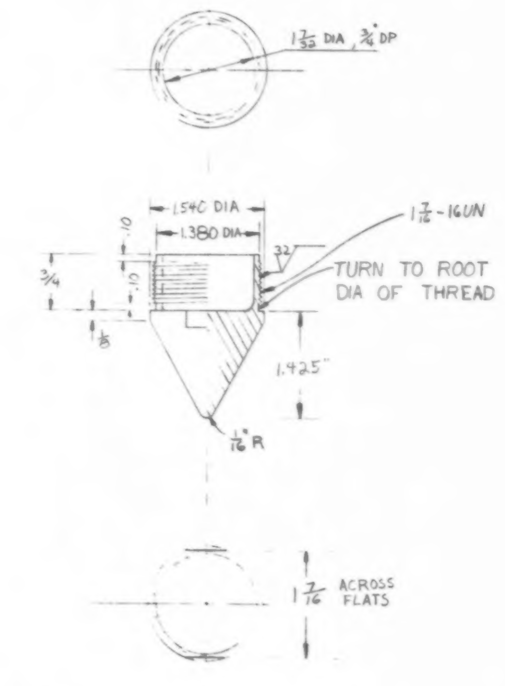

1 7/32 DIA, 3/4 DP
1.540 DIA
1.380 DIA
.10
.10
3/4
1/8
32
1 7/16-16UN
TURN TO ROOT DIA OF THREAD
1.425"
1/16 R
1 7/16 ACROSS FLATS

CYCLONE III COLLECTION CUP (901)

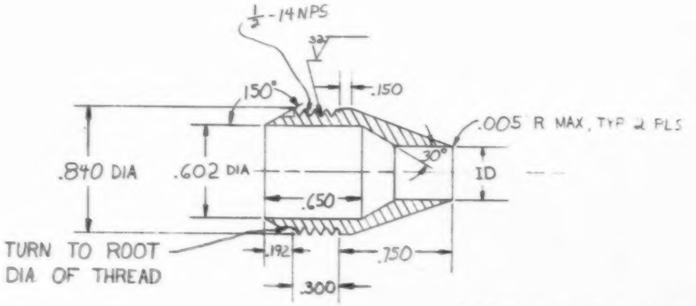

1/2-14NPS
32
150°
.150
.005 R MAX, TYP 2 PLS
30°
.840 DIA
.602 DIA
.650
ID
TURN TO ROOT DIA OF THREAD
.192
.750
.300

CYCLONE IX NOZZLES

2" = 1"

	ITEM	ID
FOR SRI USE ONLY	902	.208"
	903	.269"
	904	.360"
	905	3.0 mm
	906	3.5mm
	907	4.0mm
	908	4.5mm
	909	5.0mm
	910	6.0mm
	911	7.0mm
	912	8.5mm
	913	10.0mm
	914	12.0mm
	915	14.5mm

DATE	REVISIONS	ZONE	NO
10-19-79	ADDED ITEMS 905-915		A

TOLERANCES UNLESS OTHERWISE NOTED		
FRACTIONS	~~± 1/32~~	± 1/64
DECIMALS	~~± .010~~	±.00
ANGLES	~~±~~	± 1/2
FINISH		
APPROVED		
CHECKED		
DRAWN	K BASSON	

SOUTHERN RESEARCH INSTITUTE
BIRMINGHAM, ALABAMA 35205

TITLE SRI CYCLONE IX

COLLECTION CUP & NOZZLES

SCALE FULL
DATE 4-17-79
DWG NO. 4181-31 -C-09

ASSY.	ITEM	QUAN.	NAME / DESCRIPTION / MATERIAL
	1001	1	COLLECTION CUP, 3.125" O.D. x 1.785" LONG
	1002	1	VORTEX TUBE, 3.125" O.D. x 4.094" LONG

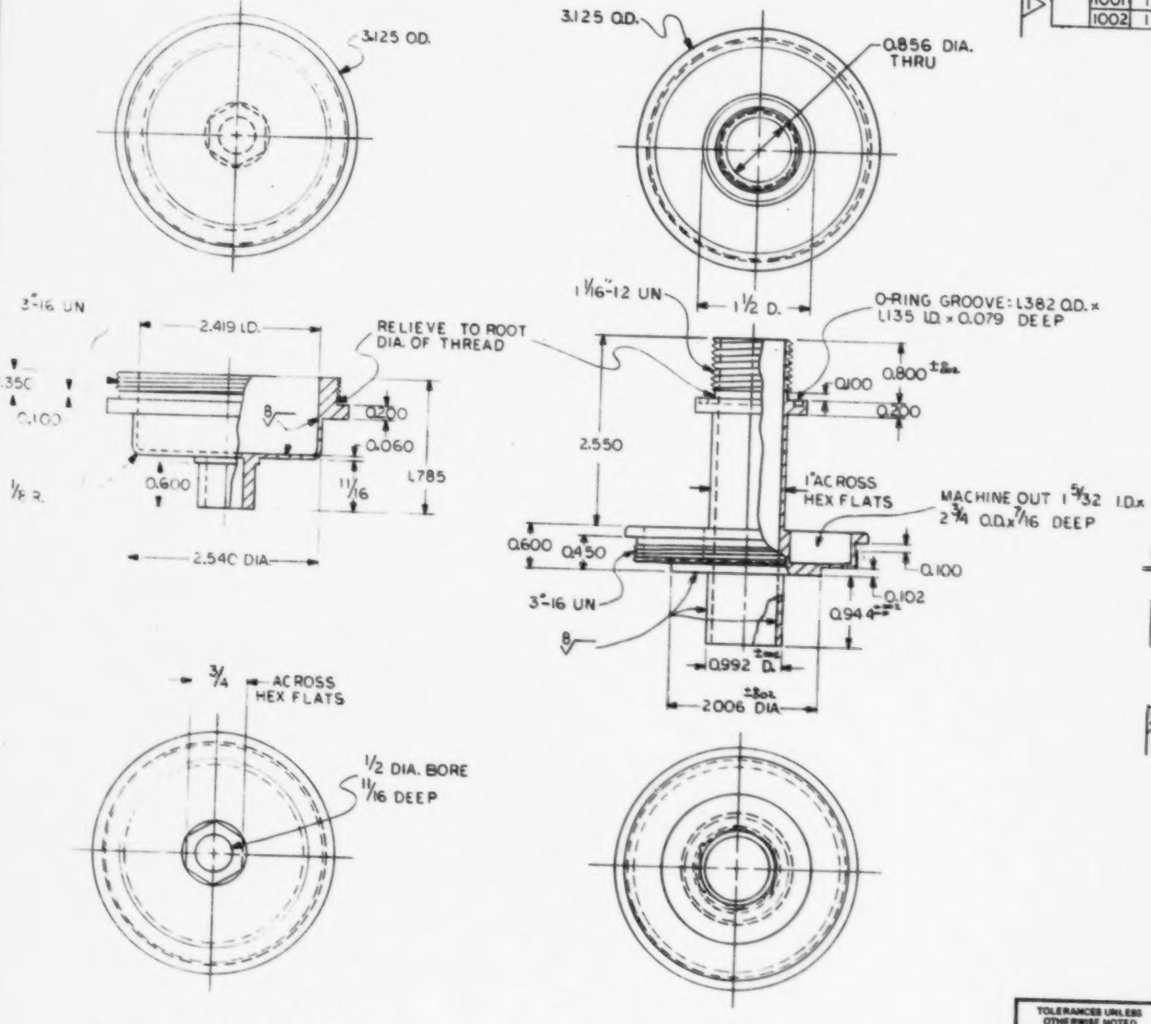
3.125 O.D.
3"-16 UN
2.419 I.D.
RELIEVE TO ROOT DIA. OF THREAD
0.350
0.100
8
0.200
0.060
1.785
11/16
0.600
1/8 R.
2.540 DIA.
3/4 ACROSS HEX FLATS
1/2 DIA. BORE 11/16 DEEP
3.125 O.D.
0.856 DIA. THRU
1 1/16"-12 UN
1 1/2 D.
O-RING GROOVE: 1.382 O.D. x 1.135 I.D. x 0.079 DEEP
0.100
0.800 ±.002
0.200
2.550
1" ACROSS HEX FLATS
MACHINE OUT 1 5/32 I.D. x 2 3/4 O.D. x 7/16 DEEP
0.600
0.450
0.100
3"-16 UN
0.102
0.944 ±.001
8
0.992 ±.002 D.
2.006 ±.002 DIA.

COLLECTION CUP (1001)

VORTEX TUBE (1002)

NOTES:

1. MATERIALS: 316 STAINLESS STEEL, 6AL-4V TITANIUM ALLOY, OR [illegible] ALUMINUM; TO BE SPECIFIED BY WORK ORDER.
2. ALL FILLETS AND ROUNDS 1/16 R. UNLESS NOTED.

TOLERANCES UNLESS OTHERWISE NOTED	
FRACTIONS	± 1/64
DECIMALS	± .005
ANGLES	± 1/2°
FINISH	
APPROVED	
CHECKED	R.R.W. J.R.
DRAWN	M. COWAN

DATE	REVISIONS	ZONE	NO.

SOUTHERN RESEARCH INSTITUTE
BIRMINGHAM, ALABAMA 35205

TITLE SRI CYCLONE X: MARK 2

COLLECTION CUP & VORTEX TUBE

SCALE FULL
DATE 8-17-79
DWG. NO. 4181-37-C-10

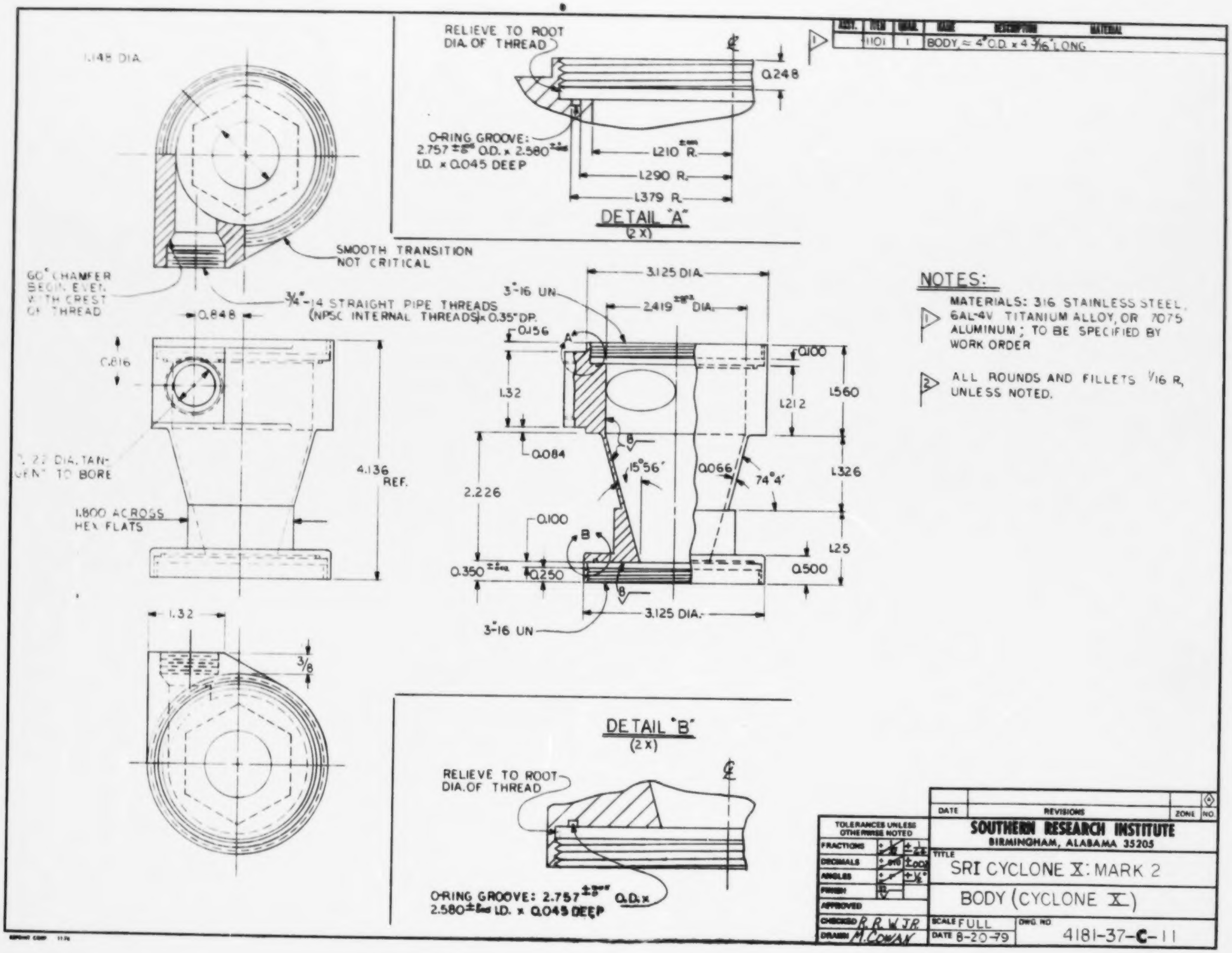
1.148 DIA.
SMOOTH TRANSITION NOT CRITICAL
60° CHAMFER BEGIN EVEN WITH CREST OF THREAD
3/4"-14 STRAIGHT PIPE THREADS (NPSC INTERNAL THREADS) x 0.35" DP.
0.848
0.816
1.22 DIA. TANGENT TO BORE
1.800 ACROSS HEX FLATS
4.136 REF.
1.32
3/8
RELIEVE TO ROOT DIA. OF THREAD
O-RING GROOVE: 2.757 O.D. x 2.580 I.D. x 0.045 DEEP
0.248
1.210 R.
1.290 R.
1.379 R.
DETAIL "A"
(2X)
3.125 DIA.
2.419 DIA.
3"-16 UN
0.156
A
1.32
0.084
2.226
0.100
B
0.350
0.250
3.125 DIA.
3"-16 UN
15°56'
0.066
74°4'
0.100
1.212
1.560
1.326
1.25
0.500
DETAIL "B"
(2X)
RELIEVE TO ROOT DIA. OF THREAD
O-RING GROOVE: 2.757 O.D. x 2.580 I.D. x 0.045 DEEP
1101
1
BODY ≈ 4" O.D. x 4 3/16" LONG
NOTES:
1 MATERIALS: 316 STAINLESS STEEL, 6AL-4V TITANIUM ALLOY, OR 7075 ALUMINUM; TO BE SPECIFIED BY WORK ORDER
2 ALL ROUNDS AND FILLETS 1/16 R, UNLESS NOTED.
TOLERANCES UNLESS OTHERWISE NOTED
FRACTIONS
DECIMALS
ANGLES
FINISH
APPROVED
CHECKED R.R.W. JR.
DRAWN M. COWAN
DATE
REVISIONS
ZONE
NO.
SOUTHERN RESEARCH INSTITUTE
BIRMINGHAM, ALABAMA 35205
TITLE
SRI CYCLONE X: MARK 2
BODY (CYCLONE X)
SCALE FULL
DATE 8-20-79
DWG. NO.
4181-37-C-11

ASSY.	ITEM	QUAN.	NAME	DESCRIPTION	MATERIAL
	1201		NOZZLE, DIA. VARIES x 2.32" LONG		1

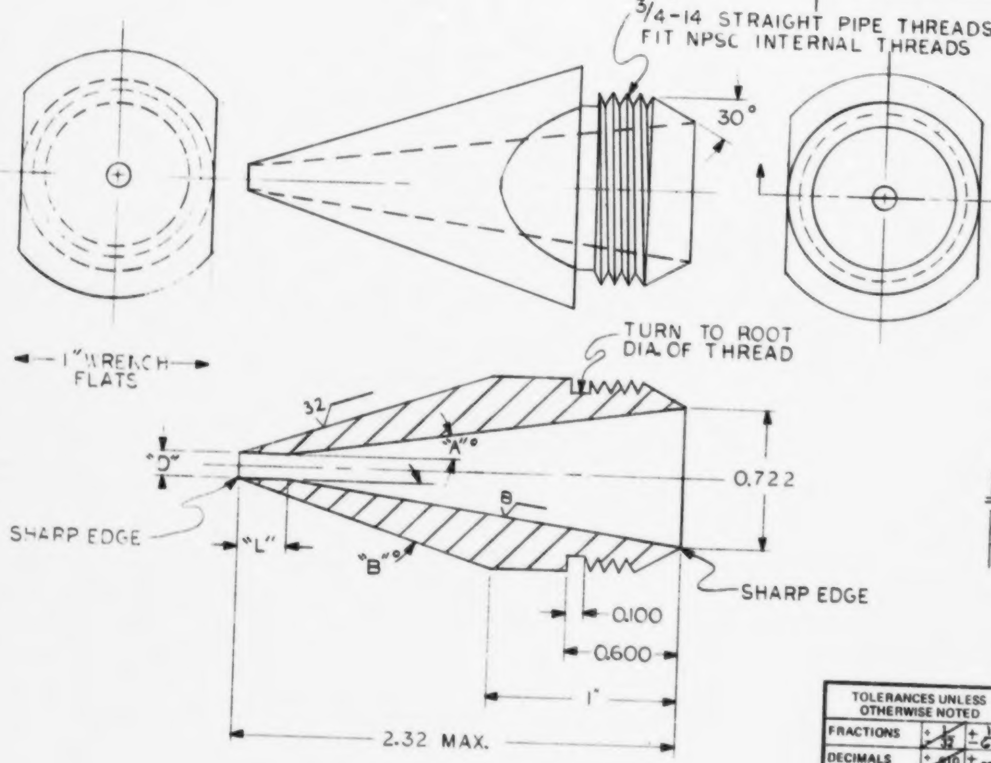

3/4"-14 STRAIGHT PIPE THREADS TO FIT NPSC INTERNAL THREADS
30°
1" WRENCH FLATS
TURN TO ROOT DIA. OF THREAD
32
"D"
"A"°
0.722
B
SHARP EDGE
"L"
"B"°
SHARP EDGE
0.100
0.600
1"
2.32 MAX.

TABULATION			
"D" (DIA) mm	"A"° DEGREES	"B"° DEGREES	"L" INCHES
3.0	8° 18′	18° 28′	0.25
3.5	8° 02′	18° 05′	0.25
4.0	7° 46′	17° 42′	0.25
4.5	7° 30′	17° 19′	0.25
5.0	7° 14′	16° 55′	0.25
6.0	6° 42′	16° 08′	0.25
7.0	6° 09′	15° 21′	0.25
8.5	5° 21′	14° 09′	0.25
10.0	5° 09′	12° 56′	0.50
12.0	3° 55′	11° 18′	0.50
14.5	2° 23′	9° 14′	0.50

NOTE:

1 MATERIAL TO BE SPECIFIED BY WORK ORDER.

DATE	REVISIONS	ZONE	NO.

SOUTHERN RESEARCH INSTITUTE
BIRMINGHAM, ALABAMA 35205

TITLE SRI CYCLONE X: MARK 2

NOZZLES

TOLERANCES UNLESS OTHERWISE NOTED		
FRACTIONS	± 1/32	± 1/64
DECIMALS	± .010	± .002
ANGLES	± 1°	± 1/2°
FINISH	32	
APPROVED		
CHECKED	R.R.W. JR.	
DRAWN	M. COWAN	

SCALE 2X

DATE 8-21-79

DWG. NO. 4181-37-**B**-12

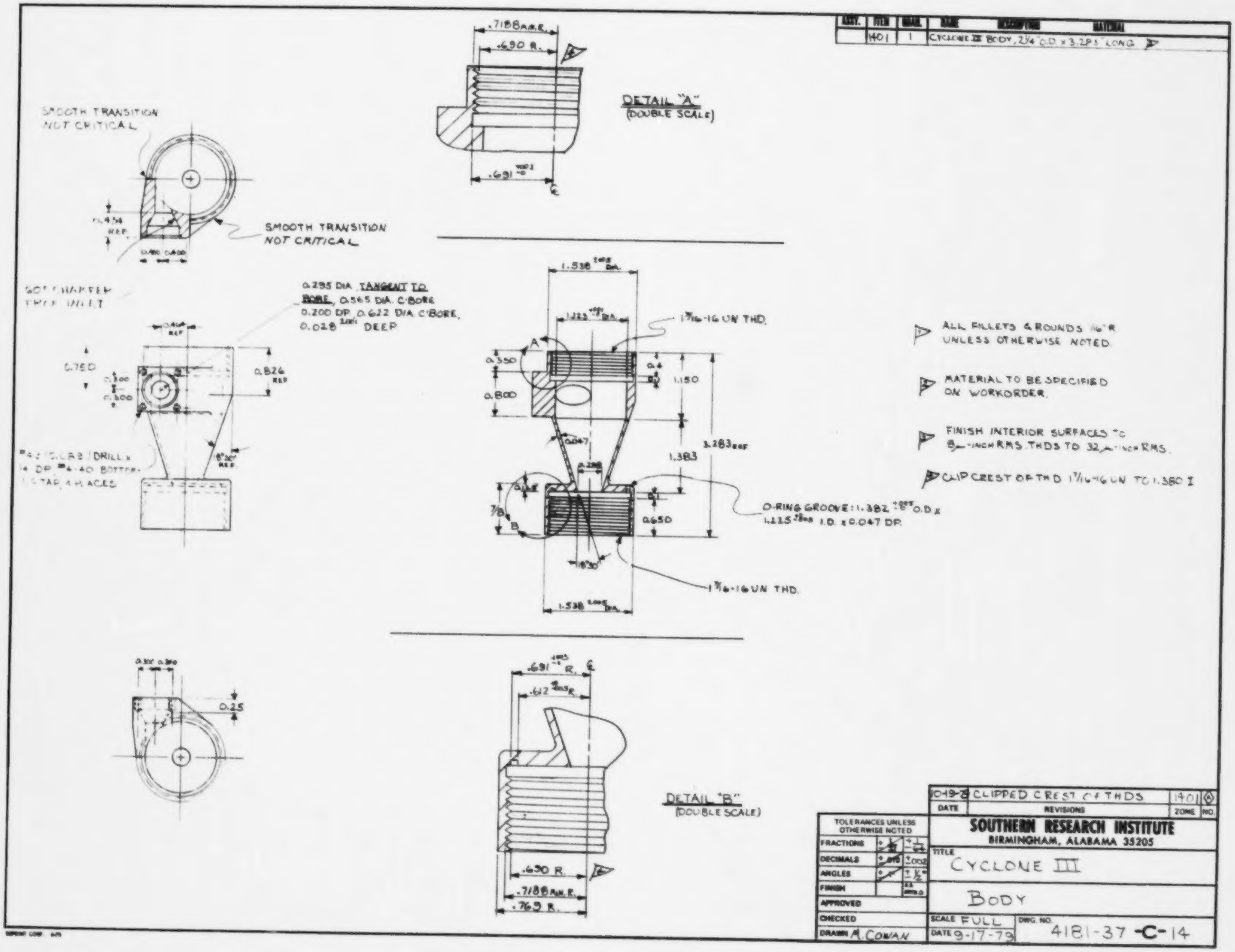
ASSY. | ITEM | QUAN. | NAME | DESCRIPTION | MATERIAL
1401 | 1 | CYCLONE III BODY, 2¼" O.D. x 3.283" LONG
.7188 A.M.R.
.690 R.
.691 +.003 −0
DETAIL "A"
(DOUBLE SCALE)
SMOOTH TRANSITION
NOT CRITICAL
0.434 REF.
0.400 0.400
SMOOTH TRANSITION
NOT CRITICAL
60° CHAMFER
THRU INLET
0.295 DIA. TANGENT TO BORE, 0.565 DIA. C'BORE 0.200 DP. 0.622 DIA. C'BORE, 0.028 ±.001 DEEP
0.414 REF
0.750
0.300
0.300
0.826 REF
#42 (0.093) DRILL x ¼ DP. #4-40 BOTTOM TAP, 4 PLACES
18°30' REF.
1.538 ±.005 DIA.
1.222 +.001 −0 DIA.
1⅜-16 UN THD.
A
0.350
0.800
0.4
1.150
0.047
1.383
3.283 REF
0.288
7/8
B
0.650
O-RING GROOVE: 1.382 +.005 −0 O.D. x 1.225 +0 −.005 I.D. x 0.047 DP.
18°30'
1⅜-16 UN THD.
1.538 ±.005 DIA.
ALL FILLETS & ROUNDS 1/16" R UNLESS OTHERWISE NOTED.
MATERIAL TO BE SPECIFIED ON WORKORDER.
FINISH INTERIOR SURFACES TO 8μ-INCH RMS. THDS TO 32μ-INCH RMS.
CLIP CREST OF THD 1⅜-16 UN TO 1.380 I
0.300 0.300
0.25
.691 +.003 −0 R.
.612 ±.005 R.
DETAIL "B"
(DOUBLE SCALE)
.630 R.
.7188 MIN. R.
.769 R.
10-19-78 | CLIPPED CREST OF THDS | 1401 | A
DATE | REVISIONS | ZONE | NO.
TOLERANCES UNLESS OTHERWISE NOTED
FRACTIONS ± 1/64
DECIMALS ± .002
ANGLES ± ½°
FINISH
APPROVED
CHECKED
DRAWN M. COWAN
SOUTHERN RESEARCH INSTITUTE
BIRMINGHAM, ALABAMA 35205
TITLE CYCLONE III
BODY
SCALE FULL
DATE 9-17-79
DWG. NO. 4181-37-C-14

APPENDIX D

DESIGN DRAWINGS OF THE INHALABLE PARTICULATE PRECUTTER CYCLONE

Figure D-1. Cyclone IX Collection Cup.
Figure D-2. Cyclone IX Vortex Tube.
Figure D-3. Cyclone IX Body.
Figure D-4. Cyclone IX Nozzles.

ASSY.	ITEM	QUAN.	PART	DESCRIPTION	MATERIAL
	601	1		COLLECTION CUP 2.500"O.D. x 1.635"LONG	

NOTES:

1. MATERIALS: 316 STAINLESS STEEL, 6AL-4V TITANIUM ALLOY, OR 7075 ALUMINUM; TO BE SPECIFIED BY WORK ORDER.
2. ALL FILLETS AND ROUNDS 1/16" R. UNLESS NOTED.

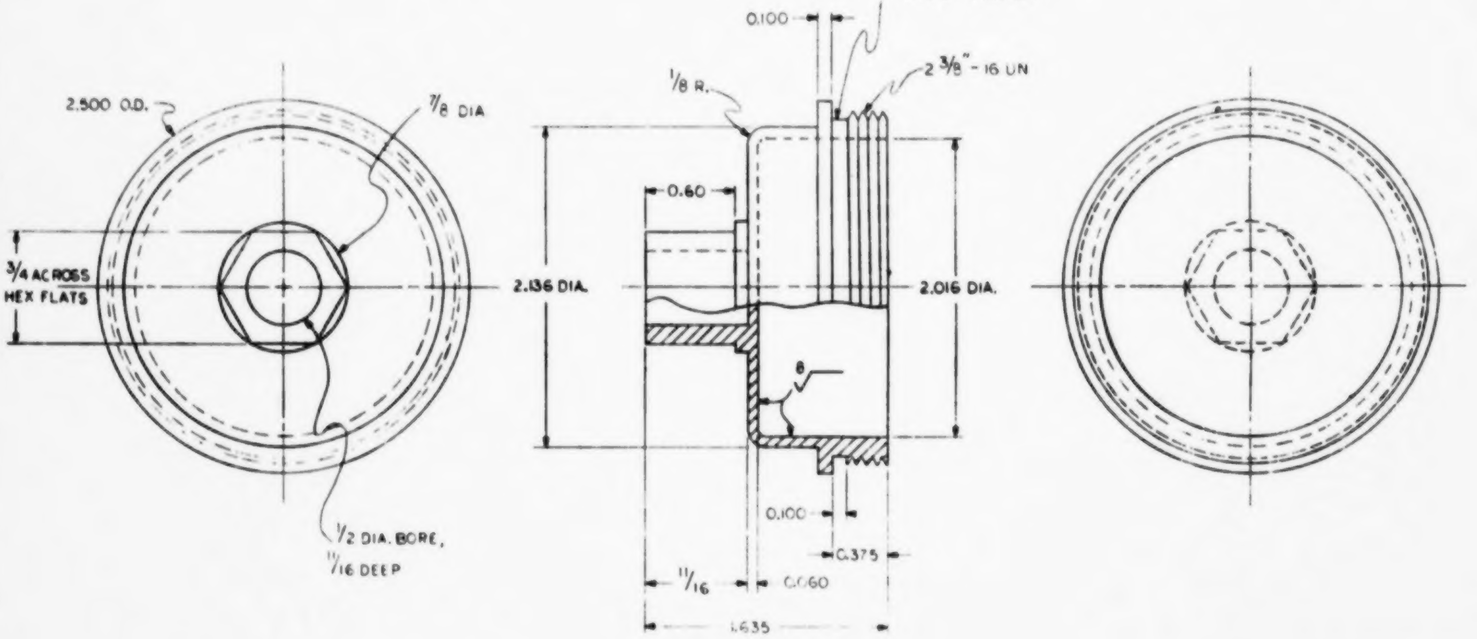
2.500 O.D.
7/8 DIA
3/4 ACROSS HEX FLATS
1/2 DIA. BORE, 11/16 DEEP
2.136 DIA.
1/8 R.
0.100
RELIEVE TO ROOT DIA. OF THREAD
2 3/8" - 16 UN
0.60
8
2.016 DIA.
0.100
0.375
11/16
0.060
1.635

DATE	REVISIONS	ZONE	NO.

SOUTHERN RESEARCH INSTITUTE
BIRMINGHAM, ALABAMA 35205

TITLE SRI CYCLONE IX : MARK 2

COLLECTION CUP

SCALE 2 X
DATE [illegible]
DWG NO 4181-37-C-06

TOLERANCES UNLESS OTHERWISE NOTED		
FRACTIONS	[illegible]	± 1/64
DECIMALS	± .010	± .002
ANGLES	[illegible]	± 1/2
FINISH	32	
APPROVED		
CHECKED	[illegible]	
DRAWN	[illegible]	

	701	1	VORTEX TUBE, 2.500"O.D. × 3.412" LONG

NOTES:

1. MATERIALS: 316 STAINLESS STEEL, 6AL-4V TITANIUM ALLOY, OR 7075 ALUMINUM; TO BE SPECIFIED BY WORK ORDER.

2. ALL FILLETS AND ROUNDS 1/16 R. UNLESS NOTED.

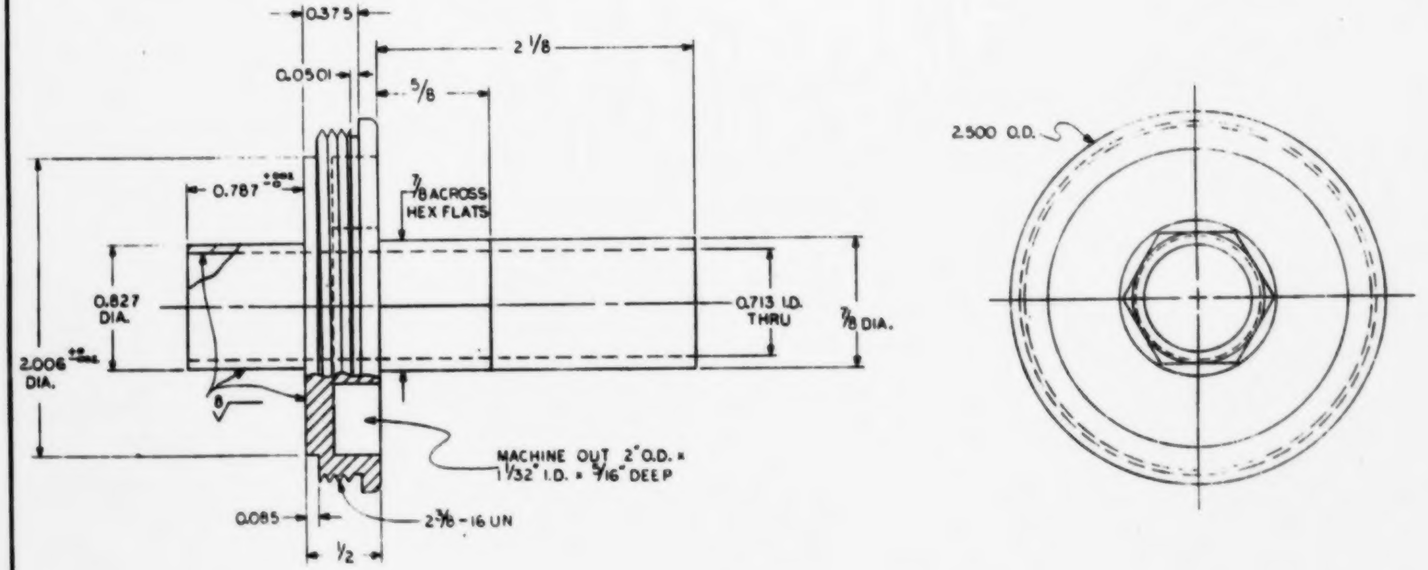
0.375
0.0501
2 1/8
5/8
0.787 +.002 −0
7/8 ACROSS HEX FLATS
0.827 DIA.
0.713 I.D. THRU
7/8 DIA.
2.006 +0 −.002 DIA.
8
MACHINE OUT 2" O.D. × 1 1/32" I.D. × 7/16" DEEP
0.085
2 3/8 - 16 UN
1/2
2.500 O.D.

TOLERANCES UNLESS OTHERWISE NOTED	
FRACTIONS	± 1/64
DECIMALS	± .002
ANGLES	± 1/2°
FINISH	
APPROVED	
CHECKED	
DRAWN	V. COWAN

DATE | REVISIONS | ZONE | NO.

SOUTHERN RESEARCH INSTITUTE
BIRMINGHAM, ALABAMA 35205

TITLE SRI CYCLONE IX: MARK 2

VORTEX TUBE

SCALE 2 X
DATE 6-13-73
DWG NO. 4181-37-C-07

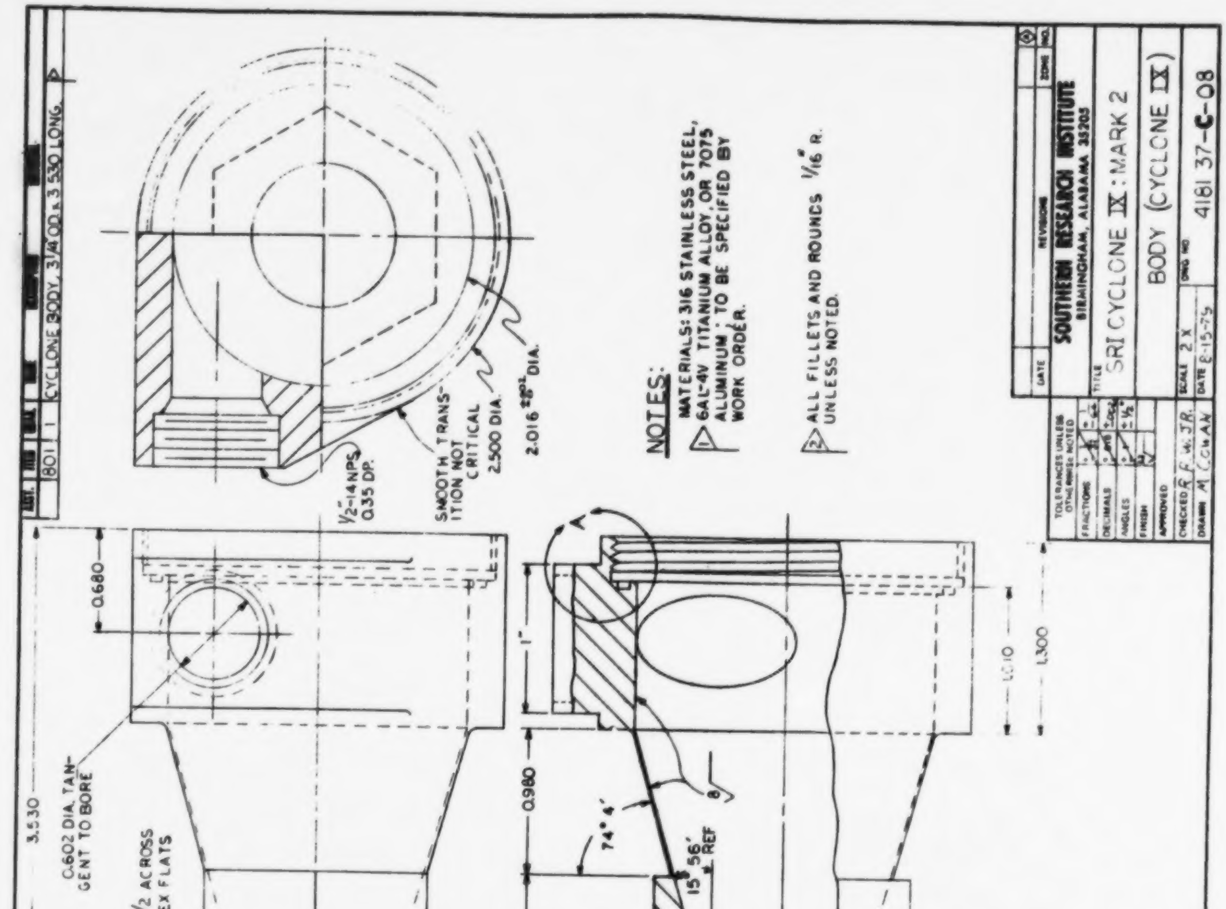
801 1 CYCLONE BODY, 3 1/4 O.D. x 3.530 LONG
1/2"-14 NPS 0.35 DP.
SMOOTH TRANSITION NOT CRITICAL
2.500 DIA.
2.016 DIA.
NOTES:
1 MATERIALS: 316 STAINLESS STEEL, 6AL-4V TITANIUM ALLOY, OR 7075 ALUMINUM; TO BE SPECIFIED BY WORK ORDER.
2 ALL FILLETS AND ROUNDS 1/16" R. UNLESS NOTED.
SOUTHERN RESEARCH INSTITUTE
BIRMINGHAM, ALABAMA 35205
SRI CYCLONE IX : MARK 2
BODY (CYCLONE IX)
SCALE 2X
DATE 8-15-75
CHECKED R. F. W. JR.
DRAWN M. COWAN
4181 37-C-08
3.530
0.680
0.602 DIA. TANGENT TO BORE
1 1/2 ACROSS HEX FLATS
0.980
74° 4'
15° 56' REF
1.25
0.50
1"
1.010
1.300
A
B
60° CHAMFER, BEGIN EVEN WITH CREST OF THREAD
5/16
1"
0.957 DIA.
RELIEVE TO ROOT DIA. OF THD.
2 3/16"-16 UN
0.045
0.240
0.050
1.008 R.
1.045 R.
1.130 R.
O-RING GROOVE 2.260 O.D. x 2.090 I.D. x 0.045 DEEP
DETAIL "A"
0.050
0.045
0.325
3/16"-16 UN
RELIEVE TO ROOT DIA. OF THREAD
DETAIL "B"

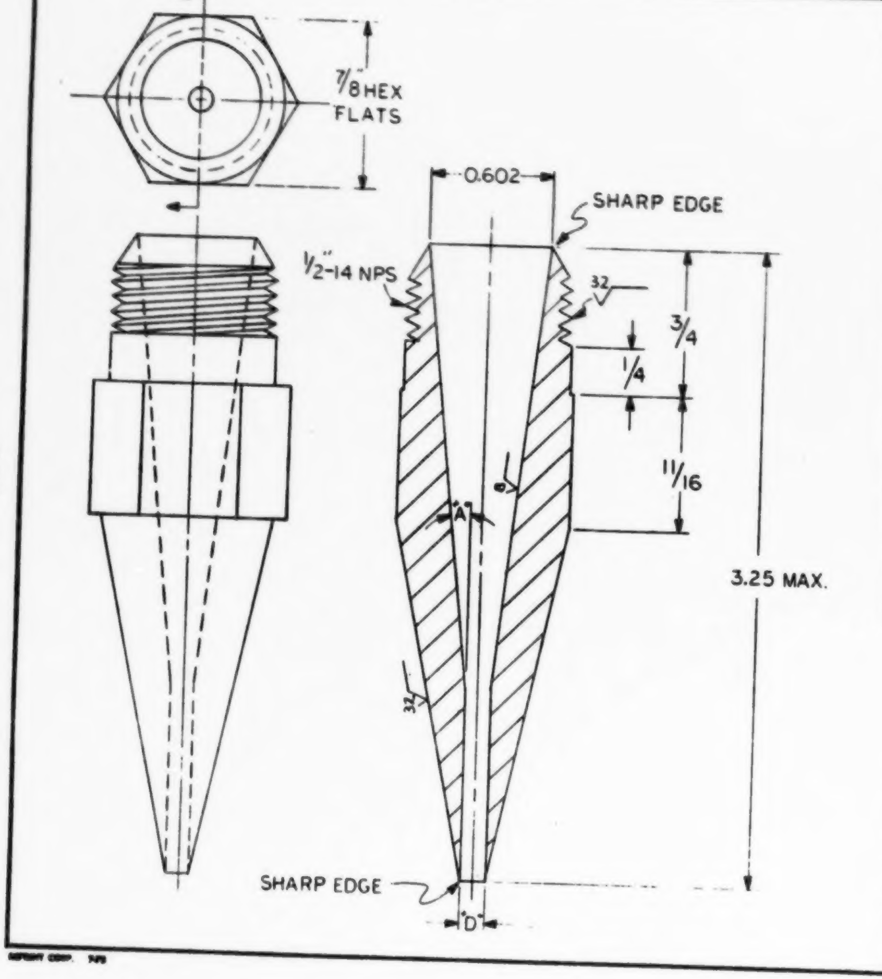

ASSY.	ITEM	QUAL.	NAME	DESCRIPTION	MATERIAL
	901		NOZZLE, ≈1 DIA." x 3.25" LONG		2

TABULATION	
"D" (DIA) mm	"A"° DEGREES
3	6
4	6
5	3 3/4
6	3 3/4
7	3 3/4
8	3 3/4
9	3 3/4
10	3 3/4
11	3 3/4
12	1 1/2
13	1 1/2
14	1 1/2
15	1 1/2

TABULATION	
"D" (DIA) IN.	"A"° DEGREES
1/8	6
3/16	3 3/4
1/4	3 3/4
5/16	3 3/4
3/8	3 3/4
7/16	1 1/2
1/2	1 1/2
9/16	1 1/2

NOTES:

1. MOST NOZZLE SIZES CAN BE MADE BY MODIFICATION OF ANDERSEN SAMPLERS, INC., STRAIGHT NOZZLES.

2. MATERIAL TO BE SPECIFIED BY WORK ORDER.

DATE	REVISIONS	ZONE	NO.

TOLERANCES UNLESS OTHERWISE NOTED		
FRACTIONS	~~± 1/32~~	± 1/64
DECIMALS	~~± .010~~	± .002
ANGLES	~~± 1°~~	± 1/2°
FINISH	32 √	
APPROVED		
CHECKED R.R.W. JR.		
DRAWN M. COWAN		

SOUTHERN RESEARCH INSTITUTE
BIRMINGHAM, ALABAMA 35205

TITLE
SRI CYCLONE IX : MARK 2

NOZZLES FOR 6" PORT

SCALE 2 X
DATE 8-15-79
DWG. NO. 4181-37-**B**-09

APPENDIX E

METRIC SYSTEM CONVERSION FACTORS

Non-metric	Multiplied by	Yields Metric
acfm	28.317	liters/min
°F	5/9 (°F-32)	°C
in.	2.54	cm
gr/acf	0.0023	g/liter
ft	30.48	cm
gr/acf	2.29	g/m^3